Severe Traumatic Brain Injury Induces Cortical Remodeling in the Pediatric Inhibitory Network.

by

Joshua Nichols

A Dissertation Presented in Partial Fulfillment
of the Requirements for the Degree
Doctorate in Philosophy

Approved November 2015
Graduate Supervisory Committee:

Trent Anderson, Co-Chair
Jason Newbern, Co-Chair
Janet Neisewander
Shenfeng Qiu
Sarah Stabenfeldt

ARIZONA STATE UNIVERSITY

December 2015

ABSTRACT

Pediatric traumatic brain injury (TBI) is a leading cause of death and disability in children. When TBI occurs in children it often results in severe cognitive and behavioral deficits. Post-injury, the pediatric brain may be sensitive to the effects of TBI while undergoing a number of age-dependent physiological and neurobiological changes. Due to the nature of the developing cortex, it is important to understand how a pediatric brain recovers from a severe TBI (sTBI) compared to an adult. Investigating major cortical and cellular changes after sTBI in a pediatric model can elucidate why pediatrics go on to suffer more neurological damage than an adult after head trauma. To model pediatric sTBI, I use controlled cortical impact (CCI) in juvenile mice (P22). First, I show that by 14 days after injury, animals begin to show recurrent, non-injury induced, electrographic seizures. Also, using whole-cell patch clamp, layer V pyramidal neurons in the peri-injury area show no changes except single-cell excitatory and inhibitory synaptic bursts. These results demonstrate that CCI induces epileptiform activity and distinct synaptic bursting within 14 days of injury without altering the intrinsic properties of layer V pyramidal neurons. Second, I characterized changes to the cortical inhibitory network and how fast-spiking (FS) interneurons in the peri-injury region function after CCI. I found that there is no loss of interneurons in the injury zone, but a 70% loss of parvalbumin immunoreactivity (PV-IR). FS neurons received less inhibitory input and greater excitatory input. Finally, I show that the cortical interneuron network is also affected in the contralateral motor cortex. The contralateral motor cortex shows a loss of interneurons and loss of PV-IR. Contralateral FS neurons in the motor cortex synaptically showed greater excitatory input and less inhibitory input 14 days after injury. In

summary, **t**his work demonstrates that by 14 days after injury, the pediatric cortex develops epileptiform activity likely due to cortical inhibitory network dysfunction. These findings provide novel insight into how pediatric cortical networks function in the injured brain and suggest potential circuit level mechanisms that may contribute to neurological disorders as a result of TBI.

ACKNOWLEDGEMENTS

I must first and foremost thank Dr. Trent Anderson. As a mentor he has played a critical role in my scientific development. He has provided me the opportunity to pursue my own ideas while challenging me to constantly improve. His understanding and patience is unmatched and I would not have been able to accomplish what I have without him. I will always be grateful to Trent for creating the opportunity for me to pursue my doctoral degree and providing endless support.

Additionally, Dr. Jason Newbern's mentorship has been invaluable and critical to my development as a scientist. He has pushed me to be critical and judiciously evaluate my work. I am grateful to Jason; not only for his everlasting support, but also for being the type young scientist I aspire to be. This would not have been possible without him. I must also thank the rest of my committee for their constant support and understanding during my graduate training: Janet Neisewander, Shenfeng Qiu, and Sarah Stabenfeldt.

I am grateful to Dr. William Jamie Tyler for introducing me to neuroscience and inviting me to join his lab during my undergraduate studies. From this, I had the privilege to work under Yusuf Tufail. I would also like to thank Dr. Carsten Duch for teaching me the rigor that science demands and also the ease with which science can be pursued.

Past and present Arizona State University graduate students also have my greatest gratitude for their advice and friendship. In particular, I must thank Dr. Joseph Georges. His willingness to teach and involve me in his own research has done more for my development as scientist than I can express.

Finally, I acknowledge my parents, Steven and Lan Nichols for their wisdom and support. Before anyone, they were the first to show me the value of science.

TABLE OF CONTENTS

CHAPTER 1

INTRODUCTION

Traumatic Brain Injury

Traumatic brain injury is the result of an external mechanical force that causes damage to the brain. The mechanical force can be the result of a rapid change in acceleration, blast waves, penetrating injury, or impact (Maas et al., 2008). Classification of TBI is based on severity of the injury, anatomical features resulting from the injury, and how the injury was caused (Saatman et al., 2008). Although TBI affects all ages, it is most common in children where it remains a leading cause of death and disability. According to the National Center for Injury Prevention and Control (2009), in children 0 - 14 years of age, TBI annually results in 435,000 trips to the emergency room and nearly 2700 deaths. Symptoms of TBI largely depend upon which area of the brain was injured. Severe TBI will often result in a relentless headache, convulsions, nausea, aphasia, slurred speech, dysarthria, loss of coordination, weakness in limbs, restlessness, and/or agitation (Kim, 2002). Frequently accompanying the primary damage to the brain is multiple secondary injury events. These events can include damage to the blood-brain barrier, inflammation, excitotoxicity, influx of calcium and sodium ions into neurons, and mitochondrial dysfunction (Park et al., 2008). An increase in intracranial pressure may arise from swelling or from a hemorrhage. Brain death or herniation can occur when the pressure within the skull becomes too great (Werner and Engelhard, 2007). Also, ischemia can result from a decrease in cerebral perfusion pressure (Ghajar, 2000). Researchers have constructed a various assortment of models such as fluid percussion injury, controlled cortical impact, blast models, and undercut models to better understand

the implications and consequences of TBI.

Pediatric Traumatic Brain Injury

Research on traumatic brain injury in the pediatric population has revealed that TBI can negatively effect on going brain development and maturation, leading to neurological changes that persist into adulthood (Anderson and Moore, 1995; Klonoff et al., 1993; Kochanek et al., 2012; Luerssen et al., 1988a). The outcome following a TBI event also seems to be age dependent as younger children (<7 years of age) will go on to have a worse outcome and take longer to recover compared with older children, adolescents, and adults (Anderson and Moore, 1995). For this reason, it is important to consider TBI as a neurological disorder that is age dependent and develops over time. Understanding the properties of the pediatric brain that alters its response to TBI may lead to better management and therapeutics to alleviate symptoms resulting from head injury. Since considerable brain maturation occurs during a child's early years (0-7 years), it is easy to understand why a child's brain before 7 years old has the most devastating consequences and effects neurological maturation.

Due to several longitudinal studies of young people with brain injuries (Anderson and Moore, 1995; Ewing-Cobbs et al., 1989, 1999, 2003, 2006; Kochanek et al., 2012; Luerssen et al., 1988a), we now understand that a young brain is not as resilient to brain injury as was once thought. Conventional thinking regarding TBI in young people was that the child's brain was resilient to trauma due to it being highly "plastic" and other parts of the brain would take over for damaged areas.

Studies in juvenile animal models to better characterize changes in the developing brain after severe TBI have been limited. However, it has been shown that juvenile brain

injury can cause alterations to the underlying corpus callosum, hippocampus, synaptic reorganization, and deficits in spatial learning memory (Adelson et al., 2013; Casella et al., 2014; Jenkins et al., 2002). One study has shown that inhibitory neurons of the adult hippocampus show reduced inhibition and increased excitation after CCI (Hunt et al., 2011). Our understanding of cortical inhibitory neurons after CCI has yet to be as thoroughly understood. In addition, evidence that a unilateral TBI can induce bilateral deficits, most TBI research has focused on the peri-injury zone, directly adjacent to the site of injury. There has been limited work addressing axonal sheering in the corpus callosum, and only one study that addresses motor cortex plasticity after CCI (Axelson et al., 2013). To address these gaps in understanding in these studies we investigated anatomical and functional cellular changes in the peri-injury and contralateral cortex after sTBI in "pediatric" animals. It is important to understand how a pediatric brain responds to TBI differently than an adult to developing new preventative and treatment options.

Epilepsy

Epilepsy is defined as the risk of recurrent seizures which can vary in length and severity (Fisher et al., 2005). It cannot be cured, but in 70% of cases seizures can be controlled by medication (Eadie, 2012). Epilepsy goes back as far as the first medical records (2005). The first recorded account of epilepsy was made by the Babylonians who believed that seizures were the result of an evil spirit invading the body. This supernatural view was not challenged until the 17th century B.C. by Hippocrates (2005). Hippocrates postulated that epilepsy should be treated like any other natural disease, with diet and drugs before it becomes chronic. He believed that once a disease becomes chronic it is ultimately incurable (Temkin, 1994). Despite Hippocrates' proposal that

heredity was a likely cause or his description of the physical characteristics and social stigma caused by it (Magiorkinis et al., 2010), it was still assumed that epilepsy was caused by evil spirits until the 17th century (2005). It was not until the mid 1800s that the first antiepileptic drug, bromide, was developed (Perucca and Gilliam, 2012). Sixty-five million people worldwide are known to have epilepsy (Thurman et al., 2011). The ways in which people develop the disease can be due to genetics or be a result of other conditions. However, in most cases for patients diagnosed with epilepsy, the cause is unknown (Fisher et al., 2005). Epilepsy can happen in a variety of ways. Genetic factors can be a cause of epilepsy because certain genes can affect the likelihood of susceptibility as well as the interaction of multiple genes (Pandolfo, 2011). However, idiopathic generalized epilepsy is the most common type of genetically determined epilepsy, but how it is inherited is still unknown (2005). The other prominent mode of the development of epilepsy is symptomatic. Symptomatic epilepsies can occur as the result of brain tumors, cerebral anoxia, brain infections, birth trauma, cortical malformations, and head trauma (2005). Compared to those that have not suffered seizures after a head injury, post-traumatic epilepsy (PTE) patients are known to have a shorter life expectancy (Corkin et al., 1984). In addition to shorter life expectancies, those with PTE recover from injuries slower and have more cognitive and motor issues (Camfield and Camfield, 2014).

Post Traumatic Epilepsy

Post-traumatic epilepsy is a possible outcome as a result of traumatic brain injury. A sufferer of a traumatic brain injury can experience post traumatic seizures as quickly as one week after initial insult (Pagni and Zenga, 2005). PTE and symptomatic epilepsy

accounts for 5% and 20% of epilepsy cases respectively (Garga and Lowenstein, 2006). A large problem to those that suffer TBI is the unknown likelihood of developing PTE (Pitkänen et al., 2007). Post traumatic seizures may occur after insult, but this does not mean that the patient will go on to develop post traumatic epilepsy (PTE). PTE is characterized as a chronic condition, where post traumatic seizures might only occur once or twice in a patient (Frey, 2003a). The likelihood of a person developing PTE is linked to the severity of the injury (Iudice and Murri, 2000). Mild TBI increases the risk, compared to that of an uninjured group, of PTE by one and a half fold (Annegers et al., 1998). However, some estimates show that as many as half of severe TBI sufferers will develop PTE (Iudice and Murri, 2000). A study done to understand the likelihood of the development of PTE in relation to severity showed that 2.1% of mild TBI sufferers will go on to develop PTE compared to 16.7% of severe TBI sufferers (Annegers et al., 1998; Pitkänen and McIntosh, 2006).

Currently, there is much to known about how cellular processes in the brain occur after trauma (Garga and Lowenstein, 2006; Mazarati, 2006). Researchers have proposed several possible mechanisms that can lead to PTE, however, multiple mechanisms may be found in an individual with PTE (Agrawal et al., 2006). Several of these proposed mechanisms can range from formation of new synapses and axons, cells undergoing apoptosis or necrosis, and altered gene expression (Herman, 2002). A particular area that is believed to give rise to PTE is the hippocampus. This is due to decreased connectivity between the parietal cortex and hippocampus (Mishra et al., 2014). However, there is much to be discovered in regard to cortical plasticity after TBI. It has been shown that excitatory and inhibitory networks undergo remodeling after insult (Jin et al., 2011). This

reorganization of neural networks may make neurons hyperexcitable (Elaine Wyllie MD and Deepak K. Lachhwani, 2005). Neurons that become hyperexcitable can create an epileptic focus that leads to seizures (Gill et al., 2013). Furthermore, an increase in neuronal hyperexcitability in conjunction with a loss of inhibitory neurons can produce PTE (Elaine Wyllie MD and Deepak K. Lachhwani, 2005).

Cortex

The human cortex has six cortical layers and each layer is characterized by the distribution of neural cell types and connections to other layers and subcortical regions. Each layer is roughly 2-3mm thick in humans. Layer I is the shallowest layer of the cortex. It is mostly free of neuronal cell bodies and is largely composed of branching apical dendrites of pyramidal neurons. Layer I, the molecular layer, receives excitatory input from other areas of the cortex (Douglas and Martin, 2007), but it has also been shown that a large number of thalamocortical neurons converge there as well (Rubio-Garrido et al., 2009). Layer II and III, the external granular layer and external pyramidal layer respectively; consist of small to medium sized pyramidal neurons that output to layer V/VI. However, the output to layer VI is weak despite layer V/VI being interconnected (Shipp, 2007). Layer IV, the internal granular layer, serves to relay signals to layers II and III and also include some inhibitory granule cells. Layer IV also directly outputs to layer VI, prominently in primary cortices. This IV to VI circuit loop is reasoned to serve as a modulatory loop as it mainly terminates upon inhibitory neurons. However, areas of the brain like the motor cortex are agranular, lacking a layer IV (Shipp, 2007). Layer V, the internal pyramidal layer, is comprised of pyramidal neurons that project to subcortical regions (Jones, 1998). Layer V is the primary output layer of

the entire cortex and is densest in the motor region. This layer outputs to a variety of regions such as the superior colliculus, brainstem oculomotor centers, cerebellum, striatum and the thalamus (Shipp, 2007). Layer VI connects to the thalamus and is an outgoing component of a cortico-thalamo-cortical loop.

Considering that layer V pyramidal neurons serve as the primary output for the brain, this led us to investigate if the pathogenesis of seizure generation after traumatic brain injury could uncover intracellular markers. It has been shown that deep layer cortical neurons initiate spike and wave discharges in seizure models (Polack et al., 2007). Cortical layer V has been suggested as an important pathogenic synchronizing mechanism as well as a contributor to the initiation of epileptiform events (Hoffman et al., 1994). Layer V neurons have shown spontaneous ictal-like epileptiform discharges after controlled cortical impact (CCI) (Yang et al., 2010). Furthermore, acute injury models that have undercut layer V have shown to cause a decrease in synaptic inhibition and an increase in synaptic excitation as a result of reorganization of synaptic circuits (Jin et al., 2011).

Cortical Development

The development of the cortex begins as progenitor cells transfer inside-out along radial glia (Noctor et al., 2001). The first pyramidal neurons migrate out of the ventricular and subventricular zones from the preplate. The preplate will eventually become layer I and the subplate will form a middle layer, or cortical plate, that will go on to develop into layers V and VI. Neurons that come later will migrate radially through the deep layers and become layers II to IV (Rakic, 1988). Pyramidal neurons, the brain's primary excitatory unit, begin to increase in soma size, apical dendrite length, and basal

dendrite length in rats between postnatal day 3 and 21 (Zhang, 2004). GABAergic interneurons serve as the brain's primary inhibitory units. During development, GABA is primarily excitatory because the gradient of chloride is reversed in immature neurons, meaning the reversal potential is higher than the resting membrane potential of the cell (Ben-Ari et al., 2007; Li and Xu, 2008). As a result of GABAergic interneurons maturing faster and the gamma-Aminobutyric acid (GABA) signaling mechanisms occurring earlier than glutamatergic transmission, GABA is the major excitatory neurotransmitter in the brain before the maturation of glutamatergic synapses (Rheims et al., 2009).

Neurons begin to extend their axons and dendrites to proper synaptic partners. As the synapses are constructed and mature within neural circuits, they undergo continuous refinement and reformation. The refinement and pruning period is dependent upon interactive mechanisms and patterned neuronal activity, and in rats occurs during the second and third postnatal week of rats (Katz, 1993; Mrzljak et al., 1990; Shatz, 1990) The pruning and refinement process of axons, dendrites, and synapses begins in late gestation and dramatically increases postnatally (Cowan et al., 1984). Although synaptogenesis differs across brain regions, the sensory and motor cortices experience the most refinement after birth, and regions that handle cognitive functions are done later (Levitt, 2003).

Cortical Interneurons

Interneurons serve as the primary source of inhibition in the cortex and release the inhibitory neurotransmitter GABA. They comprise about 20% of the total cortical neuron population (Markram et al., 2004a; Rudy et al., 2011), with the excitatory population

making up the remaining 80%. GABAergic interneurons play a major role in controlling information flow in the cortex by targeting specific subcellular domains of the principle excitatory neurons and by altering the input and output of neurons (Bacci and Huguenard, 2006). Specifically, GABAergic interneurons to play important roles in controlling the timing of cortical pyramidal neuron firing (Bacci and Huguenard, 2006) , synchronizing network activity (Sohal et al., 2009), and the generation of cortical rhythms (Nakamura et al., 2015). Malfunction of these neurons has been implicated in a number of neurological diseases including epilepsy (Jin et al., 2011) to schizophrenia (Lewis et al., 2012), anxiety disorders and autism (Wöhr et al., 2015).

Cortical interneurons are a diverse group of neurons that have been classified based on anatomy, physiology, and gene expression. In general, approximately 85% of cortical interneurons can be subdivided into three types based upon their expression of the calcium chelators parvalbumin (PV), somatostatin (SST), and the neuropeptide vasoactive intestinal polypeptide (VIP) (Hioki et al., 2013; Nathanson et al., 2009; Rudy et al., 2011; Xu et al., 2010). Within the cortical layers these three groups of interneurons (PV, SST and VIP) are varied in distribution and have distinct functional roles (Markram et al., 2004a). At this time, the presence or absence of the said calcium chelators remains a leading method for distinguishing types of interneurons histologically. VIP neurons are primarily found in upper layers, such as layers II and III. In layers II/III, PV and SST make up almost half of the interneuron population. As the layers descend into layers 4-6 the VIP neurons decrease and the majority (~80%) of neurons are SST and PV positive.

PV neurons are the most abundant of the interneuron subtypes, making up about 40-50% of all cortical interneurons (Markram et al., 2004a; Rudy et al., 2011). PV

expression has been associated with the fast-spiking firing pattern since it was first published in the 1980s (Kawaguchi et al., 1987). There has since been a number of reports and laboratories that have confirmed this correlation between fast-spiking and PV expression (Cauli et al., 1997; Chow et al., 1999; Gibson et al., 1999; Kawaguchi and Kubota, 1997; Petilla Interneuron Nomenclature Group et al., 2008; Xu et al., 2010). There are two types of PV neurons, basket cells and chandelier cells. Basket cells typically make synapses at the soma and proximal dendrites of target neurons and usually have multipolar morphology. Chandelier cells typically target the axon initial segment of pyramidal neurons (Kawaguchi and Kubota, 1997; Petilla Interneuron Nomenclature Group et al., 2008). These FS neurons fire high-frequency spike trains with little to no spike frequency adaptation. When close to firing threshold, they fire abrupt episodes of non-adapting repetitive charges. They also have low input resistance, when mature, and the fastest membrane time constant of all interneurons, a feature that contributes to fast synaptic responses (Cauli et al., 1997; Connors and Gutnick, 1990; Gibson et al., 1999; Goldberg et al., 2008; Kawaguchi and Kubota, 1997; Markram et al., 2004a). PV cells mediate fast and powerful inhibition of target neurons and are involved in mediating feedforward inhibition of cortical circuits, including the thalamocortical input of sensory response. This is important for creating a tight temporal integration window of excitatory inputs and spike generation by pyramidal neurons (Cruikshank et al., 2007; Gabernet et al., 2005; Lawrence and McBain, 2003; Miller et al., 2001; Pinto et al., 2000, 2003; Pouille and Scanziani, 2001). They have also been shown to play an important role in gamma oscillations (Barberis et al., 2007; Nakamura et al., 2015; Traub et al., 2004). Their role in the cortex is vital, as they are likely the key contributors of maintaining

excitatory/inhibitory balance (Haider and McCormick, 2009; Hasenstaub et al., 2005).

Summary

Studies have shown that young children have a 42.5% chance of developing early post-traumatic seizures (EPTS) after TBI. Which is almost double that of adult sufferers (Arndt et al., 2013). Through our research, our goal is to understand what sensitizes the pediatric brain to have a worse outcome following TBI than an adult. Specifically we want to address why children have a greater risk of developing EPTS. This is accompanied by unique sensitivity of PV interneurons to sTBI that has not been reported in adult studies. Also in contrast to adult studies, sTBI in juvenile animals does not raise global excitability but induces discrete changes to cortical inhibition and excitation. Future studies will need to examine how these changes are integrated at a functional network level and may be targeted to reduce the development of adverse outcomes following TBI.

In chapter 2, we study changes in the synaptic and intrinsic properties of layer V pyramidal neurons. We identify that there are no synaptic or intrinsic changes, but we do find that all animals developed epileptic activity within 2 weeks of a severe TBI. This was indicated by presence of epileptic activity on in-vivo EEG as well as the presence of synaptic bursting in-vitro in over 80% of animals that suffered a severe TBI.

In chapter 3, we characterize changes in the inhibitory cortical network in the peri-injury zone. We find that sTBI induces select loss of parvalbumin (PV) expression in this area. PV interneurons are predominantly of a fast-spiking (FS) phenotype. Functionally, it is shown that sTBI disrupts synaptic input onto fast-spiking interneurons as they receive less inhibition and stronger excitation following sTBI.

In chapter 4, we examine that sTBI induces changes to the contralateral motor cortex. Specifically, we determined that sTBI induces a discrete loss of inhibitory interneurons in the pediatric contralateral motor cortex. This work is supported by human studies which examine changes in contralateral motor cortex following TBI (De Beaumont et al., 2007, 2009) . However, these changes may be unique to the pediatric brain as they are not observed in studies in adult animals (Jones et al., 2012; Nishibe et al., 2010). To our knowledge, this is the first work that demonstrates specific loss of interneurons in the contralateral cortex with preferential loss of parvalbumin immunoreactivity. In associated fast-spiking interneurons, sTBI reduces inhibition while enhancing excitation. Furthermore, sTBI alters the kinetic properties of both inhibitory and excitatory synaptic events.

In chapter 5, we examine if the severity of impact plays a role in the observed changes to cortical function. We used a model of repetitive mild traumatic brain injury to further identify changes to the pediatric brain after injury. We identify that there is no change in the synaptic and intrinsic properties of excitatory neurons, but morphological analysis shows cortical thinning and increased ventricle size occurs after repetitive mild injury in pediatric animals.

Overall, this dissertation characterizes unique changes to the pediatric brain. Focusing more on how severe injury alters neuronal populations in the developing cortex, but also how a differing injury model reveals unique changes. This work suggests that pediatric injury is different from adult. To better treat the pediatric population a differential approach is required to ensure effective treatment. This is necessary to improve pediatric recovery and minimize neurological deficits long into adulthood.

CHAPTER 2

SPONTANEOUS SYNAPTIC BURST ACTIVITY IN JUVENILE RATS AFTER CONTROLLED CORTICAL IMPACT

Following a traumatic brain injury 5-50% of patients will develop posttraumatic epilepsy. Pediatric patients are particularly susceptible with the highest incidence of PTE. Currently we cannot prevent the development of PTE and we have a limited understanding of the basic epileptogenic mechanisms that are initiated by TBI. We hypothesize that early on following injury the cortex undergoes distinct cellular and synaptic reorganization that facilitates cortical excitability and promotes the development of seizures. To induce traumatic brain injury, we performed controlled cortical impact (CCI) in juvenile rats (post-natal day 17). Controlled cortical impact has been shown to induce the development of cellular and synaptic changes that are thought to promote increased cortical excitability. In–vivo we performed EEG epidural recordings for 14 days following CCI. All animals initially displayed electrographic seizures that terminated within the first week and were presumed to be injury induced. Following a quiescent period 40% (6 of 15) animals had the reemergence of recurrent electrographic seizures with average event duration of 15.5s. These seizures were primarily "silent" with no overt behavioral seizure phenotype but demonstrated sustained changes in cortical excitability. To further study these changes, we performed in-vitro whole cell patch clamp recording on layer V pyramidal neurons in the peri-injury zone from CCI or sham (craniotomy only) animals. Pyramidal neurons represent the major source of excitatory output from neocortical layer V, a lamina that has been implicated in both acute and chronic models of neocortical epileptogenesis. First we examined for changes

in intrinsic excitability and found no significant difference in input resistance, action potential threshold, firing rate or resting membrane potential. Next, we examined for changes in excitatory synaptic function by recording spontaneous excitatory post-synaptic currents (sEPSCs) and found enhanced excitatory activity suggested by a decrease in the inter-event interval of CCI versus control animals with no change in the amplitude of events. This increased in excitatory activity was not accompanied by a change in inhibitory drive suggesting CCI alters the E-I balance. Specifically, we observed no change in the amplitude or inter-event interval (IEI) of spontaneous inhibitory synaptic currents (sIPSCs). In addition, both excitatory and inhibitory synaptic activity in CCI animals showed the development of distinct burst discharges that were not present in control animals. The results suggest that CCI induces early "silent" seizures that are detectable on EEG and correlate with distinct changes to the synaptic excitability in the cortex. The synaptic changes and development of burst discharges may play an important role in synchronizing the network and promoting the development of PTE.

Introduction

Traumatic brain injury (TBI) is a leading cause of death and disability in children (Faul., et al, 2010) and often leads to the development of post-traumatic epilepsy (PTE) . PTE develops in up to 20% of children and depends on several factors including the severity of injury, age of the patient, and injury site (Appleton and Demellweek, 2002) . The underlying pathophysiology of PTE is poorly understood, but develops in the wake of injury and leads to spontaneous recurrent seizures. Over the long term these post-traumatic seizures (PTS) may cause secondary brain damage through mechanisms including increased metabolic requirements, hypoxia, increased intracranial pressure, and/or excessive release of neurotransmitters (Medelow and Crawford, 1997; Teasdale and Bannan, 1997 and Graham et al., 2006 for review). Exacerbating the clinical management of PTE is that the seizures are often refractory to anti-epileptic drugs (Bauer and Burr, 2001) and are ineffective at reducing the risk of developing PTE (Adelson et al., 2003; Arango et al., 2012; Kochanek et al., 2012). However, evidence suggests that there may be a critical window following TBI for clinical intervention (Graber and Prince, 2004). Development of new therapeutic strategies in children requires an improved understanding of the processes and timing of events that occur early after injury in the genesis stages of PTE.

In humans, PTE develops slowly over months and even years. The slow development of PTE provides a unique temporal window to study and identify the epileptic changes as they occur "on the road" to PTE. We hypothesize that understanding the early changes that occur following TBI may help to define the critical period for intervention and potentially identify unique therapeutic targets. The pediatric brain is in

the midst of neurodevelopment and is undergoing a host of age-dependent physiological changes including synaptogenesis, use-dependent pruning, enhanced glucose metabolism(Chugani et al., 1987), increased neurotrophic factors (Friedman et al., 1991), and increased excitatory amino acid receptors (Insel et al., 1990). These changes may confer unique advantages and disadvantages to the outcome of a TBI event and shape the development of PTE.

Injuries ranging from mild (concussion) to severe penetrating wounds and skull fractures may fall under the broad term of TBI. The incidence of PTE is significantly higher following severe TBI which is effectively modeled in animals by controlled cortical impact (CCI). CCI has been used extensively as a model of head injury (Lighthall et al., 1989; Liu et al., 2013; Mannix et al., 2011) and more recently as an effective means to model severe TBI (Cantu et al., 2014; Hunt et al., 2009)(Yang et al., 2010). Following CCI, studies have shown significant cavitation and neuronal cell loss at the site of injury (Anderson et al., 2005a; Fox et al., 1998; Goodman et al., 1994; Hall et al., 2005a; Smith et al., 1995), hippocampal neurogenesis, and synaptogenesis in the hippocampus (Rola et al., 2006; Scheff et al., 2005). Direct injury induced seizures have been reported to occur within the first 48 hours following CCI (Nilsson et al., 1994) but the development of spontaneous recurrent post-traumatic seizures (PTS) occurs in 12.5 to 36% of animals following a latent period of weeks to months (Statler et al., 2009)(Hunt et al., 2009). In juvenile animals we have previously shown that CCI induces necrotic loss of cortex, damage to the underlying corpus callosum and hippocampus, synaptic reorganization (Card et al., 2005)(Jenkins et al., 2002) and deficits in spatial learning and memory (Adelson et al., 2013). In this study, we examined the underlying mechanisms

that may contribute to cortical hyperexcitability and epileptogenesis in juvenile animals following CCI.

Pyramidal (PYR) neurons are the major source of excitatory output from layer V, a lamina that has been implicated as the site of origin of interictal epileptiform discharge in both acute and chronic models of neocortical epileptogenesis (Hoffman et al., 1994; Prince and Tseng, 1993). A recent preliminary report by Yang and colleagues has shown that CCI performed in juvenile rats rapidly induces spontaneous epileptiform activity and burst firing in layer V cortical pyramidal neurons (Yang et al., 2010). Burst firing is known to increase the fidelity of synaptic information transfer (Izhikevich et al., 2003; Lisman, 1997) and may help to promote epilepsy by facilitating the propagation of local areas of hyperexcitability and synchrony. In the present study we examined the underlying mechanisms that may contribute to the development of epileptiform activity in juvenile rats following CCI. Utilizing electrophysiolgical approaches, we determine that CCI in juvenile rats induces the rapid development of *in-vivo* epileptiform activity and the preferential enhancement of *in-vitro* excitatory pre-synaptic burst discharges. These synaptic bursts occurred in the absence of significant changes in intrinsic excitability of layer V pyramidal neurons and may be driven by altered afferent cortical synaptic input. Our findings suggest that juvenile animals undergo unique pathophysiological changes early after TBI that may be involved in the pathogenesis of PTE.

Materials and Methods

Protocols used for all experiments were approved by the University of Arizona Institutional Animal Care and Use Committee.

CCI Injury

To experimentally model TBI, a controlled cortical impact (CCI) was performed on 29 post-natal day 17 (P17) Sprague-Dawley rats as previously described (Adelson et al., 2013) (Card et al., 2005) (Jenkins et al., 2002). In brief, male Sprague Dawley rats were sedated with isoflurane and injected interperitoneal (IP) with a mixture of ketamine (50mg/kg) and xylazine (5mg/kg) at 0.01mL per 10g of rat weight. Surgery site was shaved and animals were fixed into a stereotaxic frame. A midline scalp incision was then performed to expose the skull and a 6-mm craniotomy over the right somatosensory region was performed. The bone flap from the craniotomy was removed and placed in saline solution. Precaution was taken during the craniotomy to avoid damaging the underlying dura and inducing significant bleeding. A frontoparietal controlled cortical impact (CCI) (5mm tip, 4m/s, 2.0 mm depth) was performed using a pneumatic impactor (Amscien Instruments, Richmond, VA). After the CCI, the bone flap that was removed during the craniotomy was placed over the injury site and secured with dental cement. During this time, electroencephalography (EEG) leads were mounted and also secured with dental cement. The skin was then sutured closed and the incision area swabbed with betadine. Animal temperature was maintained with an electric heating pad and monitored post-surgery until ambulatory (< 3 hours). Following the initial recovery, animals were returned to standard housing and monitored daily. Animals that were to be connected to EEG were given 24 hours post-injury to recover prior to EEG monitoring. All other animals were allowed to recover until further experimentation began on post-injury day (PID) 14.

Seizure Monitoring with Electroencephalograpy (EEG)

Rats subjected to CCI or age-matched controls were implanted with epidural recording electrodes. Experimental evidence indicates craniotomy may induce alterations to the cortex (Cole et al., 2011; Olesen, 1987). As such, we considered the craniotomy a component of the injury process and used appropriate naïve age-matched control animals. Epidural recording electrodes were made from #0-80 x 1/8 inch stainless steel screws at the following stereotaxic co-ordinates: AP: 2.0mm, Lateral: ± 3.0, Depth: 1mm; AP: -4.0mm, Lateral: -3.0mm, Depth: 1mm; AP: -8.0mm, Lateral: +3.0, Depth: 1mm (Fig. 1). After recovery from surgery, animals were placed in acrylic cages where they could move freely and were connected through commutators to the recording system. Animals were singly housed during this period. EEG signals were recorded continuously for 13 days post-injury using an Xltek 128 channel Neurolink IP amplifier (1.0Hz and 70Hz cutoffs, 512Hz sampling rate). Two independent, blinded, and trained personnel analyzed the digital EEG files and their results were compared for consistency and averaged. As previously described, epileptiform activity was defined by the presence of epileptiform discharges or seizure-like events (Ziyatdinova et al., 2011). Epileptiform discharges (ED) were defined by rhythmic transients containing spikes and uniform sharp waves that lasted between 1 and 5 seconds. High-amplitude rhythmic discharges that were clearly distinguishable from background and lasted for greater than 5 seconds have been considered seizures (Horita et al., 1991). As simultaneous behavioral seizure activity was not monitored, this activity has been classified as seizure-like and most likely represents subclinical electrographic seizures.

Preparation and maintenance of brain slices

Coronal brain slices were prepared as previously described (Anderson et al.,

2005b, 2010) from CCI or age-matched control animals. Slices were prepared from the somatosensory cortex beneath the injury site in CCI animals or from corresponding control cortex. Male Sprague-Dawley rats aged 31-35 days (PID 14-19) were deeply anaesthetized with inhalation of isoflurane and decapitated. The brain was rapidly removed and and coronal slices (350um thick) of the somatosensory cortex taken using a vibratome (VT 1200; Leica, Nussloch, Germany). Harvesting of slices was performed beneath the site of CCI or in corresponding control cortex. The site of CCI was readily identifiable in slices as significant cavitation and tissue loss. Initial harvesting was performed in an cold (4°C) carboxygenated (95% O_2, 5% CO_2) high sucrose solution containing the following (in mM): 234 sucrose, 11 glucose, 26 $NaHCO_3$, 2.5 KCl, 1.25 $NaH_2PO_4H_20$, 10 MgS_47H_20, 0.5 $CaCl_22H_20$. Slices were then incubated for 1h at 32°C in carboxygenated artificial CSF (aCSF) containing (in mM): 126 NaCl, 26 $NaHCO_3$, 2.5 KCl, 10 Glucose, 1.25 $Na_2H_2PO_4H_20$, 1 $MgSO_47H_20$, 2 $CaCl_2H_20$, pH 7.4 and then returned to room temperature before being moved to the recording chamber for whole-cell patch clamp recording.

Electrophysiological recording

Slices prepared from CCI or control animals were submerged in flowing carboxygenated aCSF heated to 32°C. Submerged slices were first visualized under 4x brightfield for identification of layer V cortex. For slices from CCI rats, recordings were made in the peri-injury zone within 2 mm of the injury-induced cavitation. Recordings from control slices were made in the recorded in the corresponding cortex. Whole-cell recordings were obtained from regular spiking cortical pyramidal neurons using an upright microscope (Axioexaminer, Carl-Zeiss, Thornwood, NY, USA) fitted with

infrared differential interference contrast optics. Regular spiking (RS) pyramidal neurons were distinguished based on their current-clamp firing behavior (Guatteo et al., 1994). The electrode capacitance and bridge circuit were appropriately adjusted. The series resistance (R_s) of neurons chosen for analysis was less than 20% of membrane input resistance and monitored for stability. Membrane potential was not corrected for a calculated 10 mV liquid junction potential. A Multiclamp 700A patch-clamp amplifier (Axon Instruments, Union City, CA, USA) was used for both current and voltage-clamp mode. Recordings were obtained at 32°C using borosilicate glass microelectrodes (tip resistance, 2.5-3.5 MΩ) filled with intracellular solution (in mM): 135 KGluconate, 4 KCl, 2 NaCl, 10 HEPES, 4 EGTA, 4 Mg ATP, 0.3 Na TRIS for excitatory recording resulting in a calculated ECl- of -16 mV. For recording of inhibitory events, an intracellular solution containing the following was used (in mM): 70 KGluconate, 70 KCl, 2 NaCl, 10 HEPES, 4 EGTA, 4 Mg ATP, 0.3 GTP. This internal solution has been used previously (Anderson et al., 2010)(Sun et al., 2006) and facilitates detection of inhibitory events. The calculated E_{Cl} was approximately −16 mV, resulting in inward $GABA_A$ currents at a holding potential of −70 mV. Inhibitory events were pharmacologically isolated by bath application of 2-Amino-5-phosphonopentanoic acid (d-APV; 50 μm) and 6,7-dinitroquinoxaline-2, 3-dione (DNQX, 20 μm) purchased from Ascent Scientific (Abcam Biochemicals, Cambridge, MA).

Data Analysis

Data was analyzed using pCLAMP (Axon Instruments), Prism (GraphPad) and MiniAnalysis (Synaptosoft) software and are presented as means ± s.e.m. For detection of spontaneous synaptic events automated threshold detection was employed through

MiniAnalysis and detected events were subsequently manually verified. Synaptic bursts events were detected based on previously published characteristics (Prince and Connors, 1986; Prince and Tseng, 1993) and were defined by a minimum of 3 synaptic events occurring in 250 milliseconds that temporally summated. Input resistance was calculated from the voltage response to the input of a current step (1s, 50mV). Adaptation index was calculated as $100 \times (1 - F_{Last}/F_2)$, where F_{Last} corresponds to the firing rate of the last interspike interval and F_2 the second interspike interval. Many of the pyramidal neurons had a high variability in the first interspike interval, so the second interspike interval was chosen for analysis. Intrinsic burst index was calculated as the inter-event interval between the first set of action potentials divided by the second. Statistical significance was tested using an unpaired *t* test and differences were determined to be significant if $P < 0.05$.

Results

To model severe TBI in pediatric patients, we subjected 17-day-old rats to controlled cortical impact (CCI (n=13) and compared them to age-matched controls (n=9). The CCI procedure results in a significant cavity in the cortex at the site of the injury and extensive necrosis (Adelson et al., 2013; Yang et al., 2010). In the weeks and months that follow after CCI, up to 36% of adult animals will develop spontaneous behavioral seizures (Hunt et al., 2009) and over 85% have been shown to develop epileptiform activity (Statler et al., 2009). In humans, PTE develops following a latent period that can last from months to years (Agrawal et al., 2006). At the point in which seizures are clinically identifiable, the underlying neural activity and networks have undergone significant change. We believe this activity begins early after the injury, and

leads to hyperexcitability and subclinical electrographic changes well in advance of PTE. To investigate the changes that occur in juvenile rats early after CCI, we examined for electrophysiological changes and mechanisms that may promote epileptogenesis.

Epileptiform Activity is rapidly induced In-Vivo following Traumatic Brain Injury

To monitor for the development of epileptiform activity, we performed electroencephalograpy (EEG) recordings of CCI animals (n=16) or age-matched controls (n=9). Following recovery from the CCI surgery, EEG activity was continuously recorded for the first two weeks. Epileptiform activity was detected post-recording based on previously published characteristics (Ziyatdinova et al., 2011) and as detailed in the methods. Two trained personnel where blinded to the animal's experimental condition and averages values taken from the independent grading of the EEG recordings. Within the first 24 hours of recording, 87.5% of CCI animals developed epileptiform activity that was absent in control animals. This epileptiform activity was considered to be injury-induced and akin to "early" post-traumatic seizures. Animals had a variable latent period (2-7 days) following this initial early stage, but all CCI animals subsequently developed recurrent epileptiform activity that was synchronized across all EEG leads (Fig. 1). On average, 16.4±3 epileptiform events were detected over the post-latency recording period. In 7 of 16 CCI animals, prolonged seizure-like events were also detected. The development of epileptiform activity within 14 days after CCI, and in advance of PTE, suggests the presence of on-going epileptogenic activity. Post-injury day 14 was chosen for further *in-vitro* experimentation, as it was the earliest time point that all animals reliably displayed *in-vivo* epileptiform activity.

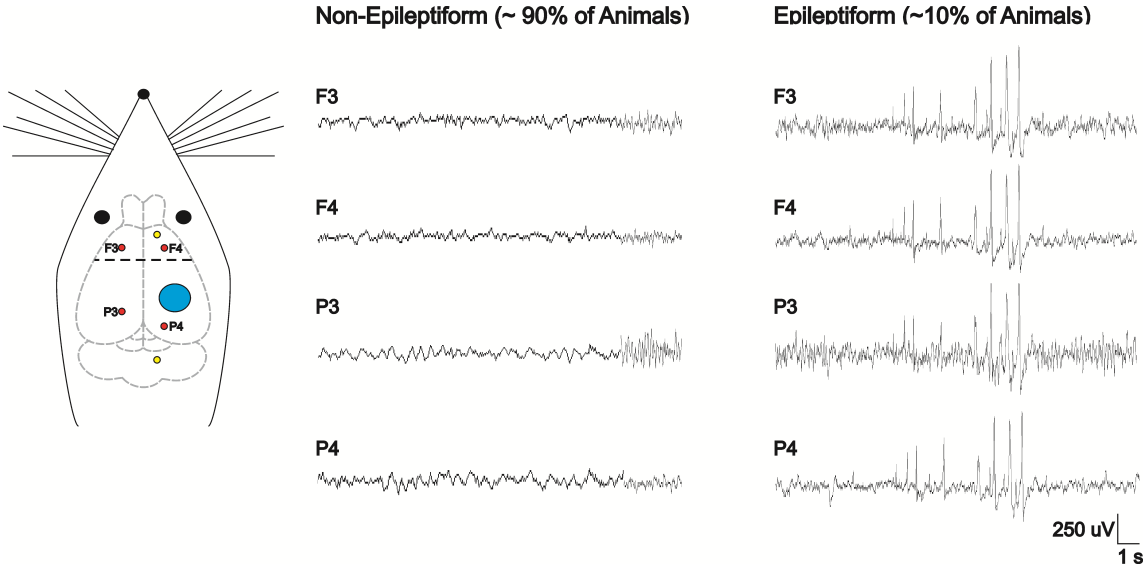

Figure 1. CCI induces epileptiform activity. Left: Schematic representation of rat brain indicating site of CCI injury (blue circle) and EEG recording electrodes (red circles). Middle and Right: Epidural EEG recordings from rats made 14 days after CCI. Middle panel is from a control animal without observable epileptiform activity and right panel from a CCI animal that displayed spontaneous epileptiform discharges.

Epileptiform synaptic bursting is induced in-vitro following TBI

Epileptogenesis has been extensively studied in numerous animal models and is generally thought to occur as the result of disruption to intrinsic excitability, synaptic inhibition and/or synaptic excitation (Prince and Connors, 1986 for review). To investigate the contribution of these mechanisms to CCI induced epileptiform activity, we examined for electrophysiological changes in cortical brain slices. Epileptiform activity detected by EEG was widespread and synchronous within and across cortical hemispheres. Pyramidal neurons in layer V are the major output pathway of the cortex and have been implicated in network synchronization (Telfeian and Connors, 1998). As such, whole-cell patch clamp recordings of physiologically-identified layer V pyramidal neurons were made 14 days after CCI or in age-matched control. All recordings were made in the peri-injury zone (i.e. within 2 mm of injury site) or corresponding control cortex.

Intrinsic Excitability

The intrinsic membrane properties of a neuron have been repeatedly shown to be altered in various models of epilepsy (Willmore, 1990; Yang et al., 2007). Neurons that are predisposed or have pathological enhancements to intrinsic excitability may be spontaneous generators of epileptic activity. To examine this possibility, we first recorded for changes in the intrinsic membrane properties from CCI and control pyramidal neurons. Recording under current-clamp, we found no statistical difference between control and CCI resting membrane potential (-67.5 ±1.0 mV (control); -67.7±0.9 mV (CCI), $P<0.92$) and input resistance (198.5 ±16.1 MΩ (control); 192.3 ±12.9 MΩ (CCI), $P<0.76$). Next, we evaluated the firing-current (f-I) relationship in control and

CCI animals. A series of current steps (-150pA to 300pa, 50pA steps, 1 second) were injected through the patch pipette and the membrane voltage response was recorded (Fig 2A). We examined for changes in the firing frequency and adaptation index but found no statistical difference (Fig 2B). Finally, using a rheobase protocol (50 msec, 5 pA steps) we examined for changes in membrane excitability. We found no statistical difference in rheobase current or action potential properties (threshold, amplitude, and half-width)(Fig 3). Overall, these results suggest that changes in the intrinsic membrane excitability of layer V pyramidal neurons do not significantly contribute to the early development of epileptiform activity following CCI.

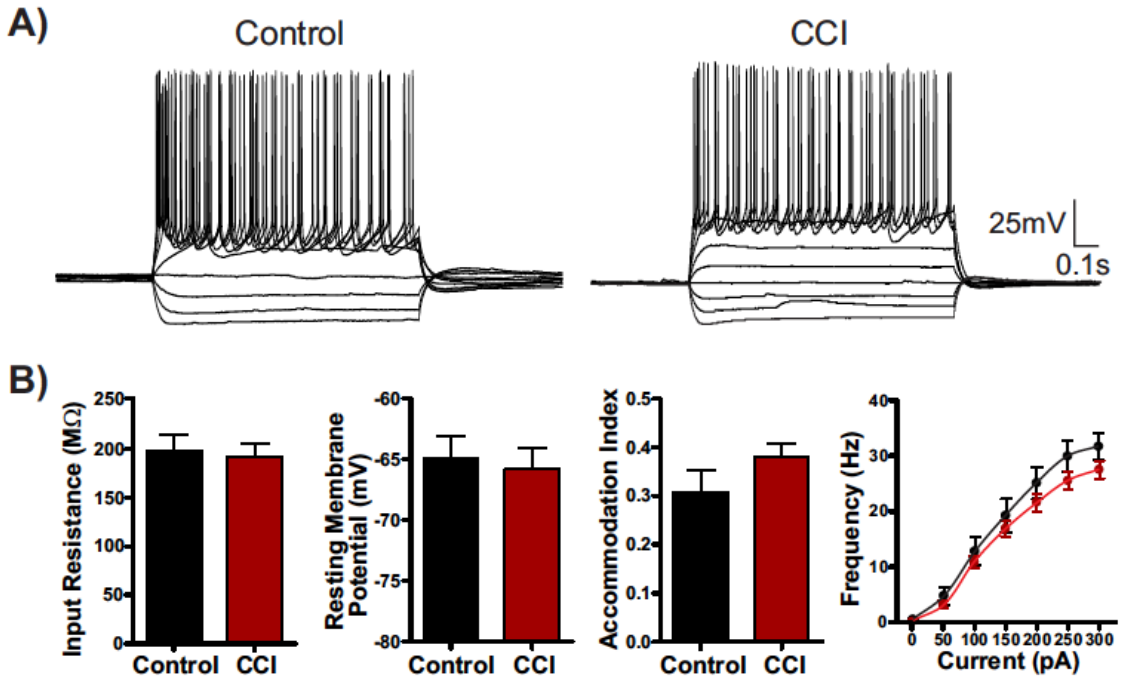

Figure 2. Intrinsic excitability is not altered by CCI. A) Current Clamp recordings in response to intracellular current steps (-150pA to 250pA, 1s) in pyramidal neurons from control or CCI injured animals. Note the similarity in the intrinsic cellular response. B) Bar charts of average response values of various intrinsic membrane properties from (control n=14, CCI n=41). n=38)n=38).n=38).animals (n=41).

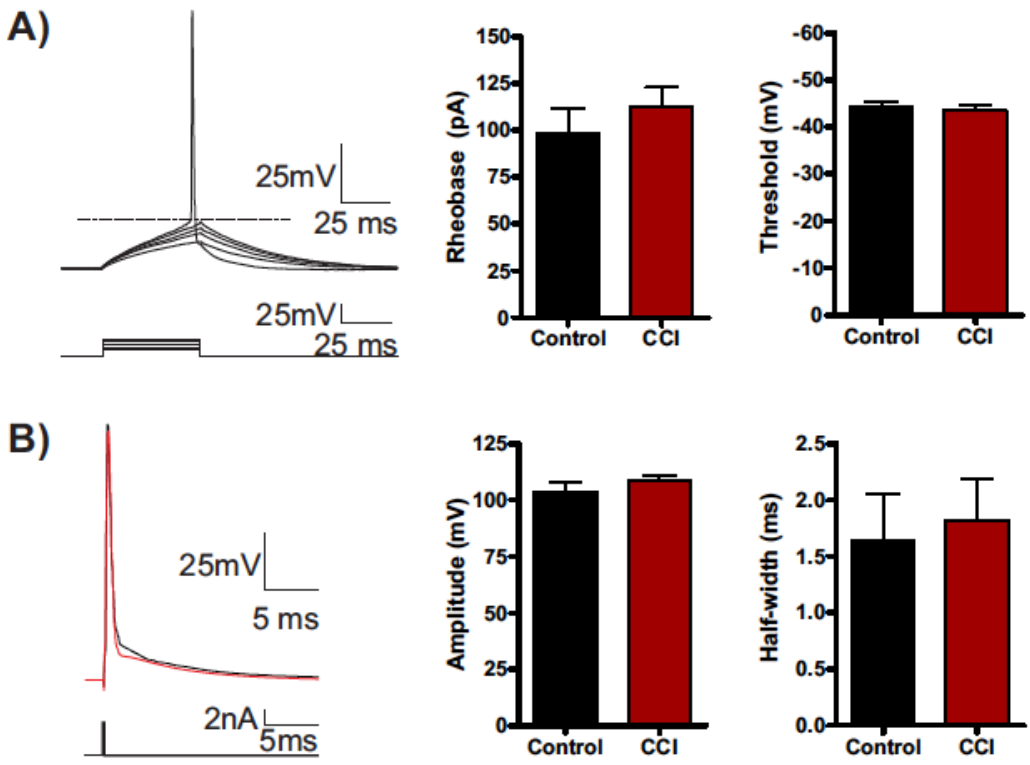

Figure 3. Action Potential Firing is not altered by CCI. A) Reprentative whole-cell current clamp recording in response to a series of 50msec injection (5pA steps). Bar charts of the average values for control or CCI. Rheobase was calculated as the minimum current which produced an action potential. Threshold was measured at the greatest change in calculated slope. B) Current clamp single action potential step (2nA, 0.5ms) was injected to measure action potential properties.

Spontaneous Synaptic Activity

The generation of epileptiform activity and seizures is thought to occur through altered network activity and increased neuronal recruitment that may involve changes to synaptic properties and efficacy (Prince and Connors, 1986 for review). We tested this possibility by examining post-synaptic currents received by layer V pyramidal neurons.

Excitation

First, under voltage clamp (V_{hold}=-70mV) we examined for changes in spontaneous post-synaptic currents. For these experiments pharmacological isolation of excitatory glutamatergic post-synaptic currents (ePSCs) was not possible as GABA antagonists are known to disinhibit the slice and promote epileptiform activity and thereby mask CCI induced changes. To minimize the detection of inhibitory events, neurons were held near and positive of the reversal potential of chloride (V_{hold} = -70mV, calculated E_{Cl^-} = -16mV). This allowed detection of only excitatory positive-directed (inward current) events in isolation from any small inhibitory outward events. First, we examined for changes in the inter-event interval (i.e. frequency) of excitatory sPSCs and found no statistical difference between control (295.6 ± 42.9 ms) and CCI (243.2 ± 26.7)(P=0.28) Similarly we found no statistical difference between control and CCI in the amplitude of excitatory sPSCs (16.8 ± 1.2 pA (control) vs 17.4 ± 1.4 pA (CCI), charge transfer (69.5 ± 7.0 fC (control) vs 73.1 ± 5.4 fC (CCI)(P=0.70) or decay (3.6 ± 0.2 ms (control) vs 3.5 ± 0.2 ms)(CCI)(P=0.77)(Fig 4). The data suggest that CCI does not alter overall excitatory synaptic activity.

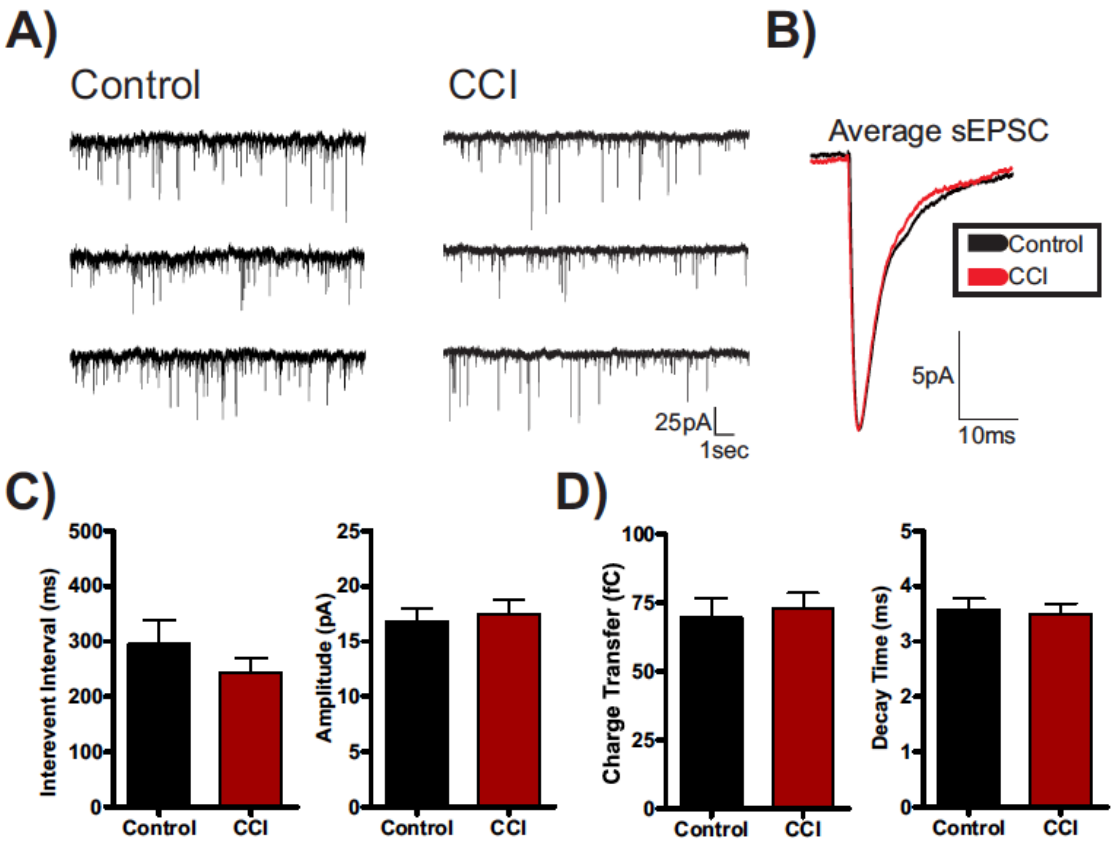

Figure 4. CCI fails to alter excitatory post-synaptic currents. A) Voltage clamp recordings of spontaneous post-synaptic current (sPSC) in control or CCI injured animals. B) Overylayed and amplitude scaled average sPSC recorded from either control (black) or CCI (red) animals. C & D) Average sPSC properties are plotted for control (n=13) or CCI (n=38). Vhold = -70mV.

Inhibition

Second, to directly examine for changes in inhibition we recorded spontaneous inhibitory post-synaptic currents (sIPSCs) that were pharmacologically isolated by bath application of d-AP-V (50uM) and DNQX (20uM). We also utilized a modified internal patch solution with an elevated chloride concentration. This internal has been extensively used(Anderson et al., 2010)(Bacci and Huguenard, 2006) and increases the signal to noise and detection fidelity of inhibitory synaptic events. Voltage clamp recordings were made at -70mV from CCI or control animals. We found no significant change in amplitude (24.6 ± 2.4 pA (control) vs 24.9 ± 3.3 pA (CCI)(P=0.95) or inter-event interval (385.1 ± 85.9 ms (control) vs 328.2 ± 50.4 ms (CCI)(P=0.55). However in contrast to excitatory synaptic activity, a significant increase in the decay time of inhibitory sIPSCs was observed (5.2 ± 0.56 ms (control) vs 7.5 ± 0.70 ms (CCI))(P<0.03)(Fig 5). A similar trend was observed in the charge transfer but it failed to reach statistical significance area (126.1 ± 17.6 fC (control); 185.1 ± 28.2 fC (CCI), P=0.15)(Figure 5B). The net effect of these changes would be to increase the efficacy of inhibition following CCI by increasing the temporal window over which inhibition acts.

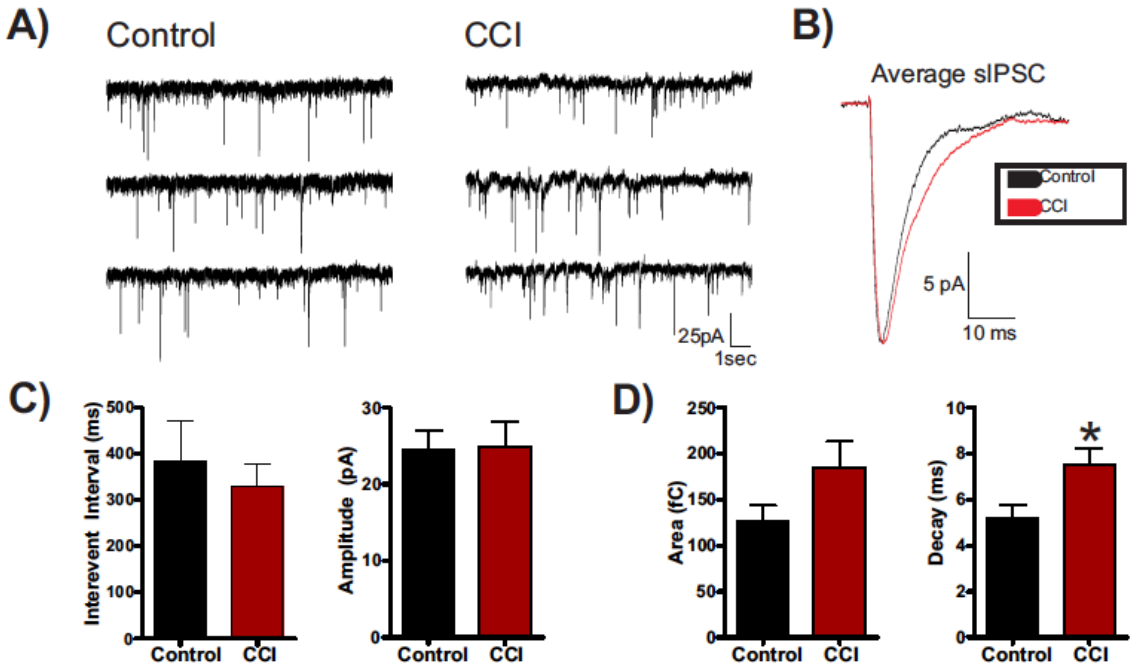

Figure 5. CCI increases inhibitory synaptic decay. A) Voltage clamp recordings of spontaneous inhibiotry post-synaptic current (sIPSC) in control or CCI injured animals. For inhibitory recording glutamate receptor antagonists (APV/DNQX or kynurenate) were applied. B) Overlayed and amplitude scaled average sIPSC recorded from either control (black) or CCI (red) animals. C & D) Average sIPSC properties for control (n=9) or CCI (n=16). Vhold = -70mV. * P<0.05.

Synaptic Burst Discharges

Excitatory burst discharges are thought to increase synaptic efficacy by increasing the probability of inducing the post-synaptic cell to fire an action potential. In our initial experiments, we examined the average sPSC properties and found that CCI had no impact on the average excitatory synaptic activity. However, during recording we observed distinct spontaneous synaptic burst discharges that resembled the epileptiform activity observed *in-vivo*. Based on previous reports detection of synaptic bursts was determined by the presence of a minimum of three simultaneous sPSCs within 250 ms that did not return to baseline. These detection parameters were highly sensitive and allowed for detection of a small number of synaptic bursts in control animals. Overall, the presence of excitatory burst discharges were significantly greater following CCI as 79.5% of recorded CCI neurons displayed synaptic bursting compared to 23.1% of control. However, the average number of synaptic bursts detected in a CCI animal (avg. of 7.7 ± 2) during a single recording session were dramatically increased over control (avg. of 0.38 ± 0.2) ($P<0.04$). The average excitatory sPSC burst in CCI animals consisted of 5.9 ±1 synaptic events and lasted on average for 858.0 ± 240 milliseconds (Fig 6). Bath application of 1um tetrodoxin (TTX) eliminated excitatory burst discharges (n=4). On the inhibitory side, similar burst discharges were observed in 75% of CCI neurons compared with 22% in control. However, the average number of sIPSC bursts in CCI (3.6 ± 1.1 neurons remained significantly increased over control (0.6 + 0.4). The average inhibitory sIPSC burst in CCI animals consisted of 11.4 ± 2.6 synaptic events with duration of 431.0 ± 71 milliseconds (Fig 7). Overall, following CCI, there was a significant increase in excitatory and inhibitory burst discharges. In comparison, CCI

induced greater excitatory bursting than inhibitory bursting by both frequency of total neurons bursting, and average number of burst per neuron. This suggests CCI induced synaptic bursting may be preferentially increasing excitatory synaptic coupling.

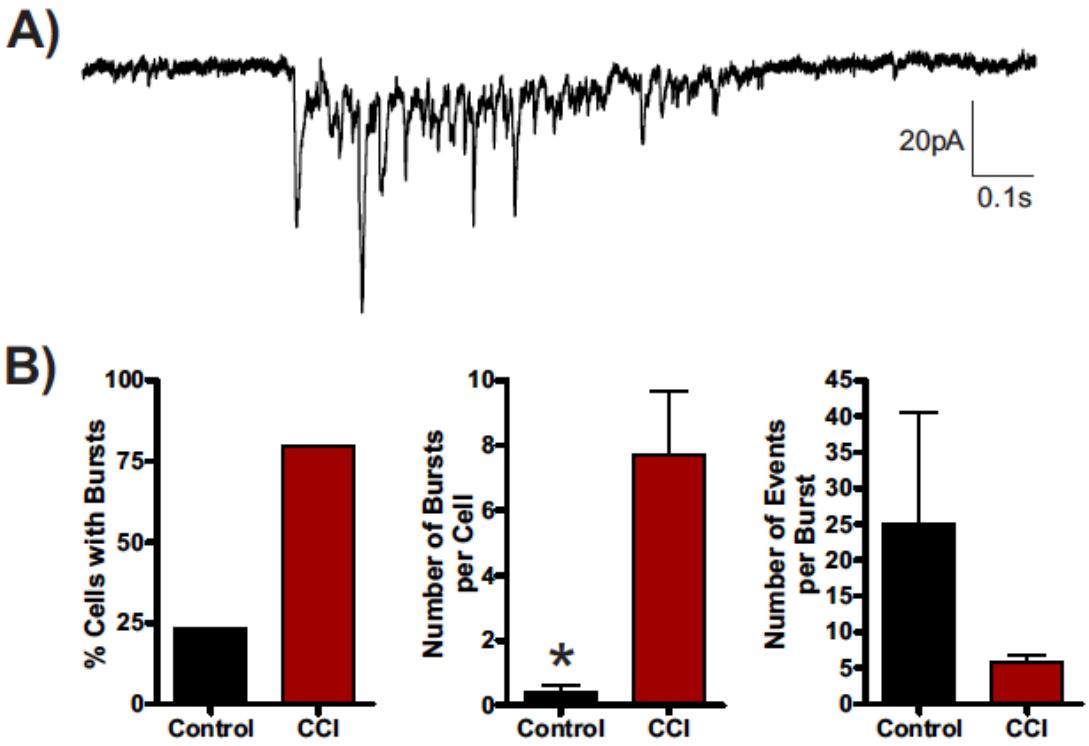

Figure 6. Excitatory Synaptic Bursts are Induced by CCI. A) Voltage clamp recording of spontaneous excitatory burst discharge observed in a CCI animal with an epileptiform EEG. Note the burst is comprised of compound sPSC and resembles paroxysmal discharges observed in epileptic animals. B) Bar charts of average values of various burst properties (control = 13, CCI = 38). *P<0.05.

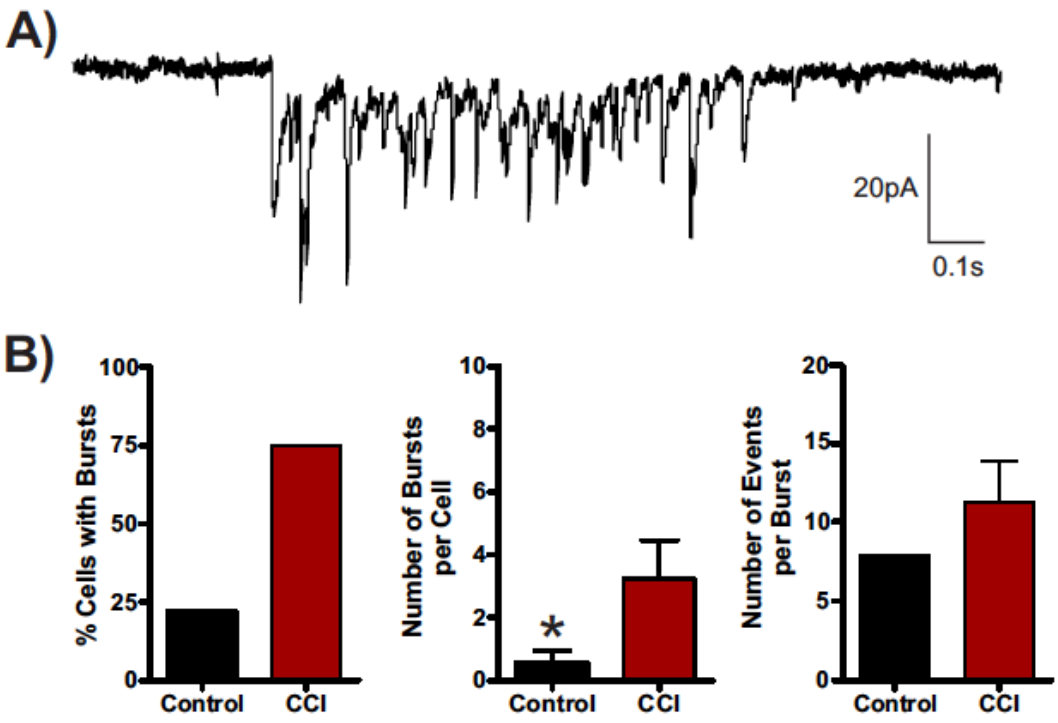

Figure 7. Inhibitory Synaptic Bursts are Induced by CCI. A) Voltage clamp recording of spontaneous inhibitory burst discharge observed in a CCI animal with an epileptiform EEG. For inhibitory recording glutamate receptor antagonists (APV/DNQX or kynurenate) were applied. Note the burst is comprised of compound sIPSC and resembles epileptiform discharges observed in epileptic animals. B) Bar charts of average values of various burst properties (control (n=9), CCI(n =16).

Discussion

This study was undertaken to better understand the early changes to cortical excitability induced by traumatic brain injury and to gain insight into how they may facilitate the development of post-traumatic epilepsy (PTE). Controlled cortical impact (CCI) in rodents has been effectively used to model traumatic brain injury (TBI)(Bolkvadze and Pitkänen, 2012; Cantu et al., 2014; Hunt et al., 2009). However, these studies have primarily focused on CCI performed in adult animals. The outcome, incidence and clinical management of TBI in children differ significantly from adults. In this study, we examined the development of epileptiform activity and the underlying pathophysiology that occurs in juvenile (PND 17) rats following CCI. The results of this study suggest that within 14 days of CCI injury epileptiform activity is induced that can be detected *in-vivo* by EEG as synchronous discharges across multiple cortical regions. At a cellular and synaptic level this epileptiform activity was accompanied by a lack of change in intrinsic membrane properties but a 44% increase in the decay of inhibitory synaptic input onto layer V pyramidal neurons. In addition, spontaneous epileptiform bursting was observed in both excitatory and inhibitory synaptic recordings. Synaptic bursting is thought to enhance synaptic coupling between neurons and may promote PTE through enhanced hyperexcitability and network synchrony.

Development of Epileptiform Activity Following CCI in Juvenile Rats

The hallmark of PTE is the development of spontaneous recurrent seizures. In humans, these seizures develop after several months to years following the initial injury(Agrawal et al., 2006). The progressive development of PTE suggests an evolving process that may begin early after injury. To directly examine the development of

epileptiform activity early after injury we performed continuous EEG for the first 14 days post-injury. Epileptiform activity and electrographic seizures were observed in 87.5% of animals within the first 24 hours after CCI. These early seizures are thought to be injury induced and may be separate from the underlying epileptogenic processes that lead to PTE. However, children are also more prone to developing early seizures and the prevalence and contribution of these early seizures to development of PTE in pediatric TBI remains to be determined. Following a variable latent period all CCI animals proceeded to develop spontaneous recurrent epileptiform activity by 14 days post-injury. This activity was primarily characterized by high-amplitude rhythmic discharges that were routinely synchronized across all 4 cortical EEG leads. This activity resembles epileptiform discharges and inter-ictal spiking that has been previously shown in other epileptic animal models (Hunt et al., 2013). This epileptiform activity and late seizures that develop after the first week of injury are positive predictors of PTE (Frey, 2003 for review). Furthermore, the presence of similar inter-ictal EEG abnormalities are strong predictors of disease severity and outcome (Ramantani, 2013). Further work recording EEG continuously for several months will be required to determine the prognostic value of the observed early epileptiform activity. To our knowledge, no other study has examined the development of early EEG changes after injury during the time period as animals transition from these presumed injury induced seizures to the development of the first recurrent spontaneous epileptiform activity. The study of PTE is

complicated by the presence of multiple injury, repair and adaptive processed initiated by

the TBI – only a portion of which are presumed to be epileptogenic. Examination of animals early after injury has a potential reductionist advantage while determining early pathophysiological changes that may define a critical window or targets for therapeutic intervention. We have now validated that 14 days after injury is the earliest time point after CCI where animals reliably display *in-vivo* and *in-vitro* epileptiform activity.

Epileptogenesis has been extensively studied in numerous animal models and may result from a variety of mechanisms. While no common epileptogenic mechanism has been found a combination of disruption to intrinsic cellular properties, synaptic inhibition and/or synaptic excitation has been frequently reported(Prince and Connors, 1986 for review). Recently, a preliminary report by Yang and colleagues has indicated the development of hyperexcitability and spontaneous epileptiform activity following CCI in juvenile animals(Yang et al., 2010). We extend these findings here to examine the underlying mechanism and determine the impact of CCI on known intrinsic and synaptic changes that are thought to be epileptogenic. Overall our results indicate that CCI fails to alter intrinsic membrane properties, neuronal firing or average excitatory synaptic activity while promoting burst discharges and enhanced inhibitory synaptic decay. Specifically, the intrinsic excitability of a neuron is determined in large part by its membrane properties and ion channels and enhanced intrinsic excitability may be epileptogenic. However, following CCI in juvenile animals layer V pyramidal neurons displayed no change in intrinsic excitability. This included resting membrane potential, input resistance, action potential threshold and rheobase. Similarly, there was no change in the firing properties (frequency or accommodation), input-output relationship (f-I curve) or single action potential waveform. Together these results suggest that alterations

to intrinsic excitability do not significantly contribute to the observed development of epileptiform activity following CCI.

At a synaptic level, our results indicate that overall excitatory synaptic input onto layer V pyramidal neurons was not altered. There was no change in the amplitude, inter-event interval or kinetics of excitatory spontaneous post-synaptic currents. Regulatory control over spontaneous synaptic activity is complex, but in general changes to amplitude and kinetics occur as a result of changes to the pre- or post-synaptic neuron including mechanisms such as quantal content or receptor subunit composition. Altered inter-event interval is thought to reflect changes to the pre-synaptic neuron (e.g. probability of release). The lack of change in sPSCs after CCI suggests that altered excitatory synaptic activity is not driving the development of epileptiform activity. In examining inhibition in the cortex, we similarly found no change in the amplitude or inter-event interval of spontaneous inhibitory post-synaptic currents. However, the decay of inhibitory responses was significantly increased following CCI. Alterations to the time course of synaptic GABAergic events will have a profound effect on the excitability of individual neurons and networks by altering the temporal integration window, the time over which a GABAergic event may reduce a coincident excitatory event. Our finding of an increase in sIPSC decay is consistent with increases observed in other models of epilepsy(Calcagnotto et al., 2005). The time course of inhibitory events is determined by both pre and post-synaptic factors including expression of synaptic GABA transporters, synchrony of GABA release and subunit composition(Overstreet and Westbrook, 2003; Keros and Hablitz, 2005; Barberis et al., 2007). In general, an increase in synaptic decay is predicted to counteract the observed hyperexcitability but may also be impacted by

neural trauma induced changes in the chloride reversal potential(van den Pol et al., 1996). Altered intracellular chloride may also impact the kinetics of chloride dependent GABAergic inhibition(Houston et al., 2009) and would be in line with the observed CCI induced changes. Determining the role of increased synaptic decay in promoting or resisting epileptic changes following CCI remains an open question.

Development of synaptic bursting following CCI in juvenile rats

The development of epilepsy is commonly associated with the synchronous discharge of cortical neurons. Excitatory burst discharges are thought to increase synaptic coupling by increasing the probability of inducing the post-synaptic cell to fire an action potential. In this study we have identified unique epileptiform burst discharges following CCI in the absence of changes to intrinsic membrane, firing properties or global changes in excitatory synaptic currents. Taken together it suggests that layer V pyramidal neurons are not the initiator of the epileptiform discharges but are driven by afferent input. As no changes were observed in excitatory synaptic IEI it suggests the synaptic bursting is not due to altered pre-synaptic probability of release. As the bursts were sensitive to blockade with TTX it suggests they are being driven by action potential dependent afferent input. How the bursts directly impact synaptic coupling and the output of layer V pyramidal neurons remains to be determined. As synchronous spontaneous epileptiform activity was observed on EEG across cortical regions and hemispheres (Fig 1) it suggests network recruitment and widespread propagation of the epileptic activity. Layer V pyramidal neurons receives input from all other cortical layers as well as from thalamus and are implicated in synchronization of cortical activity(Peters and Jones, 1984; Telfeian and Connors, 1998; Wise, 1975). The increase in excitatory

burst discharges may therefore promote epileptiform activity by increasing the excitability of layer V pyramidal neurons that are perfectly placed to increase cortical output and network synchrony. Determining if the epileptiform activity is specific to layer V pyramidal neurons, the location of the afferent driver of the epileptiform activity and the specific contribution of layer V changes to in-vivo epileptiform activity are areas of current investigation.

In addition to excitatory bursting, distinct inhibitory bursting was similarly observed. To isolate inhibitory synaptic currents we routinely blocked glutamatergic neurotransmission with bath application of APV and DNQX. As inhibitory bursting persisted in the presence of glutamatergic blockade this suggests inhibitory bursting is not mediated by afferent glutamatergic input. This appears is in contrast to our findings on excitatory bursting and may reflect intrinsic excitability changes and spontaneous burst discharges form inhibitory interneurons themselves. Inhibitory interneurons in the cortex are a diverse group of neurons that have distinct anatomical, morphological and cellular properties(Markram et al., 2004a). Based upon our results we cannot ascertain if changes to inhibition are confined to one class of interneuron and future work will be needed to determine its specific role in mediating CCI induced epileptiform activity and PTE.

Pediatric Traumatic Brain Injury

Traumatic brain injury that occurs in children differs from adults with a decreased mortality rate(Luerssen et al., 1988b), increased incidence of skull fractures and epidural hematomas (Sarkar et al., 2014) and greater deficits in cognitive and behavioral functioning(Anderson et al., 2005c; McKinlay et al., 2002). In this study we have begun examining if the pathophysiology of TBI in children V pyramidal neurons. The

development of epileptiform activity early after injury may be the first step “on the road” to PTE. Understanding how TBI alters cortical excitability early after injury may help define therapeutic targets and a critical window of intervention.

References

Abdul-Muneer, P.M., Schuetz, H., Wang, F., Skotak, M., Jones, J., Gorantla, S., Zimmerman, M.C., Chandra, N., and Haorah, J. (2013). Induction of oxidative and nitrosative damage leads to cerebrovascular inflammation in an animal model of mild traumatic brain injury induced by primary blast. Free Radic. Biol. Med. *60*, 282–291.

Adelson, P.D. (1999). Animal models of traumatic brain injury in the immature: a review. Exp. Toxicol. Pathol. Off. J. Ges. Für Toxikol. Pathol. *51*, 130–136.

Adelson, P.D., Bratton, S.L., Carney, N.A., Chesnut, R.M., du Coudray, H.E.M., Goldstein, B., Kochanek, P.M., Miller, H.C., Partington, M.P., Selden, N.R., et al. (2003). Guidelines for the acute medical management of severe traumatic brain injury in infants, children, and adolescents. Chapter 19. The role of anti-seizure prophylaxis following severe pediatric traumatic brain injury. Pediatr. Crit. Care Med. J. Soc. Crit. Care Med. World Fed. Pediatr. Intensive Crit. Care Soc. *4*, S72–S75.

Adelson, P.D., Fellows-Mayle, W., Kochanek, P.M., and Dixon, C.E. (2013). Morris water maze function and histologic characterization of two age-at-injury experimental models of controlled cortical impact in the immature rat. Childs Nerv. Syst. ChNS Off. J. Int. Soc. Pediatr. Neurosurg. *29*, 43–53.

Agrawal, A., Timothy, J., Pandit, L., and Manju, M. (2006). Post-traumatic epilepsy: an overview. Clin. Neurol. Neurosurg. *108*, 433–439.

Almeida-Suhett, C.P., Prager, E.M., Pidoplichko, V., Figueiredo, T.H., Marini, A.M., Li, Z., Eiden, L.E., and Braga, M.F.M. (2015). GABAergic interneuronal loss and reduced inhibitory synaptic transmission in the hippocampal CA1 region after mild traumatic brain injury. Exp. Neurol. *273*, 11–23.

Andersen, S.L. (2003). Trajectories of brain development: point of vulnerability or window of opportunity? Neurosci. Biobehav. Rev. *27*, 3–18.

Anderson, V., and Moore, C. (1995). Age at injury as a predictor of outcome following pediatric head injury: A longitudinal perspective. Child Neuropsychol. *1*, 187–202.

Anderson, K.J., Miller, K.M., Fugaccia, I., and Scheff, S.W. (2005a). Regional distribution of Fluoro-Jade B staining in the hippocampus following traumatic brain injury. Exp. Neurol. *193*, 125–130.

Anderson, T.R., Jarvis, C.R., Biedermann, A.J., Molnar, C., and Andrew, R.D. (2005b). Blocking the anoxic depolarization protects without functional compromise following simulated stroke in cortical brain slices. J. Neurophysiol. *93*, 963–979.

Anderson, T.R., Huguenard, J.R., and Prince, D.A. (2010). Differential effects of Na+-K+ ATPase blockade on cortical layer V neurons. J. Physiol. *588*, 4401–4414.

Anderson, V., Catroppa, C., Morse, S., Haritou, F., and Rosenfeld, J. (2005c). Functional plasticity or vulnerability after early brain injury? Pediatrics *116*, 1374–1382.

Annegers, J.F., Hauser, W.A., Coan, S.P., and Rocca, W.A. (1998). A population-based study of seizures after traumatic brain injuries. N. Engl. J. Med. *338*, 20–24.

Appleton, R.E., and Demellweek, C. (2002). Post-traumatic epilepsy in children requiring inpatient rehabilitation following head injury. J. Neurol. Neurosurg. Psychiatry *72*, 669–672.

Arango, J.I., Deibert, C.P., Brown, D., Bell, M., Dvorchik, I., and Adelson, P.D. (2012). Posttraumatic seizures in children with severe traumatic brain injury. Childs Nerv. Syst. ChNS Off. J. Int. Soc. Pediatr. Neurosurg. *28*, 1925–1929.

Atallah, B.V., Bruns, W., Carandini, M., and Scanziani, M. (2012). Parvalbumin-Expressing Interneurons Linearly Transform Cortical Responses to Visual Stimuli. Neuron *73*, 159.

Axelson, H.W., Winkler, T., Flygt, J., Djupsjö, A., Hånell, A., and Marklund, N. (2013). Plasticity of the contralateral motor cortex following focal traumatic brain injury in the rat. Restor. Neurol. Neurosci. *31*, 73–85.

Bacci, A., and Huguenard, J.R. (2006). Enhancement of spike-timing precision by autaptic transmission in neocortical inhibitory interneurons. Neuron *49*, 119–130.

Balan, I.S., Saladino, A.J., Aarabi, B., Castellani, R.J., Wade, C., Stein, D.M., Eisenberg, H.M., Chen, H.H., and Fiskum, G. (2013). Cellular alterations in human traumatic brain injury: changes in mitochondrial morphology reflect regional levels of injury severity. J. Neurotrauma *30*, 367–381.

Barberis, A., Mozrzymas, J.W., Ortinski, P.I., and Vicini, S. (2007). Desensitization and binding properties determine distinct alpha1beta2gamma2 and alpha3beta2gamma2 GABA(A) receptor-channel kinetic behavior. Eur. J. Neurosci. *25*, 2726–2740.

Barlow, K.M., Spowart, J.J., and Minns, R.A. (2000). Early posttraumatic seizures in non-accidental head injury: relation to outcome. Dev. Med. Child Neurol. *42*, 591–594.

Bauer, J., and Burr, W. (2001). Course of chronic focal epilepsy resistant to anticonvulsant treatment. Seizure J. Br. Epilepsy Assoc. *10*, 239–246.

Behrens, M.M., and Sejnowski, T.J. (2009). Does schizophrenia arise from oxidative dysregulation of parvalbumin-interneurons in the developing cortex? Neuropharmacology *57*, 193–200.

Behrens, M.M., Ali, S.S., Dao, D.N., Lucero, J., Shekhtman, G., Quick, K.L., and Dugan, L.L. (2007). Ketamine-Induced Loss of Phenotype of Fast-Spiking Interneurons Is Mediated by NADPH-Oxidase. Science *318*, 1645–1647.

Ben-Ari, Y., Gaiarsa, J.-L., Tyzio, R., and Khazipov, R. (2007). GABA: a pioneer transmitter that excites immature neurons and generates primitive oscillations. Physiol. Rev. *87*, 1215–1284.

Biernaskie, J., and Corbett, D. (2001). Enriched rehabilitative training promotes improved forelimb motor function and enhanced dendritic growth after focal ischemic injury. J. Neurosci. Off. J. Soc. Neurosci. *21*, 5272–5280.

Biernaskie, J., Szymanska, A., Windle, V., and Corbett, D. (2005). Bi-hemispheric contribution to functional motor recovery of the affected forelimb following focal ischemic brain injury in rats. Eur. J. Neurosci. *21*, 989–999.

Bolkvadze, T., and Pitkänen, A. (2012). Development of post-traumatic epilepsy after controlled cortical impact and lateral fluid-percussion-induced brain injury in the mouse. J. Neurotrauma *29*, 789–812.

Brody, D.L., Mac Donald, C., Kessens, C.C., Yuede, C., Parsadanian, M., Spinner, M., Kim, E., Schwetye, K.E., Holtzman, D.M., and Bayly, P.V. (2007). Electromagnetic controlled cortical impact device for precise, graded experimental traumatic brain injury. J. Neurotrauma *24*, 657–673.

Buriticá, E., Villamil, L., Guzmán, F., Escobar, M.I., García-Cairasco, N., and Pimienta, H.J. (2009). Changes in calcium-binding protein expression in human cortical contusion tissue. J. Neurotrauma *26*, 2145–2155.

Cabungcal, J.-H., Steullet, P., Morishita, H., Kraftsik, R., Cuenod, M., Hensch, T.K., and Do, K.Q. (2013a). Perineuronal nets protect fast-spiking interneurons against oxidative stress. Proc. Natl. Acad. Sci. U. S. A. *110*, 9130–9135.

Cabungcal, J.-H., Steullet, P., Kraftsik, R., Cuenod, M., and Do, K.Q. (2013b). Early-life insults impair parvalbumin interneurons via oxidative stress: reversal by N-acetylcysteine. Biol. Psychiatry *73*, 574–582.

Caillard, O., Moreno, H., Schwaller, B., Llano, I., Celio, M.R., and Marty, A. (2000). Role of the calcium-binding protein parvalbumin in short-term synaptic plasticity. Proc. Natl. Acad. Sci. U. S. A. *97*, 13372–13377.

Calcagnotto, M.E., Paredes, M.F., Tihan, T., Barbaro, N.M., and Baraban, S.C. (2005). Dysfunction of synaptic inhibition in epilepsy associated with focal cortical dysplasia. J. Neurosci. Off. J. Soc. Neurosci. *25*, 9649–9657.

Camfield, P.R., and Camfield, C.S. (2014). What Happens to Children With Epilepsy When They Become Adults? Some Facts and Opinions. Pediatr. Neurol.

Cantu, D., Walker, K., Andresen, L., Taylor-Weiner, A., Hampton, D., Tesco, G., and Dulla, C.G. (2014). Traumatic Brain Injury Increases Cortical Glutamate Network

Activity by Compromising GABAergic Control. Cereb. Cortex N. Y. N 1991.

Cao, Y., Vikingstad, E.M., Huttenlocher, P.R., Towle, V.L., and Levin, D.N. (1994). Functional magnetic resonance studies of the reorganization of the human hand sensorimotor area after unilateral brain injury in the perinatal period. Proc. Natl. Acad. Sci. U. S. A. *91*, 9612–9616.

Card, J.P., Santone, D.J., Gluhovsky, M.Y., and Adelson, P.D. (2005). Plastic reorganization of hippocampal and neocortical circuitry in experimental traumatic brain injury in the immature rat. J. Neurotrauma *22*, 989–1002.

Casella, E.M., Thomas, T.C., Vanino, D.L., Fellows-Mayle, W., Lifshitz, J., Card, J.P., and Adelson, P.D. (2014). Traumatic brain injury alters long-term hippocampal neuron morphology in juvenile, but not immature, rats. Childs Nerv. Syst. *30*, 1333–1342.

Cauli, B., Audinat, E., Lambolez, B., Angulo, M.C., Ropert, N., Tsuzuki, K., Hestrin, S., and Rossier, J. (1997). Molecular and physiological diversity of cortical nonpyramidal cells. J. Neurosci. Off. J. Soc. Neurosci. *17*, 3894–3906.

Caveness, W.F., Meirowsky, A.M., Rish, B.L., Mohr, J.P., Kistler, J.P., Dillon, J.D., and Weiss, G.H. (1979). The nature of posttraumatic epilepsy. J. Neurosurg. *50*, 545–553.

Chen, P., Goldberg, D.E., Kolb, B., Lanser, M., and Benowitz, L.I. (2002). Inosine induces axonal rewiring and improves behavioral outcome after stroke. Proc. Natl. Acad. Sci. U. S. A. *99*, 9031–9036.

Cheng, G., Kong, R., Zhang, L., and Zhang, J. (2012). Mitochondria in traumatic brain injury and mitochondrial-targeted multipotential therapeutic strategies. Br. J. Pharmacol. *167*, 699–719.

Chow, A., Erisir, A., Farb, C., Nadal, M.S., Ozaita, A., Lau, D., Welker, E., and Rudy, B. (1999). K(+) channel expression distinguishes subpopulations of parvalbumin- and somatostatin-containing neocortical interneurons. J. Neurosci. Off. J. Soc. Neurosci. *19*, 9332–9345.

Chugani, H.T., Phelps, M.E., and Mazziotta, J.C. (1987). Positron emission tomography study of human brain functional development. Ann. Neurol. *22*, 487–497.

Cole, J.T., Yarnell, A., Kean, W.S., Gold, E., Lewis, B., Ren, M., McMullen, D.C., Jacobowitz, D.M., Pollard, H.B., O'Neill, J.T., et al. (2010). Craniotomy: True Sham for Traumatic Brain Injury, or a Sham of a Sham? J. Neurotrauma *28*, 359–369.

Cole, J.T., Yarnell, A., Kean, W.S., Gold, E., Lewis, B., Ren, M., McMullen, D.C., Jacobowitz, D.M., Pollard, H.B., O'Neill, J.T., et al. (2011). Craniotomy: True Sham for Traumatic Brain Injury, or a Sham of a Sham? J. Neurotrauma *28*, 359–369.

Connors, B.W., and Gutnick, M.J. (1990). Intrinsic firing patterns of diverse neocortical

neurons. Trends Neurosci. *13*, 99–104.

Cook, L.G., Chapman, S.B., Elliott, A.C., Evenson, N.N., and Vinton, K. (2014). Cognitive Gains from Gist Reasoning Training in Adolescents with Chronic-Stage Traumatic Brain Injury. Front. Neurol. *5*.

Corkin, S., Sullivan, E.V., and Carr, F.A. (1984). Prognostic factors for life expectancy after penetrating head injury. Arch. Neurol. *41*, 975–977.

Cowan, W.M., Fawcett, J.W., O'Leary, D.D., and Stanfield, B.B. (1984). Regressive events in neurogenesis. Science *225*, 1258–1265.

Cramer, S.C., Shah, R., Juranek, J., Crafton, K.R., and Le, V. (2006). Activity in the peri-infarct rim in relation to recovery from stroke. Stroke J. Cereb. Circ. *37*, 111–115.

Cruikshank, S.J., Lewis, T.J., and Connors, B.W. (2007). Synaptic basis for intense thalamocortical activation of feedforward inhibitory cells in neocortex. Nat. Neurosci. *10*, 462–468.

Dávid, C., Schleicher, A., Zuschratter, W., and Staiger, J.F. (2007). The innervation of parvalbumin-containing interneurons by VIP-immunopositive interneurons in the primary somatosensory cortex of the adult rat. Eur. J. Neurosci. *25*, 2329–2340.

De Beaumont, L., Lassonde, M., Leclerc, S., and Théoret, H. (2007). Long-term and cumulative effects of sports concussion on motor cortex inhibition. Neurosurgery *61*, 329–336; discussion 336–337.

De Beaumont, L., Théoret, H., Mongeon, D., Messier, J., Leclerc, S., Tremblay, S., Ellemberg, D., and Lassonde, M. (2009). Brain function decline in healthy retired athletes who sustained their last sports concussion in early adulthood. Brain J. Neurol. *132*, 695–708.

Dichter, M.A., and Ayala, G.F. (1987). Cellular mechanisms of epilepsy: a status report. Science *237*, 157–164.

Ding, M.-C., Wang, Q., Lo, E.H., and Stanley, G.B. (2011). Cortical excitation and inhibition following focal traumatic brain injury. J. Neurosci. Off. J. Soc. Neurosci. *31*, 14085–14094.

Doischer, D., Hosp, J.A., Yanagawa, Y., Obata, K., Jonas, P., Vida, I., and Bartos, M. (2008). Postnatal differentiation of basket cells from slow to fast signaling devices. J. Neurosci. Off. J. Soc. Neurosci. *28*, 12956–12968.

Douglas, R.J., and Martin, K.A.C. (2007). Mapping the Matrix: The Ways of Neocortex. Neuron *56*, 226–238.

Eadie, M.J. (2012). Shortcomings in the current treatment of epilepsy. Expert Rev.

Neurother. *12*, 1419–1427.

Elaine Wyllie MD, A.G., and Deepak K. Lachhwani (2005). The Treatment of Epilepsy: Principles and Practice (Philadelphia: Lippincott Williams & Wilkins).

Emery, D.L., Raghupathi, R., Saatman, K.E., Fischer, I., Grady, M.S., and McIntosh, T.K. (2000). Bilateral growth-related protein expression suggests a transient increase in regenerative potential following brain trauma. J. Comp. Neurol. *424*, 521–531.

Ewing-Cobbs, L., Miner, M.E., Fletcher, J.M., and Levin, H.S. (1989). Intellectual, Motor, and Language Sequelae Following Closed Head Injury in Infants and Preschoolers. J. Pediatr. Psychol. *14*, 531–547.

Ewing-Cobbs, L., Prasad, M., Kramer, L., and Landry, S. (1999). Inflicted traumatic brain injury: relationship of developmental outcome to severity of injury. Pediatr. Neurosurg. *31*, 251–258.

Ewing-Cobbs, L., Barnes, M.A., and Fletcher, J.M. (2003). Early brain injury in children: development and reorganization of cognitive function. Dev. Neuropsychol. *24*, 669–704.

Ewing-Cobbs, L., Prasad, M.R., Kramer, L., Cox, C.S., Baumgartner, J., Fletcher, S., Mendez, D., Barnes, M., Zhang, X., and Swank, P. (2006). Late intellectual and academic outcomes following traumatic brain injury sustained during early childhood. J. Neurosurg. *105*, 287–296.

Fisher, R.S., van Emde Boas, W., Blume, W., Elger, C., Genton, P., Lee, P., and Engel, J., Jr (2005). Epileptic seizures and epilepsy: definitions proposed by the International League Against Epilepsy (ILAE) and the International Bureau for Epilepsy (IBE). Epilepsia *46*, 470–472.

Fox, G., Fan, L., Levasseur, R.A., and Faden, A.I. (1998). Sustained Sensory/Motor and Cognitive Deficits With Neuronal Apoptosis Following Controlled Cortical Impact Brain Injury in the Mouse. J. Neurotrauma *15*, 599–614.

Frey, L.C. (2003a). Epidemiology of posttraumatic epilepsy: a critical review. Epilepsia *44 Suppl 10*, 11–17.

Frey, L.C. (2003b). Epidemiology of posttraumatic epilepsy: a critical review. Epilepsia *44 Suppl 10*, 11–17.

Friedman, D., Claassen, J., and Hirsch, L.J. (2009). Continuous electroencephalogram monitoring in the intensive care unit. Anesth. Analg. *109*, 506–523.

Friedman, W.J., Olson, L., and Persson, H. (1991). Cells that Express Brain-Derived Neurotrophic Factor mRNA in the Developing Postnatal Rat Brain. Eur. J. Neurosci. *3*, 688–697.

Frost, S.B., Barbay, S., Friel, K.M., Plautz, E.J., and Nudo, R.J. (2003). Reorganization

of Remote Cortical Regions After Ischemic Brain Injury: A Potential Substrate for Stroke Recovery. J. Neurophysiol. *89*, 3205–3214.

Fujimoto, S.T., Longhi, L., Saatman, K.E., Conte, V., Stocchetti, N., and McIntosh, T.K. (2004). Motor and cognitive function evaluation following experimental traumatic brain injury. Neurosci. Biobehav. Rev. *28*, 365–378.

Gabernet, L., Jadhav, S.P., Feldman, D.E., Carandini, M., and Scanziani, M. (2005). Somatosensory integration controlled by dynamic thalamocortical feed-forward inhibition. Neuron *48*, 315–327.

Galarreta, M., and Hestrin, S. (1998). Frequency-dependent synaptic depression and the balance of excitation and inhibition in the neocortex. Nat. Neurosci. *1*, 587–594.

Galarreta, M., and Hestrin, S. (1999). A network of fast-spiking cells in the neocortex connected by electrical synapses. Nature *402*, 72–75.

Garga, N., and Lowenstein, D.H. (2006). Posttraumatic epilepsy: a major problem in desperate need of major advances. Epilepsy Curr. Am. Epilepsy Soc. *6*, 1–5.

Ghajar, J. (2000). Traumatic brain injury. Lancet *356*, 923–929.

Gibson, J.R., Beierlein, M., and Connors, B.W. (1999). Two networks of electrically coupled inhibitory neurons in neocortex. Nature *402*, 75–79.

Gill, R., Chang, P.K.-Y., Prenosil, G.A., Deane, E.C., and McKinney, R.A. (2013). Blocking brain-derived neurotrophic factor inhibits injury-induced hyperexcitability of hippocampal CA3 neurons. Eur. J. Neurosci. *38*, 3554–3566.

Goddeyne, C., Nichols, J., Wu, C., and Anderson, T. (2015). Repetitive mild traumatic brain injury induces ventriculomegaly and cortical thinning in juvenile rats. J. Neurophysiol. *113*, 3268–3280.

Goldberg, E.M., Clark, B.D., Zagha, E., Nahmani, M., Erisir, A., and Rudy, B. (2008). K+ channels at the axon initial segment dampen near-threshold excitability of neocortical fast-spiking GABAergic interneurons. Neuron *58*, 387–400.

Goldberg, J.H., Yuste, R., and Tamas, G. (2003). Ca2+ imaging of mouse neocortical interneurone dendrites: Contribution of Ca2+-permeable AMPA and NMDA receptors to subthreshold Ca2+dynamics. J. Physiol. *551*, 67–78.

Goodman, J.C., Cherian, L., Bryan, R.M., and Robertson, C.S. (1994). Lateral Cortical Impact Injury in Rats: Pathologic Effects of Varying Cortical Compression and Impact Velocity. J. Neurotrauma *11*, 587–597.

Graber, K.D., and Prince, D.A. (2004). A critical period for prevention of posttraumatic neocortical hyperexcitability in rats. Ann. Neurol. *55*, 860–870.

Guatteo, E., Bacci, A., Franceschetti, S., Avanzini, G., and Wanke, E. (1994). Neurons dissociated from neocortex fire with “burst” and “regular” trains of spikes. Neurosci. Lett. *175*, 117–120.

Guerriero, R.M., Giza, C.C., and Rotenberg, A. (2015). Glutamate and GABA Imbalance Following Traumatic Brain Injury. Curr. Neurol. Neurosci. Rep. *15*, 545.

Gupta, A., Wang, Y., and Markram, H. (2000). Organizing principles for a diversity of GABAergic interneurons and synapses in the neocortex. Science *287*, 273–278.

Haider, B., and McCormick, D.A. (2009). Rapid neocortical dynamics: cellular and network mechanisms. Neuron *62*, 171–189.

Hall, E.D., Sullivan, P.G., Gibson, T.R., Pavel, K.M., Thompson, B.M., and Scheff, S.W. (2005a). Spatial and Temporal Characteristics of Neurodegeneration after Controlled Cortical Impact in Mice: More than a Focal Brain Injury. J. Neurotrauma *22*, 252–265.

Hall, R.C.W., Hall, R.C.W., and Chapman, M.J. (2005b). Definition, diagnosis, and forensic implications of postconcussional syndrome. Psychosomatics *46*, 195–202.

Hamm, R.J., Pike, B.R., O’Dell, D.M., Lyeth, B.G., and Jenkins, L.W. (1994). The rotarod test: an evaluation of its effectiveness in assessing motor deficits following traumatic brain injury. J. Neurotrauma *11*, 187–196.

Hånell, A., Clausen, F., Björk, M., Jansson, K., Philipson, O., Nilsson, L.N.G., Hillered, L., Weinreb, P.H., Lee, D., McIntosh, T.K., et al. (2010). Genetic deletion and pharmacological inhibition of Nogo-66 receptor impairs cognitive outcome after traumatic brain injury in mice. J. Neurotrauma *27*, 1297–1309.

Hasenstaub, A., Shu, Y., Haider, B., Kraushaar, U., Duque, A., and McCormick, D.A. (2005). Inhibitory postsynaptic potentials carry synchronized frequency information in active cortical networks. Neuron *47*, 423–435.

Hensch, T.K. (2005). Critical period plasticity in local cortical circuits. Nat. Rev. Neurosci. *6*, 877–888.

Herman, S.T. (2002). Epilepsy after brain insult: targeting epileptogenesis. Neurology *59*, S21–S26.

Hioki, H., Okamoto, S., Konno, M., Kameda, H., Sohn, J., Kuramoto, E., Fujiyama, F., and Kaneko, T. (2013). Cell Type-Specific Inhibitory Inputs to Dendritic and Somatic Compartments of Parvalbumin-Expressing Neocortical Interneuron. J. Neurosci. *33*, 544–555.

Hoffman, S.N., Salin, P.A., and Prince, D.A. (1994). Chronic neocortical epileptogenesis in vitro. J. Neurophysiol. *71*, 1762–1773.

Horita, H., Uchida, E., and Maekawa, K. (1991). Circadian rhythm of regular spike-wave

discharges in childhood absence epilepsy. Brain Dev. *13*, 200–202.

Houston, C.M., Bright, D.P., Sivilotti, L.G., Beato, M., and Smart, T.G. (2009). Intracellular chloride ions regulate the time course of GABA-mediated inhibitory synaptic transmission. J. Neurosci. Off. J. Soc. Neurosci. *29*, 10416–10423.

Houweling, A.R., Bazhenov, M., Timofeev, I., Steriade, M., and Sejnowski, T.J. (2005). Homeostatic Synaptic Plasticity Can Explain Post-traumatic Epileptogenesis in Chronically Isolated Neocortex. Cereb. Cortex N. Y. N 1991 *15*, 834–845.

Hu, H., Gan, J., and Jonas, P. (2014). Fast-spiking, parvalbumin+ GABAergic interneurons: From cellular design to microcircuit function. Science *345*, 1255263.

Hulsebosch, C.E., DeWitt, D.S., Jenkins, L.W., and Prough, D.S. (1998). Traumatic brain injury in rats results in increased expression of Gap-43 that correlates with behavioral recovery. Neurosci. Lett. *255*, 83–86.

Hunt, R.F., Scheff, S.W., and Smith, B.N. (2009). Posttraumatic epilepsy after controlled cortical impact injury in mice. Exp. Neurol. *215*, 243–252.

Hunt, R.F., Scheff, S.W., and Smith, B.N. (2011). Synaptic reorganization of inhibitory hilar interneuron circuitry after traumatic brain injury in mice. J. Neurosci. Off. J. Soc. Neurosci. *31*, 6880–6890.

Huusko, N., Römer, C., Ndode-Ekane, X.E., Lukasiuk, K., and Pitkänen, A. (2015). Loss of hippocampal interneurons and epileptogenesis: a comparison of two animal models of acquired epilepsy. Brain Struct. Funct. *220*, 153–191.

Insel, T.R., Miller, L.P., and Gelhard, R.E. (1990). The ontogeny of excitatory amino acid receptors in rat forebrain--I. N-methyl-D-aspartate and quisqualate receptors. Neuroscience *35*, 31–43.

Isomura, Y., Harukuni, R., Takekawa, T., Aizawa, H., and Fukai, T. (2009). Microcircuitry coordination of cortical motor information in self-initiation of voluntary movements. Nat. Neurosci. *12*, 1586–1593.

Itami, C., Kimura, F., and Nakamura, S. (2007). Brain-derived neurotrophic factor regulates the maturation of layer 4 fast-spiking cells after the second postnatal week in the developing barrel cortex. J. Neurosci. Off. J. Soc. Neurosci. *27*, 2241–2252.

Iudice, A., and Murri, L. (2000). Pharmacological prophylaxis of post-traumatic epilepsy. Drugs *59*, 1091–1099.

Izhikevich, E.M., Desai, N.S., Walcott, E.C., and Hoppensteadt, F.C. (2003). Bursts as a unit of neural information: selective communication via resonance. Trends Neurosci. *26*, 161–167.

Jacobs, K.M., Graber, K.D., Kharazia, V.N., Parada, I., and Prince, D.A. (2000).

Postlesional epilepsy: the ultimate brain plasticity. Epilepsia *41 Suppl 6*, S153–S161.

Jenkins, L.W., Peters, G.W., Dixon, C.E., Zhang, X., Clark, R.S.B., Skinner, J.C., Marion, D.W., Adelson, P.D., and Kochanek, P.M. (2002). Conventional and functional proteomics using large format two-dimensional gel electrophoresis 24 hours after controlled cortical impact in postnatal day 17 rats. J. Neurotrauma *19*, 715–740.

Jin, X., Prince, D.A., and Huguenard, J.R. (2006). Enhanced Excitatory Synaptic Connectivity in Layer V Pyramidal Neurons of Chronically Injured Epileptogenic Neocortex in Rats. J. Neurosci. *26*, 4891–4900.

Jin, X., Huguenard, J.R., and Prince, D.A. (2011). Reorganization of inhibitory synaptic circuits in rodent chronically injured epileptogenic neocortex. Cereb. Cortex N. Y. N 1991 *21*, 1094–1104.

Jin, X., Jiang, K., and Prince, D.A. (2014). Excitatory and Inhibitory Synaptic Connectivity to Layer V Fast-spiking Interneurons in the Freeze Lesion Model of Cortical Microgyria. J. Neurophysiol.

Johnson, V.E., Stewart, J.E., Begbie, F.D., Trojanowski, J.Q., Smith, D.H., and Stewart, W. (2013). Inflammation and white matter degeneration persist for years after a single traumatic brain injury. Brain J. Neurol. *136*, 28–42.

Jones, E.G. (1998). Viewpoint: the core and matrix of thalamic organization. Neuroscience *85*, 331–345.

Jones, T.A., Liput, D.J., Maresh, E.L., Donlan, N., Parikh, T.J., Marlowe, D., and Kozlowski, D.A. (2012). Use-Dependent Dendritic Regrowth Is Limited after Unilateral Controlled Cortical Impact to the Forelimb Sensorimotor Cortex. J. Neurotrauma *29*, 1455–1468.

Katz, L.C. (1993). Coordinate activity in retinal and cortical development. Curr. Opin. Neurobiol. *3*, 93–99.

Kawaguchi, Y., and Kondo, S. (2002). Parvalbumin, somatostatin and cholecystokinin as chemical markers for specific GABAergic interneuron types in the rat frontal cortex. J. Neurocytol. *31*, 277–287.

Kawaguchi, Y., and Kubota, Y. (1997). GABAergic cell subtypes and their synaptic connections in rat frontal cortex. Cereb. Cortex *7*, 476–486.

Kawaguchi, Y., Katsumaru, H., Kosaka, T., Heizmann, C.W., and Hama, K. (1987). Fast spiking cells in rat hippocampus (CA1 region) contain the calcium-binding protein parvalbumin. Brain Res. *416*, 369–374.

Keros, S., and Hablitz, J.J. (2005). Subtype-specific GABA transporter antagonists synergistically modulate phasic and tonic GABAA conductances in rat neocortex. J.

Neurophysiol. *94*, 2073–2085.

Kim, E. (2002). Agitation, aggression, and disinhibition syndromes after traumatic brain injury. NeuroRehabilitation *17*, 297–310.

Kinney, J.W., Davis, C.N., Tabarean, I., Conti, B., Bartfai, T., and Behrens, M.M. (2006). A specific role for NR2A-containing NMDA receptors in the maintenance of parvalbumin and GAD67 immunoreactivity in cultured interneurons. J. Neurosci. Off. J. Soc. Neurosci. *26*, 1604–1615.

Kleschevnikov, A.M., Belichenko, P.V., Villar, A.J., Epstein, C.J., Malenka, R.C., and Mobley, W.C. (2004). Hippocampal long-term potentiation suppressed by increased inhibition in the Ts65Dn mouse, a genetic model of Down syndrome. J. Neurosci. Off. J. Soc. Neurosci. *24*, 8153–8160.

Klonoff, H., Clark, C., and Klonoff, P.S. (1993). Long-term outcome of head injuries: a 23 year follow up study of children with head injuries. J. Neurol. Neurosurg. Psychiatry *56*, 410–415.

Kobayashi, M., Wen, X., and Buckmaster, P.S. (2003). Reduced inhibition and increased output of layer II neurons in the medial entorhinal cortex in a model of temporal lobe epilepsy. J. Neurosci. Off. J. Soc. Neurosci. *23*, 8471–8479.

Kobori, N., Clifton, G.L., and Dash, P. (2002). Altered expression of novel genes in the cerebral cortex following experimental brain injury. Brain Res. Mol. Brain Res. *104*, 148–158.

Kochanek, P.M., Carney, N., Adelson, P.D., Ashwal, S., Bell, M.J., Bratton, S., Carson, S., Chesnut, R.M., Ghajar, J., Goldstein, B., et al. (2012). Guidelines for the acute medical management of severe traumatic brain injury in infants, children, and adolescents--second edition. Pediatr. Crit. Care Med. J. Soc. Crit. Care Med. World Fed. Pediatr. Intensive Crit. Care Soc. *13 Suppl 1*, S1–S82.

Kuhlman, S.J., Olivas, N.D., Tring, E., Ikrar, T., Xu, X., and Trachtenberg, J.T. (2013). A disinhibitory microcircuit initiates critical-period plasticity in the visual cortex. Nature *501*, 543–546.

Lawrence, J.J., and McBain, C.J. (2003). Interneuron diversity series: containing the detonation--feedforward inhibition in the CA3 hippocampus. Trends Neurosci. *26*, 631–640.

Lenzlinger, P.M., Shimizu, S., Marklund, N., Thompson, H.J., Schwab, M.E., Saatman, K.E., Hoover, R.C., Bareyre, F.M., Motta, M., Luginbuhl, A., et al. (2005). Delayed inhibition of Nogo-A does not alter injury-induced axonal sprouting but enhances recovery of cognitive function following experimental traumatic brain injury in rats. Neuroscience *134*, 1047–1056.

Letzkus, J.J., Wolff, S.B.E., Meyer, E.M.M., Tovote, P., Courtin, J., Herry, C., and Lüthi, A. (2011). A disinhibitory microcircuit for associative fear learning in the auditory cortex. Nature *480*, 331–335.

Levitt, P. (2003). Structural and functional maturation of the developing primate brain. J. Pediatr. *143*, S35–S45.

Levitt, P., Eagleson, K.L., and Powell, E.M. (2004). Regulation of neocortical interneuron development and the implications for neurodevelopmental disorders. Trends Neurosci. *27*, 400–406.

Lewis, D.A., Curley, A.A., Glausier, J., and Volk, D.W. (2012). Cortical Parvalbumin Interneurons and Cognitive Dysfunction in Schizophrenia. Trends Neurosci. *35*, 57–67.

Li, K., and Xu, E. (2008). The role and the mechanism of gamma-aminobutyric acid during central nervous system development. Neurosci. Bull. *24*, 195–200.

Li, H.H., Lee, S.M., Cai, Y., Sutton, R.L., and Hovda, D.A. (2004). Differential gene expression in hippocampus following experimental brain trauma reveals distinct features of moderate and severe injuries. J. Neurotrauma *21*, 1141–1153.

Lighthall, J.W., Dixon, C.E., and Anderson, T.E. (1989). Experimental models of brain injury. J. Neurotrauma *6*, 83–97.

Lisman, J.E. (1997). Bursts as a unit of neural information: making unreliable synapses reliable. Trends Neurosci. *20*, 38–43.

Liu, N.-K., Zhang, Y.-P., O'Connor, J., Gianaris, A., Oakes, E., Lu, Q.-B., Verhovshek, T., Walker, C.L., Shields, C.B., and Xu, X.-M. (2013). A bilateral head injury that shows graded brain damage and behavioral deficits in adultmice. Brain Res. *1499*, 121–128.

Lowenstein, D.H., Thomas, M.J., Smith, D.H., and McIntosh, T.K. (1992). Selective vulnerability of dentate hilar neurons following traumatic brain injury: a potential mechanistic link between head trauma and disorders of the hippocampus. J. Neurosci. Off. J. Soc. Neurosci. *12*, 4846–4853.

Luerssen, T.G., Klauber, M.R., and Marshall, L.F. (1988a). Outcome from head injury related to patient's age. A longitudinal prospective study of adult and pediatric head injury. J. Neurosurg. *68*, 409–416.

Luerssen, T.G., Klauber, M.R., and Marshall, L.F. (1988b). Outcome from head injury related to patient's age. A longitudinal prospective study of adult and pediatric head injury. J. Neurosurg. *68*, 409–416.

Ma, Y., and Prince, D.A. (2012). Functional alterations in GABAergic fast-spiking interneurons in chronically injured epileptogenic neocortex. Neurobiol. Dis. *47*, 102–113.

Ma, Y., Hu, H., Berrebi, A.S., Mathers, P.H., and Agmon, A. (2006). Distinct Subtypes

of Somatostatin-Containing Neocortical Interneurons Revealed in Transgenic Mice. J. Neurosci. *26*, 5069–5082.

Maas, A.I., Stocchetti, N., and Bullock, R. (2008). Moderate and severe traumatic brain injury in adults. Lancet Neurol. *7*, 728–741.

Magiorkinis, E., Sidiropoulou, K., and Diamantis, A. (2010). Hallmarks in the history of epilepsy: epilepsy in antiquity. Epilepsy Behav. EB *17*, 103–108.

Mannix, R.C., Zhang, J., Park, J., Lee, C., and Whalen, M.J. (2011). Detrimental effect of genetic inhibition of B-site APP-cleaving enzyme 1 on functional outcome after controlled cortical impact in young adult mice. J. Neurotrauma *28*, 1855–1861.

Marklund, N., Bareyre, F.M., Royo, N.C., Thompson, H.J., Mir, A.K., Grady, M.S., Schwab, M.E., and McIntosh, T.K. (2007). Cognitive outcome following brain injury and treatment with an inhibitor of Nogo-A in association with an attenuated downregulation of hippocampal growth-associated protein-43 expression. J. Neurosurg. *107*, 844–853.

Markram, H., Toledo-Rodriguez, M., Wang, Y., Gupta, A., Silberberg, G., and Wu, C. (2004a). Interneurons of the neocortical inhibitory system. Nat. Rev. Neurosci. *5*, 793–807.

Markram, H., Toledo-Rodriguez, M., Wang, Y., Gupta, A., Silberberg, G., and Wu, C. (2004b). Interneurons of the neocortical inhibitory system. Nat. Rev. Neurosci. *5*, 793–807.

Matsumoto, H., and Marsan, C.A. (1964). Cortical cellular phenomena in experimental epilepsy: Interictal manifestations. Exp. Neurol. *9*, 286–304.

Mazarati, A. (2006). Is posttraumatic epilepsy the best model of posttraumatic epilepsy? Epilepsy Curr. Am. Epilepsy Soc. *6*, 213–214.

McKinlay, A., Dalrymple-Alford, J.C., Horwood, L.J., and Fergusson, D.M. (2002). Long term psychosocial outcomes after mild head injury in early childhood. J. Neurol. Neurosurg. Psychiatry *73*, 281–288.

Mello, L.E., Cavalheiro, E.A., Tan, A.M., Kupfer, W.R., Pretorius, J.K., Babb, T.L., and Finch, D.M. (1993). Circuit mechanisms of seizures in the pilocarpine model of chronic epilepsy: cell loss and mossy fiber sprouting. Epilepsia *34*, 985–995.

Menon, D.K., Schwab, K., Wright, D.W., Maas, A.I., and Demographics and Clinical Assessment Working Group of the International and Interagency Initiative toward Common Data Elements for Research on Traumatic Brain Injury and Psychological Health (2010). Position statement: definition of traumatic brain injury. Arch. Phys. Med. Rehabil. *91*, 1637–1640.

Michael, A.P., Stout, J., Roskos, P.T., Bolzenius, J., Gfeller, J., Mogul, D., and Bucholz,

R. (2015). Evaluation of Cortical Thickness after Traumatic Brain Injury in Military Veterans. J. Neurotrauma *32*, 1751–1758.

Miller, L.M., Escabí, M.A., and Schreiner, C.E. (2001). Feature selectivity and interneuronal cooperation in the thalamocortical system. J. Neurosci. Off. J. Soc. Neurosci. *21*, 8136–8144.

Miller, M.N., Okaty, B.W., Kato, S., and Nelson, S.B. (2011). Activity-dependent changes in the firing properties of neocortical fast-spiking interneurons in the absence of large changes in gene expression. Dev. Neurobiol. *71*, 62–70.

Mishra, A.M., Bai, X., Sanganahalli, B.G., Waxman, S.G., Shatillo, O., Grohn, O., Hyder, F., Pitkanen, A., and Blumenfeld, H. (2014). Decreased Resting Functional Connectivity after Traumatic Brain Injury in the Rat. PLoS ONE *9*.

Mitchell, S.J., and Silver, R.A. (2003). Shunting Inhibition Modulates Neuronal Gain during Synaptic Excitation. Neuron *38*, 433–445.

Morris, N.P., and Henderson, Z. (2000). Perineuronal nets ensheath fast spiking, parvalbumin-immunoreactive neurons in the medial septum/diagonal band complex. Eur. J. Neurosci. *12*, 828–838.

Mrzljak, L., Uylings, H.B., Van Eden, C.G., and Judás, M. (1990). Neuronal development in human prefrontal cortex in prenatal and postnatal stages. Prog. Brain Res. *85*, 185–222.

Nakamura, T., Matsumoto, J., Takamura, Y., Ishii, Y., Sasahara, M., Ono, T., and Nishijo, H. (2015). Relationships among parvalbumin-immunoreactive neuron density, phase-locked gamma oscillations, and autistic/schizophrenic symptoms in PDGFR-β knock-out and control mice. PloS One *10*, e0119258.

Nathanson, J.L., Yanagawa, Y., Obata, K., and Callaway, E.M. (2009). Preferential labeling of inhibitory and excitatory cortical neurons by endogenous tropism of AAV and lentiviral vectors. Neuroscience *161*, 441–450.

Nelson, S.B., and Turrigiano, G.G. (1998). Synaptic depression: a key player in the cortical balancing act. Nat. Neurosci. *1*, 539–541.

Nichols, J., Perez, R., Wu, C., Adelson, P.D., and Anderson, T. (2015). Traumatic Brain Injury Induces Rapid Enhancement of Cortical Excitability in Juvenile Rats. CNS Neurosci. Ther. *21*, 193–203.

Nilsson, P., Ronne-Engström, E., Flink, R., Ungerstedt, U., Carlson, H., and Hillered, L. (1994). Epileptic seizure activity in the acute phase following cortical impact trauma in rat. Brain Res. *637*, 227–232.

Nishibe, M., Barbay, S., Guggenmos, D., and Nudo, R.J. (2010). Reorganization of

Motor Cortex after Controlled Cortical Impact in Rats and Implications for Functional Recovery. J. Neurotrauma *27*, 2221–2232.

Noctor, S.C., Flint, A.C., Weissman, T.A., Dammerman, R.S., and Kriegstein, A.R. (2001). Neurons derived from radial glial cells establish radial units in neocortex. Nature *409*, 714–720.

Nudo, R.J. (2006). Mechanisms for recovery of motor function following cortical damage. Curr. Opin. Neurobiol. *16*, 638–644.

Okaty, B.W., Miller, M.N., Sugino, K., Hempel, C.M., and Nelson, S.B. (2009). Transcriptional and electrophysiological maturation of neocortical fastspiking GABAergic interneurons. J. Neurosci. Off. J. Soc. Neurosci. *29*, 7040–7052.

Olesen, S.P. (1987). Leakiness of rat brain microvessels to fluorescent probes following craniotomy. Acta Physiol. Scand. *130*, 63–68.

Orduz, D., Bischop, D.P., Schwaller, B., Schiffmann, S.N., and Gall, D. (2013). Parvalbumin tunes spike-timing and efferent short-term plasticity in striatal fast spiking interneurons. J. Physiol. *591*, 3215–3232.

Orlando, C., and Raineteau, O. (2015). Integrity of cortical perineuronal nets influences corticospinal tract plasticity after spinal cord injury. Brain Struct. Funct. *220*, 1077–1091.

Overstreet, L.S., and Westbrook, G.L. (2003). Synapse density regulates independence at unitary inhibitory synapses. J. Neurosci. Off. J. Soc. Neurosci. *23*, 2618–2626.

Pagni, C.A., and Zenga, F. (2005). Posttraumatic epilepsy with special emphasis on prophylaxis and prevention. Acta Neurochir. Suppl. *93*, 27–34.

Pandolfo, M. (2011). Genetics of epilepsy. Semin. Neurol. *31*, 506–518.

Park, E., Bell, J.D., and Baker, A.J. (2008). Traumatic brain injury: Can the consequences be stopped? CMAJ Can. Med. Assoc. J. *178*, 1163–1170.

Pavlov, I., Huusko, N., Drexel, M., Kirchmair, E., Sperk, G., Pitkänen, A., and Walker, M.C. (2011). Progressive loss of phasic, but not tonic, GABAA receptor-mediated inhibition in dentate granule cells in a model of post-traumatic epilepsy in rats. Neuroscience *194*, 208–219.

Paxinos, G., and Watson, C. (2007). The rat brain in stereotaxic coordinates (Amsterdam; Boston: Elsevier).

Pearce, A.J., Hoy, K., Rogers, M.A., Corp, D.T., Davies, C.B., Maller, J.J., and Fitzgerald, P.B. (2015). Acute motor, neurocognitive and neurophysiological change following concussion injury in Australian amateur football. A prospective multimodal investigation. J. Sci. Med. Sport *18*, 500–506.

Pearson, W.S., Ovalle, F., Faul, M., and Sasser, S.M. (2012a). A review of traumatic brain injury trauma center visits meeting physiologic criteria from The American College of Surgeons Committee on Trauma/Centers for Disease Control and Prevention Field Triage Guidelines. Prehospital Emerg. Care Off. J. Natl. Assoc. EMS Physicians Natl. Assoc. State EMS Dir. *16*, 323–328.

Pearson, W.S., Sugerman, D.E., McGuire, L.C., and Coronado, V.G. (2012b). Emergency Department Visits for Traumatic Brain Injury in Older Adults in the United States: 2006–08. West. J. Emerg. Med. *13*, 289–293.

Perucca, P., and Gilliam, F.G. (2012). Adverse effects of antiepileptic drugs. Lancet Neurol. *11*, 792–802.

Peters, A., and Jones, E.G. (1984). Cerebral Cortex: Volume 1: Cellular Components of the Cerebral Cortex (New York: Springer).

Petilla Interneuron Nomenclature Group, Ascoli, G.A., Alonso-Nanclares, L., Anderson, S.A., Barrionuevo, G., Benavides-Piccione, R., Burkhalter, A., Buzsáki, G., Cauli, B., Defelipe, J., et al. (2008). Petilla terminology: nomenclature of features of GABAergic interneurons of the cerebral cortex. Nat. Rev. Neurosci. *9*, 557–568.

Pi, H.-J., Hangya, B., Kvitsiani, D., Sanders, J.I., Huang, Z.J., and Kepecs, A. (2013). Cortical interneurons that specialize in disinhibitory control. Nature *advance online publication*.

Pinto, D.J., Brumberg, J.C., and Simons, D.J. (2000). Circuit dynamics and coding strategies in rodent somatosensory cortex. J. Neurophysiol. *83*, 1158–1166.

Pinto, D.J., Hartings, J.A., Brumberg, J.C., and Simons, D.J. (2003). Cortical damping: analysis of thalamocortical response transformations in rodent barrel cortex. Cereb. Cortex N. Y. N 1991 *13*, 33–44.

Pitkänen, A., and McIntosh, T.K. (2006). Animal models of post-traumatic epilepsy. J. Neurotrauma *23*, 241–261.

Pitkänen, A., Kharatishvili, I., Karhunen, H., Lukasiuk, K., Immonen, R., Nairismägi, J., Gröhn, O., and Nissinen, J. (2007). Epileptogenesis in experimental models. Epilepsia *48 Suppl 2*, 13–20.

Polack, P.-O., Guillemain, I., Hu, E., Deransart, C., Depaulis, A., and Charpier, S. (2007). Deep Layer Somatosensory Cortical Neurons Initiate Spike-and-Wave Discharges in a Genetic Model of Absence Seizures. J. Neurosci. *27*, 6590–6599.

Pouille, F., and Scanziani, M. (2001). Enforcement of temporal fidelity in pyramidal cells by somatic feed-forward inhibition. Science *293*, 1159–1163.

Powell, S.B., Sejnowski, T.J., and Behrens, M.M. (2012). Behavioral and neurochemical

consequences of cortical oxidative stress on parvalbumin-interneuron maturation in rodent models of schizophrenia. Neuropharmacology *62*, 1322–1331.

Prince, D.A. (1978). Neurophysiology of Epilepsy. Annu. Rev. Neurosci. *1*, 395–415.

Prince, D.A., and Connors, B.W. (1986). Mechanisms of interictal epileptogenesis. Adv. Neurol. *44*, 275–299.

Prince, D.A., and Tseng, G.F. (1993). Epileptogenesis in chronically injured cortex: in vitro studies. J. Neurophysiol. *69*, 1276–1291.

Prinz, A., Selesnew, L.-M., Liss, B., Roeper, J., and Carlsson, T. (2013). Increased excitability in serotonin neurons in the dorsal raphe nucleus in the 6-OHDA mouse model of Parkinson's disease. Exp. Neurol. *248*, 236–245.

Rakic, P. (1988). Specification of cerebral cortical areas. Science *241*, 170–176.

Ramantani, G. (2013). Neonatal epilepsy and underlying aetiology: to what extent do seizures and EEG abnormalities influence outcome? Epileptic Disord. Int. Epilepsy J. Videotape *15*, 365–375.

Rheims, S., Holmgren, C.D., Chazal, G., Mulder, J., Harkany, T., Zilberter, T., and Zilberter, Y. (2009). GABA action in immature neocortical neurons directly depends on the availability of ketone bodies. J. Neurochem. *110*, 1330–1338.

Rola, R., Mizumatsu, S., Otsuka, S., Morhardt, D., Noblehaeusslein, L., Fishman, K., Potts, M., and Fike, J. (2006). Alterations in hippocampal neurogenesis following traumatic brain injury in mice. Exp. Neurol. *202*, 189–199.

Romcy-Pereira, R.N., and Garcia-Cairasco, N. (2003). Hippocampal cell proliferation and epileptogenesis after audiogenic kindling are not accompanied by mossy fiber sprouting or Fluoro-Jade staining. Neuroscience *119*, 533–546.

Routbort, M.J., Bausch, S.B., and McNamara, J.O. (1999). Seizures, cell death, and mossy fiber sprouting in kainic acid-treated organotypic hippocampal cultures. Neuroscience *94*, 755–765.

Rubio-Garrido, P., Pérez-de-Manzo, F., Porrero, C., Galazo, M.J., and Clascá, F. (2009). Thalamic input to distal apical dendrites in neocortical layer 1 is massive and highly convergent. Cereb. Cortex N. Y. N 1991 *19*, 2380–2395.

Rudy, B., Fishell, G., Lee, S., and Hjerling-Leffler, J. (2011). Three Groups of Interneurons Account for Nearly 100% of Neocortical GABAergic Neurons. Dev. Neurobiol. *71*, 45–61.

Saatman, K.E., Duhaime, A.-C., Bullock, R., Maas, A.I.R., Valadka, A., Manley, G.T., and Workshop Scientific Team and Advisory Panel Members (2008). Classification of

traumatic brain injury for targeted therapies. J. Neurotrauma *25*, 719–738.

Salin, P., Tseng, G.F., Hoffman, S., Parada, I., and Prince, D.A. (1995). Axonal sprouting in layer V pyramidal neurons of chronically injured cerebral cortex. J. Neurosci. *15*, 8234–8245.

Sarkar, K., Keachie, K., Nguyen, U., Muizelaar, J.P., Zwienenberg-Lee, M., and Shahlaie, K. (2014). Computed tomography characteristics in pediatric versus adult traumatic brain injury. J. Neurosurg. Pediatr. *13*, 307–314.

Scheff, S.W., Price, D.A., Hicks, R.R., Baldwin, S.A., Robinson, S., and Brackney, C. (2005). Synaptogenesis in the Hippocampal CA1 Field following Traumatic Brain Injury. J. Neurotrauma *22*, 719–732.

Schmidt, A.T., Hanten, G.R., Li, X., Vasquez, A.C., Wilde, E.A., Chapman, S.B., and Levin, H.S. (2012). Decision making after pediatric traumatic brain injury: trajectory of recovery and relationship to age and gender. Int. J. Dev. Neurosci. Off. J. Int. Soc. Dev. Neurosci. *30*, 225–230.

Schwaller, B., Tetko, I.V., Tandon, P., Silveira, D.C., Vreugdenhil, M., Henzi, T., Potier, M.-C., Celio, M.R., and Villa, A.E.P. (2004). Parvalbumin deficiency affects network properties resulting in increased susceptibility to epileptic seizures. Mol. Cell. Neurosci. *25*, 650–663.

Shatz, C.J. (1990). Impulse activity and the patterning of connections during cns development. Neuron *5*, 745–756.

Shipp, S. (2007). Structure and function of the cerebral cortex. Curr. Biol. *17*, R443–R449.

Smith, C., Gentleman, S.M., Leclercq, P.D., Murray, L.S., Griffin, W.S.T., Graham, D.I., and Nicoll, J.A.R. (2013). The neuroinflammatory response in humans after traumatic brain injury. Neuropathol. Appl. Neurobiol. *39*, 654–666.

Smith, D.H., Soares, H.D., Pierce, J.S., Perlman, K.G., Saatman, K.M., Meaney, D.F., Dixon, C.E., and McIntosh, T.K. (1995). A Model of Parasagittal Controlled Cortical Impact in the Mouse: Cognitive and Histopathologic Effects. J. Neurotrauma *12*, 169–178.

Sohal, V.S., Zhang, F., Yizhar, O., and Deisseroth, K. (2009). Parvalbumin neurons and gamma rhythms enhance cortical circuit performance. Nature *459*, 698–702.

Somjen, G.G. (2004). Ions in the Brain : Normal Function, Seizures, and Stroke: Normal Function, Seizures, and Stroke (Oxford University Press).

Statler, K.D., Scheerlinck, P., Pouliot, W., Hamilton, M., White, H.S., and Dudek, F.E. (2009). A potential model of pediatric posttraumatic epilepsy. Epilepsy Res. *86*, 221–223.

Steriade, M., Amzica, F., Neckelmann, D., and Timofeev, I. (1998). Spike-wave complexes and fast components of cortically generated seizures. II. Extra- and intracellular patterns. J. Neurophysiol. *80*, 1456–1479.

Sun, Q.-Q., Huguenard, J.R., and Prince, D.A. (2006). Barrel cortex microcircuits: thalamocortical feedforward inhibition in spiny stellate cells is mediated by a small number of fast-spiking interneurons. J. Neurosci. Off. J. Soc. Neurosci. *26*, 1219–1230.

Tanaka, Y.H., Tanaka, Y., Fujiyama, F., Furuta, T., Yanagawa, Y., and Kaneko, T. (2011). Local connections of layer 5 GABAergic interneurons to corticospinal neurons. Front. Neural Circuits *5*, 12.

Tasker, J.G., and Dudek, F.E. (1991). Electrophysiology of GABA-mediated synaptic transmission and possible roles in epilepsy. Neurochem. Res. *16*, 251–262.

Telfeian, A.E., and Connors, B.W. (1998). Layer-specific pathways for the horizontal propagation of epileptiform discharges in neocortex. Epilepsia *39*, 700–708.

Temkin, O. (1994). The Falling Sickness: A History of Epilepsy from the Greeks to the Beginnings of Modern Neurology (JHU Press).

Thompson, H.J., Lifshitz, J., Marklund, N., Grady, M.S., Graham, D.I., Hovda, D.A., and McIntosh, T.K. (2005). Lateral fluid percussion brain injury: a 15-year review and evaluation. J. Neurotrauma *22*, 42–75.

Thurman, D.J., Beghi, E., Begley, C.E., Berg, A.T., Buchhalter, J.R., Ding, D., Hesdorffer, D.C., Hauser, W.A., Kazis, L., Kobau, R., et al. (2011). Standards for epidemiologic studies and surveillance of epilepsy. Epilepsia *52 Suppl 7*, 2–26.

Timofeev, I., and Steriade, M. (2004). Neocortical seizures: initiation, development and cessation. Neuroscience *123*, 299–336.

Traub, R.D., and Wong, R.K. (1982). Cellular mechanism of neuronal synchronization in epilepsy. Science *216*, 745–747.

Traub, R.D., Bibbig, A., LeBeau, F.E.N., Buhl, E.H., and Whittington, M.A. (2004). Cellular mechanisms of neuronal population oscillations in the hippocampus in vitro. Annu. Rev. Neurosci. *27*, 247–278.

Tremblay, S., de Beaumont, L., Lassonde, M., and Théoret, H. (2011). Evidence for the specificity of intracortical inhibitory dysfunction in asymptomatic concussed athletes. J. Neurotrauma *28*, 493–502.

Ueno, M., Hayano, Y., Nakagawa, H., and Yamashita, T. (2012). Intraspinal rewiring of the corticospinal tract requires target-derived brain-derived neurotrophic factor and compensates lost function after brain injury. Brain J. Neurol. *135*, 1253–1267.

Uhlhaas, P.J., and Singer, W. (2010). Abnormal neural oscillations and synchrony in

schizophrenia. Nat. Rev. Neurosci. *11*, 100–113.

van den Pol, A.N., Obrietan, K., and Chen, G. (1996). Excitatory actions of GABA after neuronal trauma. J. Neurosci. Off. J. Soc. Neurosci. *16*, 4283–4292.

Wang, Y., Kakizaki, T., Sakagami, H., Saito, K., Ebihara, S., Kato, M., Hirabayashi, M., Saito, Y., Furuya, N., and Yanagawa, Y. (2009). Fluorescent labeling of both GABAergic and glycinergic neurons in vesicular GABA transporter (VGAT)–Venus transgenic mouse. Neuroscience *164*, 1031–1043.

Werner, C., and Engelhard, K. (2007). Pathophysiology of traumatic brain injury. Br. J. Anaesth. *99*, 4–9.

Wilde, E.A., Merkley, T.L., Bigler, E.D., Max, J.E., Schmidt, A.T., Ayoub, K.W., McCauley, S.R., Hunter, J.V., Hanten, G., Li, X., et al. (2012). Longitudinal changes in cortical thickness in children after traumatic brain injury and their relation to behavioral regulation and emotional control. Int. J. Dev. Neurosci. Off. J. Int. Soc. Dev. Neurosci. *30*, 267–276.

Willmore, L.J. (1990). Post-traumatic epilepsy: cellular mechanisms and implications for treatment. Epilepsia *31 Suppl 3*, S67–S73.

Wilson, N.R., Runyan, C.A., Wang, F.L., and Sur, M. (2012). Division and subtraction by distinct cortical inhibitory networks in vivo. Nature *488*, 343–348.

Wise, S.P. (1975). The laminar organization of certain afferent and efferent fiber systems in the rat somatosensory cortex. Brain Res. *90*, 139–142.

Wöhr, M., Orduz, D., Gregory, P., Moreno, H., Khan, U., Vörckel, K.J., Wolfer, D.P., Welzl, H., Gall, D., Schiffmann, S.N., et al. (2015). Lack of parvalbumin in mice leads to behavioral deficits relevant to all human autism core symptoms and related neural morphofunctional abnormalities. Transl. Psychiatry *5*, e525.

Wojcik, S.M., Katsurabayashi, S., Guillemin, I., Friauf, E., Rosenmund, C., Brose, N., and Rhee, J.-S. (2006). A shared vesicular carrier allows synaptic corelease of GABA and glycine. Neuron *50*, 575–587.

Xu, X., Roby, K.D., and Callaway, E.M. (2010). Immunochemical characterization of inhibitory mouse cortical neurons: Three chemically distinct classes of inhibitory cells. J. Comp. Neurol. *518*, 389–404.

Yang, L., Benardo, L.S., Valsamis, H., and Ling, D.S.F. (2007). Acute injury to superficial cortex leads to a decrease in synaptic inhibition and increase in excitation in neocortical layer V pyramidal cells. J. Neurophysiol. *97*, 178–187.

Yang, L., Afroz, S., Michelson, H.B., Goodman, J.H., Valsamis, H.A., and Ling, D.S.F. (2010). Spontaneous epileptiform activity in rat neocortex after controlled cortical impact

injury. J. Neurotrauma *27*, 1541–1548.

Yoshimura, Y., and Callaway, E.M. (2005). Fine-scale specificity of cortical networks depends on inhibitory cell type and connectivity. Nat. Neurosci. *8*, 1552–1559.

Zhang, Z. (2004). Maturation of Layer V Pyramidal Neurons in the Rat Prefrontal Cortex: Intrinsic Properties and Synaptic Function. J. Neurophysiol. *91*, 1171–1182.

Zhang, Q.-G., Laird, M.D., Han, D., Nguyen, K., Scott, E., Dong, Y., Dhandapani, K.M., and Brann, D.W. (2012). Critical Role of NADPH Oxidase in Neuronal Oxidative Damage and Microglia Activation following Traumatic Brain Injury. PLoS ONE *7*, e34504.

Ziyatdinova, S., Gurevicius, K., Kutchiashvili, N., Bolkvadze, T., Nissinen, J., Tanila, H., and Pitkänen, A. (2011). Spontaneous epileptiform discharges in a mouse model of Alzheimer's disease are suppressed by antiepileptic drugs that block sodium channels. Epilepsy Res. *94*, 75–85.

van Zundert, B., Izaurieta, P., Fritz, E., and Alvarez, F.J. (2012). Early pathogenesis in the adult-onset neurodegenerative disease amyotrophic lateral sclerosis. J. Cell. Biochem. *113*, 3301–3312.

(2005). Atlas epilepsy care in the world. (Geneva: Programme for Neurological Diseases and Neuroscience, Dept. of Mental Health and Substance Abuse, World Health Organization).

(2012). Jasper's Basic Mechanisms of the Epilepsies (Bethesda (MD): National Center for Biotechnology Information (US)).

CHAPTER 3

SELECTIVE LOSS OF CORTICAL INHIBITORY FUNCTION

Pediatric traumatic brain injury is a leading cause of death and disability in children and often results in permanent cognitive and behavioral deficits. Recent findings indicate that the pediatric brain is more sensitive to brain injury compared to adult. To assess the pathogenesis of pediatric TBI, we focused on the cortical inhibitory network as it has been implicated in cortical remodeling after injury. The actions of inhibitory interneurons are essential for maintaining and regulating cortical function and are imp-licated in the pathogenesis of TBI. In this study, using a severe model of TBI in a pediatric mouse (P22), controlled cortical impact (CCI), we have found that TBI selectively alters inhibition in the cortex. Specifically, to understand how cortical inter-neurons are affected by TBI we utilized whole cell patch clamp and immunohistochemical approaches in juvenile cre-dependent transgenic mice that express tdTomato in all interneurons (VGAT-Cre; Ai9). At an anatomical level, we found that near the injury site there was no change in the global interneurons population (Ai9) but a select loss of expression of the calcium binding protein parvalbumin (PV). At a functional level, PV expressing neurons primarily have a fast-spiking (FS) electro-physiological phenotype. In FS interneurons, TBI induced a decrease in the frequency of spontaneous inhibitory postsynaptic currents (sIPSCs) while increasing the amplitude of spontaneous excitatory postsynaptic currents (sEPSCs). These results suggest that there is significant reorganization of the inhibitory cortical network in the pediatric brain after controlled cortical impact, resulting in greater excitatory drive and decreased inhibition onto FS neurons.

Introduction

The pediatric population is the most "at risk" group for receiving a traumatic brain injury (TBI) with nearly 1 million annual emergency room visits in the United States (Pearson et al., 2012a). TBI remains the leading cause of death and disability in children and often leads to development of lifelong cognitive and behavioral deficits (Annegers et al., 1998; Barlow et al., 2000; Caveness et al., 1979). Traumatic brain injury (TBI) represents a continuum ranging from mild to severe, with probability of adverse outcome increasing with injury severity (Adelson, 1999). Emerging research suggests that the pediatric brain has unique physiology that may have a profound effect on response and recovery to TBI. Pediatric TBI can have a negative impact on continued brain function and maturation that is unique from adult TBI (Anderson and Moore, 1995; Cook et al., 2014, 2014; Schmidt et al., 2012). Examination of TBI in adult animals has implicated reduction in GABAergic synaptic inhibition a major contributing factor to epileptogenesis after brain injury (Jin et al., 2011; Kobayashi et al., 2003). In addition, TBI in adult animals has been shown to induce loss of expression of known markers for multiple subtypes of interneurons and enhanced cortical excitability (Cantu et al., 2014). However, we have previously found that in juvenile mice after controlled cortical impact (CCI), synaptic excitation and inhibition onto pyramidal neurons is largely unchanged (Goddeyne et al., 2015; Nichols et al., 2015). This suggests the pathophysiology of TBI in juvenile animals may be distinct from adults.

To better understand TBI induced changes to cortical inhibition, it is important to understand which GABAergic subtypes are most vulnerable in the pediatric cortex. Cortical interneurons are a diverse population of cells with unique intrinsic and synaptic

properties (Rudy et al., 2011). Immunohistochemical markers have often been used to determine presence of interneuron subtypes, however, these approaches are unable to differentiate between a loss of immunoreactivity and loss of cell number (i.e. cell death). All GABAergic interneurons selectively express the vesicular GABA transporter (VGAT) (Wojcik et al., 2006). In this study, we use transgenic mice that express an endogenous fluorophore (tdTomato) wherever VGAT is present. This allows us to directly examine for TBI induced interneuron loss and functional changes to cortical inhibition. As previously reported, (Brody et al., 2007; Hunt et al., 2009; Nichols et al., 2015) severe TBI is effectively modeled using controlled cortical impact (CCI). Combined with whole-cell patch clamp and conventional immunohistochemical (IHC) approaches we quantified CCI induced changes to cortical interneurons. While CCI did not induce general interneuron loss, a significant reduction in expression of parvalbumin (PV) positive interneurons was observed. Parvalbumin positive interneurons are predominantly of a fast-spiking (FS) phenotype (Hu et al., 2014) and make up 40-50% of the inhibitory interneuron population (Rudy et al., 2011). FS interneurons are known to target somatic and proximal dendrites and provide powerful inhibition and regulation of action potential timing and output (Kinney et al., 2006).

Overall, the loss of PV in FS interneurons following CCI did not alter the intrinsic properties. However, there was a marked decrease in synaptic inhibition accompanied by an increase in excitatory synaptic events. These findings contrast with reports from adult animals (Cantu et al., 2014) and when taken along with our previous findings (Nichols et al., 2015)(Nichols et al., *In Preparation*) and recent human epidemiological reports (Anderson and Moore, 1995; Schmidt et al., 2012) suggest the response of the "pediatric"

brain to TBI is unique from adults and that age at injury is a critical factor determining the underlying pathophysiology.

Materials and Methods

CCI Injury

Juvenile mice (PID 14) were subjected to a severe controlled cortical impact as previously described (Hunt et al., 2009; Nichols et al., 2015). Mice were anesthetized with isoflurane (2%) and placed in a stereotaxic frame. Animal temperature was maintained and monitored for the duration of the surgery and until ambulatory post-surgery. The skull was exposed with a midline incision and a 5mm craniotomy was made lateral to the sagittal suture between bregma and lamda, over the right somatosensory region. Precaution was taken during the craniotomy not to disturb the underlying dura. A frontoparietal CCI (3mm diameter tip, 3.0 m/s, 2mm depth, 500ms duration) was performed using an electromagnetic cortical impactor (Hatteras Instruments, Cary, North Carolina). After the impact, the removed bone flap was placed over the site of injury and sealed with dental cement. Control animals were naïve, as previous reports have found that a craniotomy can cause an inflammatory response (Cole et al., 2010; Olesen, 1987)

Preparation of Brain Slices

On PID 14–19, the rats were deeply anaesthetized with inhalation of isoflurane and decapitated. The brain was rapidly removed and coronal slices (350 μm thick) prepared on a vibratome (VT 1200; Leica, Nussloch, Germany) as previously described (Anderson et al., 2010; Nichols et al., 2015). Slices were obtained from the somatosensory cortex that contained the injury site in CCI animals or from corresponding control cortex in sham animals. The site of CCI was readily identifiable in slices as

significant cavitation and tissue loss. Initial harvesting of brain slices was performed in an ice-cooled (4°C) carboxygenated (95% O_2, 5% CO_2) high sucrose solution containing the following (in mM): 234 sucrose, 11 glucose, 26 $NaHCO_3$, 2.5 KCl, 1.25 $NaH_2PO_4H_2O$, 10 MgS_47H_2O, 0.5 $CaCl_22H_2O$. Slices were then incubated for 1 h at 32°C in carboxygenated artificial CSF (aCSF) containing (in mM): 126 NaCl, 26 $NaHCO_3$, 2.5 KCl, 10 Glucose, 1.25 $Na_2H_2PO_4H_2O$, 1 $MgSO_47H_2O$, 2 $CaCl_2H_2O$, pH 7.4. Slices were then returned to room temperature before being moved to the recording chamber for whole-cell patch-clamp recording.

In Vitro Electrophysiological Recording

Coronal slices were prepared from CCI or sham animals were submerged in flowing carboxygenated aCSF heated to 32°C. Submerged slices were first visualized under 4× brightfield for identification of layer V cortex. For slices from impacted mice, recordings were made in the peri-injury zone within 2 mm of the injury-induced cavitation. Recordings from control slices were made in the corresponding cortex to the peri-injury zone of CCI animals. Whole-cell recordings were obtained from fast-spiking interneurons using an upright microscope (Axioexaminer; Carl-Zeiss, Thornwood, NY, USA) fitted with infrared differential interference contrast optics. Regular spiking (RS) pyramidal neurons were distinguished based on their current-clamp firing behavior (Guatteo et al., 1994). The electrode capacitance and bridge circuit were appropriately adjusted. The series resistance (R_s) of neurons chosen for analysis was <20% of membrane input resistance and monitored for stability. Membrane potential was not corrected for a calculated 10 mV liquid junction potential. A Multiclamp 700 A patch-clamp amplifier (Axon Instruments, Union City, CA, USA) was used for both current-

and voltage-clamp mode. Recordings were obtained at 32°C using borosilicate glass microelectrodes (tip resistance, 2.5–3.5 MΩ). For excitatory recordings, electrodes were filled with an intracellular solution containing (in mM): 135 KGluconate, 4 KCl, 2 NaCl, 10 HEPES, 4 EGTA, 4 Mg ATP, 0.3 Na TRIS. For recording of inhibitory events, an intracellular solution containing the following was used (in mM): 70 KGluconate, 70 KCl, 2 NaCl, 10 HEPES, 4 EGTA, 4 Mg ATP, 0.3 GTP. This internal solution has been used previously (Anderson et al., 2010; Nichols et al., 2015) and shown to facilitate detection of inhibitory events. The calculated E_{Cl} was approximately −16 mV, resulting in inward $GABA_A$ currents at a holding potential of −70 mV. Inhibitory events were pharmacologically isolated by bath application of 2-Amino-5-phosphonopentanoic acid (d-APV; 50 μM) and 6,7-dinitroquinoxaline-2,3-dione (DNQX, 20 μM).

Immunohistochemistry

At PID 14 mice underwent cardiac perfusion using 4% paraformaldehyde. Brains were extracted and place in 4% paraformaldehyde for post fixation for 24 hours before being sectioned. Immunohistochemistry was performed using 60μm free floating vibratome sections of brains were collected in PBS, blocked with 5% normal serum in TBS with 0.1% Triton X-100, and incubated with primary antibodies in blocking solution overnight at 4°C. The following primary antibodies were used in our study: anti-NeuN (1:1000, Chemicon), anti-parvalbumin (1:1000, SWant), anti-somatostatin (1:1000, SWant), DAPI (1:2000, Roche). After rinsing, sections were then incubated with Alexa conjugated secondary antibodies (Invitrogen) overnight at 4°C, rinsed 3 times in PBS, and mounted with Vectashield (Vector Labs).

Image Acquisition and Data Analysis

Images were collected on a Leica SP5 and Zeiss 710 laser scanning confocal microscope using 10X or 20X objectives. Single fields were tiled together to generate high-resolution images of whole brain coronal sections. Images were corrected for brightness and contrast in Photoshop. For assessment of Parvalbumin neuron density, we defined a region of interest (ROI), 350um wide that expanded all cortical layers and was perpendicular to the white matter. The ROI was positioned 3.15mm lateral to midline on the contralateral hemisphere, positioned over the peri-injury site. The area immediately adjacent to the injury (peri-injury) was examined using ROIs which were extended across all cortical layers and 350um lateral from the edge of the injury. Data obtained from ROIs from CCI animals were compared to corresponding areas in control animals. To determine density, the area of cortex within the ROI from three separate coronal sections was measured and the number of Parvalbumin or Somatostatin labeled soma was manually assayed. For assessment of Ai9 and NeuN density, single channel images from three separate sections were imported into ImageJ, manually thresholded, and the watershed algorithm was applied. The analyze particle plugin was employed using a minimal particle size of 70 pixels^2 for Ai9. The number of labeled neurons and the size of Ai9$^+$ soma were recorded. For PV and SST, somal size was manually measured in Photoshop. Results were averaged from at least three independent mice from separate litters from control or CCI mice (Hunt et al., 2009; Nichols et al., 2015).

Results

Inhibitory Interneuron (Ai9) Cell Density was Unchanged after CCI

To quantify CCI induced changes in total neuron and inhibitory neuron number in the cortex, we performed IHC staining using the neuron specific marker NeuN or

examination of the transgenic fluorescently labeled interneurons with tdTomato. CCI was performed on juvenile VGAT-Cre;Ai9 mice at post-natal day 22. Animals were sacrificed 14 days after CCI (post-injury day 14), coronal brain slices cut from control or CCI mice and confocal images taken. As previously reported, CCI induced ablates motor and most of somatosensory region, as well as resulting in severe damage of the hippocampus (Fig. 1) (Hunt et al., 2009; Nichols et al., 2015). Previous reports have indicated that TBI may induce cortical thinning (i.e. atrophy) (Michael et al., 2015; Wilde et al., 2012). However, following CCI we noted only a small decrease in the thickness of the cortex when comparing CCI (1093.83 ± 56.33 CCI) with control (1219.27 ± 21.98 control) that failed to reach significance (P=0.13). To examine for changes in the total neuronal population we next examined immunoreactivity of the pan-neuronal marker NeuN. CCI induced change in total number of NeuN positive cells (912.7 ± 69.47 control, 706.7 ± 41.29 CCI) (p = 0.02). However, when adjusted for small changes in effective area by using cell density no significant difference was detected between CCI and control animals (232.1 ± 10.55 control, 221.3 ± 7.37 CCI)(P=0.15). This data suggest that outside of the direct injury zone CCI induces very little neuronal loss.

Next, to isolate changes in the interneuron population we examined CCI induced changes to the endogenously labeled Ai9 positive population of neurons. In contrast to the total neuronal population marked trend was observed following CCI whereby total Ai9 positive cells were reduced (160.90 ± 5.27 control, 112.67 ± 17.39 CCI)(P=0.057). However, Ai9 cell density was not significantly different (62.43 ± 3.25 control, 56.23± 2.94 CCI) were reduced (P=0.23)(Fig. 1B). The reduction of total Ai9 neurons without a commensurate change in Ai9 density may reflect the influence of the observed small

change in cortical thickness. . These experiments confirmed that although the peri-injury zone is often a site from which seizure activity develops (Friedman et al., 2009), at PID 14 in the pediatric brain there is no change in the total number of neurons. However, the total interneuron population trended towards being reduced by 30% and cell density by 10%. As VGAT is expressed in nearly all interneurons our use of a Vgat:Cre; Ai9 transgenic mouse allowed us to directly examine for changes in the global interneuron population versus traditional immunoreactivity approaches. However, the trend in the data suggested the possibility of a significant change in a subtype of cortical interneuron.

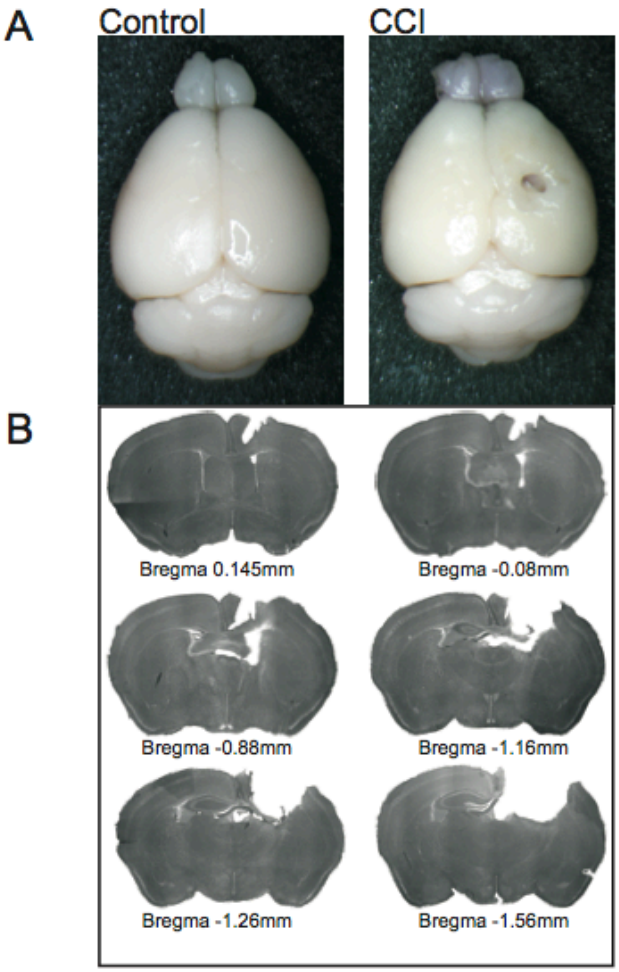

Figure 1. CCI Induces loss of cortical tissue. (A) Example figures of perfused control and CCI mice brains. (B) Serial images of 60um slices showing extent of injury and CCI at Bregma coordinates.

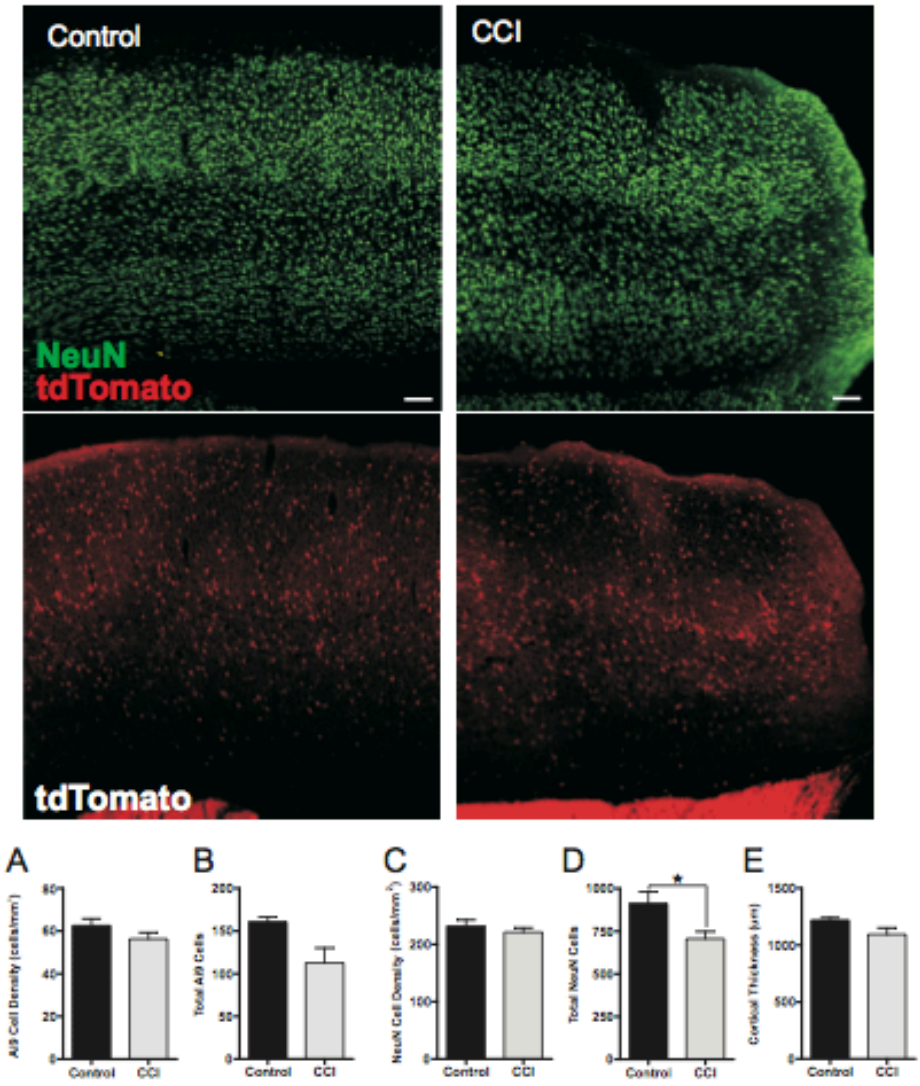

Figure 2. Ai9 cell density is unchanged in the peri-injury zone after CCI. (Top) NeuN (green) is qualitatively similar between control and CCI. (Bottom) Ai9 (red) distribution is not altered after CCI. NeuN and Ai9 show to be unchanged throughout injury zone. (n=3) (A) Quantitative analysis shows that Ai9 density is unchanged. (B) Total Ai9 cells are not changed between control and CCI. (C) NeuN cell density is not changed. (D) NeuN total cells are significantly down after injury. (n=3, P=0.04). (E) Cortical height, measured at the peri-injury region, is similar between control and CCI animals. (n=3).

Parvalbumin Expression is Reduced Following CCI

Cortical interneurons are a varied population of neurons with unique physiological roles (Gupta et al., 2000). No single classification system can uniquely identify the numerous subtypes but they can be effectively segregated based on the presence of unique calcium chelator proteins (Rudy et al., 2011). In the cortex, the two principal interneuron subtypes are parvalbumin (PV) (40-50%) and somatostatin (SST)(~30%) (Markram et al., 2004b). To directly examine for potential CCI induced changes in interneuron subtypes we examined for changes in expression of PV and SST in VGAT:Cre; Ai9 mice using standard immunohistochemical approaches. Parvalbumin neurons have been implicated in a number of neurological diseases (Hu et al., 2014). Specifically, it has been shown that PV deficiency in the cortex can increase epileptic seizure susceptibility (Schwaller et al., 2004) and is reduced in the schizophrenic brain (Lewis et al., 2012). Intracellularly, PV plays a critical role in preventing synaptic facilitation and maintaining rhythmic firing in fast-spiking interneurons (Orduz et al., 2013). To examine for CCI induced changes in PV expression we again sacrificed animals 14 days after CCI and harvested coronal cortical slices for IHC processing. Examination of the peri-injury zone revealed a dramatic reduction in expression of PV. We found that CCI significantly reduced the overall number of PV cells (control 35.11 ± 0.11 versus CCI 8.60 ± 1.09) ($P<0.0001$). In addition, the density of PV positive neurons was reduced by over 71% ($p<0.0001$)(Fig. 2, A). Finally, we examined if CCI induced changes in PV expression were correlated with distance from the site of the injury. We extended 100um bins radially from the site of injury for 1mm. In comparison to control

values, the density of PV expressing neurons was significantly decreased by CCI across the entire range. Within the data collected from the CCI data, PV density was more reduced closer to the site of injury (Fig 3C). This suggests that CCI induces both a focal and more generalized loss of PV expression.

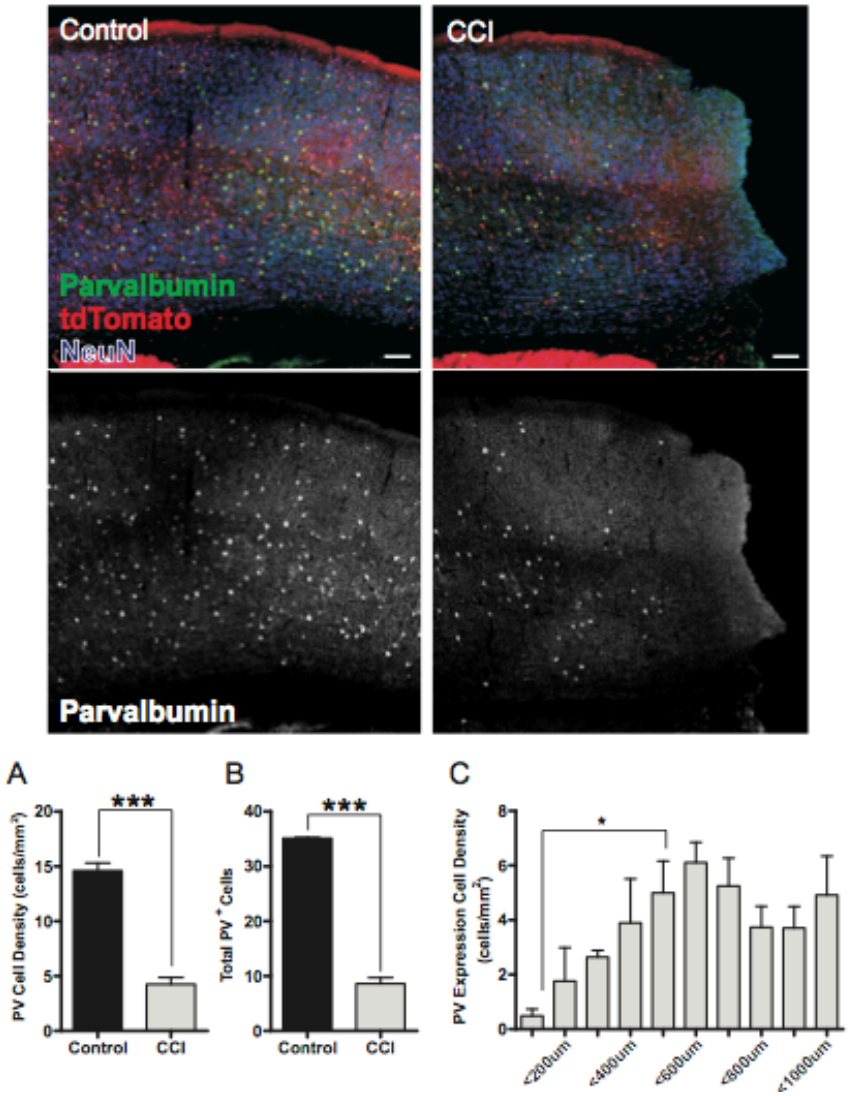

Figure 3. Parvalbumin immunoreactivity is reduced after CCI. (Top) Peri-injury regions with parvalubumin (Green), Ai9 (tdTomato), and NeuN (Blue). (Bottom) Immunostaining of parvalbumin shows loss of expression after injury. (A) Quantification of parvalbumin density is significantly reduced after CCI. (n=3) ***$p<0.0001$, unpaired Student's t-test. (B) Total cells with parvalbumin expression was analyzed in control and CCI, and quantitatively displays no significant differences. (n=3). (C) Distal analysis with 100um wide columns was used to analyze changes in parvalbumin expression in relation to injury. PV expression loss was greatest near the injury site (One-way Anova, *$p<0.05$). Scale bar = 100um.

Somatostatin Expression is not Altered by CCI

Second to PV, SST interneurons are the second most abundant subtype in the cortex. (Markram et al., 2004b). Using a similar approach to that detailed for PV expression changes, we examined for changes in SST expression in the peri-injury after injury. In contrast to PV, we found that CCI induced no statistically significant difference in SST cell number (control 44.89 ± 8.39 versus 33.00 ± 1.35) (P=0.23) or cell density (16.79 ± 14.56 control, 14.56 ± 1.57 CCI) when compared to control animals (P=0.60)(Fig. 3, A). A regional analysis relative to the site of injury again was again performed and revealed no statistically significant difference in SST cell density relative to the injury site or in comparison with values for control animals (Fig 4, A-B). Taken together, these results suggest that CCI does not induce overall loss of interneurons or SST expression but only selectively induces loss of PV expression in interneurons.

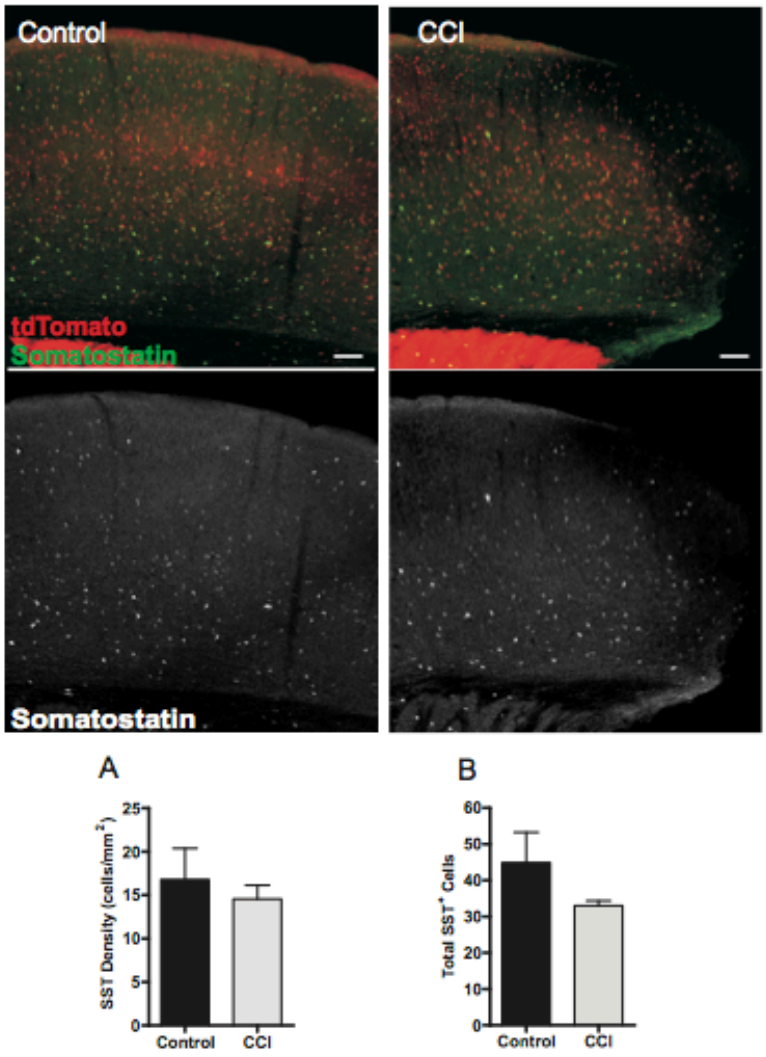

Figure 4. CCI does not alter the density of somatostatin neurons in the cortex after CCI. (Top) Control slice with co-labelling of Ai9 interneurons (red) and somatostatin interneurons (green). (Bottom) Immunostaining of somatostatin interneurons reveals no change in number after injury. (A) Quantification of somatostatin density in the peri-injury region between control and CCI animals shows no change. (B) Quantification of somatostatin interneuron total cells is not different between control and CCI animals. Scale bar = 100um.

Fast-spiking Interneurons are not Altered Following CCI

As another mechanism of identification, electrophysiological firing patterns effectively distinguish cortical interneuron subtypes (Kawaguchi and Kondo, 2002). PV positive interneurons are predominantly fast-spiking (FS) (Galarreta and Hestrin, 1999). PV is thought to play a important role in the functional properties of FS interneurons including maintenance of spike timing (Kinney et al., 2006) and rhythmic firing (Orduz et al., 2013). Consequently, the selective loss of PV expression in the peri-injury led us to investigate if CCI alters the intrinsic properties of fast-spiking interneurons. We performed whole cell patch clamp experiments in the peri-injury zone of coronal brain slices taken from Vgat:Cre; Ai9 mice 14 days after CCI or in corresponding control cortex. Neurons were first visually identified through DIC bright field imaging and confirmed to be Ai9 positive. Under current clamp, neurons were verified to have a FS firing pattern as previously described (Anderson et al., 2010; Hu et al., 2014)(Fig 4.A). Intrinsic properties of FS interneurons from control and CCI mice were examined and found to be not statistically different. This included resting membrane potential, input resistance and firing frequency (Fig 4. C-E). In a subset of neurons (n=11) we intra-cellularly labelled neurons with biocytin for post hoc analysis. These electro-physiologically identified FS neurons were confirmed to be Ai9 positive but as compared to a control neuron were all PV negative (Fig. 4, B). The intrinsic properties of the CCI PV^{-}-FS interneurons did not differ from control PV^{+}-FS interneurons. These findings confirmed that the FS interneuron phenotype remains in the peri-injury zone and that the loss of PV expression has no significant effect on the intrinsic membrane properties tested.

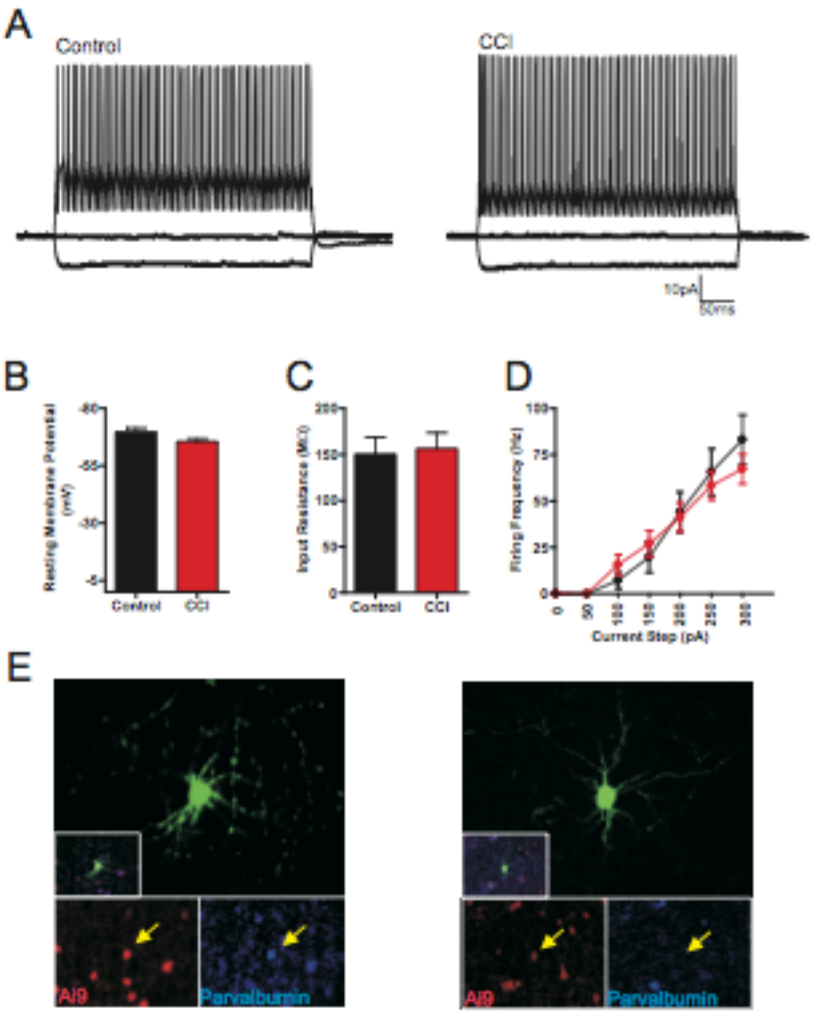

Figure 5. Fast-spiking interneurons do not have altered intrinsic properties after CCI. (A) Firing patterns at a 250pA current step does not elicit different firing patterns between control and CCI. (B) Resting membrane potential of fast-spiking interneurons is similar among control and CCI animals. (C) Input resistance of fast-spiking interneurons is not changed after CCI. (D) Analysis of firing frequency shows that CCI does not differ from control. (E) Biocytin fills with immunostaining for parvalbumin show that fast-spiking interneurons, indicated by the Ai9, lose parvalbumin expression after CCI.

CCI Reduces Inhibitory sIPSC Frequency and Increases Synaptic Kinetics

To examine for changes in synaptic inhibition we recorded spontaneous inhibitory post-synaptic currents (sIPSCs) onto layer V FS interneurons 14 days after CCI or from age-matched control animals. sIPSCs were pharmacologically isolated by bath application of the glutamate receptor antagonist kynurenic acid (2mM). A modified internal solution (Ecl=-16mV) was also used as previously described (Anderson et al., 2010) to increase detection of inhibitory synaptic events. We found that CCI significantly reduced the frequency of sIPSCs over 54% from 4.34 ± 0.75 (n=10) to 1.96 ± 0.33 (n=15) (P=0.004). No significant change was observed in the amplitude or charge of sIPSCs. However, the kinetics of the sIPSCs were significantly altered by CCI as both the rise (P=0.03) and decay (P=0.03) time were significantly increased. This suggests that CCI primarily induces a loss of inhibition onto FS interneurons.

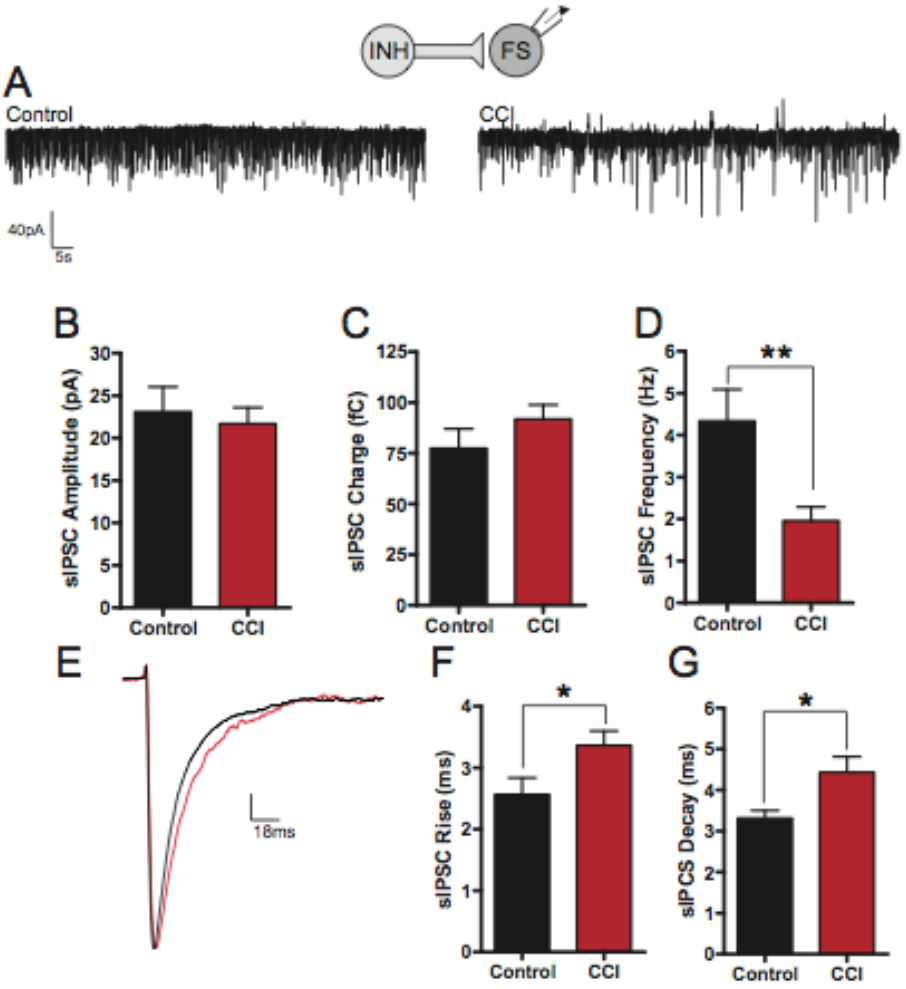

Figure 6. Spontaneous IPCSs are decreased after CCI, and synaptic rise and decay times are increased after injury. (A) Gap-free traces in voltage clamp, holding at -70mV, recording sIPSCs from fast-spiking interneurons. (B&C) sIPSCs of CCI animals did not show a change compared to control. (D) Frequency of sIPSC events was significantly reduced after injury. ** p=0.0035. (E) Overlaid normalized average sIPSC after injury demonstrates the increased rise and decay time. (F) sIPSC rise time is significantly increased after injury. * p=0.03. (G) sIPSC decay time is significantly increased after injury. * p=0.03. (control n=10, CCI n=15)

Excitatory sEPSC Amplitude and Charge Increase after CCI

Finally, we examined for changes in excitatory input onto FS interneurons by recording spontaneous post-synaptic currents (sPSCs). For these experiments, a physiological internal was used (ECl = -80mV) that allowed detection of inward glutamatergic events isolated from outward GABAergic synaptic events. As previously reported (Nichols et al., 2015), excitatory activity was not pharmacologically isolated as blocking GABAergic activity may disinhibit the network and alter the ability to record CCI induced changes directly. Whole cell recording of sPSCs in FS interneurons revealed a statistically significant increase in the amplitude ($P=0.0009$) and charge ($P<0.0001$) of excitatory sPSCS following CCI as compared to control recordings ($n=13$)(Fig. 6). In contrast to inhibitory sPSCs, no change in the frequency of events, or decay and rise time were observed (Fig. 6). This suggests that CCI induces an increase in the strength of excitation onto FS interneurons.

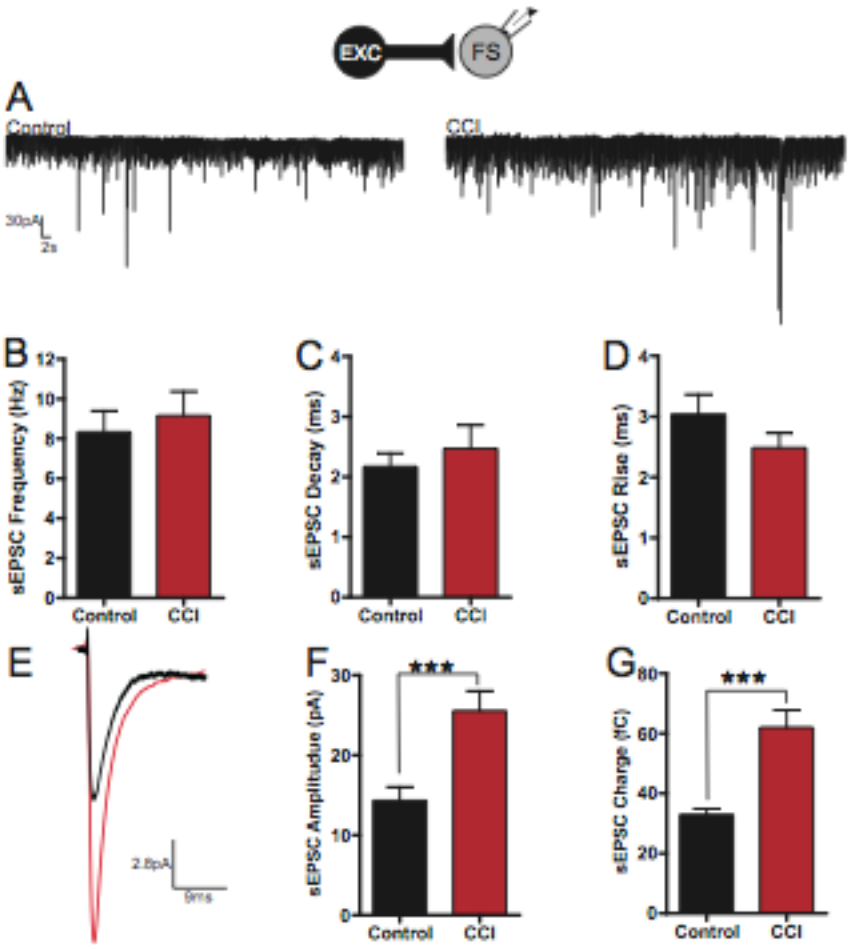

Figure 7. CCI results in increased synaptic excitatory input onto fast-spiking neurons. (A) Gap-free voltage clamp traces, holding at -70mV, from fast-spiking interneurons monitoring sEPSCs in control and CCI. (B-D) sEPSC frequency, decay, and rise time were not changed after injury. (E) Overlaid averaged sEPSCs demonstrate the dramatic change in amplitude after CCI. (F) Quantitatively sEPSC amplitude is significantly increased after injury. *** p=0.0009. (G) Charge transfer after injury significantly increased after injury. p<0.0001. (Control n=13, CCI n=12).

Discussion

We analyzed for changes in cortical interneurons and intrinsic and synaptic physiology of genetically labeled cortical fast-spiking (FS) parvalbumin (PV) expressing GABAergic interneurons 14 days after in pediatric mice. Previous studies have assayed adult TBI and/or subcortical regions after injury (Cantu et al., 2014; Card et al., 2005; Hall et al., 2005a; Hunt et al., 2011), however ours is the first to analyze cortical inhibitory neurons in transgenic pediatric mice. In doing so, we were able to reveal by 14 days after injury a loss of PV expression without a loss of interneurons and that these PV-FS neurons had altered synaptic activity. We found that by 14 days after injury, pediatric mice showed no loss of interneurons, but a 75% reduction in PV expression. When FS neurons were examined for electrophysiological properties after injury, they received a significant reduction in inhibition. Synaptic excitation onto FS neurons showed an increase in synaptic strength (i.e. amplitude and charge). Despite FS neurons showing synaptic changes and PV expression, intrinsic properties remained unchanged after CCI. Our observations likely reflect that TBI leads to anatomical and neurophysiological network remodeling of the interneuron network in the peri-injury region after CCI.

Overall cortical density neurons (NeuN) and interneurons (Ai9) were not reduced by 14 days after injury. This is in contrast to other TBI studies that have examined for interneuron loss in the hippocampus (Ding et al., 2011; Huusko et al., 2015; Lowenstein et al., 1992; Pavlov et al., 2011). However, to investigate interneuron subtype changes, we analyzed for PV and SST. Despite no reduction in SST density, we did find PV expression was significantly reduced. Loss of PV expression has been shown in humans after TBI (Buriticá et al., 2009) and animal models (Cabungcal et al., 2013a, 2013b). Our

select loss of PV differentiates from adults where more global changes in the inhibitory network have been observed by showing a loss of PV and SST (Cantu et al., 2014). However, this study focused more on adult CCI. Our study provides a novel approach by using transgenic mice with fluorescent labeling of interneurons provides an advantage of being able to differentiate between expression loss and neuronal loss not detected in the previously mentioned studies.

It has been shown that PV neurons have an electrophysiological fast-spiking phonotype (Kawaguchi and Kubota, 1997; Kawaguchi et al., 1987). To electrophysiologically characterize FS neurons after CCI, we performed whole-cell patch clamp 14 days after injury. We found that FS neurons did not show a change in intrinsic properties. Synaptically, we found that FS neurons received less frequent inhibition and a change in sIPSC kinetics (i.e. increased rise and decay time). These results have been seen in GABAergic dentate hilar cells after CCI in adult mice (Hunt et al., 2011). sEPSC onto FS neurons showed greater synaptic strength with increased amplitude and charge after CCI. Increased excitatory synaptic activity has been seen onto pyramidal neurons of the peri-injury region after CCI (Almeida-Suhett et al., 2015; Cantu et al., 2014). These results suggest that CCI induces increased excitability and decreased inhibition onto FS neurons.

The select vulnerability of PV-FS neurons after CCI and their contribution to the pathology of TBI remains speculative. However, previous injury models have implicated inhibitory FS neurons in contributing to post injury hyperexcitability (Jin et al., 2014; Ma and Prince, 2012). FS have unique physiological properties that may make them more sensitive to TBI. First, FS spike fast and have unique NaKATPase, maybe unique

metabolic demands (Anderson et al., 2010; Cabungcal et al., 2013a). FS have perineuronal nets that protect against oxidative stress when they are fully condensed during maturity (Cabungcal et al., 2013a; Morris and Henderson, 2000; Orlando and Raineteau, 2015). However, in juvenile animals (P20) these nets are not fully mature and may sensitize PV interneurons. In fact, overproduction of superoxides have been shown to NMDA dependently reduce PV immunoreactivity without inducing cell death (Behrens et al., 2007; Cabungcal et al., 2013a; Goldberg et al., 2003; Kinney et al., 2006; Powell et al., 2012; Zhang et al., 2012).

The findings of this study suggest that PV-FS interneurons in juvenile animals are differentially affected and sensitive to traumatic brain injury. In contrast to the loss of both PV and SST interneurons observed previously in adult TBI, the selective loss of PV-FS neurons observed in the juvenile mice that underwent CCI in the present study suggests that interneuron sensitivity to injury is developmentally regulated. PV-FS interneurons play a vital role in cortical function. Disruption of PV-FS functioning may play an important role in the recovery and outcomes following TBI. Taken together the data suggest that sTBI may surprisingly disinhibit FS cortical interneurons. At present, elucidating if PV expression loss and disinhibition are adaptive or maladaptive responses to injury remains to be determined. Identifying novel pathophysiological mechanisms that may be targeted is of critical importance to developing targeted therapeutic approaches.

References

Adelson, P.D. (1999). Animal models of traumatic brain injury in the immature: a review. Exp. Toxicol. Pathol. Off. J. Ges. Für Toxikol. Pathol. *51*, 130–136.

Anderson, V., and Moore, C. (1995). Age at injury as a predictor of outcome following pediatric head injury: A longitudinal perspective. Child Neuropsychol. *1*, 187–202.

Anderson, T.R., Huguenard, J.R., and Prince, D.A. (2010). Differential effects of Na+-K+ ATPase blockade on cortical layer V neurons. J. Physiol. *588*, 4401–4414.

Annegers, J.F., Hauser, W.A., Coan, S.P., and Rocca, W.A. (1998). A population-based study of seizures after traumatic brain injuries. N. Engl. J. Med. *338*, 20–24.

Atallah, B.V., Bruns, W., Carandini, M., and Scanziani, M. (2012). Parvalbumin-Expressing Interneurons Linearly Transform Cortical Responses to Visual Stimuli. Neuron *73*, 159.

Barlow, K.M., Spowart, J.J., and Minns, R.A. (2000). Early posttraumatic seizures in non-accidental head injury: relation to outcome. Dev. Med. Child Neurol. *42*, 591–594.

Brody, D.L., Mac Donald, C., Kessens, C.C., Yuede, C., Parsadanian, M., Spinner, M., Kim, E., Schwetye, K.E., Holtzman, D.M., and Bayly, P.V. (2007). Electromagnetic controlled cortical impact device for precise, graded experimental traumatic brain injury. J. Neurotrauma *24*, 657–673.

Buriticá, E., Villamil, L., Guzmán, F., Escobar, M.I., García-Cairasco, N., and Pimienta, H.J. (2009). Changes in calcium-binding protein expression in human cortical contusion tissue. J. Neurotrauma *26*, 2145–2155.

Caillard, O., Moreno, H., Schwaller, B., Llano, I., Celio, M.R., and Marty, A. (2000). Role of the calcium-binding protein parvalbumin in short-term synaptic plasticity. Proc. Natl. Acad. Sci. U. S. A. *97*, 13372–13377.

Cantu, D., Walker, K., Andresen, L., Taylor-Weiner, A., Hampton, D., Tesco, G., and Dulla, C.G. (2014). Traumatic Brain Injury Increases Cortical Glutamate Network Activity by Compromising GABAergic Control. Cereb. Cortex N. Y. N 1991.

Caveness, W.F., Meirowsky, A.M., Rish, B.L., Mohr, J.P., Kistler, J.P., Dillon, J.D., and Weiss, G.H. (1979). The nature of posttraumatic epilepsy. J. Neurosurg. *50*, 545–553.

Cole, J.T., Yarnell, A., Kean, W.S., Gold, E., Lewis, B., Ren, M., McMullen, D.C., Jacobowitz, D.M., Pollard, H.B., O'Neill, J.T., et al. (2010). Craniotomy: True Sham for Traumatic Brain Injury, or a Sham of a Sham? J. Neurotrauma *28*, 359–369.

Colicos, M.A., Dixon, C.E., and Dash, P.K. (1996). Delayed, selective neuronal death following experimental cortical impact injury in rats: possible role in memory deficits.

Brain Res. *739*, 111–119.

Cook, L.G., Chapman, S.B., Elliott, A.C., Evenson, N.N., and Vinton, K. (2014). Cognitive Gains from Gist Reasoning Training in Adolescents with Chronic-Stage Traumatic Brain Injury. Front. Neurol. *5*.

Ding, M.-C., Wang, Q., Lo, E.H., and Stanley, G.B. (2011). Cortical excitation and inhibition following focal traumatic brain injury. J. Neurosci. Off. J. Soc. Neurosci. *31*, 14085–14094.

Friedman, D., Claassen, J., and Hirsch, L.J. (2009). Continuous electroencephalogram monitoring in the intensive care unit. Anesth. Analg. *109*, 506–523.

Galarreta, M., and Hestrin, S. (1999). A network of fast-spiking cells in the neocortex connected by electrical synapses. Nature *402*, 72–75.

Goddeyne, C., Nichols, J., Wu, C., and Anderson, T. (2015). Repetitive mild traumatic brain injury induces ventriculomegaly and cortical thinning in juvenile rats. J. Neurophysiol. *113*, 3268–3280.

Guatteo, E., Bacci, A., Franceschetti, S., Avanzini, G., and Wanke, E. (1994). Neurons dissociated from neocortex fire with “burst” and “regular” trains of spikes. Neurosci. Lett. *175*, 117–120.

Gupta, A., Wang, Y., and Markram, H. (2000). Organizing principles for a diversity of GABAergic interneurons and synapses in the neocortex. Science *287*, 273–278.

Hensch, T.K. (2005). Critical period plasticity in local cortical circuits. Nat. Rev. Neurosci. *6*, 877–888.

Hu, H., Gan, J., and Jonas, P. (2014). Fast-spiking, parvalbumin+ GABAergic interneurons: From cellular design to microcircuit function. Science *345*, 1255263.

Hunt, R.F., Scheff, S.W., and Smith, B.N. (2009). Posttraumatic epilepsy after controlled cortical impact injury in mice. Exp. Neurol. *215*, 243–252.

Huusko, N., Römer, C., Ndode-Ekane, X.E., Lukasiuk, K., and Pitkänen, A. (2015). Loss of hippocampal interneurons and epileptogenesis: a comparison of two animal models of acquired epilepsy. Brain Struct. Funct. *220*, 153–191.

Jin, X., Prince, D.A., and Huguenard, J.R. (2006). Enhanced Excitatory Synaptic Connectivity in Layer V Pyramidal Neurons of Chronically Injured Epileptogenic Neocortex in Rats. J. Neurosci. *26*, 4891–4900.

Jin, X., Huguenard, J.R., and Prince, D.A. (2011). Reorganization of inhibitory synaptic circuits in rodent chronically injured epileptogenic neocortex. Cereb. Cortex N. Y. N 1991 *21*, 1094–1104.

Jin, X., Jiang, K., and Prince, D.A. (2014). Excitatory and Inhibitory Synaptic Connectivity to Layer V Fast-spiking Interneurons in the Freeze Lesion Model of Cortical Microgyria. J. Neurophysiol.

Kawaguchi, Y. (1997). Selective cholinergic modulation of cortical GABAergic cell subtypes. J. Neurophysiol. *78*, 1743–1747.

Kawaguchi, Y., and Kondo, S. (2002). Parvalbumin, somatostatin and cholecystokinin as chemical markers for specific GABAergic interneuron types in the rat frontal cortex. J. Neurocytol. *31*, 277–287.

Kawaguchi, Y., Katsumaru, H., Kosaka, T., Heizmann, C.W., and Hama, K. (1987). Fast spiking cells in rat hippocampus (CA1 region) contain the calcium-binding protein parvalbumin. Brain Res. *416*, 369–374.

Kinney, J.W., Davis, C.N., Tabarean, I., Conti, B., Bartfai, T., and Behrens, M.M. (2006). A specific role for NR2A-containing NMDA receptors in the maintenance of parvalbumin and GAD67 immunoreactivity in cultured interneurons. J. Neurosci. Off. J. Soc. Neurosci. *26*, 1604–1615.

Kobayashi, M., Wen, X., and Buckmaster, P.S. (2003). Reduced inhibition and increased output of layer II neurons in the medial entorhinal cortex in a model of temporal lobe epilepsy. J. Neurosci. Off. J. Soc. Neurosci. *23*, 8471–8479.

Larner, S.F., McKinsey, D.M., Hayes, R.L., and W. Wang, K.K. (2005). Caspase 7: increased expression and activation after traumatic brain injury in rats. J. Neurochem. *94*, 97–108.

Letzkus, J.J., Wolff, S.B.E., Meyer, E.M.M., Tovote, P., Courtin, J., Herry, C., and Lüthi, A. (2011). A disinhibitory microcircuit for associative fear learning in the auditory cortex. Nature *480*, 331–335.

Lewis, D.A., Curley, A.A., Glausier, J., and Volk, D.W. (2012). Cortical Parvalbumin Interneurons and Cognitive Dysfunction in Schizophrenia. Trends Neurosci. *35*, 57–67.

Lowenstein, D.H., Thomas, M.J., Smith, D.H., and McIntosh, T.K. (1992). Selective vulnerability of dentate hilar neurons following traumatic brain injury: a potential mechanistic link between head trauma and disorders of the hippocampus. J. Neurosci. Off. J. Soc. Neurosci. *12*, 4846–4853.

Ma, Y., and Prince, D.A. (2012). Functional alterations in GABAergic fast-spiking interneurons in chronically injured epileptogenic neocortex. Neurobiol. Dis. *47*, 102–113.

Markram, H., Toledo-Rodriguez, M., Wang, Y., Gupta, A., Silberberg, G., and Wu, C. (2004). Interneurons of the neocortical inhibitory system. Nat. Rev. Neurosci. *5*, 793–807.

Nichols, J., Perez, R., Wu, C., Adelson, P.D., and Anderson, T. (2015). Traumatic Brain Injury Induces Rapid Enhancement of Cortical Excitability in Juvenile Rats. CNS Neurosci. Ther. *21*, 193–203.

Olesen, S.P. (1987). Leakiness of rat brain microvessels to fluorescent probes following craniotomy. Acta Physiol. Scand. *130*, 63–68.

Orduz, D., Bischop, D.P., Schwaller, B., Schiffmann, S.N., and Gall, D. (2013). Parvalbumin tunes spike-timing and efferent short-term plasticity in striatal fast spiking interneurons. J. Physiol. *591*, 3215–3232.

Pavlov, I., Huusko, N., Drexel, M., Kirchmair, E., Sperk, G., Pitkänen, A., and Walker, M.C. (2011). Progressive loss of phasic, but not tonic, GABAA receptor-mediated inhibition in dentate granule cells in a model of post-traumatic epilepsy in rats. Neuroscience *194*, 208–219.

Pearson, W.S., Ovalle, F., Faul, M., and Sasser, S.M. (2012). A review of traumatic brain injury trauma center visits meeting physiologic criteria from The American College of Surgeons Committee on Trauma/Centers for Disease Control and Prevention Field Triage Guidelines. Prehospital Emerg. Care Off. J. Natl. Assoc. EMS Physicians Natl. Assoc. State EMS Dir. *16*, 323–328.

Prinz, A., Selesnew, L.-M., Liss, B., Roeper, J., and Carlsson, T. (2013). Increased excitability in serotonin neurons in the dorsal raphe nucleus in the 6-OHDA mouse model of Parkinson's disease. Exp. Neurol. *248*, 236–245.

Rudy, B., Fishell, G., Lee, S., and Hjerling-Leffler, J. (2011). Three Groups of Interneurons Account for Nearly 100% of Neocortical GABAergic Neurons. Dev. Neurobiol. *71*, 45–61.

Schmidt, A.T., Hanten, G.R., Li, X., Vasquez, A.C., Wilde, E.A., Chapman, S.B., and Levin, H.S. (2012). Decision making after pediatric traumatic brain injury: trajectory of recovery and relationship to age and gender. Int. J. Dev. Neurosci. Off. J. Int. Soc. Dev. Neurosci. *30*, 225–230.

Schwaller, B., Tetko, I.V., Tandon, P., Silveira, D.C., Vreugdenhil, M., Henzi, T., Potier, M.-C., Celio, M.R., and Villa, A.E.P. (2004). Parvalbumin deficiency affects network properties resulting in increased susceptibility to epileptic seizures. Mol. Cell. Neurosci. *25*, 650–663.

Sohal, V.S., Zhang, F., Yizhar, O., and Deisseroth, K. (2009). Parvalbumin neurons and gamma rhythms enhance cortical circuit performance. Nature *459*, 698–702.

Uhlhaas, P.J., and Singer, W. (2010). Abnormal neural oscillations and synchrony in schizophrenia. Nat. Rev. Neurosci. *11*, 100–113.

Wilson, N.R., Runyan, C.A., Wang, F.L., and Sur, M. (2012). Division and subtraction

by distinct cortical inhibitory networks in vivo. Nature *488*, 343–348.

Wöhr, M., Orduz, D., Gregory, P., Moreno, H., Khan, U., Vörckel, K.J., Wolfer, D.P., Welzl, H., Gall, D., Schiffmann, S.N., et al. (2015). Lack of parvalbumin in mice leads to behavioral deficits relevant to all human autism core symptoms and related neural morphofunctional abnormalities. Transl. Psychiatry *5*, e525.

Wojcik, S.M., Katsurabayashi, S., Guillemin, I., Friauf, E., Rosenmund, C., Brose, N., and Rhee, J.-S. (2006). A shared vesicular carrier allows synaptic corelease of GABA and glycine. Neuron *50*, 575–587.

Yang, L., Benardo, L.S., Valsamis, H., and Ling, D.S.F. (2007). Acute injury to superficial cortex leads to a decrease in synaptic inhibition and increase in excitation in neocortical layer V pyramidal cells. J. Neurophysiol. *97*, 178–187.

van Zundert, B., Izaurieta, P., Fritz, E., and Alvarez, F.J. (2012). Early pathogenesis in the adult-onset neurodegenerative disease amyotrophic lateral sclerosis. J. Cell. Biochem. *113*, 3301–3312.

CHAPTER 4

CONTROLLED CORTICAL IMPACT RESULTS IN SELECTIVE LOSS OF INHIBITION IN CONTRALATERAL MOTOR CORTEX

Traumatic brain injury (TBI) affects over 1 in 5 children by 15 years of age and almost half a million emergency room visits each year. Deficits that can result from TBI range from cognitive dysfunction, to physical and emotional impairments that adversely affect the everyday life of a child. Previous work from our laboratory has shown that near the site of injury TBI causes a preferential loss of cortical inhibition. However, TBI patients often report symptoms related to dysfunction in brain areas contralateral to the site of injury. The consequence of TBI on the contralateral cortex remains poorly understood and is the focus of this study. Following unilateral TBI in juvenile mice, we examined the contralateral motor cortex for induced neuronal dysfunction. TBI was induced by controlled cortical impact (CCI) and animals examined for changes in inhibitory and excitatory neuronal activity 14 days after injury. First using transgenic mice (Vgat:Cre; Ai9) we determined that CCI induces a select loss of total interneurons in the motor cortex. We found that not only were total interneurons reduced, but CCI induced a select loss of expression of the interneuron specific marker parvalbumin without altering somatostatin expression. To assess the functional consequence of these changes we examined for alteration in excitatory and inhibitory synaptic activity onto onto layer 5 fast-spiking interneurons. Layer 5 fast-spiking interneurons where chosen for there powerful inhibitory input onto cortical pyramidal neurons (Yoshimura and Callaway, 2005) and have specifically been identified as potential regulators of corticospinal output (Tanaka et al., 2011). Following CCI a marked decrease in inhibition

and increase in excitation onto fast-spiking neurons in the motor cortex was observed. These results suggest that TBI leads to anatomical and neurophysiological remodeling, distant from the direct site of injury, in the contralateral motor cortex.

Introduction

Traumatic brain injury (TBI) is a leading cause of death and disability worldwide (Pearson et al., 2012b). It is recognized as a global health problem with significant negative social and economic implications (Maas et al., 2008; Menon et al., 2010). Children are the most at risk group for receiving a TBI and in the United States this results in over half a million injuries annually (Annegers et al., 1998; Barlow et al., 2000; Iudice and Murri, 2000; Kochanek et al., 2012). Recent evidence has shown that contrary to a popular belief, following a TBI younger children are more sensitive and have worse outcomes than adults (Adelson et al., 2003; Anderson and Moore, 1995; Schmidt et al., 2012). TBI is a significant risk factor for a number of neurological diseases and ailments, including epilepsy (Arango et al., 2012) and cognitive complications (Cook et al., 2014; Hall et al., 2005b; Schmidt et al., 2012). In addition, TBI often leads to impairments in locomotion and other motor function (Axelson et al., 2013; Cao et al., 1994; Fox et al., 1998; Fujimoto et al., 2004; Hamm et al., 1994). Even after a unilateral TBI, these motor impairments are often observed bilaterally suggesting the possibility of secondary injuries to the contralateral brain. A CCI injury in the frontoparietal brain region of the somatosensory cortex of the mouse cortex has been shown to have have axonal projecting fibers to the contralateral motor cortex (Oh, S.W., et al., 2014). Recent work in our laboratory has revealed that inhibitory interneurons are particularly sensitive to TBI

(Nichols et al., *In Preparation*). We examined if the same inhibitory network remodeling seen near the injury was present in the contralateral motor cortex.

Cortical interneurons are a heterogenous cell population with unique physiological, immunohistochemical, intrinsic and synaptic properties with distinct laminar distributions (Markram et al., 2004b). In this study we perform CCI in juvenile animals which cre-dependently express the fluorescent protein tdTomato in all inhibitory interneurons (Vgat:Cre; Ai9). Following CCI there is a marked loss of inhibitory interneurons in the contralateral motor cortex. Fast-spiking interneurons have been shown to be recruited during the execution of motor activity in awake animals, and the associated movement activity of fast-spiking neurons occurs at the same time or later than pyramidal neuron activity (Isomura et al., 2009). Also, it has been shown that corticospinal neurons receive the majority of their inhibitory input from fast-spiking neurons and the layer 5 fast-spiking neurons might serve as a feedback or lateral inhibition mechanism for corticospinal neurons by increasing time and spatial resolution of motor executions (Tanaka et al., 2011). Consequently, we targeted whole cell patch clamp recordings from layer V fast-spiking interneurons to determine functional changes to inhibitory and excitatory activity in the contralateral motor cortex. Using this approach we show inhibitory synaptic transmission onto FS neurons is decreased after CCI.

Materials and Methods

CCI Injury

Juvenile mice, post-natal date 22 (P22) were subjected to a severe controlled

cortical impact as previously described (Hunt et al., 2009; Nichols et al., 2015). Mice were anesthetized with isoflurane (2%) and placed in a stereotaxic frame. Animal temperature was maintained and monitored for the duration of the surgery and until ambulatory post-surgery. The skull was exposed with a midline incision and a 5mm craniotomy was made lateral to the sagittal suture between bregma and lamda, over the right somatosensory region. Precaution was taken during the craniotomy not to disturb the underlying dura. A frontoparietal CCI (3mm diameter tip, 3.0 m/s, 2mm depth, 500ms duration) was performed using an electromagnetic cortical impactor (Hatteras Instruments, Cary, North Carolina). After the impact, the removed bone flap was placed over the site of injury and sealed with dental cement.

Preparation of Brain Slices

On post-injury date (PID) 14–19, the mice were deeply anaesthetized with inhalation of isoflurane and decapitated. The brain was rapidly removed and coronal slices (350 μm thick) prepared on a vibratome (VT 1200; Leica, Nussloch, Germany) as previously described (Anderson et al., 2010; Nichols et al., 2015). Coronal slices were obtained from CCI animals within the region of CCI injury or in corresponding control cortex. The site of CCI was readily identifiable in slices as significant cavitation and tissue loss. Cortex contralateral to the injury site was then examined in CCI animals or in corresponding control regions. Initial harvesting of brain slices was performed in an ice-cooled (4°C) carboxygenated (95% O_2, 5% CO_2) high sucrose solution containing the following (in mM): 234 sucrose, 11 glucose, 26 $NaHCO_3$, 2.5 KCl, 1.25 $NaH_2PO_4H_2O$, 10 MgS_47H_2O, 0.5 $CaCl_22H_2O$. Slices were then incubated for 1 h at 32°C in

carboxygenated artificial CSF (aCSF) containing (in mM): 126 NaCl, 26 $NaHCO_3$, 2.5 KCl, 10 Glucose, 1.25 $Na_2H_2PO_4H_2O$, 1 $MgSO_47H_2O$, 2 $CaCl_2H_2O$, pH 7.4. Slices were then returned to room temperature before being moved to the recording chamber for whole-cell patch-clamp recording.

In Vitro Electrophysiological Recording

Coronal slices were prepared from CCI or sham animals and were submerged in flowing carboxygenated aCSF heated to 32°C. Submerged slices were first visualized under 4× brightfield for identification of layer V cortex. For slices from impacted mice, recordings were made in the peri-injury zone within 2 mm of the injury-induced cavitation. Recordings from control slices were made in the corresponding cortex to the peri-injury zone of CCI animals. Whole-cell recordings were obtained from fast-spiking interneurons using an upright microscope (Axioexaminer; Carl-Zeiss, Thornwood, NY, USA) fitted with infrared differential interference contrast optics. Fast-spiking neurons were distinguished based on their current-clamp firing behavior (Guatteo et al., 1994) and well as with the endogenous tdTomato fluorofluore in the Vgat:Cre Ai9 mouse. The electrode capacitance and bridge circuit were appropriately adjusted. The series resistance (R_s) of neurons chosen for analysis was <20% of membrane input resistance and monitored for stability. Membrane potential was not corrected for a calculated 10 mV liquid junction potential. A Multiclamp 700A patch-clamp amplifier (Axon Instruments, Union City, CA, USA) was used for both current- and voltage-clamp mode. Recordings were obtained at 32°C using borosilicate glass microelectrodes (tip resistance, 3–4.5 MΩ). For excitatory recordings, electrodes were filled with an intracellular solution containing (in mM): 135 KGluconate, 4 KCl, 2 NaCl, 10 HEPES, 4 EGTA, 4 Mg ATP,

0.3 Na TRIS. For recording of inhibitory events, an intracellular solution containing the following was used (in mM): 70 KGluconate, 70 KCl, 2 NaCl, 10 HEPES, 4 EGTA, 4 Mg ATP, 0.3 GTP. This internal solution has been used previously (Anderson et al., 2010; Nichols et al., 2015) and shown to facilitate detection of inhibitory events. The calculated E_{Cl} was approximately −16 mV, resulting in inward $GABA_A$ currents at a holding potential of −70 mV. Inhibitory events were pharmacologically isolated by bath application of 2-Amino-5-phosphonopentanoic acid (d-APV; 50 μM) and 6,7-dinitroquinoxaline-2,3-dione (DNQX, 20 μM).

Image Acquisition and Analysis

Images were collected on a Leica SP5 and Zeiss 710 laser scanning confocal microscope using 10X or 20X objectives. Single fields were tiled together to generate high-resolution images of whole brain coronal sections. Images were corrected for brightness and contrast in Photoshop. For assessment of Parvalbumin neuron density, we defined a region of interest (ROI), 350um wide that expanded all cortical layers and was perpendicular to the white matter. The ROI was positioned 465um lateral to midline on the contralateral hemisphere, positioned over secondary and primary motor cortex. To determine density, the area of cortex within the ROI from three separate coronal sections was measured and the number of Parvalbumin or Somatostatin labeled soma was manually assayed. For assessment of Ai9 and NeuN density, single channel images from three separate sections were imported into ImageJ, manually thresholded, and the watershed algorithm was applied. The analyze particle plugin was employed using a minimal particle size of 70 $pixels^2$ for Ai9. The number of labeled neurons and the size of $Ai9^+$ soma were recorded. For PV and SST, somal size was manually measured in

Photoshop. Results were averaged from at least three independent mice from separate litters per condition.

Results

Inhibitory Interneurons (Ai9) are Reduced in Contralateral Motor Cortex

To examine for changes in the contralateral cortex following TBI we performed a frontoparietal CCI in the somatosensory cortex of juvenile mice (post-natal day 22). The transgenic mice used in this study express the fluorescent protein tdtomato (Ai9) cre-dependently targeted to all inhibitory interneurons (Vgat:Cre; Ai9) (Wang et al., 2009; Wojcik et al., 2006). At 14 days after CCI, regions of interests (ROIs) of 350um width were radially overlaid images taken from control of CCI. The ROI extending from 350 to 700um from midline corresponded to the motor cortex, including both primary and secondary regions (Paxinos and Watson, 2007). An analysis of the density of Ai9 positive neurons within the contralateral motor cortex ROI revealed a significant reduction of 27% following CCI (i.e. 54.53 ± 2.94 cells/mm^2 in CCI vs 74.52 ± 2.59 cells/mm^2 in control) (P=0.009). This loss of Ai9 cell density resulted in an overall loss of number of Ai9 positive neurons (CCI (359.1± 17.72) vs control (255.4 ± 9.05) (P< 0.0001) and was accompanied by a reduction of soma size (CCI 87.75 ± 2.03 um^2 vs control 147.0 ± 2.16 um^2) (P<0.0001). In contrast, as previously reported for the ipsilateral cortex (Nichols et al., *In Preparation*) we observed no qualitative change in the density of neurons labelled with the pan-neuronal marker NeuN in the contralateral motor cortex. Taken together with the loss of Ai9 cell density this suggests CCI disrupts the balance in number of excitatory and inhibitory neurons in the contralateral motor cortex. Finally, in some TBI models cortical atrophy has been reported that may account for

overall loss of neuron number (Goddeyne et al., 2015). However in these experiments no significant change in cortical thickness was observed following CCI suggesting a true loss of the number of interneurons with the contralateral motor cortex (Fig 1C).

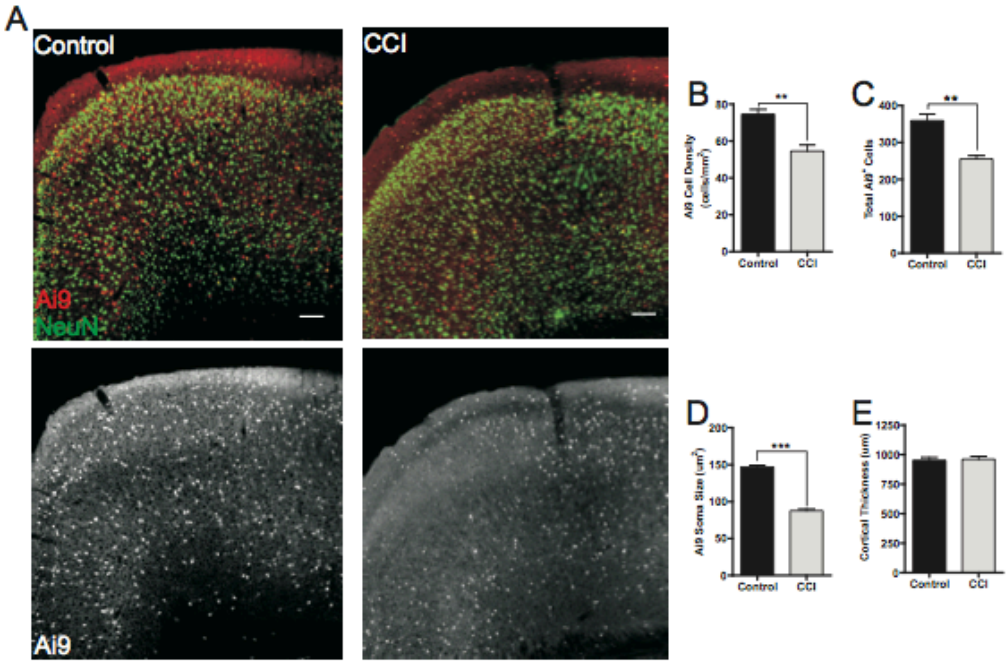

Figure 1. Control motor cortex experiences Ai9 loss after CCI. (A, Top) Control versus CCI image of contralateral motor cortex with NeuN (Green) and Ai9 (tdTomato) showing that after CCI, Ai9 density is reduced. (A, Bottom) Monochrome image displaying only interneurons (Ai9) to highlight the loss of interneurons after injury. (B) Quantitative analysis showing that Ai9 cell density is significantly decreased after injury (**P=0.009). (C) Total Ai9 was significantly decreased after CCI. (**P<0.0001). (D) Interneurons in the motor cortex also showed a dramatic loss of soma size. (***P<0.0001). (E) Cortical thickness between control and CCI animals did not change.

Parvalbumin Expression in the Motor Cortex is Reduced After Injury

To assess if a certain subpopulation of interneurons are decreased in the contralateral motor cortex after injury we examined immnohistochemical markers of cortical interneurons. Parvalbumin (PV) positive interneurons comprise approximately 50% of the interneuron cortical population (Rudy et al., 2011) and play a significant role in regulating cortical output (Mitchell and Silver, 2003) including of corticalspinal (motor) neurons (Tanaka et al., 2011). Fourteen days after CCI there was a significant loss of PV expression in the contralateral motor cortex (Fig. 2, A). Specifically, PV cell density was significantly reduced by 63% from control values (control 12.46 ± 0.41 vs CCI 4.66 ± 1.05) (P = 0.0016) (Fig. 2, B). Looking at the total number of PV positive cells there was a significant difference following CCI (control 63.22 ± 1.78, CCI 14.93 ± 4.70) (P=0.0003). The loss of PV expression (63%) was far greater than overall Ai9 loss (27%) and highlights an advantage of the transgenic approach employed in this study in separating loss of immunoreactivity and cell death.

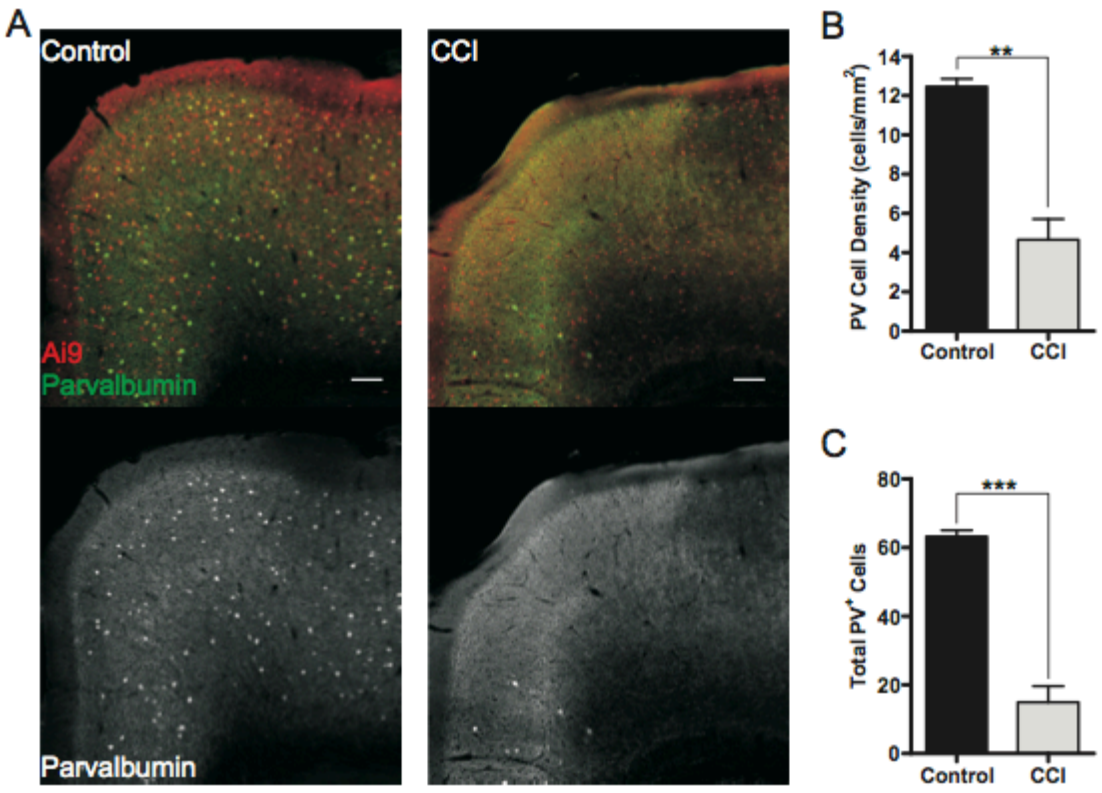

Figure 2. Parvalbumin expression is significantly lost after injury. (A, Top) Control animal with Ai9 (tdTomato) and parvalbumin (green) showing a significant loss of parvalbumin after injury. (A, Bottom) Monochrome image to highlight the dramatic loss of parvalbumin after CCI. (B) Quantification of parvalbumin cell density shows a significant loss after injury (P=0.0016). (C) Total parvalbumin positive neurons were significantly reduced after CCI. (P=0.0003).

Somatostatin Expression is not Altered after CCI

Somatostatin (SST) interneurons have been shown to play an important role in regulating excitability in the dendrites of pyramidal neurons (Ma et al., 2006). While to a lesser extent than PV neurons, SST neurons also play a role in maintaining inhibition to corticalspinal neurons (Tanaka et al., 2011). However in contrast to PV neurons, we found that SST cell density was not significantly changed in contralateral motor cortex after CCI (control 13.45 ± 1.72, CCI 12.73 ± 0.99)(P=0.73) (Fig. 3, A-B). Similarly, total SST neuron number was not significantly altered in SST neurons after CCI (control 71.78 ± 7.23 vs CCI 57.44 ± 4.59)(P=0.17). Taken together this suggests that 14 days after CCI there is a select loss of PV expression in the contralateral motor cortex.

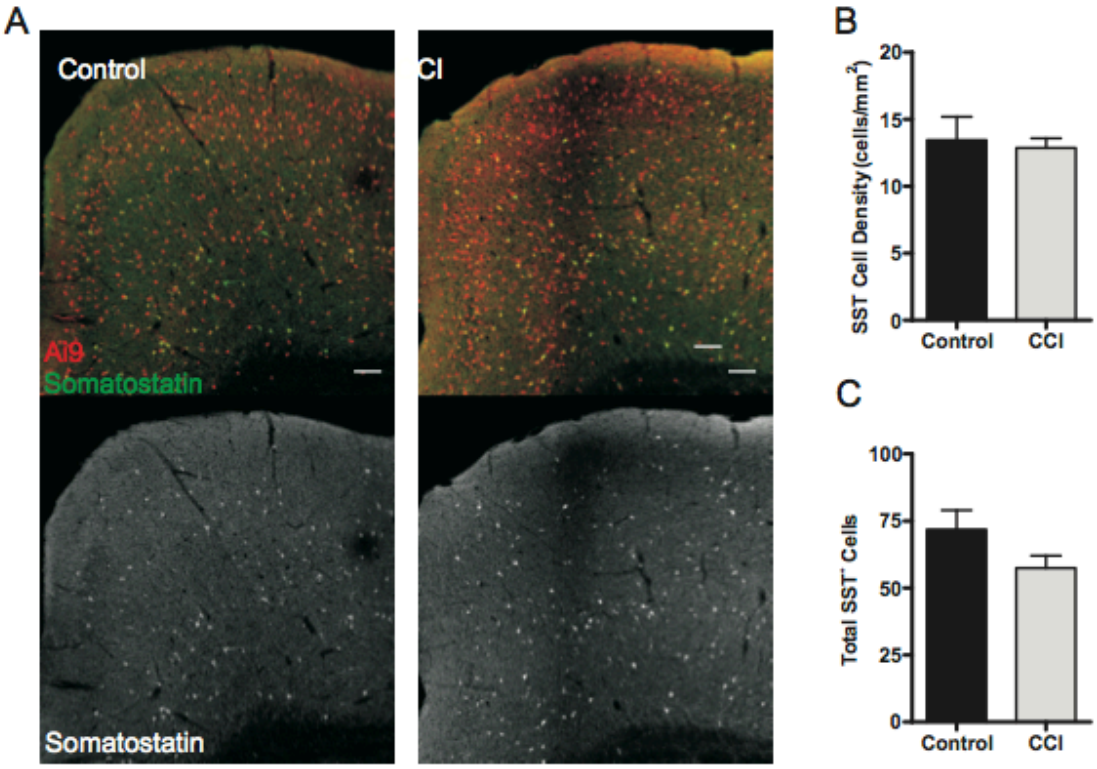

Figure 3. Somatostatin expression is not changed after injury. (A, Top) Somatostain (green) and Ai9 (tdTomato) show equal distribution across the motor cortex in both control and CCI. (A, Bottom) Monochrome image to highlight the somatostatin distribution in control and CCI motor cortex.

Fast-Spiking Interneurons are not Altered Following CCI

Parvalbumin positive cortical interneurons are predominantly of a fast-spiking (FS) phenotype (Hu et al., 2014). Similar to most other cortical cell-types, the firing properties of fast-spiking interneurons are developmentally regulated but shown to be well established by time of our CCI (i.e. P22) (Doischer et al., 2008; Itami et al., 2007; Okaty et al., 2009). Mature fast-spiking cells are characterized by low input resistance, narrow action potentials, and the production of high-frequency spike trains with little to no spike-frequency adaptation. The loss of interneurons and PV expression in this study prompted us to first examine changes in the intrinsic properties of fast-spiking neurons of the contralateral motor cortex. To examine FS interneurons directly we employed whole-cell patch clamp electrophysiology combined with intracellular biocytin fill and post-hoc immunostaining for PV. FS interneurons were recorded from control or CCI animals 14 days after injury. Biocytin filled fast spiking interneurons still maintained their endogenous Ai9-tdTomato expression. Biocytin fills confirmed that the recorded neurons were basket cells. (Fig. 4, B). FS electrophysiological phenotype was confirmed as previously described (Anderson et al., 2010; Miller et al., 2011). We found that fast-spiking interneurons maintained their high frequency spiking phenotype in CCI animals (Fig 4. A). Injection of a 1 second depolarizing current step (0 to 300 pA) showed no significant change in firing properties of FS interneurons between control and CCI animals (Fig. 4, A,E). FS interneurons recorded in CCI animals also showed no change in resting membrane potential when compared to control (control -62.78 ± 1.99, CCI -66.72 ± 0.99) (Fig. 4, C). Similarly, no significant change was observed in input resistance of

FS interneurons between control (238.7 ± 35.08 MΩ and CCI 187.6 ± 17.53) recordings (Fig. 4, D). Therefore, despite the loss of PV expression CCI failed to alter the tested intrinsic membrane properties of FS interneurons.

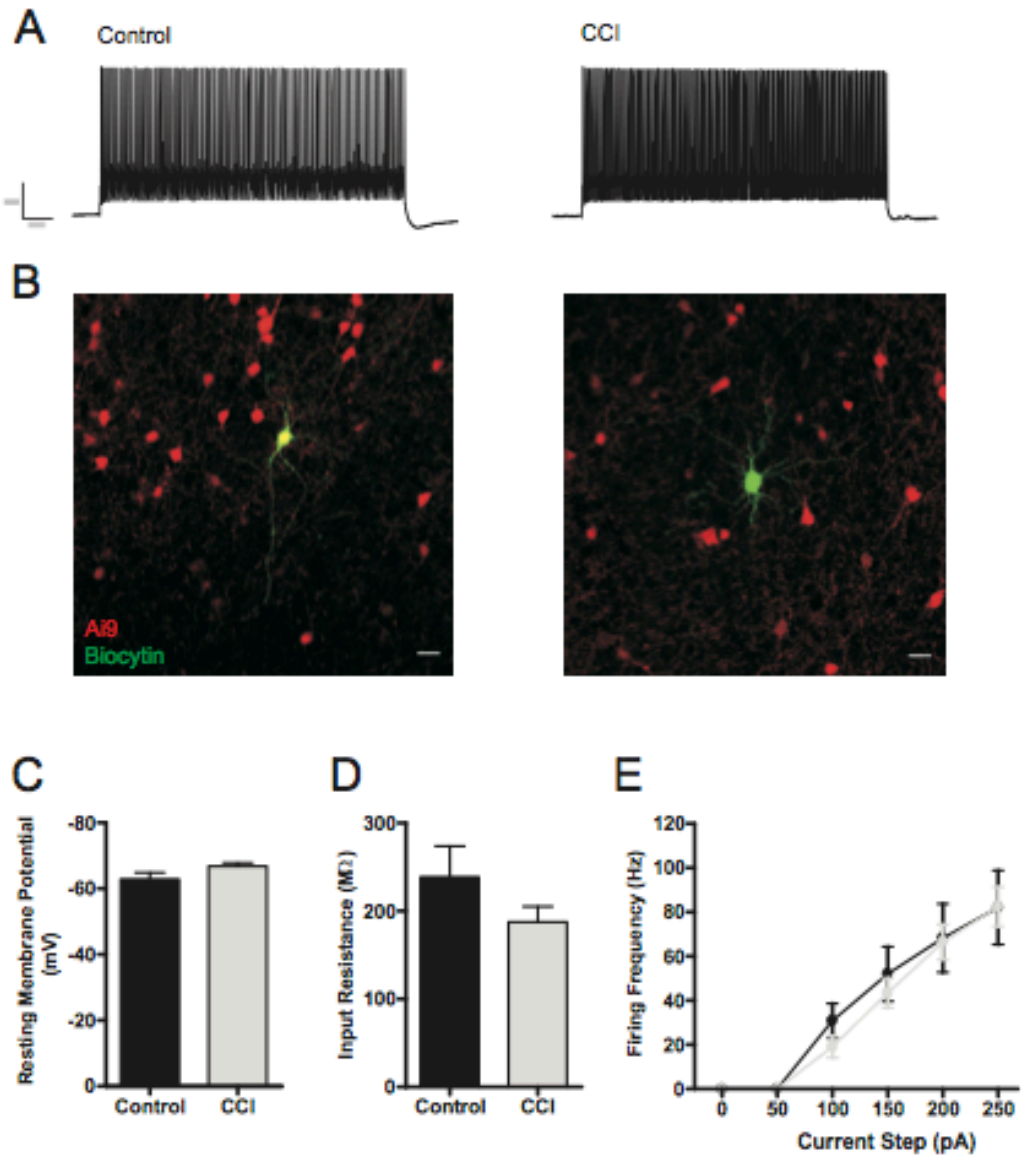

Figure 4. Fast-spiking interneurons do not have altered intrinsic properties after CCI. (A) Fast-spiking interneurons do not have altered intrinsic properties after CCI. (A) Firing patterns at a 250pA current step does not elicit different firing patterns between control and CCI. (B) Biocytin (green) against Ai9 (tdTomato) show neurons patched were confirmed as fast-spiking basket cells. (C) Resting membrane potential of fast-spiking interneurons is similar among control and CCI animals. (D) Input resistance of fast-spiking interneurons is not changed after CCI. (E) Analysis of firing frequency shows that CCI does not differ from control.

CCI Reduces Inhibitory sIPSC Inter-Event Interval and Increases Decay

Fast-spiking interneurons are known to play a key role in regulating pyramidal neuron excitability. As such, any changes on inhibition onto FS intereneurons may have a profound effect on network dynamics. To examine for changes of synaptic inhibition onto fast-spiking interneurons, spontaneous inhibitory post-synaptic currents (sIPSCs) were pharmacologically isolated with 2mm kynurenic acid and electrophysiologically recorded (Fig. 5A). For these recordings, FS interneurons were held at -70mV using a modified internal solution (Ecl=-16mV) that improves detection of inhibitory synaptic events (Anderson et al., 2010). Following CCI, there was significant reduction in the average frequency of sIPSCs onto FS interneurons as evidenced by an almost a 2-fold increase in inter-event interval (control 294.0 ± 53.13 vs CCI 610.5 ± 98.14) ($p=0.02$) (Fig. 5, B). This was accompanied by a significant increase in sIPSC charge (control 57.34 ± 5.91, CCI 91.92 ± 8.62) and decay time (control 2.90 ± 0.22 vs CCI 4.98 ± 0.67) without an associated change in amplitude (control 17.28 ± 1.99, CCI 20.13 ± 1.45) (Fig. 5, B).

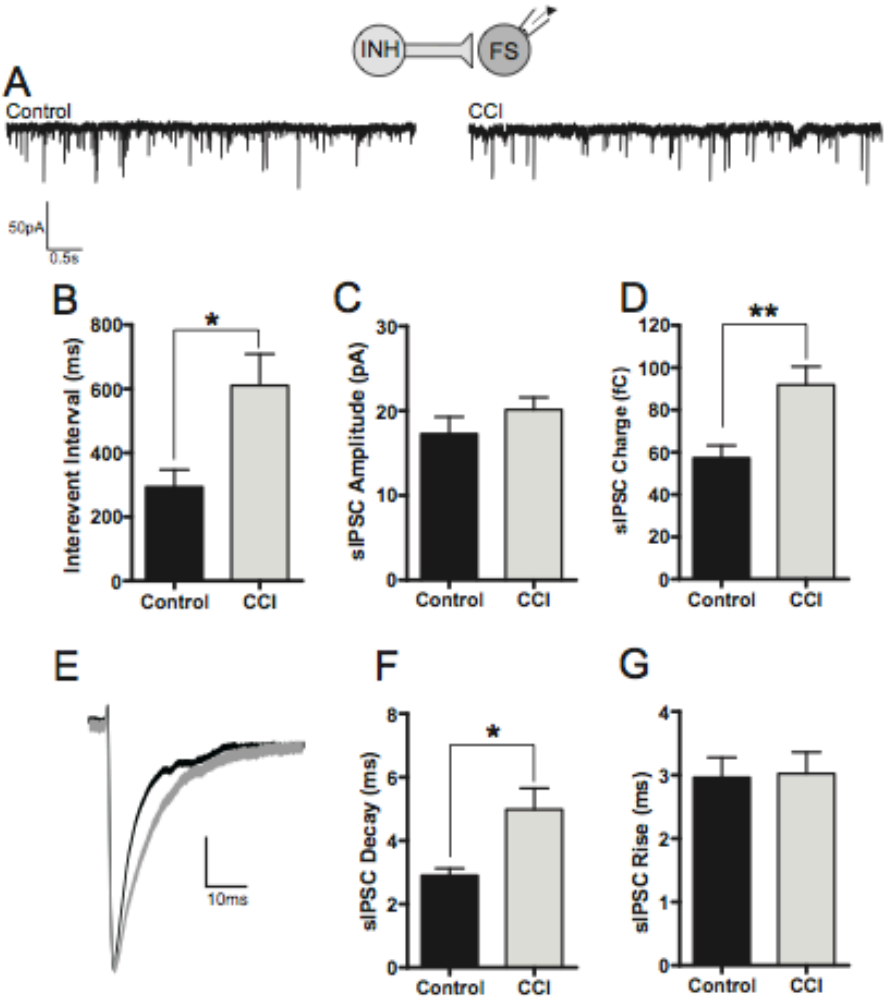

Figure 5. Spontaneous IPCSs are decreased after CCI, and synaptic rise and decay times are increased after injury. (A) Gap-free traces in voltage clamp, holding at -70mV, recording sIPSCs from fast-spiking interneurons (B) Inter-event interval of sIPSC events was significantly reduced after injury. (* P=0.02). (C) Amplitude was not different between control and CCI. (D) sIPSC charge was significantly increased after injury. (E) Overlaid normalized average sIPSC after injury demonstrates the increased decay time. (F) sIPSC decay time is significantly increased after injury. * p=0.03. (G) sIPSC rise time did not change after injury. (control n=8, CCI n=15)

CCI Increases sEPSC Inter-Event Interval and Decreases Synaptic Decay

To better understand the balance of excitation and inhibition onto fast-spiking interneurons, we similarly examined for changes in spontaneous excitatory postsynaptic currents (sEPSCs). For these recordings, FS interneurons were again held at -70mV using a physiological internal solution (ECl = -80). This allows detection of isolated excitatory events without the need for pharmacological blockers that would alter and prevent testing of baseline network excitability (Anderson et al., 2010). Recordings performed 14 days following CCI revealed a significant increase in average sEPSC inter-event interval (control 220.0 ± 48.19 vs CCI 99.00 ± 12.61)(P=0.0062) without any change in sEPSC amplitude, charge, or rise time (Fig. 6, B-G). In contrast to sIPSC, overall decay time of sEPSCs were significantly reduced (control 2.33 ± 0.20 vs CCI 1.85 ± 0.09) (p = 0.02) (Fig 6, F). These findings suggest that following CCI FS interneurons receive more frequent but weaker (reduced decay) excitatory input.

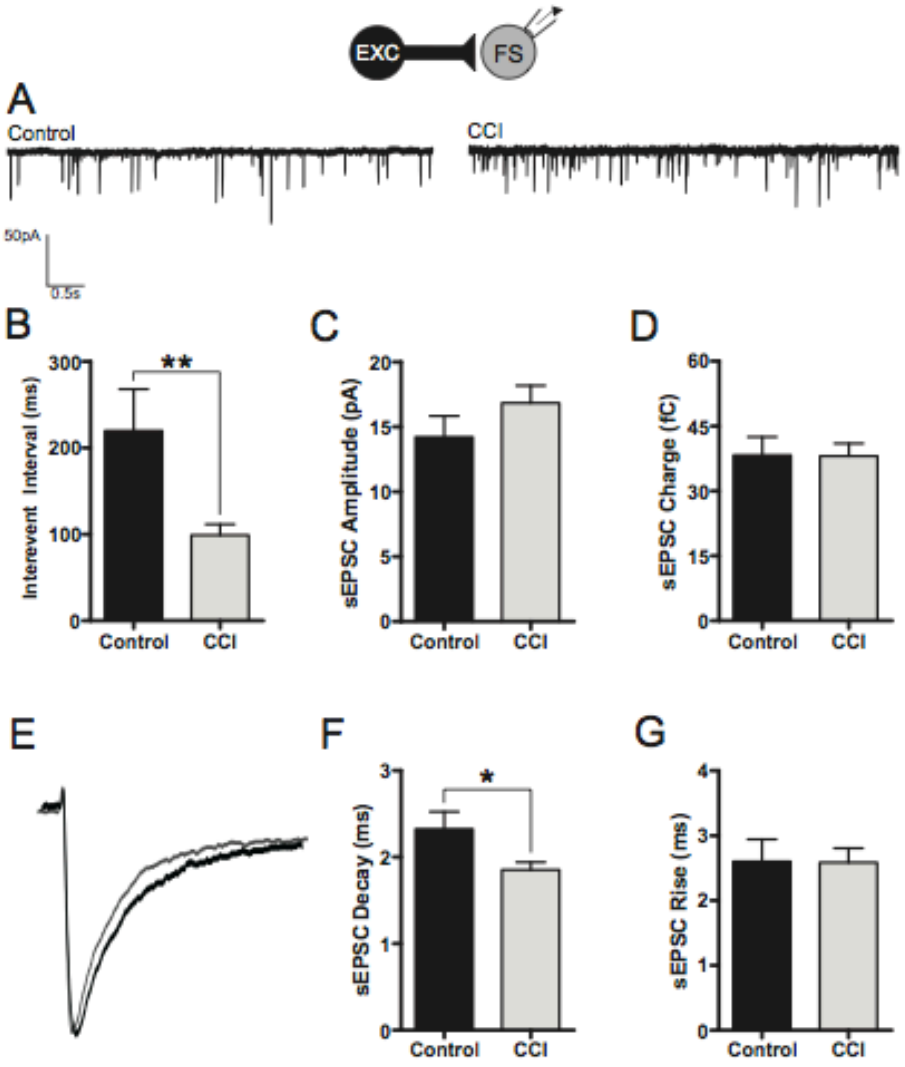

Figure 6. CCI results in increased synaptic excitatory input onto fast-spiking neurons. (A) Gap-free voltage clamp traces, holding at -70mV, from fast-spiking interneurons monitoring sEPSCs in control and CCI. (B) Inter-event interval is significantly reduced after CCI (**P=0.0062). (C-D) sEPSC amplitude and charge is not altered after CCI. (E) Overlaid averaged sEPSCs demonstrate the change in decay time after injury. (F) Quantitatively sEPSC decay is significantly reduced (*P=0.02) (G) Rise time after injury was not changed after CCI. (Control n=8, CCI n=14).

Discussion

We combined whole-cell patch clamp electrophysiology with fluorescent immunohistochemistry in fluorescently labeled inhibitory interneurons to ask whether inhibition in the contralateral motor cortex is altered after controlled cortical impact (CCI). In this study, we found that 14 days after CCI in juvenile animals the total interneuron population and PV expression cell density was significantly decreased, but SST expression was unchanged. PV expressing neurons are known to have a unique FS phenotype which can be identified electrophysiologically (Kawaguchi and Kubota, 1997; Kawaguchi et al., 1987). Using a combined electrophysiological and immunohistochemical approach we determined that CCI induced loss of PV expression that did not alter the intrinsic properties of FS interneurons. However, when examining afferent synaptic input on FS interneurons, CCI increased the IEI while increasing the strength (i.e. increased charge and decay) of synaptic inhibition. Conversely, the IEI of synaptic excitation onto FS interneurons was increased following CCI with an overall decrease of synaptic strength (i.e. decreased decay time). These findings suggest that in the contralateral motor cortex in contrast to SST interneurons, CCI selectively alters PV-FS neurons. Specifically, CCI alters the balance of synaptic excitation and inhibition (E/I) onto FS interneurons and is associated with an overall loss of the total number of interneurons. These observations argue that TBI leads to anatomical and neurophysiological remodeling of the otherwise morphologically intact contralateral motor cortex, which may play important roles in the pathophysiology of pediatric TBI. Despite evidence that suggests the deficits induced by TBI predict contralateral brain dysfunction, very few studies have undertaken a direct examination. To our knowledge,

this is the first study to directly examine changes in inhibition of contralateral motor cortex of a "pediatric" brain.

Loss of inhibitory interneurons has been previously reported following TBI. However, these studies have primarily focused on changes in the hippocampus (Ding et al., 2011; Lowenstein et al., 1992; Pavlov et al., 2011). Furthermore, the majority of studies have used immunohistochemical means to investigate changes in the interneuron population following TBI. This approach may be limited to identification of changes in immunoreactivity over direct neuronal loss. To overcome this limitation we employed a transgenic mouse approach whereby all inhibitory interneurons were endogenously labeled with the fluorescent protein tdTomato (Ai9). This provided us the ability to better differentiate if CCI induced cell death or loss of immunoreactivity. We found that in juvenile mice the total number and overall density of cortical interneurons (Ai9) in the contralateral motor cortex was significantly reduced at PID14 after CCI. As the interneuron population is late to develop in mice (Levitt et al., 2004) this study specifically examined the outcome of CCI in juvenile animals impacted at P22. We believe this time point is within the pediatric time window but ensured a significant degree of interneuron maturation was complete at the time of impact (Andersen, 2003).

Cortical interneurons are a heterogeneous population of neurons comprised of numerous subtypes (Chow et al., 1999; Markram et al., 2004b; Rudy et al., 2011). As with previous studies, we next examined for specific CCI induced changes to immunohistochemically defined populations of cortical interneurons. Specifically, examination of PV and SST interneurons was choosen as they comprise ~80% of the total cortical interneuron population(Rudy et al., 2011) and are implicated in numerous

neurological diseases (Behrens and Sejnowski, 2009; Levitt et al., 2004; Ma and Prince, 2012; Nakamura et al., 2015; Powell et al., 2012; Uhlhaas and Singer, 2010). The data revealed that while there was no change in SST expression, there was selective loss of PV expression in the contralateral motor cortex following CCI. This finding is supported by humans studies indicating loss of PV expression after TBI (Buriticá et al., 2009). In animal models, it has also been shown that PV interneurons are more sensitive to insult in pediatric animals than adults (Cabungcal et al., 2013a, 2013b). However, studies of TBI in adult animals have indicated loss of both SST and PV expression following CCI (Cantu et al., 2014). Taken together, this suggests that in the contralateral motor cortex TBI induces both loss of the total number of cortical interneurons (i.e. Ai9 number and density) along with the targeted loss of PV expression.

At an inhibitory synaptic level, our results indicate that the frequency of inhibition onto fast-spiking interneurons was reduced while the strength (i.e. increased charge and decay) was increased. As changes to intrinsic membrane properties may alter the ability or properties of detected synaptic activity (e.g. input resistance) of note is that CCI and the induced PV expression loss failed to alter the intrinsic properties of FS interneurons. While no other studies have directly examined cortical inhibitory interneurons following CCI similar results have been observed in excitatory pyramidal neurons, in adult mice after CCI (Cantu et al., 2014) as well as in the hippocampus after mild TBI (Almeida-Suhett et al., 2015). The increase in synaptic decay has also been shown in dentate hilar GABAergic neurons in adult mice after CCI (Hunt et al., 2011). In juvenile animals, we have also previously shown an increase decay time from sIPSCs onto pyramidal neurons after CCI (Nichols et al., 2015). This increase in decay time could potentially be the

result of a compensatory response to increase the temporal integration window or maintain proper excitatory and inhibitory network function. In general, inhibitory decay kinetics play an important role in shunting excitatory events (Mitchell and Silver, 2003) that may help limit the development of hyperexcitability (Guerriero et al., 2015). As FS interneurons are known to receive input from multiple types of cortical interneurons (Yoshimura and Callaway, 2005), the specific source and cell-type involved in the change in kinetics remains to be determined, but may include changes in synaptic connectivity or alteration of GABAergic subunits. Given the faster kinetics of FS versus low-threshold spiking (i.e. SST positive) interneurons (Bacci and Huguenard, 2006) and loss of PV expression it is tempting to speculate of an alteration in the relative synaptic contributions from these two interneuron populations. Another possibility is that the overall loss of synaptic inhibition might be the result of other interneurons subtypes untested in this study. To account for this, mapping cortical connectivity and unitary functional assessment of individual subtypes will be required to confirm the cell-type specific actions of TBI.

At an excitatory synaptic level, the number of spontaneous excitatory events was increased in the motor cortex contralateral to the site of injury. This has been seen in a previous adult CCI study that characterized contralateral sEPSCs from dentate hilar interneurons (Hunt et al., 2011) Increased excitation has previously been seen in pyramidal neurons in the peri-injury region after adult CCI (Cantu et al., 2014; Yang et al., 2010). Additionally, decay time of sEPSCs in FS neurons was significantly reduced. This contrasts an adult CCI study that found contralateral dentate hilar GABAergic neurons did not show a changed to sEPSC decay time (Hunt et al., 2011). However, we

have shown this in FS neurons recorded from the peri-injury region after pediatric CCI (Nichols et. al., *In Preparation*). Abnormal reorganization of brain circuits can also result in disturbed function and manifest as various neurological disorders (Kleschevnikov et al., 2004; Mello et al., 1993; Romcy-Pereira and Garcia-Cairasco, 2003; Routbort et al., 1999) It will be important to determine the mechanism and action of these changes in promoting or restricting the development of the pathophysiology and symptomology induced by TBI.

In conclusion, we found a loss of interneurons and PV expression in the contralateral motor cortex. Additionally, the frequency of excitation was increased and inhibition was decreased after CCI onto FS neurons in the same region. The role of interneurons in TBI have been shown to be key in regulating network activity after injury (Cantu et al., 2014; Jin et al., 2014). Evidence suggests that when compared to the somatosensory cortex the motor cortex may be specifically sensitive to the effects of TBI (Pearce et al., 2015; Tremblay et al., 2011). In human longitudinal studies studying the motor cortex after injury, excitation normalizes while changes to inhibition are sustained for years after injury (De Beaumont et al., 2007, 2009; Tremblay et al., 2011). Little is known regarding cortical interneurons in the contralateral motor cortex after CCI, however, similar GABAergic dysfunction has been seen in dentate hilar neurons contralateral to injury (Hunt et al., 2011). Other studies have shown the motor cortex contralateral to injury undergo synaptic and morphological changes after insult (Axelson et al., 2013; Jones et al., 2012; Nudo, 2006). This may be due to corticalspinal tract rewiring to compensate for lost motor function, which has been shown in a focal TBI in mice (Ueno et al., 2012). Similar results have been seen in human ischemia studies. For

example, clinical studies of stroke patients showed that larger infarcts caused greater activation of the intact contralateral hemisphere (Cramer et al., 2006; Frost et al., 2003). In rodent ischemia models, dendritic growth and axonal sprouting within the contralateral motor cortex have been shown following unilateral ischemia (Biernaskie and Corbett, 2001; Biernaskie et al., 2005; Chen et al., 2002). Despite these similar results, the cellular and molecular mechanisms that can account for the loss of interneurons and PV expression in the contralateral motor cortex after CCI needs to be studied further. Overall, our findings suggest that extended "injury" induced changes to the contralateral cortex may play an important, and as of yet understudied, role in the pathophysiology of TBI.

References

Abdul-Muneer, P.M., Schuetz, H., Wang, F., Skotak, M., Jones, J., Gorantla, S., Zimmerman, M.C., Chandra, N., and Haorah, J. (2013). Induction of oxidative and nitrosative damage leads to cerebrovascular inflammation in an animal model of mild traumatic brain injury induced by primary blast. Free Radic. Biol. Med. *60*, 282–291.

Adelson, P.D. (1999). Animal models of traumatic brain injury in the immature: a review. Exp. Toxicol. Pathol. Off. J. Ges. Für Toxikol. Pathol. *51*, 130–136.

Adelson, P.D., Bratton, S.L., Carney, N.A., Chesnut, R.M., du Coudray, H.E.M., Goldstein, B., Kochanek, P.M., Miller, H.C., Partington, M.P., Selden, N.R., et al. (2003). Guidelines for the acute medical management of severe traumatic brain injury in infants, children, and adolescents. Chapter 19. The role of anti-seizure prophylaxis following severe pediatric traumatic brain injury. Pediatr. Crit. Care Med. J. Soc. Crit. Care Med. World Fed. Pediatr. Intensive Crit. Care Soc. *4*, S72–S75.

Adelson, P.D., Fellows-Mayle, W., Kochanek, P.M., and Dixon, C.E. (2013). Morris water maze function and histologic characterization of two age-at-injury experimental models of controlled cortical impact in the immature rat. Childs Nerv. Syst. ChNS Off. J. Int. Soc. Pediatr. Neurosurg. *29*, 43–53.

Agrawal, A., Timothy, J., Pandit, L., and Manju, M. (2006). Post-traumatic epilepsy: an overview. Clin. Neurol. Neurosurg. *108*, 433–439.

Almeida-Suhett, C.P., Prager, E.M., Pidoplichko, V., Figueiredo, T.H., Marini, A.M., Li, Z., Eiden, L.E., and Braga, M.F.M. (2015). GABAergic interneuronal loss and reduced inhibitory synaptic transmission in the hippocampal CA1 region after mild traumatic brain injury. Exp. Neurol. *273*, 11–23.

Andersen, S.L. (2003). Trajectories of brain development: point of vulnerability or window of opportunity? Neurosci. Biobehav. Rev. *27*, 3–18.

Anderson, V., and Moore, C. (1995). Age at injury as a predictor of outcome following pediatric head injury: A longitudinal perspective. Child Neuropsychol. *1*, 187–202.

Anderson, K.J., Miller, K.M., Fugaccia, I., and Scheff, S.W. (2005a). Regional distribution of Fluoro-Jade B staining in the hippocampus following traumatic brain injury. Exp. Neurol. *193*, 125–130.

Anderson, T.R., Jarvis, C.R., Biedermann, A.J., Molnar, C., and Andrew, R.D. (2005b). Blocking the anoxic depolarization protects without functional compromise following simulated stroke in cortical brain slices. J. Neurophysiol. *93*, 963–979.

Anderson, T.R., Huguenard, J.R., and Prince, D.A. (2010). Differential effects of Na+-

K+ ATPase blockade on cortical layer V neurons. J. Physiol. *588*, 4401–4414.

Anderson, V., Catroppa, C., Morse, S., Haritou, F., and Rosenfeld, J. (2005c). Functional plasticity or vulnerability after early brain injury? Pediatrics *116*, 1374–1382.

Annegers, J.F., Hauser, W.A., Coan, S.P., and Rocca, W.A. (1998). A population-based study of seizures after traumatic brain injuries. N. Engl. J. Med. *338*, 20–24.

Appleton, R.E., and Demellweek, C. (2002). Post-traumatic epilepsy in children requiring inpatient rehabilitation following head injury. J. Neurol. Neurosurg. Psychiatry *72*, 669–672.

Arango, J.I., Deibert, C.P., Brown, D., Bell, M., Dvorchik, I., and Adelson, P.D. (2012). Posttraumatic seizures in children with severe traumatic brain injury. Childs Nerv. Syst. ChNS Off. J. Int. Soc. Pediatr. Neurosurg. *28*, 1925–1929.

Atallah, B.V., Bruns, W., Carandini, M., and Scanziani, M. (2012). Parvalbumin-Expressing Interneurons Linearly Transform Cortical Responses to Visual Stimuli. Neuron *73*, 159.

Axelson, H.W., Winkler, T., Flygt, J., Djupsjö, A., Hånell, A., and Marklund, N. (2013). Plasticity of the contralateral motor cortex following focal traumatic brain injury in the rat. Restor. Neurol. Neurosci. *31*, 73–85.

Bacci, A., and Huguenard, J.R. (2006). Enhancement of spike-timing precision by autaptic transmission in neocortical inhibitory interneurons. Neuron *49*, 119–130.

Balan, I.S., Saladino, A.J., Aarabi, B., Castellani, R.J., Wade, C., Stein, D.M., Eisenberg, H.M., Chen, H.H., and Fiskum, G. (2013). Cellular alterations in human traumatic brain injury: changes in mitochondrial morphology reflect regional levels of injury severity. J. Neurotrauma *30*, 367–381.

Barberis, A., Mozrzymas, J.W., Ortinski, P.I., and Vicini, S. (2007). Desensitization and binding properties determine distinct alpha1beta2gamma2 and alpha3beta2gamma2 GABA(A) receptor-channel kinetic behavior. Eur. J. Neurosci. *25*, 2726–2740.

Barlow, K.M., Spowart, J.J., and Minns, R.A. (2000). Early posttraumatic seizures in non-accidental head injury: relation to outcome. Dev. Med. Child Neurol. *42*, 591–594.

Bauer, J., and Burr, W. (2001). Course of chronic focal epilepsy resistant to anticonvulsant treatment. Seizure J. Br. Epilepsy Assoc. *10*, 239–246.

Behrens, M.M., and Sejnowski, T.J. (2009). Does schizophrenia arise from oxidative dysregulation of parvalbumin-interneurons in the developing cortex? Neuropharmacology *57*, 193–200.

Behrens, M.M., Ali, S.S., Dao, D.N., Lucero, J., Shekhtman, G., Quick, K.L., and Dugan, L.L. (2007). Ketamine-Induced Loss of Phenotype of Fast-Spiking Interneurons Is

Mediated by NADPH-Oxidase. Science *318*, 1645–1647.

Ben-Ari, Y., Gaiarsa, J.-L., Tyzio, R., and Khazipov, R. (2007). GABA: a pioneer transmitter that excites immature neurons and generates primitive oscillations. Physiol. Rev. *87*, 1215–1284.

Biernaskie, J., and Corbett, D. (2001). Enriched rehabilitative training promotes improved forelimb motor function and enhanced dendritic growth after focal ischemic injury. J. Neurosci. Off. J. Soc. Neurosci. *21*, 5272–5280.

Biernaskie, J., Szymanska, A., Windle, V., and Corbett, D. (2005). Bi-hemispheric contribution to functional motor recovery of the affected forelimb following focal ischemic brain injury in rats. Eur. J. Neurosci. *21*, 989–999.

Bolkvadze, T., and Pitkänen, A. (2012). Development of post-traumatic epilepsy after controlled cortical impact and lateral fluid-percussion-induced brain injury in the mouse. J. Neurotrauma *29*, 789–812.

Brody, D.L., Mac Donald, C., Kessens, C.C., Yuede, C., Parsadanian, M., Spinner, M., Kim, E., Schwetye, K.E., Holtzman, D.M., and Bayly, P.V. (2007). Electromagnetic controlled cortical impact device for precise, graded experimental traumatic brain injury. J. Neurotrauma *24*, 657–673.

Buriticá, E., Villamil, L., Guzmán, F., Escobar, M.I., García-Cairasco, N., and Pimienta, H.J. (2009). Changes in calcium-binding protein expression in human cortical contusion tissue. J. Neurotrauma *26*, 2145–2155.

Cabungcal, J.-H., Steullet, P., Morishita, H., Kraftsik, R., Cuenod, M., Hensch, T.K., and Do, K.Q. (2013a). Perineuronal nets protect fast-spiking interneurons against oxidative stress. Proc. Natl. Acad. Sci. U. S. A. *110*, 9130–9135.

Cabungcal, J.-H., Steullet, P., Kraftsik, R., Cuenod, M., and Do, K.Q. (2013b). Early-life insults impair parvalbumin interneurons via oxidative stress: reversal by N-acetylcysteine. Biol. Psychiatry *73*, 574–582.

Caillard, O., Moreno, H., Schwaller, B., Llano, I., Celio, M.R., and Marty, A. (2000). Role of the calcium-binding protein parvalbumin in short-term synaptic plasticity. Proc. Natl. Acad. Sci. U. S. A. *97*, 13372–13377.

Calcagnotto, M.E., Paredes, M.F., Tihan, T., Barbaro, N.M., and Baraban, S.C. (2005). Dysfunction of synaptic inhibition in epilepsy associated with focal cortical dysplasia. J. Neurosci. Off. J. Soc. Neurosci. *25*, 9649–9657.

Camfield, P.R., and Camfield, C.S. (2014). What Happens to Children With Epilepsy When They Become Adults? Some Facts and Opinions. Pediatr. Neurol.

Cantu, D., Walker, K., Andresen, L., Taylor-Weiner, A., Hampton, D., Tesco, G., and

Dulla, C.G. (2014). Traumatic Brain Injury Increases Cortical Glutamate Network Activity by Compromising GABAergic Control. Cereb. Cortex N. Y. N 1991.

Cao, Y., Vikingstad, E.M., Huttenlocher, P.R., Towle, V.L., and Levin, D.N. (1994). Functional magnetic resonance studies of the reorganization of the human hand sensorimotor area after unilateral brain injury in the perinatal period. Proc. Natl. Acad. Sci. U. S. A. *91*, 9612–9616.

Card, J.P., Santone, D.J., Gluhovsky, M.Y., and Adelson, P.D. (2005). Plastic reorganization of hippocampal and neocortical circuitry in experimental traumatic brain injury in the immature rat. J. Neurotrauma *22*, 989–1002.

Casella, E.M., Thomas, T.C., Vanino, D.L., Fellows-Mayle, W., Lifshitz, J., Card, J.P., and Adelson, P.D. (2014). Traumatic brain injury alters long-term hippocampal neuron morphology in juvenile, but not immature, rats. Childs Nerv. Syst. *30*, 1333–1342.

Cauli, B., Audinat, E., Lambolez, B., Angulo, M.C., Ropert, N., Tsuzuki, K., Hestrin, S., and Rossier, J. (1997). Molecular and physiological diversity of cortical nonpyramidal cells. J. Neurosci. Off. J. Soc. Neurosci. *17*, 3894–3906.

Caveness, W.F., Meirowsky, A.M., Rish, B.L., Mohr, J.P., Kistler, J.P., Dillon, J.D., and Weiss, G.H. (1979). The nature of posttraumatic epilepsy. J. Neurosurg. *50*, 545–553.

Chen, P., Goldberg, D.E., Kolb, B., Lanser, M., and Benowitz, L.I. (2002). Inosine induces axonal rewiring and improves behavioral outcome after stroke. Proc. Natl. Acad. Sci. U. S. A. *99*, 9031–9036.

Cheng, G., Kong, R., Zhang, L., and Zhang, J. (2012). Mitochondria in traumatic brain injury and mitochondrial-targeted multipotential therapeutic strategies. Br. J. Pharmacol. *167*, 699–719.

Chow, A., Erisir, A., Farb, C., Nadal, M.S., Ozaita, A., Lau, D., Welker, E., and Rudy, B. (1999). K(+) channel expression distinguishes subpopulations of parvalbumin- and somatostatin-containing neocortical interneurons. J. Neurosci. Off. J. Soc. Neurosci. *19*, 9332–9345.

Chugani, H.T., Phelps, M.E., and Mazziotta, J.C. (1987). Positron emission tomography study of human brain functional development. Ann. Neurol. *22*, 487–497.

Cole, J.T., Yarnell, A., Kean, W.S., Gold, E., Lewis, B., Ren, M., McMullen, D.C., Jacobowitz, D.M., Pollard, H.B., O'Neill, J.T., et al. (2010). Craniotomy: True Sham for Traumatic Brain Injury, or a Sham of a Sham? J. Neurotrauma *28*, 359–369.

Cole, J.T., Yarnell, A., Kean, W.S., Gold, E., Lewis, B., Ren, M., McMullen, D.C., Jacobowitz, D.M., Pollard, H.B., O'Neill, J.T., et al. (2011). Craniotomy: True Sham for Traumatic Brain Injury, or a Sham of a Sham? J. Neurotrauma *28*, 359–369.

Connors, B.W., and Gutnick, M.J. (1990). Intrinsic firing patterns of diverse neocortical neurons. Trends Neurosci. *13*, 99–104.

Cook, L.G., Chapman, S.B., Elliott, A.C., Evenson, N.N., and Vinton, K. (2014). Cognitive Gains from Gist Reasoning Training in Adolescents with Chronic-Stage Traumatic Brain Injury. Front. Neurol. *5*.

Corkin, S., Sullivan, E.V., and Carr, F.A. (1984). Prognostic factors for life expectancy after penetrating head injury. Arch. Neurol. *41*, 975–977.

Cowan, W.M., Fawcett, J.W., O'Leary, D.D., and Stanfield, B.B. (1984). Regressive events in neurogenesis. Science *225*, 1258–1265.

Cramer, S.C., Shah, R., Juranek, J., Crafton, K.R., and Le, V. (2006). Activity in the peri-infarct rim in relation to recovery from stroke. Stroke J. Cereb. Circ. *37*, 111–115.

Cruikshank, S.J., Lewis, T.J., and Connors, B.W. (2007). Synaptic basis for intense thalamocortical activation of feedforward inhibitory cells in neocortex. Nat. Neurosci. *10*, 462–468.

Dávid, C., Schleicher, A., Zuschratter, W., and Staiger, J.F. (2007). The innervation of parvalbumin-containing interneurons by VIP-immunopositive interneurons in the primary somatosensory cortex of the adult rat. Eur. J. Neurosci. *25*, 2329–2340.

De Beaumont, L., Lassonde, M., Leclerc, S., and Théoret, H. (2007). Long-term and cumulative effects of sports concussion on motor cortex inhibition. Neurosurgery *61*, 329–336; discussion 336–337.

De Beaumont, L., Théoret, H., Mongeon, D., Messier, J., Leclerc, S., Tremblay, S., Ellemberg, D., and Lassonde, M. (2009). Brain function decline in healthy retired athletes who sustained their last sports concussion in early adulthood. Brain J. Neurol. *132*, 695–708.

Dichter, M.A., and Ayala, G.F. (1987). Cellular mechanisms of epilepsy: a status report. Science *237*, 157–164.

Ding, M.-C., Wang, Q., Lo, E.H., and Stanley, G.B. (2011). Cortical excitation and inhibition following focal traumatic brain injury. J. Neurosci. Off. J. Soc. Neurosci. *31*, 14085–14094.

Doischer, D., Hosp, J.A., Yanagawa, Y., Obata, K., Jonas, P., Vida, I., and Bartos, M. (2008). Postnatal differentiation of basket cells from slow to fast signaling devices. J. Neurosci. Off. J. Soc. Neurosci. *28*, 12956–12968.

Douglas, R.J., and Martin, K.A.C. (2007). Mapping the Matrix: The Ways of Neocortex. Neuron *56*, 226–238.

Eadie, M.J. (2012). Shortcomings in the current treatment of epilepsy. Expert Rev.

Neurother. *12*, 1419–1427.

Elaine Wyllie MD, A.G., and Deepak K. Lachhwani (2005). The Treatment of Epilepsy: Principles and Practice (Philadelphia: Lippincott Williams & Wilkins).

Emery, D.L., Raghupathi, R., Saatman, K.E., Fischer, I., Grady, M.S., and McIntosh, T.K. (2000). Bilateral growth-related protein expression suggests a transient increase in regenerative potential following brain trauma. J. Comp. Neurol. *424*, 521–531.

Ewing-Cobbs, L., Miner, M.E., Fletcher, J.M., and Levin, H.S. (1989). Intellectual, Motor, and Language Sequelae Following Closed Head Injury in Infants and Preschoolers. J. Pediatr. Psychol. *14*, 531–547.

Ewing-Cobbs, L., Prasad, M., Kramer, L., and Landry, S. (1999). Inflicted traumatic brain injury: relationship of developmental outcome to severity of injury. Pediatr. Neurosurg. *31*, 251–258.

Ewing-Cobbs, L., Barnes, M.A., and Fletcher, J.M. (2003). Early brain injury in children: development and reorganization of cognitive function. Dev. Neuropsychol. *24*, 669–704.

Ewing-Cobbs, L., Prasad, M.R., Kramer, L., Cox, C.S., Baumgartner, J., Fletcher, S., Mendez, D., Barnes, M., Zhang, X., and Swank, P. (2006). Late intellectual and academic outcomes following traumatic brain injury sustained during early childhood. J. Neurosurg. *105*, 287–296.

Fisher, R.S., van Emde Boas, W., Blume, W., Elger, C., Genton, P., Lee, P., and Engel, J., Jr (2005). Epileptic seizures and epilepsy: definitions proposed by the International League Against Epilepsy (ILAE) and the International Bureau for Epilepsy (IBE). Epilepsia *46*, 470–472.

Fox, G., Fan, L., Levasseur, R.A., and Faden, A.I. (1998). Sustained Sensory/Motor and Cognitive Deficits With Neuronal Apoptosis Following Controlled Cortical Impact Brain Injury in the Mouse. J. Neurotrauma *15*, 599–614.

Frey, L.C. (2003a). Epidemiology of posttraumatic epilepsy: a critical review. Epilepsia *44 Suppl 10*, 11–17.

Frey, L.C. (2003b). Epidemiology of posttraumatic epilepsy: a critical review. Epilepsia *44 Suppl 10*, 11–17.

Friedman, D., Claassen, J., and Hirsch, L.J. (2009). Continuous electroencephalogram monitoring in the intensive care unit. Anesth. Analg. *109*, 506–523.

Friedman, W.J., Olson, L., and Persson, H. (1991). Cells that Express Brain-Derived Neurotrophic Factor mRNA in the Developing Postnatal Rat Brain. Eur. J. Neurosci. *3*, 688–697.

Frost, S.B., Barbay, S., Friel, K.M., Plautz, E.J., and Nudo, R.J. (2003). Reorganization

of Remote Cortical Regions After Ischemic Brain Injury: A Potential Substrate for Stroke Recovery. J. Neurophysiol. *89*, 3205–3214.

Fujimoto, S.T., Longhi, L., Saatman, K.E., Conte, V., Stocchetti, N., and McIntosh, T.K. (2004). Motor and cognitive function evaluation following experimental traumatic brain injury. Neurosci. Biobehav. Rev. *28*, 365–378.

Gabernet, L., Jadhav, S.P., Feldman, D.E., Carandini, M., and Scanziani, M. (2005). Somatosensory integration controlled by dynamic thalamocortical feed-forward inhibition. Neuron *48*, 315–327.

Galarreta, M., and Hestrin, S. (1998). Frequency-dependent synaptic depression and the balance of excitation and inhibition in the neocortex. Nat. Neurosci. *1*, 587–594.

Galarreta, M., and Hestrin, S. (1999). A network of fast-spiking cells in the neocortex connected by electrical synapses. Nature *402*, 72–75.

Garga, N., and Lowenstein, D.H. (2006). Posttraumatic epilepsy: a major problem in desperate need of major advances. Epilepsy Curr. Am. Epilepsy Soc. *6*, 1–5.

Ghajar, J. (2000). Traumatic brain injury. Lancet *356*, 923–929.

Gibson, J.R., Beierlein, M., and Connors, B.W. (1999). Two networks of electrically coupled inhibitory neurons in neocortex. Nature *402*, 75–79.

Gill, R., Chang, P.K.-Y., Prenosil, G.A., Deane, E.C., and McKinney, R.A. (2013). Blocking brain-derived neurotrophic factor inhibits injury-induced hyperexcitability of hippocampal CA3 neurons. Eur. J. Neurosci. *38*, 3554–3566.

Goddeyne, C., Nichols, J., Wu, C., and Anderson, T. (2015). Repetitive mild traumatic brain injury induces ventriculomegaly and cortical thinning in juvenile rats. J. Neurophysiol. *113*, 3268–3280.

Goldberg, E.M., Clark, B.D., Zagha, E., Nahmani, M., Erisir, A., and Rudy, B. (2008). K+ channels at the axon initial segment dampen near-threshold excitability of neocortical fast-spiking GABAergic interneurons. Neuron *58*, 387–400.

Goldberg, J.H., Yuste, R., and Tamas, G. (2003). Ca2+ imaging of mouse neocortical interneurone dendrites: Contribution of Ca2+-permeable AMPA and NMDA receptors to subthreshold Ca2+dynamics. J. Physiol. *551*, 67–78.

Goodman, J.C., Cherian, L., Bryan, R.M., and Robertson, C.S. (1994). Lateral Cortical Impact Injury in Rats: Pathologic Effects of Varying Cortical Compression and Impact Velocity. J. Neurotrauma *11*, 587–597.

Graber, K.D., and Prince, D.A. (2004). A critical period for prevention of posttraumatic neocortical hyperexcitability in rats. Ann. Neurol. *55*, 860–870.

Guatteo, E., Bacci, A., Franceschetti, S., Avanzini, G., and Wanke, E. (1994). Neurons dissociated from neocortex fire with “burst” and “regular” trains of spikes. Neurosci. Lett. *175*, 117–120.

Guerriero, R.M., Giza, C.C., and Rotenberg, A. (2015). Glutamate and GABA Imbalance Following Traumatic Brain Injury. Curr. Neurol. Neurosci. Rep. *15*, 545.

Gupta, A., Wang, Y., and Markram, H. (2000). Organizing principles for a diversity of GABAergic interneurons and synapses in the neocortex. Science *287*, 273–278.

Haider, B., and McCormick, D.A. (2009). Rapid neocortical dynamics: cellular and network mechanisms. Neuron *62*, 171–189.

Hall, E.D., Sullivan, P.G., Gibson, T.R., Pavel, K.M., Thompson, B.M., and Scheff, S.W. (2005a). Spatial and Temporal Characteristics of Neurodegeneration after Controlled Cortical Impact in Mice: More than a Focal Brain Injury. J. Neurotrauma *22*, 252–265.

Hall, R.C.W., Hall, R.C.W., and Chapman, M.J. (2005b). Definition, diagnosis, and forensic implications of postconcussional syndrome. Psychosomatics *46*, 195–202.

Hamm, R.J., Pike, B.R., O’Dell, D.M., Lyeth, B.G., and Jenkins, L.W. (1994). The rotarod test: an evaluation of its effectiveness in assessing motor deficits following traumatic brain injury. J. Neurotrauma *11*, 187–196.

Hånell, A., Clausen, F., Björk, M., Jansson, K., Philipson, O., Nilsson, L.N.G., Hillered, L., Weinreb, P.H., Lee, D., McIntosh, T.K., et al. (2010). Genetic deletion and pharmacological inhibition of Nogo-66 receptor impairs cognitive outcome after traumatic brain injury in mice. J. Neurotrauma *27*, 1297–1309.

Hasenstaub, A., Shu, Y., Haider, B., Kraushaar, U., Duque, A., and McCormick, D.A. (2005). Inhibitory postsynaptic potentials carry synchronized frequency information in active cortical networks. Neuron *47*, 423–435.

Hensch, T.K. (2005). Critical period plasticity in local cortical circuits. Nat. Rev. Neurosci. *6*, 877–888.

Herman, S.T. (2002). Epilepsy after brain insult: targeting epileptogenesis. Neurology *59*, S21–S26.

Hioki, H., Okamoto, S., Konno, M., Kameda, H., Sohn, J., Kuramoto, E., Fujiyama, F., and Kaneko, T. (2013). Cell Type-Specific Inhibitory Inputs to Dendritic and Somatic Compartments of Parvalbumin-Expressing Neocortical Interneuron. J. Neurosci. *33*, 544–555.

Hoffman, S.N., Salin, P.A., and Prince, D.A. (1994). Chronic neocortical epileptogenesis in vitro. J. Neurophysiol. *71*, 1762–1773.

Horita, H., Uchida, E., and Maekawa, K. (1991). Circadian rhythm of regular spike-wave

discharges in childhood absence epilepsy. Brain Dev. *13*, 200–202.

Houston, C.M., Bright, D.P., Sivilotti, L.G., Beato, M., and Smart, T.G. (2009). Intracellular chloride ions regulate the time course of GABA-mediated inhibitory synaptic transmission. J. Neurosci. Off. J. Soc. Neurosci. *29*, 10416–10423.

Houweling, A.R., Bazhenov, M., Timofeev, I., Steriade, M., and Sejnowski, T.J. (2005). Homeostatic Synaptic Plasticity Can Explain Post-traumatic Epileptogenesis in Chronically Isolated Neocortex. Cereb. Cortex N. Y. N 1991 *15*, 834–845.

Hu, H., Gan, J., and Jonas, P. (2014). Fast-spiking, parvalbumin+ GABAergic interneurons: From cellular design to microcircuit function. Science *345*, 1255263.

Hulsebosch, C.E., DeWitt, D.S., Jenkins, L.W., and Prough, D.S. (1998). Traumatic brain injury in rats results in increased expression of Gap-43 that correlates with behavioral recovery. Neurosci. Lett. *255*, 83–86.

Hunt, R.F., Scheff, S.W., and Smith, B.N. (2009). Posttraumatic epilepsy after controlled cortical impact injury in mice. Exp. Neurol. *215*, 243–252.

Hunt, R.F., Scheff, S.W., and Smith, B.N. (2011). Synaptic reorganization of inhibitory hilar interneuron circuitry after traumatic brain injury in mice. J. Neurosci. Off. J. Soc. Neurosci. *31*, 6880–6890.

Huusko, N., Römer, C., Ndode-Ekane, X.E., Lukasiuk, K., and Pitkänen, A. (2015). Loss of hippocampal interneurons and epileptogenesis: a comparison of two animal models of acquired epilepsy. Brain Struct. Funct. *220*, 153–191.

Insel, T.R., Miller, L.P., and Gelhard, R.E. (1990). The ontogeny of excitatory amino acid receptors in rat forebrain--I. N-methyl-D-aspartate and quisqualate receptors. Neuroscience *35*, 31–43.

Isomura, Y., Harukuni, R., Takekawa, T., Aizawa, H., and Fukai, T. (2009). Microcircuitry coordination of cortical motor information in self-initiation of voluntary movements. Nat. Neurosci. *12*, 1586–1593.

Itami, C., Kimura, F., and Nakamura, S. (2007). Brain-derived neurotrophic factor regulates the maturation of layer 4 fast-spiking cells after the second postnatal week in the developing barrel cortex. J. Neurosci. Off. J. Soc. Neurosci. *27*, 2241–2252.

Iudice, A., and Murri, L. (2000). Pharmacological prophylaxis of post-traumatic epilepsy. Drugs *59*, 1091–1099.

Izhikevich, E.M., Desai, N.S., Walcott, E.C., and Hoppensteadt, F.C. (2003). Bursts as a unit of neural information: selective communication via resonance. Trends Neurosci. *26*, 161–167.

Jacobs, K.M., Graber, K.D., Kharazia, V.N., Parada, I., and Prince, D.A. (2000).

Postlesional epilepsy: the ultimate brain plasticity. Epilepsia *41 Suppl 6*, S153–S161.

Jenkins, L.W., Peters, G.W., Dixon, C.E., Zhang, X., Clark, R.S.B., Skinner, J.C., Marion, D.W., Adelson, P.D., and Kochanek, P.M. (2002). Conventional and functional proteomics using large format two-dimensional gel electrophoresis 24 hours after controlled cortical impact in postnatal day 17 rats. J. Neurotrauma *19*, 715–740.

Jin, X., Prince, D.A., and Huguenard, J.R. (2006). Enhanced Excitatory Synaptic Connectivity in Layer V Pyramidal Neurons of Chronically Injured Epileptogenic Neocortex in Rats. J. Neurosci. *26*, 4891–4900.

Jin, X., Huguenard, J.R., and Prince, D.A. (2011). Reorganization of inhibitory synaptic circuits in rodent chronically injured epileptogenic neocortex. Cereb. Cortex N. Y. N 1991 *21*, 1094–1104.

Jin, X., Jiang, K., and Prince, D.A. (2014). Excitatory and Inhibitory Synaptic Connectivity to Layer V Fast-spiking Interneurons in the Freeze Lesion Model of Cortical Microgyria. J. Neurophysiol.

Johnson, V.E., Stewart, J.E., Begbie, F.D., Trojanowski, J.Q., Smith, D.H., and Stewart, W. (2013). Inflammation and white matter degeneration persist for years after a single traumatic brain injury. Brain J. Neurol. *136*, 28–42.

Jones, E.G. (1998). Viewpoint: the core and matrix of thalamic organization. Neuroscience *85*, 331–345.

Jones, T.A., Liput, D.J., Maresh, E.L., Donlan, N., Parikh, T.J., Marlowe, D., and Kozlowski, D.A. (2012). Use-Dependent Dendritic Regrowth Is Limited after Unilateral Controlled Cortical Impact to the Forelimb Sensorimotor Cortex. J. Neurotrauma *29*, 1455–1468.

Katz, L.C. (1993). Coordinate activity in retinal and cortical development. Curr. Opin. Neurobiol. *3*, 93–99.

Kawaguchi, Y., and Kondo, S. (2002). Parvalbumin, somatostatin and cholecystokinin as chemical markers for specific GABAergic interneuron types in the rat frontal cortex. J. Neurocytol. *31*, 277–287.

Kawaguchi, Y., and Kubota, Y. (1997). GABAergic cell subtypes and their synaptic connections in rat frontal cortex. Cereb. Cortex *7*, 476–486.

Kawaguchi, Y., Katsumaru, H., Kosaka, T., Heizmann, C.W., and Hama, K. (1987). Fast spiking cells in rat hippocampus (CA1 region) contain the calcium-binding protein parvalbumin. Brain Res. *416*, 369–374.

Keros, S., and Hablitz, J.J. (2005). Subtype-specific GABA transporter antagonists synergistically modulate phasic and tonic GABAA conductances in rat neocortex. J.

Neurophysiol. *94*, 2073–2085.

Kim, E. (2002). Agitation, aggression, and disinhibition syndromes after traumatic brain injury. NeuroRehabilitation *17*, 297–310.

Kinney, J.W., Davis, C.N., Tabarean, I., Conti, B., Bartfai, T., and Behrens, M.M. (2006). A specific role for NR2A-containing NMDA receptors in the maintenance of parvalbumin and GAD67 immunoreactivity in cultured interneurons. J. Neurosci. Off. J. Soc. Neurosci. *26*, 1604–1615.

Kleschevnikov, A.M., Belichenko, P.V., Villar, A.J., Epstein, C.J., Malenka, R.C., and Mobley, W.C. (2004). Hippocampal long-term potentiation suppressed by increased inhibition in the Ts65Dn mouse, a genetic model of Down syndrome. J. Neurosci. Off. J. Soc. Neurosci. *24*, 8153–8160.

Klonoff, H., Clark, C., and Klonoff, P.S. (1993). Long-term outcome of head injuries: a 23 year follow up study of children with head injuries. J. Neurol. Neurosurg. Psychiatry *56*, 410–415.

Kobayashi, M., Wen, X., and Buckmaster, P.S. (2003). Reduced inhibition and increased output of layer II neurons in the medial entorhinal cortex in a model of temporal lobe epilepsy. J. Neurosci. Off. J. Soc. Neurosci. *23*, 8471–8479.

Kobori, N., Clifton, G.L., and Dash, P. (2002). Altered expression of novel genes in the cerebral cortex following experimental brain injury. Brain Res. Mol. Brain Res. *104*, 148–158.

Kochanek, P.M., Carney, N., Adelson, P.D., Ashwal, S., Bell, M.J., Bratton, S., Carson, S., Chesnut, R.M., Ghajar, J., Goldstein, B., et al. (2012). Guidelines for the acute medical management of severe traumatic brain injury in infants, children, and adolescents--second edition. Pediatr. Crit. Care Med. J. Soc. Crit. Care Med. World Fed. Pediatr. Intensive Crit. Care Soc. *13 Suppl 1*, S1–S82.

Kuhlman, S.J., Olivas, N.D., Tring, E., Ikrar, T., Xu, X., and Trachtenberg, J.T. (2013). A disinhibitory microcircuit initiates critical-period plasticity in the visual cortex. Nature *501*, 543–546.

Lawrence, J.J., and McBain, C.J. (2003). Interneuron diversity series: containing the detonation--feedforward inhibition in the CA3 hippocampus. Trends Neurosci. *26*, 631–640.

Lenzlinger, P.M., Shimizu, S., Marklund, N., Thompson, H.J., Schwab, M.E., Saatman, K.E., Hoover, R.C., Bareyre, F.M., Motta, M., Luginbuhl, A., et al. (2005). Delayed inhibition of Nogo-A does not alter injury-induced axonal sprouting but enhances recovery of cognitive function following experimental traumatic brain injury in rats. Neuroscience *134*, 1047–1056.

Letzkus, J.J., Wolff, S.B.E., Meyer, E.M.M., Tovote, P., Courtin, J., Herry, C., and Lüthi, A. (2011). A disinhibitory microcircuit for associative fear learning in the auditory cortex. Nature *480*, 331–335.

Levitt, P. (2003). Structural and functional maturation of the developing primate brain. J. Pediatr. *143*, S35–S45.

Levitt, P., Eagleson, K.L., and Powell, E.M. (2004). Regulation of neocortical interneuron development and the implications for neurodevelopmental disorders. Trends Neurosci. *27*, 400–406.

Lewis, D.A., Curley, A.A., Glausier, J., and Volk, D.W. (2012). Cortical Parvalbumin Interneurons and Cognitive Dysfunction in Schizophrenia. Trends Neurosci. *35*, 57–67.

Li, K., and Xu, E. (2008). The role and the mechanism of gamma-aminobutyric acid during central nervous system development. Neurosci. Bull. *24*, 195–200.

Li, H.H., Lee, S.M., Cai, Y., Sutton, R.L., and Hovda, D.A. (2004). Differential gene expression in hippocampus following experimental brain trauma reveals distinct features of moderate and severe injuries. J. Neurotrauma *21*, 1141–1153.

Lighthall, J.W., Dixon, C.E., and Anderson, T.E. (1989). Experimental models of brain injury. J. Neurotrauma *6*, 83–97.

Lisman, J.E. (1997). Bursts as a unit of neural information: making unreliable synapses reliable. Trends Neurosci. *20*, 38–43.

Liu, N.-K., Zhang, Y.-P., O'Connor, J., Gianaris, A., Oakes, E., Lu, Q.-B., Verhovshek, T., Walker, C.L., Shields, C.B., and Xu, X.-M. (2013). A bilateral head injury that shows graded brain damage and behavioral deficits in adultmice. Brain Res. *1499*, 121–128.

Lowenstein, D.H., Thomas, M.J., Smith, D.H., and McIntosh, T.K. (1992). Selective vulnerability of dentate hilar neurons following traumatic brain injury: a potential mechanistic link between head trauma and disorders of the hippocampus. J. Neurosci. Off. J. Soc. Neurosci. *12*, 4846–4853.

Luerssen, T.G., Klauber, M.R., and Marshall, L.F. (1988a). Outcome from head injury related to patient's age. A longitudinal prospective study of adult and pediatric head injury. J. Neurosurg. *68*, 409–416.

Luerssen, T.G., Klauber, M.R., and Marshall, L.F. (1988b). Outcome from head injury related to patient's age. A longitudinal prospective study of adult and pediatric head injury. J. Neurosurg. *68*, 409–416.

Ma, Y., and Prince, D.A. (2012). Functional alterations in GABAergic fast-spiking interneurons in chronically injured epileptogenic neocortex. Neurobiol. Dis. *47*, 102–113.

Ma, Y., Hu, H., Berrebi, A.S., Mathers, P.H., and Agmon, A. (2006). Distinct Subtypes

of Somatostatin-Containing Neocortical Interneurons Revealed in Transgenic Mice. J. Neurosci. *26*, 5069–5082.

Maas, A.I., Stocchetti, N., and Bullock, R. (2008). Moderate and severe traumatic brain injury in adults. Lancet Neurol. *7*, 728–741.

Magiorkinis, E., Sidiropoulou, K., and Diamantis, A. (2010). Hallmarks in the history of epilepsy: epilepsy in antiquity. Epilepsy Behav. EB *17*, 103–108.

Mannix, R.C., Zhang, J., Park, J., Lee, C., and Whalen, M.J. (2011). Detrimental effect of genetic inhibition of B-site APP-cleaving enzyme 1 on functional outcome after controlled cortical impact in young adult mice. J. Neurotrauma *28*, 1855–1861.

Marklund, N., Bareyre, F.M., Royo, N.C., Thompson, H.J., Mir, A.K., Grady, M.S., Schwab, M.E., and McIntosh, T.K. (2007). Cognitive outcome following brain injury and treatment with an inhibitor of Nogo-A in association with an attenuated downregulation of hippocampal growth-associated protein-43 expression. J. Neurosurg. *107*, 844–853.

Markram, H., Toledo-Rodriguez, M., Wang, Y., Gupta, A., Silberberg, G., and Wu, C. (2004a). Interneurons of the neocortical inhibitory system. Nat. Rev. Neurosci. *5*, 793–807.

Markram, H., Toledo-Rodriguez, M., Wang, Y., Gupta, A., Silberberg, G., and Wu, C. (2004b). Interneurons of the neocortical inhibitory system. Nat. Rev. Neurosci. *5*, 793–807.

Matsumoto, H., and Marsan, C.A. (1964). Cortical cellular phenomena in experimental epilepsy: Interictal manifestations. Exp. Neurol. *9*, 286–304.

Mazarati, A. (2006). Is posttraumatic epilepsy the best model of posttraumatic epilepsy? Epilepsy Curr. Am. Epilepsy Soc. *6*, 213–214.

McKinlay, A., Dalrymple-Alford, J.C., Horwood, L.J., and Fergusson, D.M. (2002). Long term psychosocial outcomes after mild head injury in early childhood. J. Neurol. Neurosurg. Psychiatry *73*, 281–288.

Mello, L.E., Cavalheiro, E.A., Tan, A.M., Kupfer, W.R., Pretorius, J.K., Babb, T.L., and Finch, D.M. (1993). Circuit mechanisms of seizures in the pilocarpine model of chronic epilepsy: cell loss and mossy fiber sprouting. Epilepsia *34*, 985–995.

Menon, D.K., Schwab, K., Wright, D.W., Maas, A.I., and Demographics and Clinical Assessment Working Group of the International and Interagency Initiative toward Common Data Elements for Research on Traumatic Brain Injury and Psychological Health (2010). Position statement: definition of traumatic brain injury. Arch. Phys. Med. Rehabil. *91*, 1637–1640.

Michael, A.P., Stout, J., Roskos, P.T., Bolzenius, J., Gfeller, J., Mogul, D., and Bucholz,

R. (2015). Evaluation of Cortical Thickness after Traumatic Brain Injury in Military Veterans. J. Neurotrauma *32*, 1751–1758.

Miller, L.M., Escabí, M.A., and Schreiner, C.E. (2001). Feature selectivity and interneuronal cooperation in the thalamocortical system. J. Neurosci. Off. J. Soc. Neurosci. *21*, 8136–8144.

Miller, M.N., Okaty, B.W., Kato, S., and Nelson, S.B. (2011). Activity-dependent changes in the firing properties of neocortical fast-spiking interneurons in the absence of large changes in gene expression. Dev. Neurobiol. *71*, 62–70.

Mishra, A.M., Bai, X., Sanganahalli, B.G., Waxman, S.G., Shatillo, O., Grohn, O., Hyder, F., Pitkanen, A., and Blumenfeld, H. (2014). Decreased Resting Functional Connectivity after Traumatic Brain Injury in the Rat. PLoS ONE *9*.

Mitchell, S.J., and Silver, R.A. (2003). Shunting Inhibition Modulates Neuronal Gain during Synaptic Excitation. Neuron *38*, 433–445.

Morris, N.P., and Henderson, Z. (2000). Perineuronal nets ensheath fast spiking, parvalbumin-immunoreactive neurons in the medial septum/diagonal band complex. Eur. J. Neurosci. *12*, 828–838.

Mrzljak, L., Uylings, H.B., Van Eden, C.G., and Judás, M. (1990). Neuronal development in human prefrontal cortex in prenatal and postnatal stages. Prog. Brain Res. *85*, 185–222.

Nakamura, T., Matsumoto, J., Takamura, Y., Ishii, Y., Sasahara, M., Ono, T., and Nishijo, H. (2015). Relationships among parvalbumin-immunoreactive neuron density, phase-locked gamma oscillations, and autistic/schizophrenic symptoms in PDGFR-β knock-out and control mice. PloS One *10*, e0119258.

Nathanson, J.L., Yanagawa, Y., Obata, K., and Callaway, E.M. (2009). Preferential labeling of inhibitory and excitatory cortical neurons by endogenous tropism of AAV and lentiviral vectors. Neuroscience *161*, 441–450.

Nelson, S.B., and Turrigiano, G.G. (1998). Synaptic depression: a key player in the cortical balancing act. Nat. Neurosci. *1*, 539–541.

Nichols, J., Perez, R., Wu, C., Adelson, P.D., and Anderson, T. (2015). Traumatic Brain Injury Induces Rapid Enhancement of Cortical Excitability in Juvenile Rats. CNS Neurosci. Ther. *21*, 193–203.

Nilsson, P., Ronne-Engström, E., Flink, R., Ungerstedt, U., Carlson, H., and Hillered, L. (1994). Epileptic seizure activity in the acute phase following cortical impact trauma in rat. Brain Res. *637*, 227–232.

Nishibe, M., Barbay, S., Guggenmos, D., and Nudo, R.J. (2010). Reorganization of

Motor Cortex after Controlled Cortical Impact in Rats and Implications for Functional Recovery. J. Neurotrauma *27*, 2221–2232.

Noctor, S.C., Flint, A.C., Weissman, T.A., Dammerman, R.S., and Kriegstein, A.R. (2001). Neurons derived from radial glial cells establish radial units in neocortex. Nature *409*, 714–720.

Nudo, R.J. (2006). Mechanisms for recovery of motor function following cortical damage. Curr. Opin. Neurobiol. *16*, 638–644.

Okaty, B.W., Miller, M.N., Sugino, K., Hempel, C.M., and Nelson, S.B. (2009). Transcriptional and electrophysiological maturation of neocortical fastspiking GABAergic interneurons. J. Neurosci. Off. J. Soc. Neurosci. *29*, 7040–7052.

Olesen, S.P. (1987). Leakiness of rat brain microvessels to fluorescent probes following craniotomy. Acta Physiol. Scand. *130*, 63–68.

Orduz, D., Bischop, D.P., Schwaller, B., Schiffmann, S.N., and Gall, D. (2013). Parvalbumin tunes spike-timing and efferent short-term plasticity in striatal fast spiking interneurons. J. Physiol. *591*, 3215–3232.

Orlando, C., and Raineteau, O. (2015). Integrity of cortical perineuronal nets influences corticospinal tract plasticity after spinal cord injury. Brain Struct. Funct. *220*, 1077–1091.

Overstreet, L.S., and Westbrook, G.L. (2003). Synapse density regulates independence at unitary inhibitory synapses. J. Neurosci. Off. J. Soc. Neurosci. *23*, 2618–2626.

Pagni, C.A., and Zenga, F. (2005). Posttraumatic epilepsy with special emphasis on prophylaxis and prevention. Acta Neurochir. Suppl. *93*, 27–34.

Pandolfo, M. (2011). Genetics of epilepsy. Semin. Neurol. *31*, 506–518.

Park, E., Bell, J.D., and Baker, A.J. (2008). Traumatic brain injury: Can the consequences be stopped? CMAJ Can. Med. Assoc. J. *178*, 1163–1170.

Pavlov, I., Huusko, N., Drexel, M., Kirchmair, E., Sperk, G., Pitkänen, A., and Walker, M.C. (2011). Progressive loss of phasic, but not tonic, GABAA receptor-mediated inhibition in dentate granule cells in a model of post-traumatic epilepsy in rats. Neuroscience *194*, 208–219.

Paxinos, G., and Watson, C. (2007). The rat brain in stereotaxic coordinates (Amsterdam; Boston: Elsevier).

Pearce, A.J., Hoy, K., Rogers, M.A., Corp, D.T., Davies, C.B., Maller, J.J., and Fitzgerald, P.B. (2015). Acute motor, neurocognitive and neurophysiological change following concussion injury in Australian amateur football. A prospective multimodal investigation. J. Sci. Med. Sport *18*, 500–506.

Pearson, W.S., Ovalle, F., Faul, M., and Sasser, S.M. (2012a). A review of traumatic brain injury trauma center visits meeting physiologic criteria from The American College of Surgeons Committee on Trauma/Centers for Disease Control and Prevention Field Triage Guidelines. Prehospital Emerg. Care Off. J. Natl. Assoc. EMS Physicians Natl. Assoc. State EMS Dir. *16*, 323–328.

Pearson, W.S., Sugerman, D.E., McGuire, L.C., and Coronado, V.G. (2012b). Emergency Department Visits for Traumatic Brain Injury in Older Adults in the United States: 2006–08. West. J. Emerg. Med. *13*, 289–293.

Perucca, P., and Gilliam, F.G. (2012). Adverse effects of antiepileptic drugs. Lancet Neurol. *11*, 792–802.

Peters, A., and Jones, E.G. (1984). Cerebral Cortex: Volume 1: Cellular Components of the Cerebral Cortex (New York: Springer).

Petilla Interneuron Nomenclature Group, Ascoli, G.A., Alonso-Nanclares, L., Anderson, S.A., Barrionuevo, G., Benavides-Piccione, R., Burkhalter, A., Buzsáki, G., Cauli, B., Defelipe, J., et al. (2008). Petilla terminology: nomenclature of features of GABAergic interneurons of the cerebral cortex. Nat. Rev. Neurosci. *9*, 557–568.

Pi, H.-J., Hangya, B., Kvitsiani, D., Sanders, J.I., Huang, Z.J., and Kepecs, A. (2013). Cortical interneurons that specialize in disinhibitory control. Nature *advance online publication*.

Pinto, D.J., Brumberg, J.C., and Simons, D.J. (2000). Circuit dynamics and coding strategies in rodent somatosensory cortex. J. Neurophysiol. *83*, 1158–1166.

Pinto, D.J., Hartings, J.A., Brumberg, J.C., and Simons, D.J. (2003). Cortical damping: analysis of thalamocortical response transformations in rodent barrel cortex. Cereb. Cortex N. Y. N 1991 *13*, 33–44.

Pitkänen, A., and McIntosh, T.K. (2006). Animal models of post-traumatic epilepsy. J. Neurotrauma *23*, 241–261.

Pitkänen, A., Kharatishvili, I., Karhunen, H., Lukasiuk, K., Immonen, R., Nairismägi, J., Gröhn, O., and Nissinen, J. (2007). Epileptogenesis in experimental models. Epilepsia *48 Suppl 2*, 13–20.

Polack, P.-O., Guillemain, I., Hu, E., Deransart, C., Depaulis, A., and Charpier, S. (2007). Deep Layer Somatosensory Cortical Neurons Initiate Spike-and-Wave Discharges in a Genetic Model of Absence Seizures. J. Neurosci. *27*, 6590–6599.

Pouille, F., and Scanziani, M. (2001). Enforcement of temporal fidelity in pyramidal cells by somatic feed-forward inhibition. Science *293*, 1159–1163.

Powell, S.B., Sejnowski, T.J., and Behrens, M.M. (2012). Behavioral and neurochemical

consequences of cortical oxidative stress on parvalbumin-interneuron maturation in rodent models of schizophrenia. Neuropharmacology *62*, 1322–1331.

Prince, D.A. (1978). Neurophysiology of Epilepsy. Annu. Rev. Neurosci. *1*, 395–415.

Prince, D.A., and Connors, B.W. (1986). Mechanisms of interictal epileptogenesis. Adv. Neurol. *44*, 275–299.

Prince, D.A., and Tseng, G.F. (1993). Epileptogenesis in chronically injured cortex: in vitro studies. J. Neurophysiol. *69*, 1276–1291.

Prinz, A., Selesnew, L.-M., Liss, B., Roeper, J., and Carlsson, T. (2013). Increased excitability in serotonin neurons in the dorsal raphe nucleus in the 6-OHDA mouse model of Parkinson's disease. Exp. Neurol. *248*, 236–245.

Rakic, P. (1988). Specification of cerebral cortical areas. Science *241*, 170–176.

Ramantani, G. (2013). Neonatal epilepsy and underlying aetiology: to what extent do seizures and EEG abnormalities influence outcome? Epileptic Disord. Int. Epilepsy J. Videotape *15*, 365–375.

Rheims, S., Holmgren, C.D., Chazal, G., Mulder, J., Harkany, T., Zilberter, T., and Zilberter, Y. (2009). GABA action in immature neocortical neurons directly depends on the availability of ketone bodies. J. Neurochem. *110*, 1330–1338.

Rola, R., Mizumatsu, S., Otsuka, S., Morhardt, D., Noblehaeusslein, L., Fishman, K., Potts, M., and Fike, J. (2006). Alterations in hippocampal neurogenesis following traumatic brain injury in mice. Exp. Neurol. *202*, 189–199.

Romcy-Pereira, R.N., and Garcia-Cairasco, N. (2003). Hippocampal cell proliferation and epileptogenesis after audiogenic kindling are not accompanied by mossy fiber sprouting or Fluoro-Jade staining. Neuroscience *119*, 533–546.

Routbort, M.J., Bausch, S.B., and McNamara, J.O. (1999). Seizures, cell death, and mossy fiber sprouting in kainic acid-treated organotypic hippocampal cultures. Neuroscience *94*, 755–765.

Rubio-Garrido, P., Pérez-de-Manzo, F., Porrero, C., Galazo, M.J., and Clascá, F. (2009). Thalamic input to distal apical dendrites in neocortical layer 1 is massive and highly convergent. Cereb. Cortex N. Y. N 1991 *19*, 2380–2395.

Rudy, B., Fishell, G., Lee, S., and Hjerling-Leffler, J. (2011). Three Groups of Interneurons Account for Nearly 100% of Neocortical GABAergic Neurons. Dev. Neurobiol. *71*, 45–61.

Saatman, K.E., Duhaime, A.-C., Bullock, R., Maas, A.I.R., Valadka, A., Manley, G.T., and Workshop Scientific Team and Advisory Panel Members (2008). Classification of

traumatic brain injury for targeted therapies. J. Neurotrauma *25*, 719–738.

Salin, P., Tseng, G.F., Hoffman, S., Parada, I., and Prince, D.A. (1995). Axonal sprouting in layer V pyramidal neurons of chronically injured cerebral cortex. J. Neurosci. *15*, 8234–8245.

Sarkar, K., Keachie, K., Nguyen, U., Muizelaar, J.P., Zwienenberg-Lee, M., and Shahlaie, K. (2014). Computed tomography characteristics in pediatric versus adult traumatic brain injury. J. Neurosurg. Pediatr. *13*, 307–314.

Scheff, S.W., Price, D.A., Hicks, R.R., Baldwin, S.A., Robinson, S., and Brackney, C. (2005). Synaptogenesis in the Hippocampal CA1 Field following Traumatic Brain Injury. J. Neurotrauma *22*, 719–732.

Schmidt, A.T., Hanten, G.R., Li, X., Vasquez, A.C., Wilde, E.A., Chapman, S.B., and Levin, H.S. (2012). Decision making after pediatric traumatic brain injury: trajectory of recovery and relationship to age and gender. Int. J. Dev. Neurosci. Off. J. Int. Soc. Dev. Neurosci. *30*, 225–230.

Schwaller, B., Tetko, I.V., Tandon, P., Silveira, D.C., Vreugdenhil, M., Henzi, T., Potier, M.-C., Celio, M.R., and Villa, A.E.P. (2004). Parvalbumin deficiency affects network properties resulting in increased susceptibility to epileptic seizures. Mol. Cell. Neurosci. *25*, 650–663.

Shatz, C.J. (1990). Impulse activity and the patterning of connections during cns development. Neuron *5*, 745–756.

Shipp, S. (2007). Structure and function of the cerebral cortex. Curr. Biol. *17*, R443–R449.

Smith, C., Gentleman, S.M., Leclercq, P.D., Murray, L.S., Griffin, W.S.T., Graham, D.I., and Nicoll, J.A.R. (2013). The neuroinflammatory response in humans after traumatic brain injury. Neuropathol. Appl. Neurobiol. *39*, 654–666.

Smith, D.H., Soares, H.D., Pierce, J.S., Perlman, K.G., Saatman, K.M., Meaney, D.F., Dixon, C.E., and McIntosh, T.K. (1995). A Model of Parasagittal Controlled Cortical Impact in the Mouse: Cognitive and Histopathologic Effects. J. Neurotrauma *12*, 169–178.

Sohal, V.S., Zhang, F., Yizhar, O., and Deisseroth, K. (2009). Parvalbumin neurons and gamma rhythms enhance cortical circuit performance. Nature *459*, 698–702.

Somjen, G.G. (2004). Ions in the Brain : Normal Function, Seizures, and Stroke: Normal Function, Seizures, and Stroke (Oxford University Press).

Statler, K.D., Scheerlinck, P., Pouliot, W., Hamilton, M., White, H.S., and Dudek, F.E. (2009). A potential model of pediatric posttraumatic epilepsy. Epilepsy Res. *86*, 221–223.

Steriade, M., Amzica, F., Neckelmann, D., and Timofeev, I. (1998). Spike-wave complexes and fast components of cortically generated seizures. II. Extra- and intracellular patterns. J. Neurophysiol. *80*, 1456–1479.

Sun, Q.-Q., Huguenard, J.R., and Prince, D.A. (2006). Barrel cortex microcircuits: thalamocortical feedforward inhibition in spiny stellate cells is mediated by a small number of fast-spiking interneurons. J. Neurosci. Off. J. Soc. Neurosci. *26*, 1219–1230.

Tanaka, Y.H., Tanaka, Y., Fujiyama, F., Furuta, T., Yanagawa, Y., and Kaneko, T. (2011). Local connections of layer 5 GABAergic interneurons to corticospinal neurons. Front. Neural Circuits *5*, 12.

Tasker, J.G., and Dudek, F.E. (1991). Electrophysiology of GABA-mediated synaptic transmission and possible roles in epilepsy. Neurochem. Res. *16*, 251–262.

Telfeian, A.E., and Connors, B.W. (1998). Layer-specific pathways for the horizontal propagation of epileptiform discharges in neocortex. Epilepsia *39*, 700–708.

Temkin, O. (1994). The Falling Sickness: A History of Epilepsy from the Greeks to the Beginnings of Modern Neurology (JHU Press).

Thompson, H.J., Lifshitz, J., Marklund, N., Grady, M.S., Graham, D.I., Hovda, D.A., and McIntosh, T.K. (2005). Lateral fluid percussion brain injury: a 15-year review and evaluation. J. Neurotrauma *22*, 42–75.

Thurman, D.J., Beghi, E., Begley, C.E., Berg, A.T., Buchhalter, J.R., Ding, D., Hesdorffer, D.C., Hauser, W.A., Kazis, L., Kobau, R., et al. (2011). Standards for epidemiologic studies and surveillance of epilepsy. Epilepsia *52 Suppl 7*, 2–26.

Timofeev, I., and Steriade, M. (2004). Neocortical seizures: initiation, development and cessation. Neuroscience *123*, 299–336.

Traub, R.D., and Wong, R.K. (1982). Cellular mechanism of neuronal synchronization in epilepsy. Science *216*, 745–747.

Traub, R.D., Bibbig, A., LeBeau, F.E.N., Buhl, E.H., and Whittington, M.A. (2004). Cellular mechanisms of neuronal population oscillations in the hippocampus in vitro. Annu. Rev. Neurosci. *27*, 247–278.

Tremblay, S., de Beaumont, L., Lassonde, M., and Théoret, H. (2011). Evidence for the specificity of intracortical inhibitory dysfunction in asymptomatic concussed athletes. J. Neurotrauma *28*, 493–502.

Ueno, M., Hayano, Y., Nakagawa, H., and Yamashita, T. (2012). Intraspinal rewiring of the corticospinal tract requires target-derived brain-derived neurotrophic factor and compensates lost function after brain injury. Brain J. Neurol. *135*, 1253–1267.

Uhlhaas, P.J., and Singer, W. (2010). Abnormal neural oscillations and synchrony in

schizophrenia. Nat. Rev. Neurosci. *11*, 100–113.

van den Pol, A.N., Obrietan, K., and Chen, G. (1996). Excitatory actions of GABA after neuronal trauma. J. Neurosci. Off. J. Soc. Neurosci. *16*, 4283–4292.

Wang, Y., Kakizaki, T., Sakagami, H., Saito, K., Ebihara, S., Kato, M., Hirabayashi, M., Saito, Y., Furuya, N., and Yanagawa, Y. (2009). Fluorescent labeling of both GABAergic and glycinergic neurons in vesicular GABA transporter (VGAT)–Venus transgenic mouse. Neuroscience *164*, 1031–1043.

Werner, C., and Engelhard, K. (2007). Pathophysiology of traumatic brain injury. Br. J. Anaesth. *99*, 4–9.

Wilde, E.A., Merkley, T.L., Bigler, E.D., Max, J.E., Schmidt, A.T., Ayoub, K.W., McCauley, S.R., Hunter, J.V., Hanten, G., Li, X., et al. (2012). Longitudinal changes in cortical thickness in children after traumatic brain injury and their relation to behavioral regulation and emotional control. Int. J. Dev. Neurosci. Off. J. Int. Soc. Dev. Neurosci. *30*, 267–276.

Willmore, L.J. (1990). Post-traumatic epilepsy: cellular mechanisms and implications for treatment. Epilepsia *31 Suppl 3*, S67–S73.

Wilson, N.R., Runyan, C.A., Wang, F.L., and Sur, M. (2012). Division and subtraction by distinct cortical inhibitory networks in vivo. Nature *488*, 343–348.

Wise, S.P. (1975). The laminar organization of certain afferent and efferent fiber systems in the rat somatosensory cortex. Brain Res. *90*, 139–142.

Wöhr, M., Orduz, D., Gregory, P., Moreno, H., Khan, U., Vörckel, K.J., Wolfer, D.P., Welzl, H., Gall, D., Schiffmann, S.N., et al. (2015). Lack of parvalbumin in mice leads to behavioral deficits relevant to all human autism core symptoms and related neural morphofunctional abnormalities. Transl. Psychiatry *5*, e525.

Wojcik, S.M., Katsurabayashi, S., Guillemin, I., Friauf, E., Rosenmund, C., Brose, N., and Rhee, J.-S. (2006). A shared vesicular carrier allows synaptic corelease of GABA and glycine. Neuron *50*, 575–587.

Xu, X., Roby, K.D., and Callaway, E.M. (2010). Immunochemical characterization of inhibitory mouse cortical neurons: Three chemically distinct classes of inhibitory cells. J. Comp. Neurol. *518*, 389–404.

Yang, L., Benardo, L.S., Valsamis, H., and Ling, D.S.F. (2007). Acute injury to superficial cortex leads to a decrease in synaptic inhibition and increase in excitation in neocortical layer V pyramidal cells. J. Neurophysiol. *97*, 178–187.

Yang, L., Afroz, S., Michelson, H.B., Goodman, J.H., Valsamis, H.A., and Ling, D.S.F. (2010). Spontaneous epileptiform activity in rat neocortex after controlled cortical impact

injury. J. Neurotrauma *27*, 1541–1548.

Yoshimura, Y., and Callaway, E.M. (2005). Fine-scale specificity of cortical networks depends on inhibitory cell type and connectivity. Nat. Neurosci. *8*, 1552–1559.

Zhang, Z. (2004). Maturation of Layer V Pyramidal Neurons in the Rat Prefrontal Cortex: Intrinsic Properties and Synaptic Function. J. Neurophysiol. *91*, 1171–1182.

Zhang, Q.-G., Laird, M.D., Han, D., Nguyen, K., Scott, E., Dong, Y., Dhandapani, K.M., and Brann, D.W. (2012). Critical Role of NADPH Oxidase in Neuronal Oxidative Damage and Microglia Activation following Traumatic Brain Injury. PLoS ONE *7*, e34504.

Ziyatdinova, S., Gurevicius, K., Kutchiashvili, N., Bolkvadze, T., Nissinen, J., Tanila, H., and Pitkänen, A. (2011). Spontaneous epileptiform discharges in a mouse model of Alzheimer's disease are suppressed by antiepileptic drugs that block sodium channels. Epilepsy Res. *94*, 75–85.

van Zundert, B., Izaurieta, P., Fritz, E., and Alvarez, F.J. (2012). Early pathogenesis in the adult-onset neurodegenerative disease amyotrophic lateral sclerosis. J. Cell. Biochem. *113*, 3301–3312.

(2005). Atlas epilepsy care in the world. (Geneva: Programme for Neurological Diseases and Neuroscience, Dept. of Mental Health and Substance Abuse, World Health Organization).

(2012). Jasper's Basic Mechanisms of the Epilepsies (Bethesda (MD): National Center for Biotechnology Information (US)).

CHAPTER 5

REPETITIVE MILD TRAUMTIC BRAIN INJURY INDUCES VENTRICULOMEGALY AND CORTICAL THINNING IN JUVENILE RATS

Traumatic brain injury (TBI) most frequently occurs in pediatric patients and remains a leading cause of childhood death and disability. Mild TBI (mTBI) accounts for nearly 75% of all TBI cases, yet its neuropathophysiology is still poorly understood. While even a single mTBI injury can lead to persistent deficits, repeat injuries increase the severity and duration of both acute symptoms and long-term deficits. In this study, to model pediatric repetitive mTBI (rmTBI) we subjected unrestrained juvenile animals (postnatal day 20) to repeat weight-drop impacts. Animals were anesthetized and subjected to sham injury or rmTBI once per day for 5 days. Magnetic resonance imaging (MRI) performed 14 days after injury revealed marked cortical atrophy and ventriculomegaly in rmTBI animals. Specifically, beneath the impact zone the thickness of the cortex was reduced by up to 46% and the area of the ventricles increased by up to 970%. Immunostaining with the neuron-specific marker NeuN revealed an overall loss of neurons within the motor cortex but no change in neuronal density. Examination of intrinsic and synaptic properties of layer II/III pyramidal neurons revealed no significant difference between sham-injured and rmTBI animals at rest or under convulsant challenge with the potassium channel blocker 4-aminopyridine. Overall, our findings indicate that the neuropathological changes reported after pediatric rmTBI can be effectively modeled by repeat weight drop in juvenile animals. Developing a better understanding of how rmTBI alters the pediatric brain may help improve patient care and direct “return to game” decision making in adolescents.

Introduction

Traumatic brain injury (TBI) is a significant health concern that affects more than 1.5 million Americans each year (Faul et al. 2010; Langlois et al. 2006; Rutland-Brown et al. 2006). At present, no single classification system has been developed that encompasses the host of clinical, pathological, behavioral, and cellular changes that occur as a result of TBI. In general, TBI is categorized into mild, moderate, and severe. Mild TBI (mTBI), including concussions, accounts for nearly 75% of all TBI cases (Cassidy et al. 2004; Elder and Cristian 2009; Langlois et al. 2005, 2006; Miniño et al. 2006). mTBI is often called an "invisible wound," as it results in a minimal loss of consciousness (<30 min) and minimal acute neuropathological findings (Carroll et al. 2004; Morey et al. 2013; Smith et al. 2013). Consequently, mTBI is often difficult to detect and diagnose in the early acute stages after injury and may result in the incidence being underreported. After mTBI patients may experience cognitive and behavioral impairments including confusion, memory and attention deficits, and headaches (Barkhoudarian et al. 2011). These symptoms usually resolve completely within 2–3 wk after a single mTBI (Lovell et al. 2003; McCrea et al. 2003). However, especially with repeat injuries, these symptoms may persist for extended periods of time (Arciniegas et al. 2005; Halstead et al. 2010; Pellman et al. 2003).

Repetitive mTBI (rmTBI) significantly increases symptom severity (Collins et al. 2002), leads to longer-term cognitive and motor deficits (De Beaumont et al. 2007; Guskiewicz 2011; Omalu et al. 2010b), and increases the risk for developing dementia (Guskiewicz et al. 2005) and neurodegenerative disorders (Masel and DeWitt 2010; McKee et al. 2009, 2010; Plassman et al. 2000). Even a single mTBI event places

patients at a greater risk for further TBI events and the ensuing consequences of rmTBI (Barkhoudarian et al. 2011; MacGregor et al. 2011; Tremblay et al. 2013; Zemper 2003). In contrast to a single mTBI event, rmTBI induces significant long-term structural changes to the brain including brain atrophy and enlargement of the ventricles (Giza 2006; Huh et al. 2007; Maxwell 2012; Smith et al. 2013; Wang et al. 2014). Currently no effective treatments are available to prevent the adverse complications associated with rmTBI. Development of new therapeutic strategies is contingent on an improved understanding of the underlying pathophysiological processes induced by rmTBI. Recent public and research attention has focused on understanding rmTBI that occurs in adult athletes and military personnel. However, recent reports indicate that children may be particularly susceptible and sensitive to the effects of TBI (Barlow et al. 2010; Eisenberg et al. 2013; Field et al. 2003; Guskiewicz et al. 2000; Kontos et al. 2013). In children, TBI remains a leading cause of death and disability (Faul et al. 2010), with >10% experiencing a mTBI by the age of 10 (Barlow et al. 2010; Bruns and Hauser 2003). As with adults, the source of TBI varies greatly in children, but it may occur from a combination of events including accidents, abuse (shaken baby syndrome), or adolescent sport concussions. The pediatric brain is different from the adult brain owing to a host of ongoing neurodevelopmental processes including cortical hypertrophy, synaptogenesis, use-dependent pruning, enhanced glucose metabolism, increased neurotrophic factors, altered excitatory amino acid receptors, and myelination of axons (Adelson 1999; Chugani et al. 1987; Friedman et al. 1991; Giza 2006; Insel et al. 1990). These processes have often been thought to confer children with an advantage in coping with brain injury, but recent evidence suggests they may be particularly sensitive to the

effects of rmTBI (Eisenberg et al. 2013; Field et al. 2003).

Several models of TBI have been developed (Angoa-Pérez et al. 2014; Cernak 2005; Xiong et al. 2013), but many are intended to induce a more severe TBI and do not effectively model mTBI. In this study, we modified a recently published adult weight-drop rmTBI model (Kane et al. 2012) for use in juvenile rats. This method of inducing rmTBI recapitulates the nature of the injury (closed head injury, unrestrained animal, linear and rotational acceleration forces) and was recently shown to produce several of the cognitive and behavioral outcomes associated with clinical mTBI (Kane et al. 2012; Meaney and Smith 2011; Viano et al. 2007). With the use of this method, in juvenile rats a single mTBI was sufficient to induce clinically relevant impairments to executive, motor, and balance functions (Mychasiuk et al. 2014). The durations of these impairments are variable, but they have been reported to persist for up to months after mTBI (McCrea et al. 2003; Petraglia et al. 2014). The purpose of this study was to examine the neuropathological and neurophysiological changes induced early after rmTBI in juvenile rats with magnetic resonance imaging (MRI), immunohistochemical, and electrophysiological approaches. The results validate the use of this repetitive weight-drop method to effectively model pediatric rmTBI. Similar to what has been reported in humans (Halstead et al. 2010; McCrea et al. 2003; Smith et al. 2013), rmTBI in juvenile rats induced marked cortical atrophy (i.e., decreased cortical thickness) and enlarged ventricles that were most pronounced beneath the impact site. Despite significant cortical atrophy, no intrinsic or synaptic electrophysiological changes were evident in layer II/III neurons recorded from rmTBI animals 14 days after injury. These findings are in contrast to the recent report from adult rodents (Kane et al. 2012) and after

single mTBI (Mychasiuk et al. 2014) and suggest that impact number, severity, and age are critical determinants of the pathophysiological changes following rmTBI.

Materials and Methods

Repetitive Mild Traumatic Brain Injury

To experimentally model rmTBI we modified a recently developed model by Kane et al. (2012). This model replicates many of the clinical characteristics and mechanics of a mTBI injury including low impact force, low incidence of skull fracture and subdural hematoma, no immediate or early seizures, and no gross cavitation at the impact site. This model has been shown to effectively induce and model rmTBI in adult mice and was here modified to model pediatric rmTBI in juvenile rats. In brief, 20-day-old (P20) male Sprague-Dawley rats were subjected to a single mTBI once per day for 5 consecutive days (Fig. 1). Rats were lightly sedated via isoflurane inhalation and immediately placed ventral side down on a tightly stretched Kimwipe secured to a Plexiglas stage (Fig. 2A). The animal's head was then carefully centered under the vertical aluminum guide tube. As the animal's skull and skin remained completely intact, the animal's position was carefully adjusted using external anatomical landmarks (i.e., ear canals, eyes) so that impacts occurred between the bregma and lambda sutures. The impact weight (92 g, 9-mm diameter) was then positioned at the top of the aluminum tube so that the bottom of the weight was precisely 865 mm above the animal's head and was allowed to fall freely down the aluminum guide tube. The guide tube is threaded to allow for careful adjustment between animals to ensure accurate positioning of the guide tube and impact location (Fig. 2A). The force of the impact caused the animal to break through the stretched Kimwipe, rotate 180°, and land dorsally on the foam pad below.

The rat falls away from the impact weight, and no secondary impacts were observed. The animal's movement after impact is not mechanically constrained, allowing simulation of the rotational and linear acceleration and deceleration forces most often associated with this type of injury. The animal was then placed in a supine position and monitored for righting reflex time. Righting reflex was defined as the animal's ability to right itself from a supine to a prone position. Once righted and ambulatory the animal was placed back into its home cage and monitored daily. In the rmTBI animal group, this procedure was repeated once per day for a total of five impacts. Age-matched sham-injured animals were given anesthesia, underwent mock impacts, and were placed in a supine position to test righting reflex times. After the fifth sham injury or rmTBI, animals were again monitored daily but left for 14 days to recover before further experimentation. All "postinjury day" (PID) descriptions were calculated as days between last impact and day of death.

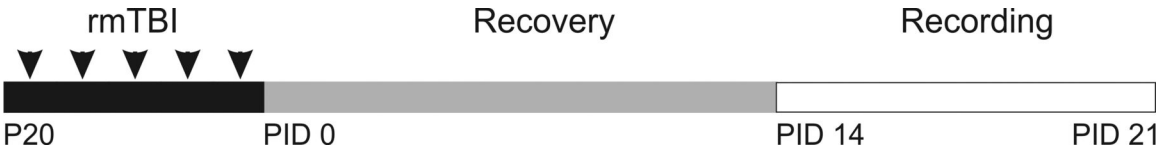

Figure 1. Experimental timeline. Overview of the timeline used to model repetitive mild traumatic brain injury (rmTBI). Arrowheads represent time of single impact repeated once daily for 5 days. Control animals were given anesthesia only. Postinjury day (PID) indicates number of days after the 5th rmTBI injury.

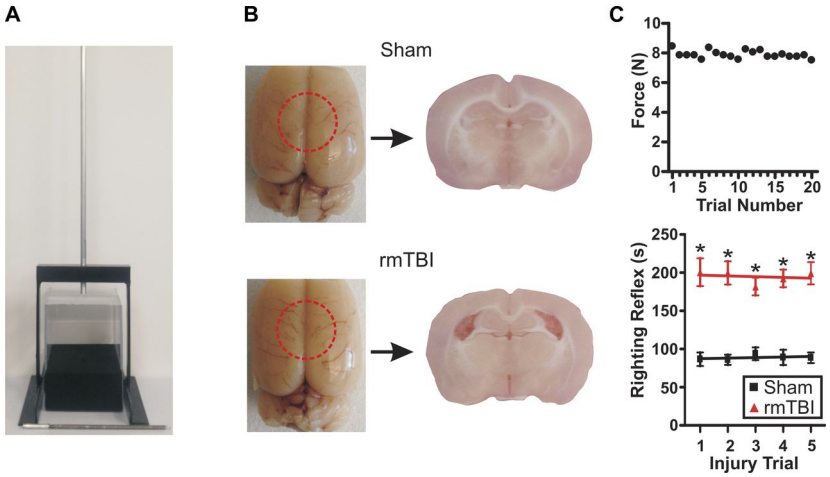

Figure 2. Experimental model of rmTBI. *A*: photograph of rmTBI device and impact weight. *B*, *left*: photographs of brains acutely prepared 14 days after sham injury or rmTBI (1 impact/day for 5 days) in juvenile (P20) rats. Red dashed circle indicates approximate site of impact. *Right*: photograph of coronal brain slices taken from respective sham-injured or rmTBI brains. Note the presence of enlarged ventricles and cortical thinning after rmTBI. *C*, *top*: scatterplot of impact force measurements taken across 20 trials (weight 92 g, drop height 865 mm). *Bottom*: line graph of average righting reflex time in sham-injured ($n = 38$) and rmTBI ($n = 42$) animals across the 5 injury trial days. *$P < 0.01$.

Brain Fixation and Tissue Processing

At 14 days after injury (PID 14) the animals were deeply anesthetized with isoflurane and perfused transcardially with cold 0.9% saline followed by a fixative containing 4% paraformaldehyde. The brains were then removed and fixed in paraformaldehyde overnight. The following day brains were cryoprotected in two stages: 15% sucrose for 24 h followed by 30% sucrose for 24 h. Brains selected for MRI were then washed in PBS for 48 h. For immunofluorescence, 30-μm-thick sections were cut serially with a cryostat (Leica Biosystems) and stored at −20°C. Sections were then stained with the mature neuronal marker NeuN (Abcam, Cambridge, MA). In brief, the sections were first washed in PBS (2 × 15 min) before being permeabilized with 0.3% Triton X for 1 h (Abcam). Nonspecific binding was blocked with CAS-Block (Life Technologies). Finally, the sections were moved into the primary NeuN antibody diluted to 1:2,000 and incubated overnight on an orbital shaker at 4°C. The sections were then washed repeatedly in PBS and incubated with a Cy3 secondary antibody (1:1,000, Jackson Immunoresearch) in the dark at 4°C overnight. Images were taken of both control and rmTBI animals with an epifluorescent or confocal microscope.

Magnetic Resonance Imaging

MRI was performed on PID 14 brains that had been previously perfusion fixed. Imaging was performed on a Bruker Biospec 7.0-T small-animal MR scanner (Bruker Medizintechnik, Karlsruhe, Germany) with a 72-mm transmitter coil and a rat brain surface receiver coil. 3D RARE sequence was used to acquire coronal a T2-weighted image (TE: 60 ms, TR: 3,000 ms, RARE factor: 8, resolution: 0.1 mm × 0.1 mm × 0.1

mm, matrix: 192 × 192 × 192, FOV: 19.2 mm × 19.2 mm × 19.2 mm, total acquisition time: 3 h 50 min) covering the posterior cerebellum to the frontal lobe. MRI data were analyzed with ImageJ software.

Electrophysiological Slice Preparation

Coronal brain slices were made as described previously (Anderson et al. 2005, 2010; Iremonger et al. 2006). In brief, male Sprague-Dawley rats aged 38–45 days (PID 14–21) were deeply sedated via isoflurane inhalation and decapitated. Brains were quickly removed and placed in ice-cold (4°C) carboxygenated (95% O_2-5% CO_2) high-sucrose solution composed of (in mM) 234 sucrose, 11 glucose, 26 $NaHCO_3$, 2.5 KCl, 1.25 $NaH_2PO_4 \cdot H_2O$, 10 $MgSO_4 \cdot 7H_2O$, 0.5 $CaCl_2 \cdot 2H_2O$. The tissue was kept in this solution while 350-µm-thick coronal slices were taken with a vibratome (VT 1200; Leica, Nussloch, Germany). Brain slices were harvested from beneath the site of impact in rmTBI animals or from the corresponding area in sham-injured animals. Slices were incubated for 1 h in a water bath-warmed (32°C) container filled with carboxygenated artificial cerebrospinal fluid (aCSF) composed of (in mM) 126 NaCl, 26 $NaHCO_3$, 2.5 KCl, 10 glucose, 1.25 $NaH_2PO_4 \cdot H_2O$, 1 $MgSO_4 \cdot 7H_2O$, 2 $CaCl_2 \cdot 2H_2O$, pH 7.4. After the 1-h incubation, the slices were returned to room temperature before the tissue was moved to a recording chamber for whole cell patch-clamp recording.

Whole-Cell Patch-Clamp Recording

Coronal brain slices prepared from rmTBI and sham-injured animals were placed in the recording chamber and immersed in carboxygenated aCSF maintained at a temperature of 32°C. Initial visualization and identification of cortical layers was done under 4× brightfield magnification. Recordings were made from layer II/III neurons of

motor cortex within the impact zone for rmTBI animals or the corresponding region in sham-injured animals. An upright microscope (Axioexaminer, Carl Zeiss) equipped with infrared differential interference contrast optics was used to acquire whole cell patch-clamp recordings from regular-spiking (RS) cortical pyramidal neurons. Current-clamp firing behavior was used to identify RS pyramidal neurons as previously described (Connors et al. 1982; Guatteo et al. 1994). Electrode capacitance and bridge circuit were appropriately adjusted. Neurons chosen for analysis had a stable membrane resistance (R_m) that was less than 20% of the input resistance (R_I), a resting membrane potential less than −55 mV, and overshooting action potentials. All current- and voltage-clamp recordings were obtained with a Multiclamp 700A patch-clamp amplifier (Axon Instruments, Union City, CA). Borosilicate glass microelectrodes (tip resistance 2.5–3.5 MΩ) were produced by a Sutter P-97 automated pipette puller (Sutter Instrument, Novato, CA) and used for patch-clamp recordings. For recording excitatory events, pipettes were filled with intracellular solution (in mM: 135 K gluconate, 4 KCl, 2 NaCl, 10 HEPES, 4 EGTA, 4 MgATP, 0.3 Na Tris). For recording inhibitory events, pipettes were filled with intracellular solution (in mM: 70 K gluconate, 70 KCl, 2 NaCl, 10 HEPES, 4 EGTA, 4 MgATP, 0.3 GTP) with a calculated reversal potential of Cl^- (E_{Cl^-}) of −16 mV, resulting in inward $GABA_A$ currents at a holding potential (V_{hold}) of −70 mV. This internal solution has been previously demonstrated (Anderson et al. 2010; Sun et al. 2006) to facilitate detection of inhibitory events.

Data Analysis

Data were analyzed with pCLAMP (Axon Instruments), Prism (GraphPad), ImageJ (National Institutes of Health), and Mini Analysis (Synaptosoft) software and are

presented as means ± SE. For immunohistochemical analysis of NeuN staining a region of interest (ROI) of the motor cortex was created with ImageJ software, and NeuN-positive cells within the ROI were manually counted. Cell count and density values are presented as the average cell count for three serial sections from each animal normalized to the width or area of the ROI, respectively. Electrophysiologically recorded spontaneous synaptic events were detected as previously described with automated threshold detection and manual verification (Nichols et al. 2015). R_I was calculated from the voltage response to the input of a current step (1 s, 50 mV). The adaptation index was calculated based on the ratio of the last interspike interval (F_{Last}) divided by the second (F_2) as per the equation $100 \times (1 - F_{Last}/F_2)$. Pyramidal neurons often displayed a highly variable first interspike interval, and consequently F_2 was chosen for analysis. Firing frequency was calculated as the number of action potentials induced by a 1-s, 250-pA current step. Rheobase current was determined as the minimum current step (50-ms duration) that produced an action potential. Action potential threshold was calculated as the voltage at the maximum slope of the rheobase voltage recording (Nichols et al. 2015). Statistical significance was determined with an unpaired *t*-test, one-way ANOVA, or Kolmogorov-Smirnov (K-S) test, and differences were determined to be significant if $P < 0.05$.

Results

rmTBI is Effectively Modeled by Repetitive Weight Drop

To model rmTBI in pediatric patients, we modified the weight-drop method recently published by Kane et al. (2012) for use with juvenile rats (Fig. 2A). Animals subjected to rmTBI demonstrated no gross morphological changes, identifiable surface

deformations, or tissue loss at the site of the impact (Fig. 2B). The rmTBI procedure resulted in no incidence of scalp lacerations, and no immediate or late seizures were observed. As previously reported, the incidence of skull fractures or intracranial bleeding was low, and any animals displaying either where removed from further study (Kane et al. 2012). At PID 14–21 rat brains were removed for further experimentation. Acute slices prepared from rmTBI brains revealed marked structural changes including cortical thinning and ventriculomegaly (Fig. 2B). To determine the reproducibility of the rmTBI method, we tested the consistency of the impact force across 20 trials. A force meter (Chatillon DFM-10, Ametek Instruments) was placed at the base of the guide tube, and the peak impact force was measured across 20 trials. We found the average impact force with a 92-g weight to be highly consistent across trials with an average force of 7.890 ± 0.06 N and a maximum variation of <1 N (Fig. 2C, top).

In humans, the duration of loss of consciousness (LOC) is an important criterion in assessing the severity of a brain injury. While brain injury may occur in the absence of LOC, it is generally accepted that "mild" TBIs induce LOC between a few seconds and <30 min (Carroll et al. 2004; Smith et al. 2013). Assessing LOC in rats is difficult, but it has been indirectly evaluated by measuring the righting reflex time as an indicator of neurological restoration (Kane et al. 2012; Zecharia et al. 2012). Righting reflex time was measured after each sham or rmTBI impact as the time for an animal to recover from the supine to the prone position. Compared with sham-injured animals the righting reflex time was significantly increased across all 5 days (Fig. 2C, bottom). However, this increase in righting reflex time was not exacerbated by repeat sham (day 1 86.92 ± 8.8 s vs. day 5 88.59 ± 6.9 s) or rmTBI (day 1 200.60 ± 18.2 s vs. day 5 199.30 ± 14.6 s)

injuries ($P > 0.05$ for both). Averaged across all five impact trials the righting reflex time remained significantly increased between in rmTBI (193.1 ± 6.7 s) vs. sham-injured (92.31 ± 4.0 s) animals.

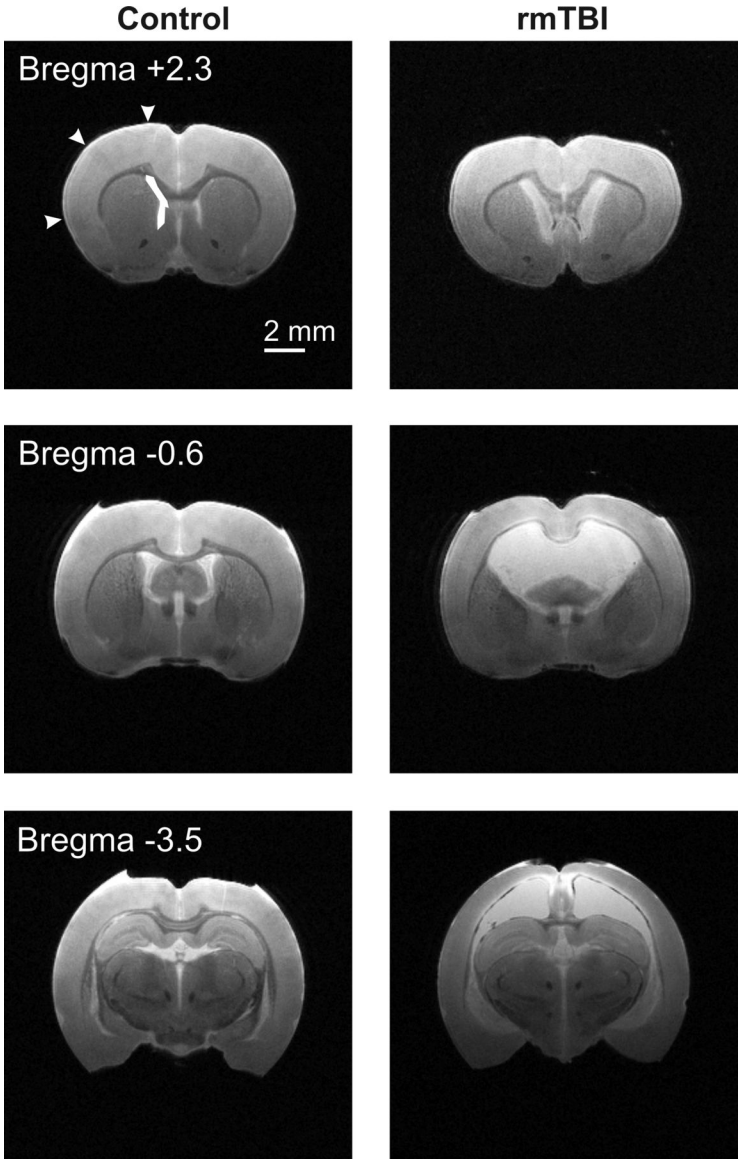

Figure 3. Magnetic resonance imaging (MRI) reveals significant structural changes after rmTBI. Coronal T2-weighted MRI images were obtained with a 7-T MRI scanner from perfusion fixed brains 14 days after sham injury or rmTBI. Representative images from sham injury (Control, *left*) or rmTBI (*right*) are presented. Approximate anatomical position of images are referenced relative to bregma. Arrowheads and box represent regions where cortical depth and lateral ventricle area measurements were taken. Similar respective measurements were made across all sham injury and rmTBI images. In T2-weighted images water and edema are bright, while gray and white matter appear darker. Note the significant cortical thinning and ventriculomegaly evident in rmTBI brains.

MRI of rmTBI reveals significant ventriculomegaly and cortical thinning.

To better assess the anatomical and structural changes to the brain following rmTBI, we performed T2-weighted MRI. Brains were perfusion fixed on PID 14 and ex vivo MRI imaging performed on control (n = 4) or rmTBI (n = 3) brains (Fig. 3). MRI imaging was performed from the frontal cortex to posterior cerebellum. To determine changes in cortical thinning, we measured the depth of the motor, somatosensory, and insular cortex across three regions—one region outside (bregma +2.3) and two regions within (bregma −0.6 and −3.5) the direct impact zone (Fig. 4A). The rmTBI was delivered by a 9-mm impact rod that spanned the region between bregma and lambda sutures in the rat. As imaging was performed ex vivo, we utilized anatomical landmarks to approximate the image location relative to the impact zone and published stereotaxic coordinates (i.e., bregma +2.3 mm, −0.6 mm, or −3.5 mm, respectively) (Paxinos and Watson 2007). In this way, we assessed changes in cortical depth across brain regions in the anterior-posterior as well as medial-lateral directions in both control and rmTBI animals.

Substantial cortical thinning was observed in the motor cortex in all three brain regions, with up to a 46% decrease in cortical depth within the impact zone (Fig. 4B). Similarly, the depth of the somatosensory cortex was significantly reduced by over 25%, but this reduction was restricted to directly within the impact zone (i.e., bregma −0.6 mm and bregma −3.5 mm). Measurement of the depth of the insular cortex revealed no significant difference across all three brain regions examined ($P > 0.05$). We next performed similar measurements on the area of the third and lateral ventricles. While no significant difference in the area of the third ventricle was observed ($P > 0.05$), the lateral ventricle area increased up to 970% after rmTBI (Fig. 5). Within the impact zone

(bregma −0.6 and −3.5), the lateral ventricle maximally increased from 1.37 ± 0.2 mm^2 to 13.30 ± 1.0 mm^2 ($P < 0.0001$). Outside of the direct impact zone (bregma +2.3), the lateral ventricles were again significantly increased from 0.84 ± 0.1 mm^2 to 4.40 ± 0.4 mm^2 ($P < 0.0001$). Collectively, the data reveal that rmTBI induces rapid and significant reduction in the depth of the cortex and ventriculomegaly that is most substantial at the site of impact.

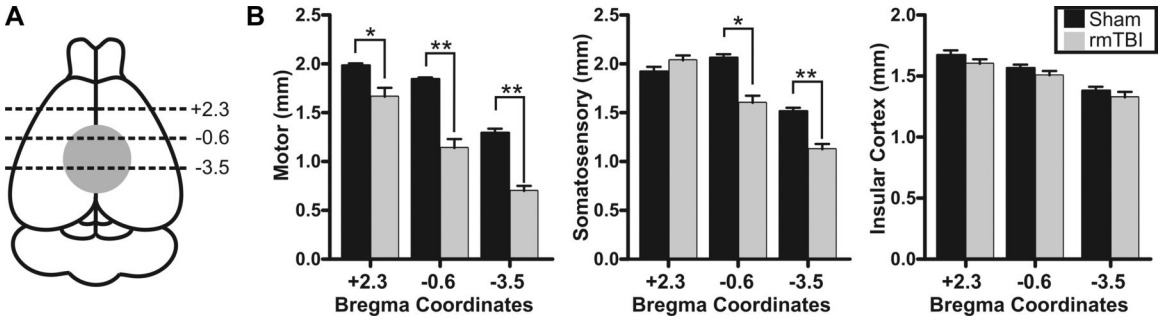

Figure 4. rmTBI induces cortical thinning. *A*: schematic indicating site of TBI impact (gray filled circle) and relative MRI image locations (black dashed lines) where cortical depth was measured. Numerical values are approximate bregma coordinates. *B*: bar charts of average cortical depth measured in MRI images at the listed bregma coordinates. Measurements of motor (*left*), somatosensory (*center*), or insular (*right*) cortical depth were made for each stereotaxic position (i.e., +2.3 mm, −0.6 mm, and −3.5 mm). Average values for sham injury and rmTBI are presented for each cortical region and location. No statistical difference was observed between sham injury and rmTBI for somatosensory cortex at +2.3 ($P > 0.05$) or for any insular cortex measurement ($P > 0.05$). *$P < 0.05$, **$P < 0.01$.

rmTBI induces no change in neuronal density or gross tissue damage.

To determine whether rmTBI altered the total number or density of neurons within the cortex, we performed immunohistochemical analysis with the neuron-specific marker NeuN (Fig. 6A). As the amount of rmTBI-induced cortical thinning was most pronounced in the motor cortex, we focused the analysis on this region. The decrease in cortical thickness resulted in an overall decrease in total NeuN-positive cells between sham-injured (476.1 ± 17) and rmTBI (296.1 ± 24) animals ($P < 0.001$). However, analysis of the density of neurons (i.e., total neurons/area) revealed no significant change between sham-injured and rmTBI animals ($P = 0.21$) (Fig. 6B). Therefore, the data suggest that rmTBI induces a significant reduction in the volume of the cortex, but the cortex that remains is of similar neuronal density as that in sham-injured animals.

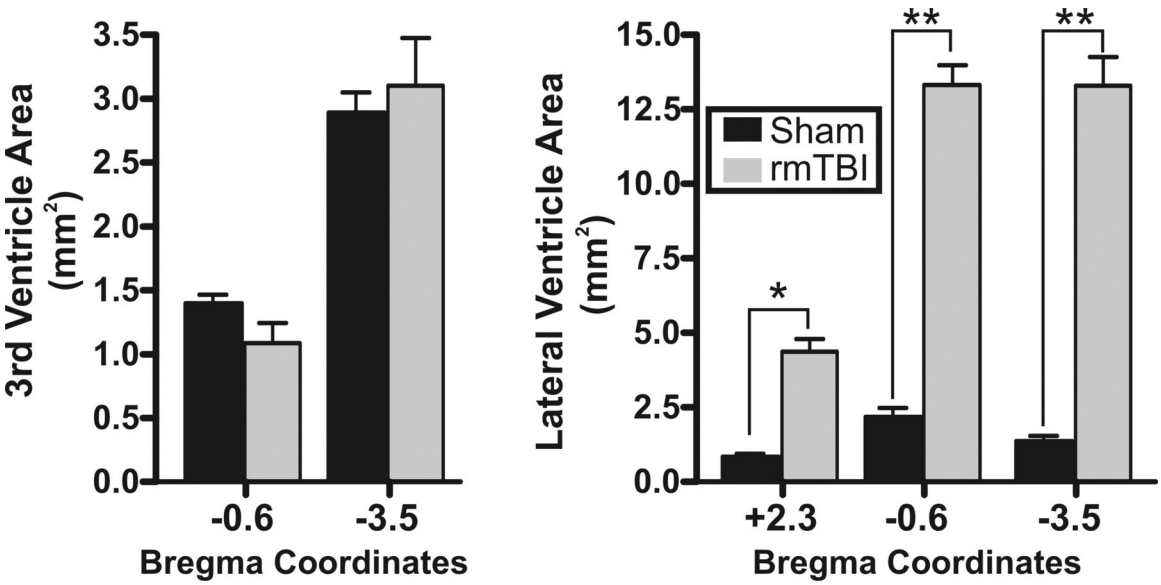

Figure 5. rmTBI induces lateral ventriculomegaly: average ventricle area measured in MRI images from the 3rd ventricle (*left*) or lateral ventricle (*right*). Corresponding sham injury and rmTBI values are presented for regions in the anterior, middle, and posterior positions in the brain. Positions in the brain are identified relative to approximated stereotaxic coordinates from bregma (i.e., +2.3 mm, −0.6 mm, and −3.5 mm). No statistical difference was observed in the area of the 3rd ventricle between sham injury and rmTBI. *$P < 0.05$, **$P < 0.01$.

rmTBI does not significantly alter electrophysiological properties of layer II/III motor neurons.

Structurally, this study has revealed that rmTBI induces a significant reduction in the depth of the cortex that is most widespread and profound within the region of the motor cortex. To determine whether these structural changes result in functional changes to the intrinsic and synaptic properties of neurons within the motor cortex we performed electrophysiological experiments. Specifically, we recorded from layer II/III motor cortex pyramidal neurons within the injury zone of rmTBI animals or from the corresponding area in age-matched sham-injured animals.

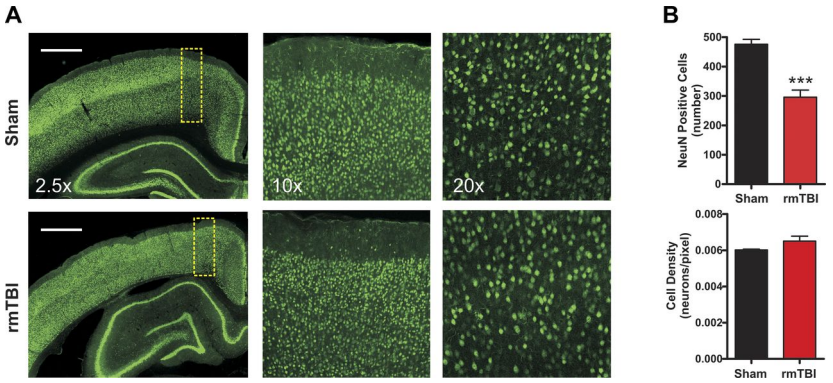

Figure 6. Effect of rmTBI on NeuN staining. *A*: representative epifluorescence and confocal images taken from sham injury ($n = 8$) or rmTBI ($n = 6$) stained with the neuron-specific marker NeuN (green). Scale bars, 1 mm. Images are at ×2.5, ×10, and ×20 magnification. *B*: bar graphs of average neuronal number (*top*) and density (*bottom*) within the motor cortex. Cell counts were made of NeuN-positive cells within standardized regions of interest (yellow dashed boxes in *A*). Note the substantial reduction of NeuN-positive cells after rmTBI but absence of neuronal density changes. ***$P < 0.0001$.

Intrinsic Excitability

Intrinsic excitability refers to the propensity of a neuron to fire an action potential and is governed by the membrane properties, currents, and channels expressed by a neuron. Alterations to intrinsic excitability have been shown in numerous models of CNS disorders (Willmore 1990; Yang et al. 2007) and may contribute to the pathophysiology of rmTBI. To examine for changes in intrinsic excitability induced by rmTBI, we recorded under current clamp the response of sham-injured (n = 10) or rmTBI (n = 14) neurons to a series of hyperpolarizing and depolarizing steps (−100 pA to 350 pA, 50-pA steps). Analysis revealed no statistical difference in R_I (P = 0.38), resting membrane potential (P = 0.77), or accommodation index (P = 0.82) between sham-injured and rmTBI neurons (Fig. 7). Using a rheobase protocol (50 ms, 5-pA steps), we performed a more detailed analysis of action potential properties but again found no statistical difference in rheobase current (P = 0.73), action potential threshold (P = 0.52), or amplitude (P = 0.31) (Fig. 8).

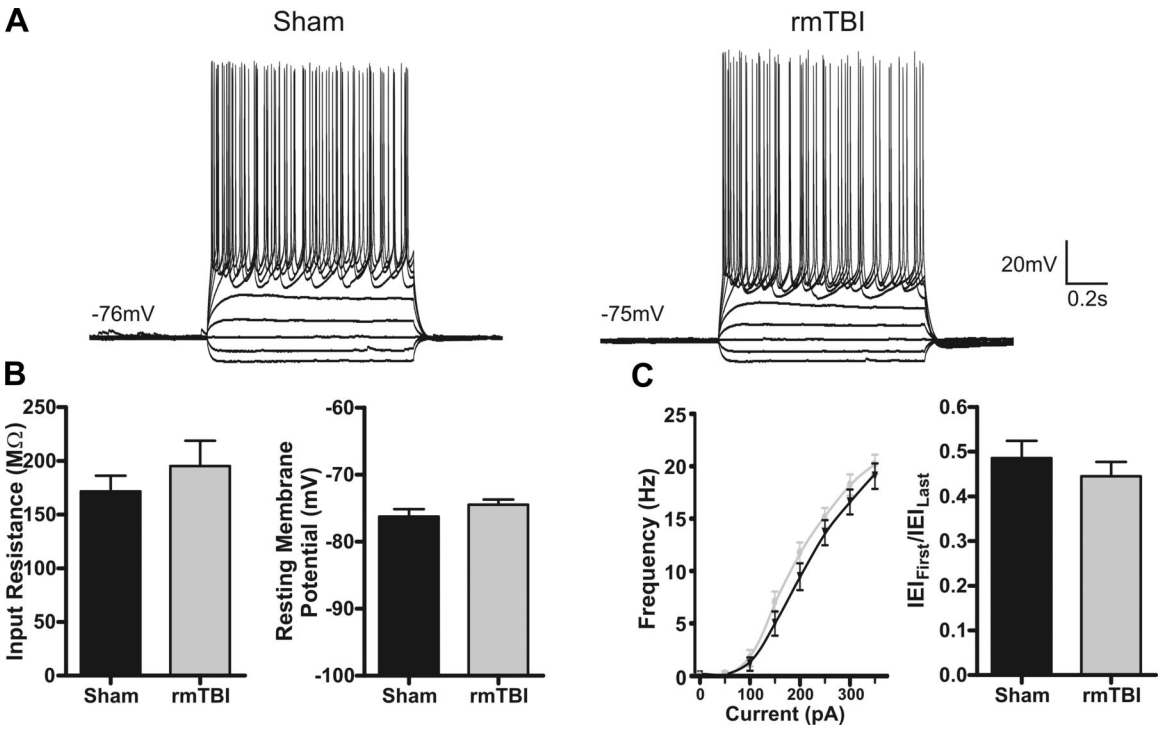

Figure 7. Intrinsic membrane properties are not altered by rmTBI. *A*: representative current-clamp recordings in response to intracellular current steps (−100 pA to 350 pA, 1 s) in layer II/III pyramidal neurons from sham-injured (n = 10) or rmTBI (n = 14) animals. Note the similarity in the intrinsic cellular response. *B*: average intrinsic membrane properties. No significant difference was found for input resistance (P = 0.38) or resting membrane potential (P = 0.77). *C*: comparison of firing properties of a sham-injured and an rmTBI animal. *Left*: plot of average firing frequency vs. current (*f-I* curve). *Right*: adaptation index [first interevent interval (IEI_{First}) between action potentials/last interevent interval (IEI_{Last})].

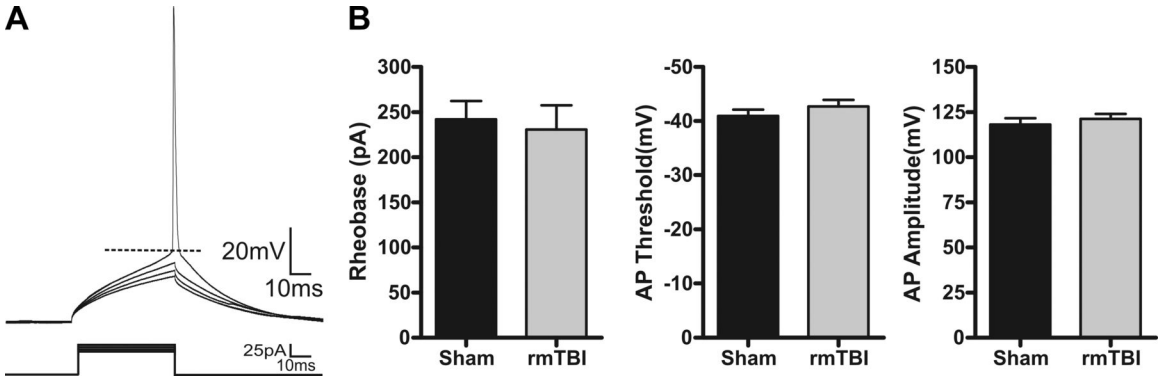

Figure 8. Action potential properties are not altered by rmTBI. *A*: representative whole cell current-clamp recording in response to a series of 50-ms injection (5-pA steps). *B*: average values for sham injury (n = 15) or rmTBI (n = 18). Rheobase was calculated as the minimum current that produced an action potential (AP). Threshold was measured at the greatest change in calculated slope. Amplitude was measured as the difference between threshold and the peak of the action potential. No statistically significant differences were found between control and rmTBI animals for rheobase (P = 0.73), action potential amplitude (P = 0.52), or threshold (P = 0.31).

Spontaneous Activity

The frequency of activity and strength of synaptic connections between neurons are fundamental to the way the brain processes and relays information. To investigate whether rmTBI disrupts or alters cortical synaptic excitability we again recorded from layer II/III pyramidal neurons in the motor cortex of sham-injured or rmTBI animals. First, under voltage clamp (V_{hold} = −70 mV), we examined for rmTBI-induced changes to spontaneous excitatory postsynaptic currents (sEPSCs). To minimize detection of inhibitory events, neurons were held near and positive of the E_{Cl}^- (V_{hold} = −70 mV, calculated E_{Cl}^- = −80 mV) and only inward synaptic events were detected. Pharmacological isolation of glutamatergic events was avoided, as the resultant synaptic disinhibition may mask rmTBI-induced changes to network excitability. In neurons from rmTBI animals, there were no significant changes in the average interevent interval (P = 0.77), amplitude (P = 0.94), decay time (P = 0.82), or charge transfer (0.34) of sEPSCs (Fig. 9). Next, we similarly examined for changes in spontaneous inhibitory postsynaptic currents (sIPSCs). Inhibitory events were pharmacologically isolated with bath application of the glutamate receptor antagonist kynurenate (2 mM). To enhance detection fidelity of inhibitory synaptic events, a modified high-intracellular Cl^- internal solution was used as previously described (Anderson et al. 2010; Sun et al. 2006). Again, no significant change was observed in sIPSC properties including interevent interval (P = 0.90), amplitude (P = 0.74), decay time (P = 0.33), and charge transfer (P = 0.46). Representative traces and summary of these results are shown in Fig. 10.

Finally, the effects of rmTBI in humans are often subtle and may not be reflected in changes to baseline synaptic activity but only become evident during periods of high

activity or demand. The observed reduction of cortical depth and neuronal number in rmTBI animals relative to sham-injured animals may result in loss of peak network or synaptic activity. To test these possibilities we challenged pyramidal neurons from sham-injured (n = 15) or rmTBI (n = 18) animals with the convulsant 4-aminopyridine (4-AP, 100 μM). Bath application of 4-AP for 15 min induced a rapid decrease in interevent interval of sEPSCs recorded in neurons from both sham-injured (53.59 ± 5.6 ms) and rmTBI (81.21 ± 20.0 ms) animals (Fig. 11A). The amplitude of sEPSCs was similarly increased by 4-AP in neurons from both sham-injured (22.47 ± 0.6 pA) and rmTBI (22.40 ± 1.1 pA) animals (Fig. 11B). However, neither the interevent interval nor amplitude during application of 4-AP was statistically different between neurons recorded from sham-injured and rmTBI animals ($P > 0.05$). Overall, this suggests that despite a significant loss of the depth of the motor cortex in rmTBI animals, the injury fails to alter excitatory or inhibitory synaptic properties or the potential peak state of synaptic excitability.

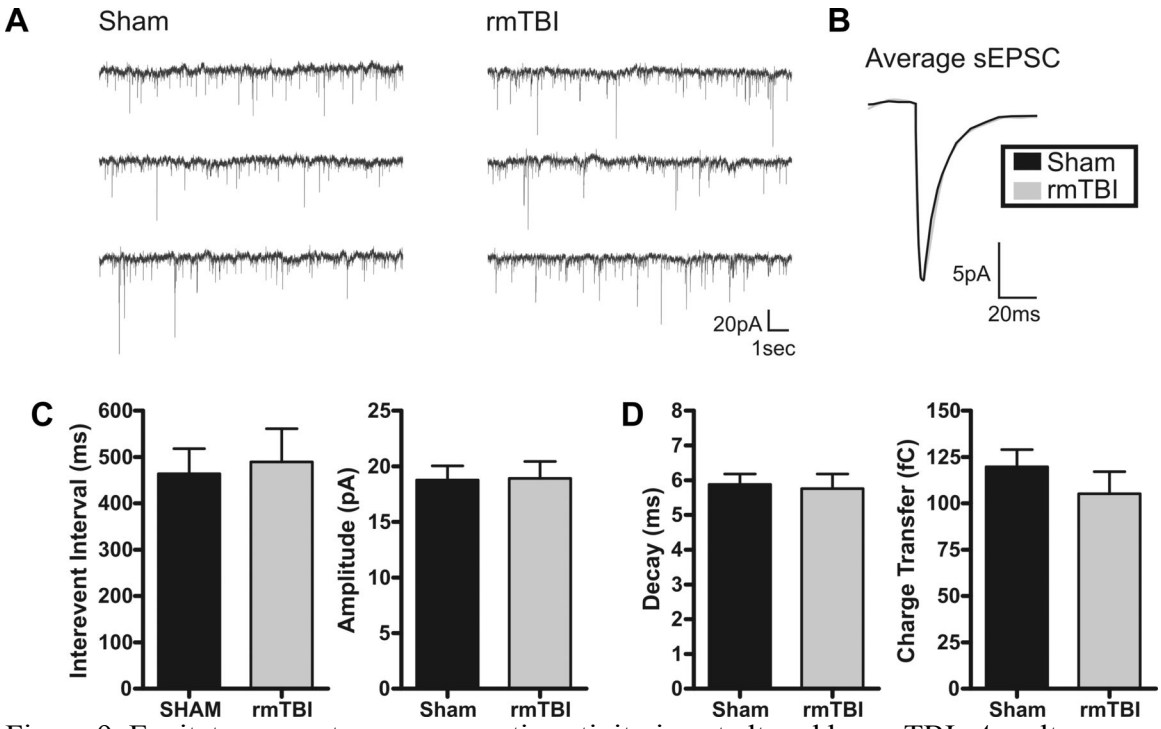

Figure 9. Excitatory spontaneous synaptic activity is not altered by rmTBI. *A*: voltage-clamp recordings of spontaneous excitatory postsynaptic currents (sEPSCs) in sham-injured (n = 19) or rmTBI (n = 14) animals. *B*: overlay of sham-injured and rmTBI scaled average sEPSC. *C*: bar charts of average sEPSC interevent interval (IEI) and amplitude for sham injury and rmTBI. No significant difference was determined for IEI (P = 0.77) or amplitude (P = 0.94). *D*: average sEPSC kinetic properties. No significant difference was detected between sham injury and rmTBI for sEPSC decay time (P = 0.82) or charge transfer (P = 0.34). Holding potential (V_{hold}) = −70 mV.

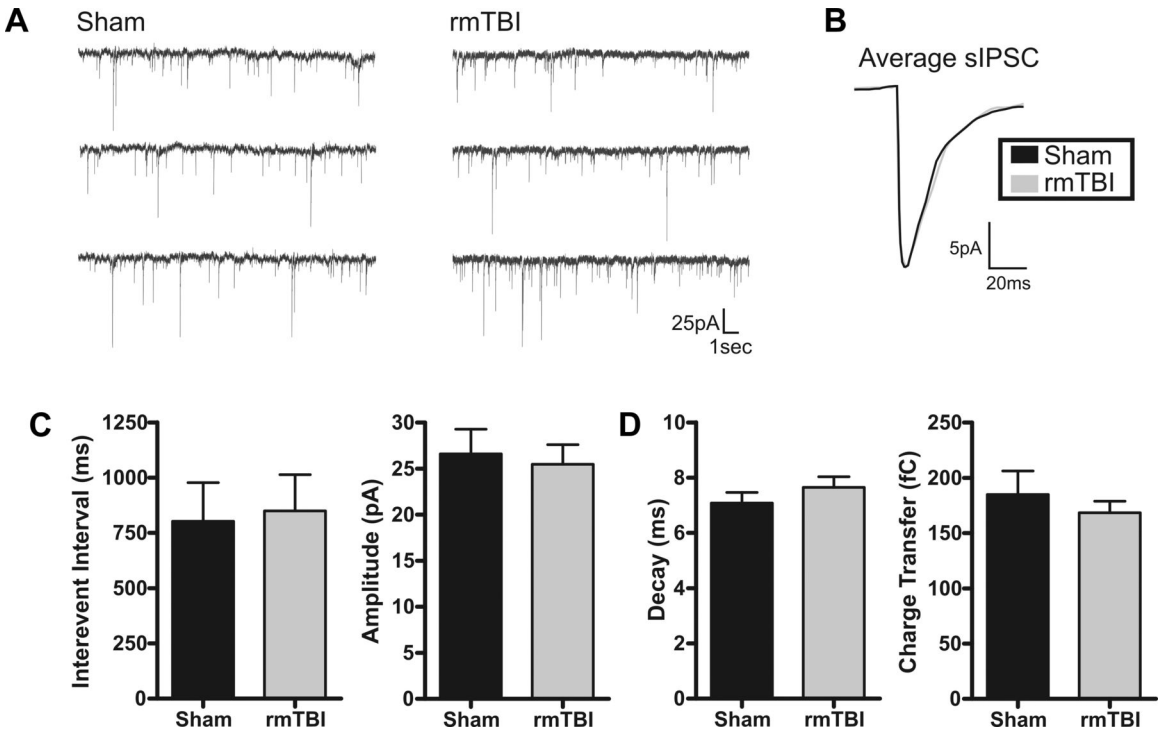

Figure 10. Inhibitory spontaneous synaptic activity is not altered by rmTBI. *A*: voltage-clamp recordings of spontaneous inhibitory postsynaptic currents (sIPSCs) in sham-injured ($n = 15$) or rmTBI ($n = 18$) animals. *B*: overlay of sham-injured and rmTBI scaled average sIPSC. *C*: average sIPSC IEI and amplitude for sham and rmTBI. No significant difference was determined for IEI ($P = 0.90$) or amplitude ($P = 0.74$). *D*: average sIPSC kinetic properties. No significant difference was detected between sham injury and rmTBI for sEPSC decay time ($P = 0.33$) or charge transfer ($P = 0.46$). $V_{hold} = -70$ mV.

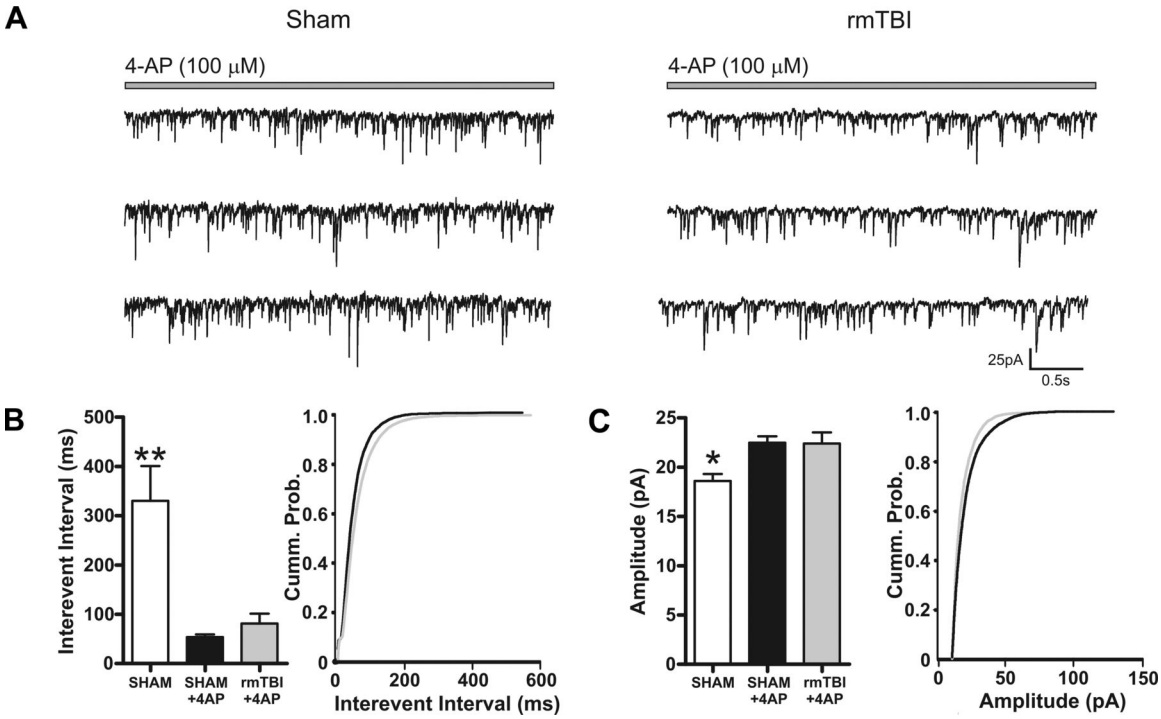

Figure 11. rmTBI does not enhance the response to the convulsant 4-aminopyridine (4-AP). *A*: voltage-clamp recordings of sEPSCs from sham-injured (n = 14) or rmTBI (n = 12) animals during bath application of 4-AP (100 μM). *B* and *C*: bar chart and cumulative probability curves of sham injury, sham injury during 4-AP, and rmTBI during 4-AP for IEI (*B*) or amplitude (*C*). Bath application of 4-AP induced a significant decrease in IEI and amplitude of sEPSCs. However, the effects of 4-AP on sEPSC IEI and amplitude were not statistically different between sham injury and rmTBI. V_{hold} = −70 mV. *P < 0.05, **P < 0.01.

Discussion

In the pediatric population, TBI remains a significant health concern that is known to place patients at risk for adverse long-term cognitive and behavioral changes. TBI may vary in severity, but >75% of all TBI is classified as mild (Cassidy et al. 2004; Elder and Cristian 2009; Langlois et al. 2005; Miniño et al. 2006). In this study, we sought to determine how rmTBI affects the pediatric brain. To effectively model human rmTBI, we modified a recently developed method for inducing rmTBI in adult animals (Kane et al. 2012) for use in juveniles. This rmTBI weight-drop method produced highly consistent impact forces across trials. The impacts occurred in a nonrestrained animal and have been shown to effectively model the direct, acceleration, and deceleration forces determined to be important to human TBI (Gennarelli and Thibault 1982; Holbourn 1943; Kane et al. 2012; Ommaya et al. 1967; Panzer et al. 2014). After mTBI, animals exhibited a significant increase in righting reflex time that suggests a brief injury-induced period of sensory and/or motor dysfunction. In contrast to what has generally been reported after single mTBI (Mychasiuk et al. 2014) or rmTBI in adult animals (Kane et al. 2012), rmTBI in juvenile animals induced significant structural changes to the brain including cortical atrophy and ventriculomegaly. This is supported by recent evidence that indicates that children may be more prone to the effects of repeat concussions (Eisenberg et al. 2013; Field et al. 2003). Neuronal specific immunostaining revealed that the cortical atrophy was accompanied by a loss of total cortical neurons. However, this overall neuronal loss was not due to a specific reduction in cortical density. The cortical atrophy was most pronounced in the motor cortex, with up to a 46% decrease in cortical

thickness beneath the site of injury in rmTBI animals. At PID 14 the significant structural changes to the motor cortex were not accompanied by significant changes in the intrinsic or synaptic properties of layer II/III pyramidal neurons at rest or under convulsant challenge. Overall, our results indicate the effectiveness of this new weight-drop method for reliably inducing a clinically relevant rmTBI. The select changes induced by rmTBI in juvenile rats suggest a potentially unique pathophysiological response to TBI in children.

Modeling Repetitive Mild Traumatic Brain Injury

Recent attention by patients, families, researchers, and the media has highlighted the significant short- and long-term consequences of rmTBI (Creeley et al. 2004; Longhi et al. 2005; Shitaka et al. 2011). Critical to understanding the pathophysiological mechanisms that drive rmTBI has been the development of new, clinically relevant models. Effective modeling of rmTBI requires an induced injury that reflects the type of impact and forces known to occur in mTBI and that results in neuropathological and clinically relevant outcomes. mTBI is characterized as occurring in a closed skull with minimal skull fractures and minimal tissue loss after a single mTBI. The impact of the mTBI induces direct force to the skull that translates into acceleration, deceleration, and shearing forces in the brain that are thought to be important to the injury process (Duhaime et al. 2012). Several models of TBI exist, including controlled cortical impact and fluid percussion (Xiong et al. 2013), but these require a craniotomy and/or a fixed skull that inadequately models these forces. Limited data exist on the exact biomechanical forces that would be classified as “mild” or concussion inducing, but the most comprehensive data have been obtained from head impact telemetry devices placed

within athletes' helmets. An in-depth review of the combined telemetry impact studies revealed that concussion is correlated with g-forces above 100g (Beckwith et al. 2013). In our study, calculated impact forces were on average 26.8g and well within the "mild" range [i.e., g-force = (F = ma)/9.8 m/s^2; F = 7.89 N, m = 30g (P20-25 rat)]. The method used in this study overcomes these limitations and effectively models both the biomechanical forces of the impact and has been shown to induce clinically relevant cognitive and behavioral changes (Gennarelli and Thibault 1982; Kane et al. 2012; Meaney and Smith 2011; Mychasiuk et al. 2014; Panzer et al. 2014).

Repetitive mild traumatic brain injury induces significant neuropathology.

A single mTBI often resolves quickly and has generally not been associated with any significant neuroimaging abnormalities (Belanger et al. 2007; Petchprapai and Winkelman 2007; Morey et al. 2013). As a result, mTBI is often referred to as an "invisible wound" and is difficult to diagnose. Whether a single mTBI induces long-term deficits is currently a source of significant debate (Carroll et al. 2004; Klein et al. 1996; Konrad et al. 2011; Vanderploeg et al. 2005; Vasterling et al. 2012; Yuh et al. 2014). It is clear, however, that when a patient receives multiple mTBIs within a short period of time it results in more severe symptoms, a longer recovery period, and increased risk for serious long-term consequences (Guskiewicz et al. 2000, 2003). In contrast to a single mTBI event, rmTBI patients show clear neuropathological findings including enlarged ventricles (ventriculomegaly) and cortical atrophy (Huh et al. 2007; Smith et al. 2013). These findings are supported by the results of this study, which indicate that after rmTBI the lateral ventricles may be increased up to 970% while the thickness of the cortex may be reduced by up to 46%. The interplay and timing of the enlarged ventricles and cortical

atrophy remain to be determined. However, the cortex appears to not be simply compressed by the enlarged ventricles, as no change in cortical neuronal density was observed. These changes were not observed after rmTBI in adult animals (Kane et al. 2012), suggesting a potentially unique response to TBI in juvenile animals. While the impact force used in this study was "mild," the neuropathological findings in rmTBI animals are more significant and may highlight the deleterious effects of receiving multiple mTBIs.

In humans, rmTBI can induce a neurodegenerative disease termed chronic traumatic encephalopathy (CTE) (Gavett et al. 2011; Smith et al. 2013) that has been most commonly found in professional athletes (McKee et al. 2009; Omalu et al. 2010a, 2010b) or soldiers exposed to blast or concussive injury (Goldstein et al. 2012). CTE can currently only be diagnosed on autopsy but results in degeneration of brain tissue (i.e., cortical atrophy) and ventriculomegaly similar to what was observed in this study. Additional characteristics of CTE include tau accumulation, cognitive impairments, memory loss, confusion, and depression (McKee et al. 2009, 2010; Miller 1966). Further work examining these characteristics will be required to determine whether the neuropathological outcome of rmTBI in this study is indicative of underlying CTE.

Cortical excitability is not altered early after repetitive mild traumatic brain injury.

Structurally, this study revealed extensive thinning of the cortex that was most pronounced beneath the site of injury in the motor cortex. Immunohistochemical staining revealed that rmTBI reduced the total number of cortical neurons, but this was not accompanied by a decrease in neuronal density. The significant loss of motor cortex is supported by several studies that have indicated persistent motor dysfunction and

abnormalities in the motor cortex after mTBI (De Beaumont et al. 2011, 2012; Tremblay et al. 2014). In addition, many of the behavioral deficits associated with rmTBI such as balance, reaction time, and visual memory involve high levels of integration across cortical regions (Covassin et al. 2008; Khurana and Kaye 2012; Slobounov et al. 2007) that are thought to be governed by input and output from layer II/III cortex (Douglas and Martin 2004; Kamper et al. 2013). This agrees with a recent study that found mTBI induces specific dendritic degeneration and synaptic reduction in cortical layer II/III pyramidal neurons (Gao and Chen 2011). As such, in this study we began by examining for rmTBI-induced changes in the intrinsic and synaptic properties of layer II/III pyramidal neurons within the motor cortex.

A neuron's intrinsic excitability determines the probability it will fire an action potential, and the output pattern of that firing has been shown to contribute to the pathophysiology of several other neurological disorders (Bush et al. 1999; Prince and Connors 1986; Prinz et al. 2013; van Zundert et al. 2012). However, at PID 14 we investigated several possible measures of intrinsic excitability and found no significant differences between our rmTBI and sham-injured groups. This finding is supported by recent work from our lab where even severe TBI in juvenile rats failed to alter the intrinsic properties of cortical pyramidal neurons (Nichols et al. 2015). At a synaptic level, again at PID 14 no significant changes were found in the strength, frequency, or kinetics of either excitatory or inhibitory synaptic neurotransmission following rmTBI. To our knowledge this is the first study to investigate detailed intracellular electrophysiological changes following rmTBI.

In humans, the use of transcranial magnetic stimulation from 72 h to 2 mo after

mTBI has shown increases in intracortical inhibition (Miller et al. 2014). Young athletes who have sustained multiple concussions have also been reported to have abnormal intracortical inhibition (De Beaumont et al. 2007, 2011; Tremblay et al. 2011). While no change in inhibition onto pyramidal neurons was observed in this study, future examination of the impact of rmTBI directly on other cortical layers and inhibitory interneurons may reveal distinct changes. Given the significant neuropathological changes following rmTBI, it is surprising to find no accompanying electrophysiological changes. The lack of synaptic excitability changes observed after rmTBI in this study contrast with recent findings after severe TBI from our lab in juvenile rats (Nichols et al. 2015) and from previous reports in adult animals (Cantu et al. 2014). As this study only examined animals at 14 days after injury it will be important to examine changes that may occur in the acute and more chronic time points after rmTBI. The data suggest that juvenile rats have a unique injury phenotype after rmTBI that may be in part due to high levels of plasticity in the juvenile brain (Akbik et al. 2013; Grutzendler et al. 2002; Li and Asante 2011; Selemon 2013), ongoing development (Kolb and Gibb 2011), and/or potential trauma-induced postnatal neurogenesis (Gregg et al. 2001; Kolb et al. 2007).

The effects of mTBI may often be subtle and only evident when the cortex is challenged with a high-demand task (Abdel et al. 2009). With the clear loss of mature neurons and significant cortical atrophy, we hypothesized that rmTBI animals may have a reduced upper limit of synaptic activity that would be evident only when the cortex was put under "stress." To test this, we examined the synaptic properties of sham-injured and rmTBI animals during application of 4-AP, a potassium channel blocker and known convulsant. 4-AP has been shown to increase synaptic excitability (Boudkkazi et al.

2011; Buckle and Haas 1982) and to affect cortical pyramidal neuron intrinsic excitability (Higgs and Spain 2011; Shu et al. 2007). As expected, both the frequency and amplitude of spontaneous excitatory activity were increased from control periods by bath application of 4-AP. However, the effects of 4-AP were not statistically different between sham-injured and rmTBI animals. Therefore, even when cortical excitability is pharmacologically increased, rmTBI animals remain equally responsive and able to enhance synaptic activity compared with sham-injured animals. However, in this study we only tested the response of a saturating dose of 4-AP that produces a near-maximal level of synaptic activity. The use of a dose-response protocol may reveal subtler changes in network excitability or 4-AP sensitivity after rmTBI.

In conclusion, rmTBI has been associated with serious clinical consequences including chronic traumatic encephalopathy and an increased risk for the development of dementia and neurodegenerative diseases (McKee et al. 2009, 2010; Omalu et al. 2010a, 2010b). In this study, we found that rmTBI can be effectively modeled in young animals with a modified weight-drop method. The impacts can be consistently delivered and replicate clinically relevant impact forces and structural changes including cortical atrophy and ventriculomegaly. This method of inducing mTBI has also recently been shown in juvenile (Mychasiuk et al. 2014) and adult (Kane et al. 2012) animals to induce clinically relevant changes to cognition and behavior. At present, the findings from this study suggest that the pathophysiology of rmTBI may be unique when occurring in pediatric patients. An improved understanding of how the pediatric brain responds to rmTBI may help identify novel therapeutic targets, influence pediatric treatment, and

improve “return to game” decision making in adolescents.

References

Abdul-Muneer, P.M., Schuetz, H., Wang, F., Skotak, M., Jones, J., Gorantla, S., Zimmerman, M.C., Chandra, N., and Haorah, J. (2013). Induction of oxidative and nitrosative damage leads to cerebrovascular inflammation in an animal model of mild traumatic brain injury induced by primary blast. Free Radic. Biol. Med. *60*, 282–291.

Adelson, P.D. (1999). Animal models of traumatic brain injury in the immature: a review. Exp. Toxicol. Pathol. Off. J. Ges. Für Toxikol. Pathol. *51*, 130–136.

Adelson, P.D., Bratton, S.L., Carney, N.A., Chesnut, R.M., du Coudray, H.E.M., Goldstein, B., Kochanek, P.M., Miller, H.C., Partington, M.P., Selden, N.R., et al. (2003). Guidelines for the acute medical management of severe traumatic brain injury in infants, children, and adolescents. Chapter 19. The role of anti-seizure prophylaxis following severe pediatric traumatic brain injury. Pediatr. Crit. Care Med. J. Soc. Crit. Care Med. World Fed. Pediatr. Intensive Crit. Care Soc. *4*, S72–S75.

Adelson, P.D., Fellows-Mayle, W., Kochanek, P.M., and Dixon, C.E. (2013). Morris water maze function and histologic characterization of two age-at-injury experimental models of controlled cortical impact in the immature rat. Childs Nerv. Syst. ChNS Off. J. Int. Soc. Pediatr. Neurosurg. *29*, 43–53.

Agrawal, A., Timothy, J., Pandit, L., and Manju, M. (2006). Post-traumatic epilepsy: an overview. Clin. Neurol. Neurosurg. *108*, 433–439.

Almeida-Suhett, C.P., Prager, E.M., Pidoplichko, V., Figueiredo, T.H., Marini, A.M., Li, Z., Eiden, L.E., and Braga, M.F.M. (2015). GABAergic interneuronal loss and reduced inhibitory synaptic transmission in the hippocampal CA1 region after mild traumatic brain injury. Exp. Neurol. *273*, 11–23.

Andersen, S.L. (2003). Trajectories of brain development: point of vulnerability or window of opportunity? Neurosci. Biobehav. Rev. *27*, 3–18.

Anderson, V., and Moore, C. (1995). Age at injury as a predictor of outcome following pediatric head injury: A longitudinal perspective. Child Neuropsychol. *1*, 187–202.

Anderson, K.J., Miller, K.M., Fugaccia, I., and Scheff, S.W. (2005a). Regional distribution of Fluoro-Jade B staining in the hippocampus following traumatic brain injury. Exp. Neurol. *193*, 125–130.

Anderson, T.R., Jarvis, C.R., Biedermann, A.J., Molnar, C., and Andrew, R.D. (2005b). Blocking the anoxic depolarization protects without functional compromise following simulated stroke in cortical brain slices. J. Neurophysiol. *93*, 963–979.

Anderson, T.R., Huguenard, J.R., and Prince, D.A. (2010). Differential effects of Na+-K+ ATPase blockade on cortical layer V neurons. J. Physiol. *588*, 4401–4414.

Anderson, V., Catroppa, C., Morse, S., Haritou, F., and Rosenfeld, J. (2005c). Functional plasticity or vulnerability after early brain injury? Pediatrics *116*, 1374–1382.

Annegers, J.F., Hauser, W.A., Coan, S.P., and Rocca, W.A. (1998). A population-based study of seizures after traumatic brain injuries. N. Engl. J. Med. *338*, 20–24.

Appleton, R.E., and Demellweek, C. (2002). Post-traumatic epilepsy in children requiring inpatient rehabilitation following head injury. J. Neurol. Neurosurg. Psychiatry *72*, 669–672.

Arango, J.I., Deibert, C.P., Brown, D., Bell, M., Dvorchik, I., and Adelson, P.D. (2012). Posttraumatic seizures in children with severe traumatic brain injury. Childs Nerv. Syst. ChNS Off. J. Int. Soc. Pediatr. Neurosurg. *28*, 1925–1929.

Atallah, B.V., Bruns, W., Carandini, M., and Scanziani, M. (2012). Parvalbumin-Expressing Interneurons Linearly Transform Cortical Responses to Visual Stimuli. Neuron *73*, 159.

Axelson, H.W., Winkler, T., Flygt, J., Djupsjö, A., Hånell, A., and Marklund, N. (2013). Plasticity of the contralateral motor cortex following focal traumatic brain injury in the rat. Restor. Neurol. Neurosci. *31*, 73–85.

Bacci, A., and Huguenard, J.R. (2006). Enhancement of spike-timing precision by autaptic transmission in neocortical inhibitory interneurons. Neuron *49*, 119–130.

Balan, I.S., Saladino, A.J., Aarabi, B., Castellani, R.J., Wade, C., Stein, D.M., Eisenberg, H.M., Chen, H.H., and Fiskum, G. (2013). Cellular alterations in human traumatic brain injury: changes in mitochondrial morphology reflect regional levels of injury severity. J. Neurotrauma *30*, 367–381.

Barberis, A., Mozrzymas, J.W., Ortinski, P.I., and Vicini, S. (2007). Desensitization and binding properties determine distinct alpha1beta2gamma2 and alpha3beta2gamma2 GABA(A) receptor-channel kinetic behavior. Eur. J. Neurosci. *25*, 2726–2740.

Barlow, K.M., Spowart, J.J., and Minns, R.A. (2000). Early posttraumatic seizures in non-accidental head injury: relation to outcome. Dev. Med. Child Neurol. *42*, 591–594.

Bauer, J., and Burr, W. (2001). Course of chronic focal epilepsy resistant to anticonvulsant treatment. Seizure J. Br. Epilepsy Assoc. *10*, 239–246.

Behrens, M.M., and Sejnowski, T.J. (2009). Does schizophrenia arise from oxidative dysregulation of parvalbumin-interneurons in the developing cortex? Neuropharmacology *57*, 193–200.

Behrens, M.M., Ali, S.S., Dao, D.N., Lucero, J., Shekhtman, G., Quick, K.L., and Dugan, L.L. (2007). Ketamine-Induced Loss of Phenotype of Fast-Spiking Interneurons Is Mediated by NADPH-Oxidase. Science *318*, 1645–1647.

Ben-Ari, Y., Gaiarsa, J.-L., Tyzio, R., and Khazipov, R. (2007). GABA: a pioneer transmitter that excites immature neurons and generates primitive oscillations. Physiol. Rev. *87*, 1215–1284.

Biernaskie, J., and Corbett, D. (2001). Enriched rehabilitative training promotes improved forelimb motor function and enhanced dendritic growth after focal ischemic injury. J. Neurosci. Off. J. Soc. Neurosci. *21*, 5272–5280.

Biernaskie, J., Szymanska, A., Windle, V., and Corbett, D. (2005). Bi-hemispheric contribution to functional motor recovery of the affected forelimb following focal ischemic brain injury in rats. Eur. J. Neurosci. *21*, 989–999.

Bolkvadze, T., and Pitkänen, A. (2012). Development of post-traumatic epilepsy after controlled cortical impact and lateral fluid-percussion-induced brain injury in the mouse. J. Neurotrauma *29*, 789–812.

Brody, D.L., Mac Donald, C., Kessens, C.C., Yuede, C., Parsadanian, M., Spinner, M., Kim, E., Schwetye, K.E., Holtzman, D.M., and Bayly, P.V. (2007). Electromagnetic controlled cortical impact device for precise, graded experimental traumatic brain injury. J. Neurotrauma *24*, 657–673.

Buriticá, E., Villamil, L., Guzmán, F., Escobar, M.I., García-Cairasco, N., and Pimienta, H.J. (2009). Changes in calcium-binding protein expression in human cortical contusion tissue. J. Neurotrauma *26*, 2145–2155.

Cabungcal, J.-H., Steullet, P., Morishita, H., Kraftsik, R., Cuenod, M., Hensch, T.K., and Do, K.Q. (2013a). Perineuronal nets protect fast-spiking interneurons against oxidative stress. Proc. Natl. Acad. Sci. U. S. A. *110*, 9130–9135.

Cabungcal, J.-H., Steullet, P., Kraftsik, R., Cuenod, M., and Do, K.Q. (2013b). Early-life insults impair parvalbumin interneurons via oxidative stress: reversal by N-acetylcysteine. Biol. Psychiatry *73*, 574–582.

Caillard, O., Moreno, H., Schwaller, B., Llano, I., Celio, M.R., and Marty, A. (2000). Role of the calcium-binding protein parvalbumin in short-term synaptic plasticity. Proc. Natl. Acad. Sci. U. S. A. *97*, 13372–13377.

Calcagnotto, M.E., Paredes, M.F., Tihan, T., Barbaro, N.M., and Baraban, S.C. (2005). Dysfunction of synaptic inhibition in epilepsy associated with focal cortical dysplasia. J. Neurosci. Off. J. Soc. Neurosci. *25*, 9649–9657.

Camfield, P.R., and Camfield, C.S. (2014). What Happens to Children With Epilepsy When They Become Adults? Some Facts and Opinions. Pediatr. Neurol.

Cantu, D., Walker, K., Andresen, L., Taylor-Weiner, A., Hampton, D., Tesco, G., and Dulla, C.G. (2014). Traumatic Brain Injury Increases Cortical Glutamate Network

Activity by Compromising GABAergic Control. Cereb. Cortex N. Y. N 1991.

Cao, Y., Vikingstad, E.M., Huttenlocher, P.R., Towle, V.L., and Levin, D.N. (1994). Functional magnetic resonance studies of the reorganization of the human hand sensorimotor area after unilateral brain injury in the perinatal period. Proc. Natl. Acad. Sci. U. S. A. *91*, 9612–9616.

Card, J.P., Santone, D.J., Gluhovsky, M.Y., and Adelson, P.D. (2005). Plastic reorganization of hippocampal and neocortical circuitry in experimental traumatic brain injury in the immature rat. J. Neurotrauma *22*, 989–1002.

Casella, E.M., Thomas, T.C., Vanino, D.L., Fellows-Mayle, W., Lifshitz, J., Card, J.P., and Adelson, P.D. (2014). Traumatic brain injury alters long-term hippocampal neuron morphology in juvenile, but not immature, rats. Childs Nerv. Syst. *30*, 1333–1342.

Cauli, B., Audinat, E., Lambolez, B., Angulo, M.C., Ropert, N., Tsuzuki, K., Hestrin, S., and Rossier, J. (1997). Molecular and physiological diversity of cortical nonpyramidal cells. J. Neurosci. Off. J. Soc. Neurosci. *17*, 3894–3906.

Caveness, W.F., Meirowsky, A.M., Rish, B.L., Mohr, J.P., Kistler, J.P., Dillon, J.D., and Weiss, G.H. (1979). The nature of posttraumatic epilepsy. J. Neurosurg. *50*, 545–553.

Chen, P., Goldberg, D.E., Kolb, B., Lanser, M., and Benowitz, L.I. (2002). Inosine induces axonal rewiring and improves behavioral outcome after stroke. Proc. Natl. Acad. Sci. U. S. A. *99*, 9031–9036.

Cheng, G., Kong, R., Zhang, L., and Zhang, J. (2012). Mitochondria in traumatic brain injury and mitochondrial-targeted multipotential therapeutic strategies. Br. J. Pharmacol. *167*, 699–719.

Chow, A., Erisir, A., Farb, C., Nadal, M.S., Ozaita, A., Lau, D., Welker, E., and Rudy, B. (1999). K(+) channel expression distinguishes subpopulations of parvalbumin- and somatostatin-containing neocortical interneurons. J. Neurosci. Off. J. Soc. Neurosci. *19*, 9332–9345.

Chugani, H.T., Phelps, M.E., and Mazziotta, J.C. (1987). Positron emission tomography study of human brain functional development. Ann. Neurol. *22*, 487–497.

Cole, J.T., Yarnell, A., Kean, W.S., Gold, E., Lewis, B., Ren, M., McMullen, D.C., Jacobowitz, D.M., Pollard, H.B., O'Neill, J.T., et al. (2010). Craniotomy: True Sham for Traumatic Brain Injury, or a Sham of a Sham? J. Neurotrauma *28*, 359–369.

Cole, J.T., Yarnell, A., Kean, W.S., Gold, E., Lewis, B., Ren, M., McMullen, D.C., Jacobowitz, D.M., Pollard, H.B., O'Neill, J.T., et al. (2011). Craniotomy: True Sham for Traumatic Brain Injury, or a Sham of a Sham? J. Neurotrauma *28*, 359–369.

Connors, B.W., and Gutnick, M.J. (1990). Intrinsic firing patterns of diverse neocortical

neurons. Trends Neurosci. *13*, 99–104.

Cook, L.G., Chapman, S.B., Elliott, A.C., Evenson, N.N., and Vinton, K. (2014). Cognitive Gains from Gist Reasoning Training in Adolescents with Chronic-Stage Traumatic Brain Injury. Front. Neurol. *5*.

Corkin, S., Sullivan, E.V., and Carr, F.A. (1984). Prognostic factors for life expectancy after penetrating head injury. Arch. Neurol. *41*, 975–977.

Cowan, W.M., Fawcett, J.W., O'Leary, D.D., and Stanfield, B.B. (1984). Regressive events in neurogenesis. Science *225*, 1258–1265.

Cramer, S.C., Shah, R., Juranek, J., Crafton, K.R., and Le, V. (2006). Activity in the peri-infarct rim in relation to recovery from stroke. Stroke J. Cereb. Circ. *37*, 111–115.

Cruikshank, S.J., Lewis, T.J., and Connors, B.W. (2007). Synaptic basis for intense thalamocortical activation of feedforward inhibitory cells in neocortex. Nat. Neurosci. *10*, 462–468.

Dávid, C., Schleicher, A., Zuschratter, W., and Staiger, J.F. (2007). The innervation of parvalbumin-containing interneurons by VIP-immunopositive interneurons in the primary somatosensory cortex of the adult rat. Eur. J. Neurosci. *25*, 2329–2340.

De Beaumont, L., Lassonde, M., Leclerc, S., and Théoret, H. (2007). Long-term and cumulative effects of sports concussion on motor cortex inhibition. Neurosurgery *61*, 329–336; discussion 336–337.

De Beaumont, L., Théoret, H., Mongeon, D., Messier, J., Leclerc, S., Tremblay, S., Ellemberg, D., and Lassonde, M. (2009). Brain function decline in healthy retired athletes who sustained their last sports concussion in early adulthood. Brain J. Neurol. *132*, 695–708.

Dichter, M.A., and Ayala, G.F. (1987). Cellular mechanisms of epilepsy: a status report. Science *237*, 157–164.

Ding, M.-C., Wang, Q., Lo, E.H., and Stanley, G.B. (2011). Cortical excitation and inhibition following focal traumatic brain injury. J. Neurosci. Off. J. Soc. Neurosci. *31*, 14085–14094.

Doischer, D., Hosp, J.A., Yanagawa, Y., Obata, K., Jonas, P., Vida, I., and Bartos, M. (2008). Postnatal differentiation of basket cells from slow to fast signaling devices. J. Neurosci. Off. J. Soc. Neurosci. *28*, 12956–12968.

Douglas, R.J., and Martin, K.A.C. (2007). Mapping the Matrix: The Ways of Neocortex. Neuron *56*, 226–238.

Eadie, M.J. (2012). Shortcomings in the current treatment of epilepsy. Expert Rev.

Neurother. *12*, 1419–1427.

Elaine Wyllie MD, A.G., and Deepak K. Lachhwani (2005). The Treatment of Epilepsy: Principles and Practice (Philadelphia: Lippincott Williams & Wilkins).

Emery, D.L., Raghupathi, R., Saatman, K.E., Fischer, I., Grady, M.S., and McIntosh, T.K. (2000). Bilateral growth-related protein expression suggests a transient increase in regenerative potential following brain trauma. J. Comp. Neurol. *424*, 521–531.

Ewing-Cobbs, L., Miner, M.E., Fletcher, J.M., and Levin, H.S. (1989). Intellectual, Motor, and Language Sequelae Following Closed Head Injury in Infants and Preschoolers. J. Pediatr. Psychol. *14*, 531–547.

Ewing-Cobbs, L., Prasad, M., Kramer, L., and Landry, S. (1999). Inflicted traumatic brain injury: relationship of developmental outcome to severity of injury. Pediatr. Neurosurg. *31*, 251–258.

Ewing-Cobbs, L., Barnes, M.A., and Fletcher, J.M. (2003). Early brain injury in children: development and reorganization of cognitive function. Dev. Neuropsychol. *24*, 669–704.

Ewing-Cobbs, L., Prasad, M.R., Kramer, L., Cox, C.S., Baumgartner, J., Fletcher, S., Mendez, D., Barnes, M., Zhang, X., and Swank, P. (2006). Late intellectual and academic outcomes following traumatic brain injury sustained during early childhood. J. Neurosurg. *105*, 287–296.

Fisher, R.S., van Emde Boas, W., Blume, W., Elger, C., Genton, P., Lee, P., and Engel, J., Jr (2005). Epileptic seizures and epilepsy: definitions proposed by the International League Against Epilepsy (ILAE) and the International Bureau for Epilepsy (IBE). Epilepsia *46*, 470–472.

Fox, G., Fan, L., Levasseur, R.A., and Faden, A.I. (1998). Sustained Sensory/Motor and Cognitive Deficits With Neuronal Apoptosis Following Controlled Cortical Impact Brain Injury in the Mouse. J. Neurotrauma *15*, 599–614.

Frey, L.C. (2003a). Epidemiology of posttraumatic epilepsy: a critical review. Epilepsia *44 Suppl 10*, 11–17.

Frey, L.C. (2003b). Epidemiology of posttraumatic epilepsy: a critical review. Epilepsia *44 Suppl 10*, 11–17.

Friedman, D., Claassen, J., and Hirsch, L.J. (2009). Continuous electroencephalogram monitoring in the intensive care unit. Anesth. Analg. *109*, 506–523.

Friedman, W.J., Olson, L., and Persson, H. (1991). Cells that Express Brain-Derived Neurotrophic Factor mRNA in the Developing Postnatal Rat Brain. Eur. J. Neurosci. *3*, 688–697.

Frost, S.B., Barbay, S., Friel, K.M., Plautz, E.J., and Nudo, R.J. (2003). Reorganization

of Remote Cortical Regions After Ischemic Brain Injury: A Potential Substrate for Stroke Recovery. J. Neurophysiol. *89*, 3205–3214.

Fujimoto, S.T., Longhi, L., Saatman, K.E., Conte, V., Stocchetti, N., and McIntosh, T.K. (2004). Motor and cognitive function evaluation following experimental traumatic brain injury. Neurosci. Biobehav. Rev. *28*, 365–378.

Gabernet, L., Jadhav, S.P., Feldman, D.E., Carandini, M., and Scanziani, M. (2005). Somatosensory integration controlled by dynamic thalamocortical feed-forward inhibition. Neuron *48*, 315–327.

Galarreta, M., and Hestrin, S. (1998). Frequency-dependent synaptic depression and the balance of excitation and inhibition in the neocortex. Nat. Neurosci. *1*, 587–594.

Galarreta, M., and Hestrin, S. (1999). A network of fast-spiking cells in the neocortex connected by electrical synapses. Nature *402*, 72–75.

Garga, N., and Lowenstein, D.H. (2006). Posttraumatic epilepsy: a major problem in desperate need of major advances. Epilepsy Curr. Am. Epilepsy Soc. *6*, 1–5.

Ghajar, J. (2000). Traumatic brain injury. Lancet *356*, 923–929.

Gibson, J.R., Beierlein, M., and Connors, B.W. (1999). Two networks of electrically coupled inhibitory neurons in neocortex. Nature *402*, 75–79.

Gill, R., Chang, P.K.-Y., Prenosil, G.A., Deane, E.C., and McKinney, R.A. (2013). Blocking brain-derived neurotrophic factor inhibits injury-induced hyperexcitability of hippocampal CA3 neurons. Eur. J. Neurosci. *38*, 3554–3566.

Goddeyne, C., Nichols, J., Wu, C., and Anderson, T. (2015). Repetitive mild traumatic brain injury induces ventriculomegaly and cortical thinning in juvenile rats. J. Neurophysiol. *113*, 3268–3280.

Goldberg, E.M., Clark, B.D., Zagha, E., Nahmani, M., Erisir, A., and Rudy, B. (2008). K+ channels at the axon initial segment dampen near-threshold excitability of neocortical fast-spiking GABAergic interneurons. Neuron *58*, 387–400.

Goldberg, J.H., Yuste, R., and Tamas, G. (2003). Ca2+ imaging of mouse neocortical interneurone dendrites: Contribution of Ca2+-permeable AMPA and NMDA receptors to subthreshold Ca2+dynamics. J. Physiol. *551*, 67–78.

Goodman, J.C., Cherian, L., Bryan, R.M., and Robertson, C.S. (1994). Lateral Cortical Impact Injury in Rats: Pathologic Effects of Varying Cortical Compression and Impact Velocity. J. Neurotrauma *11*, 587–597.

Graber, K.D., and Prince, D.A. (2004). A critical period for prevention of posttraumatic neocortical hyperexcitability in rats. Ann. Neurol. *55*, 860–870.

Guatteo, E., Bacci, A., Franceschetti, S., Avanzini, G., and Wanke, E. (1994). Neurons dissociated from neocortex fire with “burst” and “regular” trains of spikes. Neurosci. Lett. *175*, 117–120.

Guerriero, R.M., Giza, C.C., and Rotenberg, A. (2015). Glutamate and GABA Imbalance Following Traumatic Brain Injury. Curr. Neurol. Neurosci. Rep. *15*, 545.

Gupta, A., Wang, Y., and Markram, H. (2000). Organizing principles for a diversity of GABAergic interneurons and synapses in the neocortex. Science *287*, 273–278.

Haider, B., and McCormick, D.A. (2009). Rapid neocortical dynamics: cellular and network mechanisms. Neuron *62*, 171–189.

Hall, E.D., Sullivan, P.G., Gibson, T.R., Pavel, K.M., Thompson, B.M., and Scheff, S.W. (2005a). Spatial and Temporal Characteristics of Neurodegeneration after Controlled Cortical Impact in Mice: More than a Focal Brain Injury. J. Neurotrauma *22*, 252–265.

Hall, R.C.W., Hall, R.C.W., and Chapman, M.J. (2005b). Definition, diagnosis, and forensic implications of postconcussional syndrome. Psychosomatics *46*, 195–202.

Hamm, R.J., Pike, B.R., O’Dell, D.M., Lyeth, B.G., and Jenkins, L.W. (1994). The rotarod test: an evaluation of its effectiveness in assessing motor deficits following traumatic brain injury. J. Neurotrauma *11*, 187–196.

Hånell, A., Clausen, F., Björk, M., Jansson, K., Philipson, O., Nilsson, L.N.G., Hillered, L., Weinreb, P.H., Lee, D., McIntosh, T.K., et al. (2010). Genetic deletion and pharmacological inhibition of Nogo-66 receptor impairs cognitive outcome after traumatic brain injury in mice. J. Neurotrauma *27*, 1297–1309.

Hasenstaub, A., Shu, Y., Haider, B., Kraushaar, U., Duque, A., and McCormick, D.A. (2005). Inhibitory postsynaptic potentials carry synchronized frequency information in active cortical networks. Neuron *47*, 423–435.

Hensch, T.K. (2005). Critical period plasticity in local cortical circuits. Nat. Rev. Neurosci. *6*, 877–888.

Herman, S.T. (2002). Epilepsy after brain insult: targeting epileptogenesis. Neurology *59*, S21–S26.

Hioki, H., Okamoto, S., Konno, M., Kameda, H., Sohn, J., Kuramoto, E., Fujiyama, F., and Kaneko, T. (2013). Cell Type-Specific Inhibitory Inputs to Dendritic and Somatic Compartments of Parvalbumin-Expressing Neocortical Interneuron. J. Neurosci. *33*, 544–555.

Hoffman, S.N., Salin, P.A., and Prince, D.A. (1994). Chronic neocortical epileptogenesis in vitro. J. Neurophysiol. *71*, 1762–1773.

Horita, H., Uchida, E., and Maekawa, K. (1991). Circadian rhythm of regular spike-wave

discharges in childhood absence epilepsy. Brain Dev. *13*, 200–202.

Houston, C.M., Bright, D.P., Sivilotti, L.G., Beato, M., and Smart, T.G. (2009). Intracellular chloride ions regulate the time course of GABA-mediated inhibitory synaptic transmission. J. Neurosci. Off. J. Soc. Neurosci. *29*, 10416–10423.

Houweling, A.R., Bazhenov, M., Timofeev, I., Steriade, M., and Sejnowski, T.J. (2005). Homeostatic Synaptic Plasticity Can Explain Post-traumatic Epileptogenesis in Chronically Isolated Neocortex. Cereb. Cortex N. Y. N 1991 *15*, 834–845.

Hu, H., Gan, J., and Jonas, P. (2014). Fast-spiking, parvalbumin+ GABAergic interneurons: From cellular design to microcircuit function. Science *345*, 1255263.

Hulsebosch, C.E., DeWitt, D.S., Jenkins, L.W., and Prough, D.S. (1998). Traumatic brain injury in rats results in increased expression of Gap-43 that correlates with behavioral recovery. Neurosci. Lett. *255*, 83–86.

Hunt, R.F., Scheff, S.W., and Smith, B.N. (2009). Posttraumatic epilepsy after controlled cortical impact injury in mice. Exp. Neurol. *215*, 243–252.

Hunt, R.F., Scheff, S.W., and Smith, B.N. (2011). Synaptic reorganization of inhibitory hilar interneuron circuitry after traumatic brain injury in mice. J. Neurosci. Off. J. Soc. Neurosci. *31*, 6880–6890.

Huusko, N., Römer, C., Ndode-Ekane, X.E., Lukasiuk, K., and Pitkänen, A. (2015). Loss of hippocampal interneurons and epileptogenesis: a comparison of two animal models of acquired epilepsy. Brain Struct. Funct. *220*, 153–191.

Insel, T.R., Miller, L.P., and Gelhard, R.E. (1990). The ontogeny of excitatory amino acid receptors in rat forebrain--I. N-methyl-D-aspartate and quisqualate receptors. Neuroscience *35*, 31–43.

Isomura, Y., Harukuni, R., Takekawa, T., Aizawa, H., and Fukai, T. (2009). Microcircuitry coordination of cortical motor information in self-initiation of voluntary movements. Nat. Neurosci. *12*, 1586–1593.

Itami, C., Kimura, F., and Nakamura, S. (2007). Brain-derived neurotrophic factor regulates the maturation of layer 4 fast-spiking cells after the second postnatal week in the developing barrel cortex. J. Neurosci. Off. J. Soc. Neurosci. *27*, 2241–2252.

Iudice, A., and Murri, L. (2000). Pharmacological prophylaxis of post-traumatic epilepsy. Drugs *59*, 1091–1099.

Izhikevich, E.M., Desai, N.S., Walcott, E.C., and Hoppensteadt, F.C. (2003). Bursts as a unit of neural information: selective communication via resonance. Trends Neurosci. *26*, 161–167.

Jacobs, K.M., Graber, K.D., Kharazia, V.N., Parada, I., and Prince, D.A. (2000).

Postlesional epilepsy: the ultimate brain plasticity. Epilepsia *41 Suppl 6*, S153–S161.

Jenkins, L.W., Peters, G.W., Dixon, C.E., Zhang, X., Clark, R.S.B., Skinner, J.C., Marion, D.W., Adelson, P.D., and Kochanek, P.M. (2002). Conventional and functional proteomics using large format two-dimensional gel electrophoresis 24 hours after controlled cortical impact in postnatal day 17 rats. J. Neurotrauma *19*, 715–740.

Jin, X., Prince, D.A., and Huguenard, J.R. (2006). Enhanced Excitatory Synaptic Connectivity in Layer V Pyramidal Neurons of Chronically Injured Epileptogenic Neocortex in Rats. J. Neurosci. *26*, 4891–4900.

Jin, X., Huguenard, J.R., and Prince, D.A. (2011). Reorganization of inhibitory synaptic circuits in rodent chronically injured epileptogenic neocortex. Cereb. Cortex N. Y. N 1991 *21*, 1094–1104.

Jin, X., Jiang, K., and Prince, D.A. (2014). Excitatory and Inhibitory Synaptic Connectivity to Layer V Fast-spiking Interneurons in the Freeze Lesion Model of Cortical Microgyria. J. Neurophysiol.

Johnson, V.E., Stewart, J.E., Begbie, F.D., Trojanowski, J.Q., Smith, D.H., and Stewart, W. (2013). Inflammation and white matter degeneration persist for years after a single traumatic brain injury. Brain J. Neurol. *136*, 28–42.

Jones, E.G. (1998). Viewpoint: the core and matrix of thalamic organization. Neuroscience *85*, 331–345.

Jones, T.A., Liput, D.J., Maresh, E.L., Donlan, N., Parikh, T.J., Marlowe, D., and Kozlowski, D.A. (2012). Use-Dependent Dendritic Regrowth Is Limited after Unilateral Controlled Cortical Impact to the Forelimb Sensorimotor Cortex. J. Neurotrauma *29*, 1455–1468.

Katz, L.C. (1993). Coordinate activity in retinal and cortical development. Curr. Opin. Neurobiol. *3*, 93–99.

Kawaguchi, Y., and Kondo, S. (2002). Parvalbumin, somatostatin and cholecystokinin as chemical markers for specific GABAergic interneuron types in the rat frontal cortex. J. Neurocytol. *31*, 277–287.

Kawaguchi, Y., and Kubota, Y. (1997). GABAergic cell subtypes and their synaptic connections in rat frontal cortex. Cereb. Cortex *7*, 476–486.

Kawaguchi, Y., Katsumaru, H., Kosaka, T., Heizmann, C.W., and Hama, K. (1987). Fast spiking cells in rat hippocampus (CA1 region) contain the calcium-binding protein parvalbumin. Brain Res. *416*, 369–374.

Keros, S., and Hablitz, J.J. (2005). Subtype-specific GABA transporter antagonists synergistically modulate phasic and tonic GABAA conductances in rat neocortex. J.

Neurophysiol. *94*, 2073–2085.

Kim, E. (2002). Agitation, aggression, and disinhibition syndromes after traumatic brain injury. NeuroRehabilitation *17*, 297–310.

Kinney, J.W., Davis, C.N., Tabarean, I., Conti, B., Bartfai, T., and Behrens, M.M. (2006). A specific role for NR2A-containing NMDA receptors in the maintenance of parvalbumin and GAD67 immunoreactivity in cultured interneurons. J. Neurosci. Off. J. Soc. Neurosci. *26*, 1604–1615.

Kleschevnikov, A.M., Belichenko, P.V., Villar, A.J., Epstein, C.J., Malenka, R.C., and Mobley, W.C. (2004). Hippocampal long-term potentiation suppressed by increased inhibition in the Ts65Dn mouse, a genetic model of Down syndrome. J. Neurosci. Off. J. Soc. Neurosci. *24*, 8153–8160.

Klonoff, H., Clark, C., and Klonoff, P.S. (1993). Long-term outcome of head injuries: a 23 year follow up study of children with head injuries. J. Neurol. Neurosurg. Psychiatry *56*, 410–415.

Kobayashi, M., Wen, X., and Buckmaster, P.S. (2003). Reduced inhibition and increased output of layer II neurons in the medial entorhinal cortex in a model of temporal lobe epilepsy. J. Neurosci. Off. J. Soc. Neurosci. *23*, 8471–8479.

Kobori, N., Clifton, G.L., and Dash, P. (2002). Altered expression of novel genes in the cerebral cortex following experimental brain injury. Brain Res. Mol. Brain Res. *104*, 148–158.

Kochanek, P.M., Carney, N., Adelson, P.D., Ashwal, S., Bell, M.J., Bratton, S., Carson, S., Chesnut, R.M., Ghajar, J., Goldstein, B., et al. (2012). Guidelines for the acute medical management of severe traumatic brain injury in infants, children, and adolescents--second edition. Pediatr. Crit. Care Med. J. Soc. Crit. Care Med. World Fed. Pediatr. Intensive Crit. Care Soc. *13 Suppl 1*, S1–S82.

Kuhlman, S.J., Olivas, N.D., Tring, E., Ikrar, T., Xu, X., and Trachtenberg, J.T. (2013). A disinhibitory microcircuit initiates critical-period plasticity in the visual cortex. Nature *501*, 543–546.

Lawrence, J.J., and McBain, C.J. (2003). Interneuron diversity series: containing the detonation--feedforward inhibition in the CA3 hippocampus. Trends Neurosci. *26*, 631–640.

Lenzlinger, P.M., Shimizu, S., Marklund, N., Thompson, H.J., Schwab, M.E., Saatman, K.E., Hoover, R.C., Bareyre, F.M., Motta, M., Luginbuhl, A., et al. (2005). Delayed inhibition of Nogo-A does not alter injury-induced axonal sprouting but enhances recovery of cognitive function following experimental traumatic brain injury in rats. Neuroscience *134*, 1047–1056.

Letzkus, J.J., Wolff, S.B.E., Meyer, E.M.M., Tovote, P., Courtin, J., Herry, C., and Lüthi, A. (2011). A disinhibitory microcircuit for associative fear learning in the auditory cortex. Nature *480*, 331–335.

Levitt, P. (2003). Structural and functional maturation of the developing primate brain. J. Pediatr. *143*, S35–S45.

Levitt, P., Eagleson, K.L., and Powell, E.M. (2004). Regulation of neocortical interneuron development and the implications for neurodevelopmental disorders. Trends Neurosci. *27*, 400–406.

Lewis, D.A., Curley, A.A., Glausier, J., and Volk, D.W. (2012). Cortical Parvalbumin Interneurons and Cognitive Dysfunction in Schizophrenia. Trends Neurosci. *35*, 57–67.

Li, K., and Xu, E. (2008). The role and the mechanism of gamma-aminobutyric acid during central nervous system development. Neurosci. Bull. *24*, 195–200.

Li, H.H., Lee, S.M., Cai, Y., Sutton, R.L., and Hovda, D.A. (2004). Differential gene expression in hippocampus following experimental brain trauma reveals distinct features of moderate and severe injuries. J. Neurotrauma *21*, 1141–1153.

Lighthall, J.W., Dixon, C.E., and Anderson, T.E. (1989). Experimental models of brain injury. J. Neurotrauma *6*, 83–97.

Lisman, J.E. (1997). Bursts as a unit of neural information: making unreliable synapses reliable. Trends Neurosci. *20*, 38–43.

Liu, N.-K., Zhang, Y.-P., O'Connor, J., Gianaris, A., Oakes, E., Lu, Q.-B., Verhovshek, T., Walker, C.L., Shields, C.B., and Xu, X.-M. (2013). A bilateral head injury that shows graded brain damage and behavioral deficits in adultmice. Brain Res. *1499*, 121–128.

Lowenstein, D.H., Thomas, M.J., Smith, D.H., and McIntosh, T.K. (1992). Selective vulnerability of dentate hilar neurons following traumatic brain injury: a potential mechanistic link between head trauma and disorders of the hippocampus. J. Neurosci. Off. J. Soc. Neurosci. *12*, 4846–4853.

Luerssen, T.G., Klauber, M.R., and Marshall, L.F. (1988a). Outcome from head injury related to patient's age. A longitudinal prospective study of adult and pediatric head injury. J. Neurosurg. *68*, 409–416.

Luerssen, T.G., Klauber, M.R., and Marshall, L.F. (1988b). Outcome from head injury related to patient's age. A longitudinal prospective study of adult and pediatric head injury. J. Neurosurg. *68*, 409–416.

Ma, Y., and Prince, D.A. (2012). Functional alterations in GABAergic fast-spiking interneurons in chronically injured epileptogenic neocortex. Neurobiol. Dis. *47*, 102–113.

Ma, Y., Hu, H., Berrebi, A.S., Mathers, P.H., and Agmon, A. (2006). Distinct Subtypes

of Somatostatin-Containing Neocortical Interneurons Revealed in Transgenic Mice. J. Neurosci. *26*, 5069–5082.

Maas, A.I., Stocchetti, N., and Bullock, R. (2008). Moderate and severe traumatic brain injury in adults. Lancet Neurol. *7*, 728–741.

Magiorkinis, E., Sidiropoulou, K., and Diamantis, A. (2010). Hallmarks in the history of epilepsy: epilepsy in antiquity. Epilepsy Behav. EB *17*, 103–108.

Mannix, R.C., Zhang, J., Park, J., Lee, C., and Whalen, M.J. (2011). Detrimental effect of genetic inhibition of B-site APP-cleaving enzyme 1 on functional outcome after controlled cortical impact in young adult mice. J. Neurotrauma *28*, 1855–1861.

Marklund, N., Bareyre, F.M., Royo, N.C., Thompson, H.J., Mir, A.K., Grady, M.S., Schwab, M.E., and McIntosh, T.K. (2007). Cognitive outcome following brain injury and treatment with an inhibitor of Nogo-A in association with an attenuated downregulation of hippocampal growth-associated protein-43 expression. J. Neurosurg. *107*, 844–853.

Markram, H., Toledo-Rodriguez, M., Wang, Y., Gupta, A., Silberberg, G., and Wu, C. (2004a). Interneurons of the neocortical inhibitory system. Nat. Rev. Neurosci. *5*, 793–807.

Markram, H., Toledo-Rodriguez, M., Wang, Y., Gupta, A., Silberberg, G., and Wu, C. (2004b). Interneurons of the neocortical inhibitory system. Nat. Rev. Neurosci. *5*, 793–807.

Matsumoto, H., and Marsan, C.A. (1964). Cortical cellular phenomena in experimental epilepsy: Interictal manifestations. Exp. Neurol. *9*, 286–304.

Mazarati, A. (2006). Is posttraumatic epilepsy the best model of posttraumatic epilepsy? Epilepsy Curr. Am. Epilepsy Soc. *6*, 213–214.

McKinlay, A., Dalrymple-Alford, J.C., Horwood, L.J., and Fergusson, D.M. (2002). Long term psychosocial outcomes after mild head injury in early childhood. J. Neurol. Neurosurg. Psychiatry *73*, 281–288.

Mello, L.E., Cavalheiro, E.A., Tan, A.M., Kupfer, W.R., Pretorius, J.K., Babb, T.L., and Finch, D.M. (1993). Circuit mechanisms of seizures in the pilocarpine model of chronic epilepsy: cell loss and mossy fiber sprouting. Epilepsia *34*, 985–995.

Menon, D.K., Schwab, K., Wright, D.W., Maas, A.I., and Demographics and Clinical Assessment Working Group of the International and Interagency Initiative toward Common Data Elements for Research on Traumatic Brain Injury and Psychological Health (2010). Position statement: definition of traumatic brain injury. Arch. Phys. Med. Rehabil. *91*, 1637–1640.

Michael, A.P., Stout, J., Roskos, P.T., Bolzenius, J., Gfeller, J., Mogul, D., and Bucholz,

R. (2015). Evaluation of Cortical Thickness after Traumatic Brain Injury in Military Veterans. J. Neurotrauma *32*, 1751–1758.

Miller, L.M., Escabí, M.A., and Schreiner, C.E. (2001). Feature selectivity and interneuronal cooperation in the thalamocortical system. J. Neurosci. Off. J. Soc. Neurosci. *21*, 8136–8144.

Miller, M.N., Okaty, B.W., Kato, S., and Nelson, S.B. (2011). Activity-dependent changes in the firing properties of neocortical fast-spiking interneurons in the absence of large changes in gene expression. Dev. Neurobiol. *71*, 62–70.

Mishra, A.M., Bai, X., Sanganahalli, B.G., Waxman, S.G., Shatillo, O., Grohn, O., Hyder, F., Pitkanen, A., and Blumenfeld, H. (2014). Decreased Resting Functional Connectivity after Traumatic Brain Injury in the Rat. PLoS ONE *9*.

Mitchell, S.J., and Silver, R.A. (2003). Shunting Inhibition Modulates Neuronal Gain during Synaptic Excitation. Neuron *38*, 433–445.

Morris, N.P., and Henderson, Z. (2000). Perineuronal nets ensheath fast spiking, parvalbumin-immunoreactive neurons in the medial septum/diagonal band complex. Eur. J. Neurosci. *12*, 828–838.

Mrzljak, L., Uylings, H.B., Van Eden, C.G., and Judás, M. (1990). Neuronal development in human prefrontal cortex in prenatal and postnatal stages. Prog. Brain Res. *85*, 185–222.

Nakamura, T., Matsumoto, J., Takamura, Y., Ishii, Y., Sasahara, M., Ono, T., and Nishijo, H. (2015). Relationships among parvalbumin-immunoreactive neuron density, phase-locked gamma oscillations, and autistic/schizophrenic symptoms in PDGFR-β knock-out and control mice. PloS One *10*, e0119258.

Nathanson, J.L., Yanagawa, Y., Obata, K., and Callaway, E.M. (2009). Preferential labeling of inhibitory and excitatory cortical neurons by endogenous tropism of AAV and lentiviral vectors. Neuroscience *161*, 441–450.

Nelson, S.B., and Turrigiano, G.G. (1998). Synaptic depression: a key player in the cortical balancing act. Nat. Neurosci. *1*, 539–541.

Nichols, J., Perez, R., Wu, C., Adelson, P.D., and Anderson, T. (2015). Traumatic Brain Injury Induces Rapid Enhancement of Cortical Excitability in Juvenile Rats. CNS Neurosci. Ther. *21*, 193–203.

Nilsson, P., Ronne-Engström, E., Flink, R., Ungerstedt, U., Carlson, H., and Hillered, L. (1994). Epileptic seizure activity in the acute phase following cortical impact trauma in rat. Brain Res. *637*, 227–232.

Nishibe, M., Barbay, S., Guggenmos, D., and Nudo, R.J. (2010). Reorganization of

Motor Cortex after Controlled Cortical Impact in Rats and Implications for Functional Recovery. J. Neurotrauma *27*, 2221–2232.

Noctor, S.C., Flint, A.C., Weissman, T.A., Dammerman, R.S., and Kriegstein, A.R. (2001). Neurons derived from radial glial cells establish radial units in neocortex. Nature *409*, 714–720.

Nudo, R.J. (2006). Mechanisms for recovery of motor function following cortical damage. Curr. Opin. Neurobiol. *16*, 638–644.

Okaty, B.W., Miller, M.N., Sugino, K., Hempel, C.M., and Nelson, S.B. (2009). Transcriptional and electrophysiological maturation of neocortical fastspiking GABAergic interneurons. J. Neurosci. Off. J. Soc. Neurosci. *29*, 7040–7052.

Olesen, S.P. (1987). Leakiness of rat brain microvessels to fluorescent probes following craniotomy. Acta Physiol. Scand. *130*, 63–68.

Orduz, D., Bischop, D.P., Schwaller, B., Schiffmann, S.N., and Gall, D. (2013). Parvalbumin tunes spike-timing and efferent short-term plasticity in striatal fast spiking interneurons. J. Physiol. *591*, 3215–3232.

Orlando, C., and Raineteau, O. (2015). Integrity of cortical perineuronal nets influences corticospinal tract plasticity after spinal cord injury. Brain Struct. Funct. *220*, 1077–1091.

Overstreet, L.S., and Westbrook, G.L. (2003). Synapse density regulates independence at unitary inhibitory synapses. J. Neurosci. Off. J. Soc. Neurosci. *23*, 2618–2626.

Pagni, C.A., and Zenga, F. (2005). Posttraumatic epilepsy with special emphasis on prophylaxis and prevention. Acta Neurochir. Suppl. *93*, 27–34.

Pandolfo, M. (2011). Genetics of epilepsy. Semin. Neurol. *31*, 506–518.

Park, E., Bell, J.D., and Baker, A.J. (2008). Traumatic brain injury: Can the consequences be stopped? CMAJ Can. Med. Assoc. J. *178*, 1163–1170.

Pavlov, I., Huusko, N., Drexel, M., Kirchmair, E., Sperk, G., Pitkänen, A., and Walker, M.C. (2011). Progressive loss of phasic, but not tonic, GABAA receptor-mediated inhibition in dentate granule cells in a model of post-traumatic epilepsy in rats. Neuroscience *194*, 208–219.

Paxinos, G., and Watson, C. (2007). The rat brain in stereotaxic coordinates (Amsterdam; Boston: Elsevier).

Pearce, A.J., Hoy, K., Rogers, M.A., Corp, D.T., Davies, C.B., Maller, J.J., and Fitzgerald, P.B. (2015). Acute motor, neurocognitive and neurophysiological change following concussion injury in Australian amateur football. A prospective multimodal investigation. J. Sci. Med. Sport *18*, 500–506.

Pearson, W.S., Ovalle, F., Faul, M., and Sasser, S.M. (2012a). A review of traumatic brain injury trauma center visits meeting physiologic criteria from The American College of Surgeons Committee on Trauma/Centers for Disease Control and Prevention Field Triage Guidelines. Prehospital Emerg. Care Off. J. Natl. Assoc. EMS Physicians Natl. Assoc. State EMS Dir. *16*, 323–328.

Pearson, W.S., Sugerman, D.E., McGuire, L.C., and Coronado, V.G. (2012b). Emergency Department Visits for Traumatic Brain Injury in Older Adults in the United States: 2006–08. West. J. Emerg. Med. *13*, 289–293.

Perucca, P., and Gilliam, F.G. (2012). Adverse effects of antiepileptic drugs. Lancet Neurol. *11*, 792–802.

Peters, A., and Jones, E.G. (1984). Cerebral Cortex: Volume 1: Cellular Components of the Cerebral Cortex (New York: Springer).

Petilla Interneuron Nomenclature Group, Ascoli, G.A., Alonso-Nanclares, L., Anderson, S.A., Barrionuevo, G., Benavides-Piccione, R., Burkhalter, A., Buzsáki, G., Cauli, B., Defelipe, J., et al. (2008). Petilla terminology: nomenclature of features of GABAergic interneurons of the cerebral cortex. Nat. Rev. Neurosci. *9*, 557–568.

Pi, H.-J., Hangya, B., Kvitsiani, D., Sanders, J.I., Huang, Z.J., and Kepecs, A. (2013). Cortical interneurons that specialize in disinhibitory control. Nature *advance online publication*.

Pinto, D.J., Brumberg, J.C., and Simons, D.J. (2000). Circuit dynamics and coding strategies in rodent somatosensory cortex. J. Neurophysiol. *83*, 1158–1166.

Pinto, D.J., Hartings, J.A., Brumberg, J.C., and Simons, D.J. (2003). Cortical damping: analysis of thalamocortical response transformations in rodent barrel cortex. Cereb. Cortex N. Y. N 1991 *13*, 33–44.

Pitkänen, A., and McIntosh, T.K. (2006). Animal models of post-traumatic epilepsy. J. Neurotrauma *23*, 241–261.

Pitkänen, A., Kharatishvili, I., Karhunen, H., Lukasiuk, K., Immonen, R., Nairismägi, J., Gröhn, O., and Nissinen, J. (2007). Epileptogenesis in experimental models. Epilepsia *48 Suppl 2*, 13–20.

Polack, P.-O., Guillemain, I., Hu, E., Deransart, C., Depaulis, A., and Charpier, S. (2007). Deep Layer Somatosensory Cortical Neurons Initiate Spike-and-Wave Discharges in a Genetic Model of Absence Seizures. J. Neurosci. *27*, 6590–6599.

Pouille, F., and Scanziani, M. (2001). Enforcement of temporal fidelity in pyramidal cells by somatic feed-forward inhibition. Science *293*, 1159–1163.

Powell, S.B., Sejnowski, T.J., and Behrens, M.M. (2012). Behavioral and neurochemical

consequences of cortical oxidative stress on parvalbumin-interneuron maturation in rodent models of schizophrenia. Neuropharmacology *62*, 1322–1331.

Prince, D.A. (1978). Neurophysiology of Epilepsy. Annu. Rev. Neurosci. *1*, 395–415.

Prince, D.A., and Connors, B.W. (1986). Mechanisms of interictal epileptogenesis. Adv. Neurol. *44*, 275–299.

Prince, D.A., and Tseng, G.F. (1993). Epileptogenesis in chronically injured cortex: in vitro studies. J. Neurophysiol. *69*, 1276–1291.

Prinz, A., Selesnew, L.-M., Liss, B., Roeper, J., and Carlsson, T. (2013). Increased excitability in serotonin neurons in the dorsal raphe nucleus in the 6-OHDA mouse model of Parkinson's disease. Exp. Neurol. *248*, 236–245.

Rakic, P. (1988). Specification of cerebral cortical areas. Science *241*, 170–176.

Ramantani, G. (2013). Neonatal epilepsy and underlying aetiology: to what extent do seizures and EEG abnormalities influence outcome? Epileptic Disord. Int. Epilepsy J. Videotape *15*, 365–375.

Rheims, S., Holmgren, C.D., Chazal, G., Mulder, J., Harkany, T., Zilberter, T., and Zilberter, Y. (2009). GABA action in immature neocortical neurons directly depends on the availability of ketone bodies. J. Neurochem. *110*, 1330–1338.

Rola, R., Mizumatsu, S., Otsuka, S., Morhardt, D., Noblehaeusslein, L., Fishman, K., Potts, M., and Fike, J. (2006). Alterations in hippocampal neurogenesis following traumatic brain injury in mice. Exp. Neurol. *202*, 189–199.

Romcy-Pereira, R.N., and Garcia-Cairasco, N. (2003). Hippocampal cell proliferation and epileptogenesis after audiogenic kindling are not accompanied by mossy fiber sprouting or Fluoro-Jade staining. Neuroscience *119*, 533–546.

Routbort, M.J., Bausch, S.B., and McNamara, J.O. (1999). Seizures, cell death, and mossy fiber sprouting in kainic acid-treated organotypic hippocampal cultures. Neuroscience *94*, 755–765.

Rubio-Garrido, P., Pérez-de-Manzo, F., Porrero, C., Galazo, M.J., and Clascá, F. (2009). Thalamic input to distal apical dendrites in neocortical layer 1 is massive and highly convergent. Cereb. Cortex N. Y. N 1991 *19*, 2380–2395.

Rudy, B., Fishell, G., Lee, S., and Hjerling-Leffler, J. (2011). Three Groups of Interneurons Account for Nearly 100% of Neocortical GABAergic Neurons. Dev. Neurobiol. *71*, 45–61.

Saatman, K.E., Duhaime, A.-C., Bullock, R., Maas, A.I.R., Valadka, A., Manley, G.T., and Workshop Scientific Team and Advisory Panel Members (2008). Classification of

traumatic brain injury for targeted therapies. J. Neurotrauma *25*, 719–738.

Salin, P., Tseng, G.F., Hoffman, S., Parada, I., and Prince, D.A. (1995). Axonal sprouting in layer V pyramidal neurons of chronically injured cerebral cortex. J. Neurosci. *15*, 8234–8245.

Sarkar, K., Keachie, K., Nguyen, U., Muizelaar, J.P., Zwienenberg-Lee, M., and Shahlaie, K. (2014). Computed tomography characteristics in pediatric versus adult traumatic brain injury. J. Neurosurg. Pediatr. *13*, 307–314.

Scheff, S.W., Price, D.A., Hicks, R.R., Baldwin, S.A., Robinson, S., and Brackney, C. (2005). Synaptogenesis in the Hippocampal CA1 Field following Traumatic Brain Injury. J. Neurotrauma *22*, 719–732.

Schmidt, A.T., Hanten, G.R., Li, X., Vasquez, A.C., Wilde, E.A., Chapman, S.B., and Levin, H.S. (2012). Decision making after pediatric traumatic brain injury: trajectory of recovery and relationship to age and gender. Int. J. Dev. Neurosci. Off. J. Int. Soc. Dev. Neurosci. *30*, 225–230.

Schwaller, B., Tetko, I.V., Tandon, P., Silveira, D.C., Vreugdenhil, M., Henzi, T., Potier, M.-C., Celio, M.R., and Villa, A.E.P. (2004). Parvalbumin deficiency affects network properties resulting in increased susceptibility to epileptic seizures. Mol. Cell. Neurosci. *25*, 650–663.

Shatz, C.J. (1990). Impulse activity and the patterning of connections during cns development. Neuron *5*, 745–756.

Shipp, S. (2007). Structure and function of the cerebral cortex. Curr. Biol. *17*, R443–R449.

Smith, C., Gentleman, S.M., Leclercq, P.D., Murray, L.S., Griffin, W.S.T., Graham, D.I., and Nicoll, J.A.R. (2013). The neuroinflammatory response in humans after traumatic brain injury. Neuropathol. Appl. Neurobiol. *39*, 654–666.

Smith, D.H., Soares, H.D., Pierce, J.S., Perlman, K.G., Saatman, K.M., Meaney, D.F., Dixon, C.E., and McIntosh, T.K. (1995). A Model of Parasagittal Controlled Cortical Impact in the Mouse: Cognitive and Histopathologic Effects. J. Neurotrauma *12*, 169–178.

Sohal, V.S., Zhang, F., Yizhar, O., and Deisseroth, K. (2009). Parvalbumin neurons and gamma rhythms enhance cortical circuit performance. Nature *459*, 698–702.

Somjen, G.G. (2004). Ions in the Brain : Normal Function, Seizures, and Stroke: Normal Function, Seizures, and Stroke (Oxford University Press).

Statler, K.D., Scheerlinck, P., Pouliot, W., Hamilton, M., White, H.S., and Dudek, F.E. (2009). A potential model of pediatric posttraumatic epilepsy. Epilepsy Res. *86*, 221–223.

Steriade, M., Amzica, F., Neckelmann, D., and Timofeev, I. (1998). Spike-wave complexes and fast components of cortically generated seizures. II. Extra- and intracellular patterns. J. Neurophysiol. *80*, 1456–1479.

Sun, Q.-Q., Huguenard, J.R., and Prince, D.A. (2006). Barrel cortex microcircuits: thalamocortical feedforward inhibition in spiny stellate cells is mediated by a small number of fast-spiking interneurons. J. Neurosci. Off. J. Soc. Neurosci. *26*, 1219–1230.

Tanaka, Y.H., Tanaka, Y., Fujiyama, F., Furuta, T., Yanagawa, Y., and Kaneko, T. (2011). Local connections of layer 5 GABAergic interneurons to corticospinal neurons. Front. Neural Circuits *5*, 12.

Tasker, J.G., and Dudek, F.E. (1991). Electrophysiology of GABA-mediated synaptic transmission and possible roles in epilepsy. Neurochem. Res. *16*, 251–262.

Telfeian, A.E., and Connors, B.W. (1998). Layer-specific pathways for the horizontal propagation of epileptiform discharges in neocortex. Epilepsia *39*, 700–708.

Temkin, O. (1994). The Falling Sickness: A History of Epilepsy from the Greeks to the Beginnings of Modern Neurology (JHU Press).

Thompson, H.J., Lifshitz, J., Marklund, N., Grady, M.S., Graham, D.I., Hovda, D.A., and McIntosh, T.K. (2005). Lateral fluid percussion brain injury: a 15-year review and evaluation. J. Neurotrauma *22*, 42–75.

Thurman, D.J., Beghi, E., Begley, C.E., Berg, A.T., Buchhalter, J.R., Ding, D., Hesdorffer, D.C., Hauser, W.A., Kazis, L., Kobau, R., et al. (2011). Standards for epidemiologic studies and surveillance of epilepsy. Epilepsia *52 Suppl 7*, 2–26.

Timofeev, I., and Steriade, M. (2004). Neocortical seizures: initiation, development and cessation. Neuroscience *123*, 299–336.

Traub, R.D., and Wong, R.K. (1982). Cellular mechanism of neuronal synchronization in epilepsy. Science *216*, 745–747.

Traub, R.D., Bibbig, A., LeBeau, F.E.N., Buhl, E.H., and Whittington, M.A. (2004). Cellular mechanisms of neuronal population oscillations in the hippocampus in vitro. Annu. Rev. Neurosci. *27*, 247–278.

Tremblay, S., de Beaumont, L., Lassonde, M., and Théoret, H. (2011). Evidence for the specificity of intracortical inhibitory dysfunction in asymptomatic concussed athletes. J. Neurotrauma *28*, 493–502.

Ueno, M., Hayano, Y., Nakagawa, H., and Yamashita, T. (2012). Intraspinal rewiring of the corticospinal tract requires target-derived brain-derived neurotrophic factor and compensates lost function after brain injury. Brain J. Neurol. *135*, 1253–1267.

Uhlhaas, P.J., and Singer, W. (2010). Abnormal neural oscillations and synchrony in

schizophrenia. Nat. Rev. Neurosci. *11*, 100–113.

van den Pol, A.N., Obrietan, K., and Chen, G. (1996). Excitatory actions of GABA after neuronal trauma. J. Neurosci. Off. J. Soc. Neurosci. *16*, 4283–4292.

Wang, Y., Kakizaki, T., Sakagami, H., Saito, K., Ebihara, S., Kato, M., Hirabayashi, M., Saito, Y., Furuya, N., and Yanagawa, Y. (2009). Fluorescent labeling of both GABAergic and glycinergic neurons in vesicular GABA transporter (VGAT)–Venus transgenic mouse. Neuroscience *164*, 1031–1043.

Werner, C., and Engelhard, K. (2007). Pathophysiology of traumatic brain injury. Br. J. Anaesth. *99*, 4–9.

Wilde, E.A., Merkley, T.L., Bigler, E.D., Max, J.E., Schmidt, A.T., Ayoub, K.W., McCauley, S.R., Hunter, J.V., Hanten, G., Li, X., et al. (2012). Longitudinal changes in cortical thickness in children after traumatic brain injury and their relation to behavioral regulation and emotional control. Int. J. Dev. Neurosci. Off. J. Int. Soc. Dev. Neurosci. *30*, 267–276.

Willmore, L.J. (1990). Post-traumatic epilepsy: cellular mechanisms and implications for treatment. Epilepsia *31 Suppl 3*, S67–S73.

Wilson, N.R., Runyan, C.A., Wang, F.L., and Sur, M. (2012). Division and subtraction by distinct cortical inhibitory networks in vivo. Nature *488*, 343–348.

Wise, S.P. (1975). The laminar organization of certain afferent and efferent fiber systems in the rat somatosensory cortex. Brain Res. *90*, 139–142.

Wöhr, M., Orduz, D., Gregory, P., Moreno, H., Khan, U., Vörckel, K.J., Wolfer, D.P., Welzl, H., Gall, D., Schiffmann, S.N., et al. (2015). Lack of parvalbumin in mice leads to behavioral deficits relevant to all human autism core symptoms and related neural morphofunctional abnormalities. Transl. Psychiatry *5*, e525.

Wojcik, S.M., Katsurabayashi, S., Guillemin, I., Friauf, E., Rosenmund, C., Brose, N., and Rhee, J.-S. (2006). A shared vesicular carrier allows synaptic corelease of GABA and glycine. Neuron *50*, 575–587.

Xu, X., Roby, K.D., and Callaway, E.M. (2010). Immunochemical characterization of inhibitory mouse cortical neurons: Three chemically distinct classes of inhibitory cells. J. Comp. Neurol. *518*, 389–404.

Yang, L., Benardo, L.S., Valsamis, H., and Ling, D.S.F. (2007). Acute injury to superficial cortex leads to a decrease in synaptic inhibition and increase in excitation in neocortical layer V pyramidal cells. J. Neurophysiol. *97*, 178–187.

Yang, L., Afroz, S., Michelson, H.B., Goodman, J.H., Valsamis, H.A., and Ling, D.S.F. (2010). Spontaneous epileptiform activity in rat neocortex after controlled cortical impact

injury. J. Neurotrauma *27*, 1541–1548.

Yoshimura, Y., and Callaway, E.M. (2005). Fine-scale specificity of cortical networks depends on inhibitory cell type and connectivity. Nat. Neurosci. *8*, 1552–1559.

Zhang, Z. (2004). Maturation of Layer V Pyramidal Neurons in the Rat Prefrontal Cortex: Intrinsic Properties and Synaptic Function. J. Neurophysiol. *91*, 1171–1182.

Zhang, Q.-G., Laird, M.D., Han, D., Nguyen, K., Scott, E., Dong, Y., Dhandapani, K.M., and Brann, D.W. (2012). Critical Role of NADPH Oxidase in Neuronal Oxidative Damage and Microglia Activation following Traumatic Brain Injury. PLoS ONE *7*, e34504.

Ziyatdinova, S., Gurevicius, K., Kutchiashvili, N., Bolkvadze, T., Nissinen, J., Tanila, H., and Pitkänen, A. (2011). Spontaneous epileptiform discharges in a mouse model of Alzheimer's disease are suppressed by antiepileptic drugs that block sodium channels. Epilepsy Res. *94*, 75–85.

van Zundert, B., Izaurieta, P., Fritz, E., and Alvarez, F.J. (2012). Early pathogenesis in the adult-onset neurodegenerative disease amyotrophic lateral sclerosis. J. Cell. Biochem. *113*, 3301–3312.

(2005). Atlas epilepsy care in the world. (Geneva: Programme for Neurological Diseases and Neuroscience, Dept. of Mental Health and Substance Abuse, World Health Organization).

(2012). Jasper's Basic Mechanisms of the Epilepsies (Bethesda (MD): National Center for Biotechnology Information (US)).

CHAPTER 6

DISCUSSION

Recent work in pediatric TBI has found that children are not as resilient as what was once thought. Several studies have shown that younger children have a worse long-term outcome after TBI than a teenager or adult (Anderson and Moore, 1995; Anderson et al., 2005c; Luerssen et al., 1988a; Schmidt et al., 2012). This work set out to determine how the unique physiology of a child's brain contributes to the pathophysiology of TBI. Using a clinically relevant model of severe TBI, controlled cortical impact (CCI), we examined anatomical and functional changes in the peri-injury area and the contralateral motor and somatosensory cortex. Disruption to the balance of the number of excitatory and inhibitory neurons within the cortex has been implicated in the pathogenesis of numerous neurological disorders including epilepsy (Jin et al., 2006, 2011). The methods and findings detailed in this dissertation provide novel insight into the effect of CCI on cortical neurons such as pyramidal and parvalbumin fast-spiking cell types.

Our initial findings discovered that 14 days post-injury was an optimal time point at which injury induced seizures took place. This allowed us to investigate how secondary insults begin to take place in pediatrics. Using EEG, we found that injury induced seizures ceased by seven days after injury and unprovoked recurrent seizures began. Further investigation into primary excitatory neurons, pyramidal cells, was performed using whole-cell patch clamp. Our results indicate that pyramidal neurons were not changed intrinsically or synaptically. However, excitatory and inhibitory synaptic bursting was seen.

No changes were found in the excitatory population in the peri-injury region. To

characterize interneurons in the peri-injury region, similarly to our investigation of the pyramidal neurons, we used a transgenic mouse (Vgat:cre Ai9). We used whole-cell patch clamp and fluorescent immunohistochemistry (IHC) to functionally and anatomically characterize how CCI alters a juvenile animal cortex. We found that the peri-injury region retained interneurons, but experienced a loss of parvalbumin expression. Functionally, inhibition onto fast-spiking (FS) neurons was reduced and excitation was increased. This result provided insight that can begin to explain why we recorded electrographic seizures in injured animals, but saw no severe change to pyramidal neurons.

To understand if this phenomenon is seen in other cortical regions, we focused on the contralateral motor cortex, which has been shown to be differentially affected (Biernaskie et al., 2005; Frost et al., 2003; Nudo, 2006). Using the same techniques and transgenic mouse to characterize the "uninjured" contralateral motor cortex we saw similar results. However, we found that the contralateral motor cortex experienced a loss of interneurons and showed functional changes similar to what was found in the peri-injury region. When this data was compared to results, in the somatosensory region, contralateral to injury, it was clear that motor cortex was uniquely affected. This indicates that a focal injury, such as CCI, can affect other "uninjured" regions of the brain.

Finally, we performed repetitive mild TBI (rmTBI) on pediatric animals and found similar results in pyramidal neurons that we saw with the CCI model. However, we found that rmTBI produces cortical thinning and ventricular myelopathy, which was not seen in the CCI. Using IHC and a pan-neuronal marker, NeuN, we found that there were a reduced number of neurons in the cortex. Functional characterization of pyramidal

neurons after rmTBI resulted in no change of intrinsic or synaptic properties. These findings suggest that even using other models of TBI, pediatrics still show a unique outcome when compared to adults.

The work of this dissertation is the first to report that the pediatric cortex undergoes unique remodeling not seen in an adult injury. Further investigation shows that a juvenile cortical inhibitory network is preferentially affected in multiple regions after injury. Understanding cellular functions in the cortex after brain injury may be important to elucidating altered network activity that can bring about neurological deficits commonly seen after TBI in pediatric patients.

Development of Post-traumatic Epilepsy and Pyramidal neurons

Using whole-cell patch clamp and EEG techniques in juvenile rats this study demonstrates: (a) all rats within fourteen days post CCI injury show epileptiform activity by EEG, (b) there were no changes to synaptic or intrinsic properties in layer V pyramidal neurons, (c) excitatory and inhibitory synaptic bursting is greater in CCI animals compared to control, and (d) there is greater excitatory synaptic bursting than inhibitory bursting, suggesting that a hyperexcitable network develops post injury. Previous studies have shown an increase in postsynaptic currents after injury, but not while examining for changes in cell properties (Yang et al., 2010). Other CCI studies that have shown increased spontaneous events have not presented findings of synaptic bursts, either inhibitory or excitatory.

Neuronal firing usually occurs in a single action potential in isolation in response to discrete input of postsynaptic potentials that combine and cause the membrane potential to depolarize. Neurons sometimes will have periods of rapid action potentials

as opposed to the single firing event. Neuronal bursting is often seen as necessary to increase the reliability of neuronal communication (Izhikevich et al., 2003). Homeostatic synaptic plasticity has been implicated in an increase of network excitability after traumatic brain injury resulting in network burst activity (Houweling et al., 2005). It has also been shown that bursting activity resulted from the upregulation of excitatory synapses between pyramidal neurons (Houweling et al., 2005).

Electrical brain activity is normally non-synchronous and when an epileptic seizure occurs, several neurons begin firing unusually, excessively, and in synchrony. When an excitatory neuron fires, the resistance to continue to fire again or to continue firing is due to the effect of inhibitory neurons or the intrinsic properties of the neuron itself (Somjen, 2004). However, during epilepsy the resistance of the excitatory neuron to fire is decreased due to changes in ion channels or irregular activity of inhibitory neurons (Somjen, 2004). When several neurons begin to burst in synchrony, a functional heterogeneity of cortical regions for seizure generation can lead to seizures (Timofeev and Steriade, 2004). Previous studies have examined mechanisms responsible for post-traumatic epileptogenesis in rodent models using techniques such as lateral fluid percussion (Thompson et al., 2005), CCI in mice (Cantu et al., 2014; Hunt et al., 2009, 2011), and cortical undercutting (Jacobs et al., 2000; Yang et al., 2010). To our knowledge, only one study has found bursting, but this was done during extracellular recordings after CCI injury (Yang et al., 2010). Our findings provide evidence that excitatory intracellular bursting is more apparent in neurons in cases of TBI. Furthermore, we show the increase in bursting in conjunction with intrinsic and synaptic properties unchanged after TBI. This suggests that pyramidal neurons of layer V are

experiencing a change in input from other regions of the brain. The surprisingly similar bursting patterns suggest the manner in which neurons are transmitting information is different following severe cortical injuries.

Epilepsy research has shown that epileptiform activity can result from a shift of balance of excitation and inhibition toward excitation (Dichter and Ayala, 1987; Galarreta and Hestrin, 1998; Nelson and Turrigiano, 1998; Tasker and Dudek, 1991). This has been shown by studies that have elicited experimental seizures by blocking inhibition (Matsumoto and Marsan, 1964; Prince, 1978; Steriade et al., 1998). Other favorable conditions to generate seizures would be to increase inhibition and decrease excitation (Timofeev and Steriade, 2004). How this balance is altered during TBI to contribute to the development of PTE is still unclear. Our findings show that there is an increase in excitation after TBI, which is consistent with other TBI studies.

There are many possibilities that play a role in TBI pathology leading to PTE including increased inflammation (Johnson et al., 2013; Smith et al., 2013), white matter degeneration (Johnson et al., 2013), oxidative and nitrosative damage (Abdul-Muneer et al., 2013), and mitochondrial changes (Balan et al., 2013; Cheng et al., 2012). Also, further work needs to be conducted to elucidate what region of the brain is driving this rapid enhancement of excitability in layer V neurons. Axon sprouting and enhanced excitatory synaptic connectivity onto layer V pyramidal neurons has been shown in chronic models of posttraumatic epileptogenesis (Jin et al., 2006; Salin et al., 1995). By analyzing biocytin filled neurons in the affected regions could provide visual data to understand axonal and dendritic projections after injury.

In conclusion, improvements in treatment and diagnosis of PTE are desperately

needed. All children admitted to the hospital for TBI are given anticonvulsants. Providing anticonvulsants to a developing brain, when there may be no risk of PTE, could have undesirable developmental and cognitive ramifications. Here we have shown that, on a cellular level, those that suffer an injury are experiencing a bursting phenomenon. This bursting phenomenon could lead to the area of the brain that may play a role in driving a hyperexcitable cortex. By studying CCI 14 days post injury in juvenile rats, we are observing the period in which PTE is developing. PTE could develop because of the modification of the cortical network during the brain's healing process.

Selective Inhibitory Functional changes in Peri-Injury Region

Using a clinically relevant model of severe TBI (sTBI), controlled cortical impact (CCI), we examined for anatomical and functional changes to cortical inhibition in juvenile mice that endogenously expressed a fluorescent marker (tdTomato) in all interneurons (Vgat:cre Ai9). At 14 days following CCI, we measured changes in immunoreactivity of calcium-binding proteins that delineate the two largest cortical interneuron populations, parvalbumin (PV) and somatostatin (SST). We found that PV expression was significantly down while SST was unaffected. Using whole-cell patch clamp we were able to characterize fast-spiking neurons intrinsically and synaptically after CCI. Intrinsic properties were not changed, but synaptic excitation was increased and synaptic inhibition was decreased onto a fast-spiking neuron. Previous studies have shown increased excitation and decreased inhibition onto pyramidal neurons (Cantu et al., 2014). However, this work is the first to examine the cortical interneuron network in a pediatric model after CCI.

Parvalbumin interneurons in relation to neurological diseases have been an

increasing topic of interest (Lewis et al., 2012; Ma and Prince, 2012; Schwaller et al., 2004; Sohal et al., 2009). Parvalbumin interneurons have been implicated in diseases such as schizophrenia (Lewis et al., 2012; Sohal et al., 2009) and epilepsy (Jin et al., 2014; Ma and Prince, 2012; Schwaller et al., 2004). Fast-spiking parvalbumin positive basket inhibitory neurons are increasingly implicated in both critical period and adult plasticity (Hensch, 2005; Letzkus et al., 2011). As they have been shown to act in response to network activity to modulate cortical response gain (Atallah et al., 2012; Wilson et al., 2012). Modulation in gain control has been shown in in the juvenile cortex by sensory input reduction which leads to decreased excitatory firing rates (Kuhlman et al., 2013). This phenotype has been shown to increase seizure threshold (Schwaller et al., 2004), alter short-term synaptic plasticity (Caillard et al., 2000), and cause deficits relevant to human autism core symptoms (Wöhr et al., 2015).

We found that the overall density of cortical interneurons was not reduced PID 14 after CCI in juvenile mice. However, CCI induced selective loss of PV expression in the cortex, with the greatest loss near the site of injury. Despite the loss of PV expression, fast-spiking interneurons did not have altered intrinsic properties. Changes to a neurons intrinsic excitability affects its probability to fire an action potential which will affect the output that has been implicated in a variety of other neurological disorders (Prinz et al., 2013; van Zundert et al., 2012).

Synaptically, inhibition onto fast-spiking interneurons received less inhibition after CCI and an increased rise and decay time of spontaneous synaptic events. This increase in kinetic rise and decay could be a compensatory mechanism to increase the temporal integration window in response to the decrease in spontaneous inhibitory

events. Excitatory strength onto fast-spiking interneurons was dramatically increased after CCI, measured by sEPSC amplitude and charge. We didn't see a greater frequency of sEPSC events indicating that presynaptic pyramidal (PYR) neurons did not have a greater probability of release and thus are not more excitatory. This is similar to what is seen in adult mice after CCI (Cantu et al., 2014).

This suggests that PV neurons are more sensitive after an injury such as CCI. We hypothesize that the GABAergic network, particularly PV positive neurons, is more susceptible to an environmental injury, especially immature PV interneurons, due to a variety of reasons. Including a lack of perineuronal nets that protect fast-spiking interneurons (Cabungcal et al., 2013a) and the effects of oxidative stress caused by NMDA disregulation in a developing cortex (Behrens and Sejnowski, 2009; Kinney et al., 2006). Our results, in conjunction with what has been shown looking at other neurological disorders, provide insight into the importance of PV immunoreactivity to GABAergic cell function. Critical experiments that lead to the molecular mechanism that might be responsible for the loss of PV immunoreactivity is an important next step in our work and are currently underway.

Contralateral Motor Cortex Experiences Preferential Inhibitory Dysfunction

We combined whole-cell patch clamp electrophysiology with fluorescent immunohistochemistry in fluorescently labeled inhibitory interneurons to ask how contralateral motor cortex inhibition is altered after controlled cortical impact. Very little work has been done looking at contralateral effects of CCI in the pediatric brain. However, the results of excitatory and inhibitory synaptic transmission agrees with adult CCI investigating pyramidal synaptic function in the peri-injury region (Cantu et al.,

2014; Hunt et al., 2009). We found that 14 days after injury the total interneuron population and PV expression cell density was decreased. When fast-spiking interneurons were examined for electrophysiological properties, they showed a decrease of presynaptic inhibition, increased charge, and longer decay times. Excitation onto fast-spiking interneurons showed an increase in sEPSCs with decreased decay times. Despite the synaptic changes, the fast-spiking neurons showed no change to their intrinsic properties, suggesting that CCI effectively altered the E/I balance of the contralateral motor cortex. These observations argue that TBI elicits a process leading to anatomical and neurophysiological remodeling of the morphologically intact, uninjured contralateral motor cortex.

We found that the overall density of cortical interneurons was reduced at PID14 after CCI in the contralateral motor cortex of juvenile mice. CCI induced a selective loss of PV expression in the uninjured motor cortex. Using an endogenous fluorescent label, we were able to discriminate if there was actual cell loss or a change in immunoreactivity. The fast-spiking interneurons that were present in the motor cortex after injury showed no change in intrinsic properties.

Parvalbumin positive cortical interneurons are predominantly of a fast-spiking (FS) phenotype (Hu et al., 2014). Similar to most other cortical cell-types, the firing properties of FS interneurons are developmentally regulated and shown to be well established by time of our CCI (i.e. P22) (Doischer et al., 2008; Itami et al., 2007; Okaty et al., 2009). Mature fast-spiking cells are characterized by low input resistance, narrow action potentials, and the production of high-frequency spike trains with little to no spike-frequency adaptation. The loss of interneurons and PV expression in this study prompted

us to first examine changes in the intrinsic properties of FS neurons of the contralateral motor cortex. Intrinsically, the FS neurons did not show a change to resting membrane potential, input resistance, or firing frequency. Synaptically, fast-spiking interneurons received less inhibition and an increase in sIPSC decay time after CCI. This increase in decay time could potentially be the result of a compensatory response to increase the temporal integration window to maintain cortical health. The number of spontaneous excitatory events was increased in the uninjured motor cortex and was accompanied by a decreased decay time. The combination of the synaptic excitatory and inhibitory response might indicate that the inhibitory network of the contralateral motor cortex is working in overdrive in response to axonal glutamatergic over activation caused by the injury.

This evidence suggests that PV neurons are sensitive to cellular and molecular processes induced by CCI. The function of PV neurons, in the cortical network is important because previous work in PV fast-spiking inhibitory motor neurons shows that they can exhibit activity-dependent modifications of firing properties (Miller et al., 2011). The results of this work can be explained by inhibitory overexcitation in response to glutamatergic activation from cross hemisphere axonal projections. Regardless, these results provide new insight into the effect a unilateral severe TBI can have on uninjured cortical regions. However, it is important to understand that the injury is very complex and it is possiblty not a single mechanism, but likely a multitude of changes occurring in the brain simultaneously giving rising to the phenomenon seen here.

Numerous compensatory mechanisms have been shown after TBI, including regenerative efforts. Regeneration-associated molecules such as proline-rich protein 1A, growth-associated protein 43, synapsin 1 and brain-derived growth factor (BDNF), are

increased following TBI in addition to growth-associated genes (Emery et al., 2000; Hulsebosch et al., 1998; Kobori et al., 2002; Li et al., 2004; Marklund et al., 2007). Increased sprouting of uninjured corticospinal tract originating from the contralateral to the injury and of contralateral hippocampal mossy fibers has also been seen after injury (Hånell et al., 2010; Lenzlinger et al., 2005; Scheff et al., 2005). Corticospinal tract rewiring within the denervated cervical spinal cord has been shown to compensate for lost motor function following a focal TBI in mice (Ueno et al., 2012). Similar results have been seen in ischemia studies. For example, clinical studies of stroke patients showed that larger infarcts caused greater activation of the intact contralateral hemisphere (Cramer et al., 2006). Similar results in rodent ischemia models have shown dendritic growth and axonal sprouting within the contralateral motor cortex following unilateral ischemia (Biernaskie and Corbett, 2001; Biernaskie et al., 2005; Chen et al., 2002). These factors may contribute to the altered motor cortex anatomy and function seen in our data. However, further investigation into molecular mechanisms responsible for the alteration in the motor cortex is needed.

Understanding a Complex Network Change Pediatric TBI

The experiments here provide novel insight into the unique nature regarding how the pediatric cortex responds to injury. However, understanding these changes on a network level is complex, as we did not see any changes in the intrinsic properties. Additionally, we did not see different excitatory and inhibitory synaptic transmission onto layer V pyramidal neurons, except for the bursting phenotype described. However, in the same region, we saw that fast-spiking interneurons received less inhibition and

more excitation. This result would make a fast-spiking interneuron release more GABA onto its post-synaptic partner, which is known to be the somatic region of a pyramidal neuron. However, we did not see increased inhibitory post-synaptic currents when recording from pyramidal neurons.

The complexity arises when understanding the inhibitory network. We did not record from somatostatin neurons, which are known to synapse onto the proximal dendrites of pyramidal neurons. Somatostatin neurons could be compensating for their activity however these additional experiments need to be performed. To understand the rise in inhibition onto fast-spiking neurons, multiple interneurons could be the culprit. Vasoactive intestinal polypeptide (VIP) neurons have been shown to disinhibit fast-spiking neurons (Dávid et al., 2007; Pi et al., 2013). However, fast-spiking neurons are known to receive input from other fast-spiking neurons (Hioki et al., 2013). These examples are only a fraction of the potential network complexities that might be the mechanism causing our results.

To further characterize the network phenomenon seen in this work, circuit mapping of fast-spiking neurons can further explain their effect on the network. Specific neuron mapping using optogenetic mice (i.e. Somatostain-cre ChR2, VIP-cre ChR2, etc.) can reveal how certain neuronal subtypes are acting on fast-spiking neurons. On a smaller scale, synaptically connected paired recordings of a fast-spiking neuron to a fast-spiking neuron, a VIP neuron to a fast-spiking neuron, etc., could explain why a juvenile mouse inhibitory network is different from an adult. However, the complexity could be greater and require patch-clamping synaptically connected VIP, PV, and pyramidal neurons. It has been suggested that VIP neurons control the activity of pyramidal cells within a

vertical column by multi-laminar disinhibition through somatic inputs to PV neurons (Hioki et al., 2013). Unfortunately, the complexity might not end there, as current research is still working to uncover how exactly the cortex is connected and how that connectivity functions in a network.

In summary, this dissertation provides evidence that pediatric sTBI is unique from adult sTBI. In contrast to adults, this select loss of PV appears specific to juvenile animals and suggests interneuron sensitivity is age and developmentally regulated. Disruption to PV-FS interneuron functioning may play an important role in the recovery and outcomes of patients following TBI. At present, elucidating if PV expression loss is an adaptive or maladaptive response to injury is of critical importance to understanding its role in the pathophysiology of TBI and developing new targeted therapeutic approaches.

REFERENCES

Abdul-Muneer, P.M., Schuetz, H., Wang, F., Skotak, M., Jones, J., Gorantla, S., Zimmerman, M.C., Chandra, N., and Haorah, J. (2013). Induction of oxidative and nitrosative damage leads to cerebrovascular inflammation in an animal model of mild traumatic brain injury induced by primary blast. Free Radic. Biol. Med. *60*, 282–291.

Adelson, P.D., Fellows-Mayle, W., Kochanek, P.M., and Dixon, C.E. (2013). Morris water maze function and histologic characterization of two age-at-injury experimental models of controlled cortical impact in the immature rat. Childs Nerv. Syst. ChNS Off. J. Int. Soc. Pediatr. Neurosurg. *29*, 43–53.

Agrawal, A., Timothy, J., Pandit, L., and Manju, M. (2006). Post-traumatic epilepsy: an overview. Clin. Neurol. Neurosurg. *108*, 433–439.

Anderson, V., and Moore, C. (1995). Age at injury as a predictor of outcome following pediatric head injury: A longitudinal perspective. Child Neuropsychol. *1*, 187–202.

Annegers, J.F., Hauser, W.A., Coan, S.P., and Rocca, W.A. (1998). A population-based study of seizures after traumatic brain injuries. N. Engl. J. Med. *338*, 20–24.

Atallah, B.V., Bruns, W., Carandini, M., and Scanziani, M. (2012). Parvalbumin-Expressing Interneurons Linearly Transform Cortical Responses to Visual Stimuli. Neuron *73*, 159.

Bacci, A., and Huguenard, J.R. (2006). Enhancement of spike-timing precision by autaptic transmission in neocortical inhibitory interneurons. Neuron *49*, 119–130.

Balan, I.S., Saladino, A.J., Aarabi, B., Castellani, R.J., Wade, C., Stein, D.M., Eisenberg, H.M., Chen, H.H., and Fiskum, G. (2013). Cellular alterations in human traumatic brain injury: changes in mitochondrial morphology reflect regional levels of injury severity. J. Neurotrauma *30*, 367–381.

Barberis, A., Mozrzymas, J.W., Ortinski, P.I., and Vicini, S. (2007). Desensitization and binding properties determine distinct alpha1beta2gamma2 and alpha3beta2gamma2 GABA(A) receptor-channel kinetic behavior. Eur. J. Neurosci. *25*, 2726–2740.

Behrens, M.M., and Sejnowski, T.J. (2009). Does schizophrenia arise from oxidative dysregulation of parvalbumin-interneurons in the developing cortex? Neuropharmacology *57*, 193–200.

Ben-Ari, Y., Gaiarsa, J.-L., Tyzio, R., and Khazipov, R. (2007). GABA: a pioneer transmitter that excites immature neurons and generates primitive oscillations. Physiol. Rev. *87*, 1215–1284.

Biernaskie, J., and Corbett, D. (2001). Enriched rehabilitative training promotes improved forelimb motor function and enhanced dendritic growth after focal ischemic

injury. J. Neurosci. Off. J. Soc. Neurosci. *21*, 5272–5280.

Biernaskie, J., Szymanska, A., Windle, V., and Corbett, D. (2005). Bi-hemispheric contribution to functional motor recovery of the affected forelimb following focal ischemic brain injury in rats. Eur. J. Neurosci. *21*, 989–999.

Bolkvadze, T., and Pitkänen, A. (2012). Development of post-traumatic epilepsy after controlled cortical impact and lateral fluid-percussion-induced brain injury in the mouse. J. Neurotrauma *29*, 789–812.

Cabungcal, J.-H., Steullet, P., Morishita, H., Kraftsik, R., Cuenod, M., Hensch, T.K., and Do, K.Q. (2013). Perineuronal nets protect fast-spiking interneurons against oxidative stress. Proc. Natl. Acad. Sci. U. S. A. *110*, 9130–9135.

Caillard, O., Moreno, H., Schwaller, B., Llano, I., Celio, M.R., and Marty, A. (2000). Role of the calcium-binding protein parvalbumin in short-term synaptic plasticity. Proc. Natl. Acad. Sci. U. S. A. *97*, 13372–13377.

Camfield, P.R., and Camfield, C.S. (2014). What Happens to Children With Epilepsy When They Become Adults? Some Facts and Opinions. Pediatr. Neurol.

Cantu, D., Walker, K., Andresen, L., Taylor-Weiner, A., Hampton, D., Tesco, G., and Dulla, C.G. (2014). Traumatic Brain Injury Increases Cortical Glutamate Network Activity by Compromising GABAergic Control. Cereb. Cortex N. Y. N 1991.

Casella, E.M., Thomas, T.C., Vanino, D.L., Fellows-Mayle, W., Lifshitz, J., Card, J.P., and Adelson, P.D. (2014). Traumatic brain injury alters long-term hippocampal neuron morphology in juvenile, but not immature, rats. Childs Nerv. Syst. *30*, 1333–1342.

Cauli, B., Audinat, E., Lambolez, B., Angulo, M.C., Ropert, N., Tsuzuki, K., Hestrin, S., and Rossier, J. (1997). Molecular and physiological diversity of cortical nonpyramidal cells. J. Neurosci. Off. J. Soc. Neurosci. *17*, 3894–3906.

Chen, P., Goldberg, D.E., Kolb, B., Lanser, M., and Benowitz, L.I. (2002). Inosine induces axonal rewiring and improves behavioral outcome after stroke. Proc. Natl. Acad. Sci. U. S. A. *99*, 9031–9036.

Cheng, G., Kong, R., Zhang, L., and Zhang, J. (2012). Mitochondria in traumatic brain injury and mitochondrial-targeted multipotential therapeutic strategies. Br. J. Pharmacol. *167*, 699–719.

Chow, A., Erisir, A., Farb, C., Nadal, M.S., Ozaita, A., Lau, D., Welker, E., and Rudy, B. (1999). K(+) channel expression distinguishes subpopulations of parvalbumin- and somatostatin-containing neocortical interneurons. J. Neurosci. Off. J. Soc. Neurosci. *19*, 9332–9345.

Connors, B.W., and Gutnick, M.J. (1990). Intrinsic firing patterns of diverse neocortical

neurons. Trends Neurosci. *13*, 99–104.

Corkin, S., Sullivan, E.V., and Carr, F.A. (1984). Prognostic factors for life expectancy after penetrating head injury. Arch. Neurol. *41*, 975–977.

Cowan, W.M., Fawcett, J.W., O'Leary, D.D., and Stanfield, B.B. (1984). Regressive events in neurogenesis. Science *225*, 1258–1265.

Cramer, S.C., Shah, R., Juranek, J., Crafton, K.R., and Le, V. (2006). Activity in the peri-infarct rim in relation to recovery from stroke. Stroke J. Cereb. Circ. *37*, 111–115.

Cruikshank, S.J., Lewis, T.J., and Connors, B.W. (2007). Synaptic basis for intense thalamocortical activation of feedforward inhibitory cells in neocortex. Nat. Neurosci. *10*, 462–468.

Dichter, M.A., and Ayala, G.F. (1987). Cellular mechanisms of epilepsy: a status report. Science *237*, 157–164.

Donovan, V., Kim, C., Anugerah, A.K., Coats, J.S., Oyoyo, U., Pardo, A.C., and Obenaus, A. (2014). Repeated mild traumatic brain injury results in long-term white-matter disruption. J. Cereb. Blood Flow Metab. Off. J. Int. Soc. Cereb. Blood Flow Metab. *34*, 715–723.

Douglas, R.J., and Martin, K.A.C. (2007). Mapping the Matrix: The Ways of Neocortex. Neuron *56*, 226–238.

Eadie, M.J. (2012). Shortcomings in the current treatment of epilepsy. Expert Rev. Neurother. *12*, 1419–1427.

Elaine Wyllie MD, A.G., and Deepak K. Lachhwani (2005). The Treatment of Epilepsy: Principles and Practice (Philadelphia: Lippincott Williams & Wilkins).

Emery, D.L., Raghupathi, R., Saatman, K.E., Fischer, I., Grady, M.S., and McIntosh, T.K. (2000). Bilateral growth-related protein expression suggests a transient increase in regenerative potential following brain trauma. J. Comp. Neurol. *424*, 521–531.

Ewing-Cobbs, L., Miner, M.E., Fletcher, J.M., and Levin, H.S. (1989). Intellectual, Motor, and Language Sequelae Following Closed Head Injury in Infants and Preschoolers. J. Pediatr. Psychol. *14*, 531–547.

Ewing-Cobbs, L., Prasad, M., Kramer, L., and Landry, S. (1999). Inflicted traumatic brain injury: relationship of developmental outcome to severity of injury. Pediatr. Neurosurg. *31*, 251–258.

Ewing-Cobbs, L., Barnes, M.A., and Fletcher, J.M. (2003). Early brain injury in children: development and reorganization of cognitive function. Dev. Neuropsychol. *24*, 669–704.

Ewing-Cobbs, L., Prasad, M.R., Kramer, L., Cox, C.S., Baumgartner, J., Fletcher, S.,

Mendez, D., Barnes, M., Zhang, X., and Swank, P. (2006). Late intellectual and academic outcomes following traumatic brain injury sustained during early childhood. J. Neurosurg. *105*, 287–296.

Fisher, R.S., van Emde Boas, W., Blume, W., Elger, C., Genton, P., Lee, P., and Engel, J., Jr (2005). Epileptic seizures and epilepsy: definitions proposed by the International League Against Epilepsy (ILAE) and the International Bureau for Epilepsy (IBE). Epilepsia *46*, 470–472.

Frey, L.C. (2003). Epidemiology of posttraumatic epilepsy: a critical review. Epilepsia *44 Suppl 10*, 11–17.

Frost, S.B., Barbay, S., Friel, K.M., Plautz, E.J., and Nudo, R.J. (2003). Reorganization of Remote Cortical Regions After Ischemic Brain Injury: A Potential Substrate for Stroke Recovery. J. Neurophysiol. *89*, 3205–3214.

Gabernet, L., Jadhav, S.P., Feldman, D.E., Carandini, M., and Scanziani, M. (2005). Somatosensory integration controlled by dynamic thalamocortical feed-forward inhibition. Neuron *48*, 315–327.

Galarreta, M., and Hestrin, S. (1998). Frequency-dependent synaptic depression and the balance of excitation and inhibition in the neocortex. Nat. Neurosci. *1*, 587–594.

Garga, N., and Lowenstein, D.H. (2006). Posttraumatic epilepsy: a major problem in desperate need of major advances. Epilepsy Curr. Am. Epilepsy Soc. *6*, 1–5.

Ghajar, J. (2000). Traumatic brain injury. Lancet *356*, 923–929.

Gibson, J.R., Beierlein, M., and Connors, B.W. (1999). Two networks of electrically coupled inhibitory neurons in neocortex. Nature *402*, 75–79.

Gill, R., Chang, P.K.-Y., Prenosil, G.A., Deane, E.C., and McKinney, R.A. (2013). Blocking brain-derived neurotrophic factor inhibits injury-induced hyperexcitability of hippocampal CA3 neurons. Eur. J. Neurosci. *38*, 3554–3566.

Goldberg, E.M., Clark, B.D., Zagha, E., Nahmani, M., Erisir, A., and Rudy, B. (2008). K+ channels at the axon initial segment dampen near-threshold excitability of neocortical fast-spiking GABAergic interneurons. Neuron *58*, 387–400.

Haider, B., and McCormick, D.A. (2009). Rapid neocortical dynamics: cellular and network mechanisms. Neuron *62*, 171–189.

Hånell, A., Clausen, F., Björk, M., Jansson, K., Philipson, O., Nilsson, L.N.G., Hillered, L., Weinreb, P.H., Lee, D., McIntosh, T.K., et al. (2010). Genetic deletion and pharmacological inhibition of Nogo-66 receptor impairs cognitive outcome after traumatic brain injury in mice. J. Neurotrauma *27*, 1297–1309.

Hasenstaub, A., Shu, Y., Haider, B., Kraushaar, U., Duque, A., and McCormick, D.A.

(2005). Inhibitory postsynaptic potentials carry synchronized frequency information in active cortical networks. Neuron *47*, 423–435.

Hensch, T.K. (2005). Critical period plasticity in local cortical circuits. Nat. Rev. Neurosci. *6*, 877–888.

Herman, S.T. (2002). Epilepsy after brain insult: targeting epileptogenesis. Neurology *59*, S21–S26.

Hioki, H., Okamoto, S., Konno, M., Kameda, H., Sohn, J., Kuramoto, E., Fujiyama, F., and Kaneko, T. (2013). Cell Type-Specific Inhibitory Inputs to Dendritic and Somatic Compartments of Parvalbumin-Expressing Neocortical Interneuron. J. Neurosci. *33*, 544–555.

Houweling, A.R., Bazhenov, M., Timofeev, I., Steriade, M., and Sejnowski, T.J. (2005). Homeostatic Synaptic Plasticity Can Explain Post-traumatic Epileptogenesis in Chronically Isolated Neocortex. Cereb. Cortex N. Y. N 1991 *15*, 834–845.

Hulsebosch, C.E., DeWitt, D.S., Jenkins, L.W., and Prough, D.S. (1998). Traumatic brain injury in rats results in increased expression of Gap-43 that correlates with behavioral recovery. Neurosci. Lett. *255*, 83–86.

Hunt, R.F., Scheff, S.W., and Smith, B.N. (2009). Posttraumatic epilepsy after controlled cortical impact injury in mice. Exp. Neurol. *215*, 243–252.

Hunt, R.F., Scheff, S.W., and Smith, B.N. (2011). Synaptic reorganization of inhibitory hilar interneuron circuitry after traumatic brain injury in mice. J. Neurosci. Off. J. Soc. Neurosci. *31*, 6880–6890.

Iudice, A., and Murri, L. (2000). Pharmacological prophylaxis of post-traumatic epilepsy. Drugs *59*, 1091–1099.

Izhikevich, E.M., Desai, N.S., Walcott, E.C., and Hoppensteadt, F.C. (2003). Bursts as a unit of neural information: selective communication via resonance. Trends Neurosci. *26*, 161–167.

Jacobs, K.M., Graber, K.D., Kharazia, V.N., Parada, I., and Prince, D.A. (2000). Postlesional epilepsy: the ultimate brain plasticity. Epilepsia *41 Suppl 6*, S153–S161.

Jenkins, L.W., Peters, G.W., Dixon, C.E., Zhang, X., Clark, R.S.B., Skinner, J.C., Marion, D.W., Adelson, P.D., and Kochanek, P.M. (2002). Conventional and functional proteomics using large format two-dimensional gel electrophoresis 24 hours after controlled cortical impact in postnatal day 17 rats. J. Neurotrauma *19*, 715–740.

Jin, X., Prince, D.A., and Huguenard, J.R. (2006). Enhanced Excitatory Synaptic Connectivity in Layer V Pyramidal Neurons of Chronically Injured Epileptogenic Neocortex in Rats. J. Neurosci. *26*, 4891–4900.

Jin, X., Huguenard, J.R., and Prince, D.A. (2011). Reorganization of inhibitory synaptic circuits in rodent chronically injured epileptogenic neocortex. Cereb. Cortex N. Y. N 1991 *21*, 1094–1104.

Jin, X., Jiang, K., and Prince, D.A. (2014). Excitatory and Inhibitory Synaptic Connectivity to Layer V Fast-spiking Interneurons in the Freeze Lesion Model of Cortical Microgyria. J. Neurophysiol.

Johnson, V.E., Stewart, J.E., Begbie, F.D., Trojanowski, J.Q., Smith, D.H., and Stewart, W. (2013). Inflammation and white matter degeneration persist for years after a single traumatic brain injury. Brain J. Neurol. *136*, 28–42.

Jones, E.G. (1998). Viewpoint: the core and matrix of thalamic organization. Neuroscience *85*, 331–345.

Katz, L.C. (1993). Coordinate activity in retinal and cortical development. Curr. Opin. Neurobiol. *3*, 93–99.

Kawaguchi, Y., and Kubota, Y. (1997). GABAergic cell subtypes and their synaptic connections in rat frontal cortex. Cereb. Cortex *7*, 476–486.

Kawaguchi, Y., Katsumaru, H., Kosaka, T., Heizmann, C.W., and Hama, K. (1987). Fast spiking cells in rat hippocampus (CA1 region) contain the calcium-binding protein parvalbumin. Brain Res. *416*, 369–374.

Kim, E. (2002). Agitation, aggression, and disinhibition syndromes after traumatic brain injury. NeuroRehabilitation *17*, 297–310.

Kinney, J.W., Davis, C.N., Tabarean, I., Conti, B., Bartfai, T., and Behrens, M.M. (2006). A specific role for NR2A-containing NMDA receptors in the maintenance of parvalbumin and GAD67 immunoreactivity in cultured interneurons. J. Neurosci. Off. J. Soc. Neurosci. *26*, 1604–1615.

Klonoff, H., Clark, C., and Klonoff, P.S. (1993). Long-term outcome of head injuries: a 23 year follow up study of children with head injuries. J. Neurol. Neurosurg. Psychiatry *56*, 410–415.

Kobori, N., Clifton, G.L., and Dash, P. (2002). Altered expression of novel genes in the cerebral cortex following experimental brain injury. Brain Res. Mol. Brain Res. *104*, 148–158.

Kochanek, P.M., Carney, N., Adelson, P.D., Ashwal, S., Bell, M.J., Bratton, S., Carson, S., Chesnut, R.M., Ghajar, J., Goldstein, B., et al. (2012). Guidelines for the acute medical management of severe traumatic brain injury in infants, children, and adolescents--second edition. Pediatr. Crit. Care Med. J. Soc. Crit. Care Med. World Fed. Pediatr. Intensive Crit. Care Soc. *13 Suppl 1*, S1–S82.

Kuhlman, S.J., Olivas, N.D., Tring, E., Ikrar, T., Xu, X., and Trachtenberg, J.T. (2013). A disinhibitory microcircuit initiates critical-period plasticity in the visual cortex. Nature *501*, 543–546.

Lawrence, J.J., and McBain, C.J. (2003). Interneuron diversity series: containing the detonation--feedforward inhibition in the CA3 hippocampus. Trends Neurosci. *26*, 631–640.

Lenzlinger, P.M., Shimizu, S., Marklund, N., Thompson, H.J., Schwab, M.E., Saatman, K.E., Hoover, R.C., Bareyre, F.M., Motta, M., Luginbuhl, A., et al. (2005). Delayed inhibition of Nogo-A does not alter injury-induced axonal sprouting but enhances recovery of cognitive function following experimental traumatic brain injury in rats. Neuroscience *134*, 1047–1056.

Letzkus, J.J., Wolff, S.B.E., Meyer, E.M.M., Tovote, P., Courtin, J., Herry, C., and Lüthi, A. (2011). A disinhibitory microcircuit for associative fear learning in the auditory cortex. Nature *480*, 331–335.

Levitt, P. (2003). Structural and functional maturation of the developing primate brain. J. Pediatr. *143*, S35–S45.

Lewis, D.A., Curley, A.A., Glausier, J., and Volk, D.W. (2012). Cortical Parvalbumin Interneurons and Cognitive Dysfunction in Schizophrenia. Trends Neurosci. *35*, 57–67.

Li, K., and Xu, E. (2008). The role and the mechanism of gamma-aminobutyric acid during central nervous system development. Neurosci. Bull. *24*, 195–200.

Li, H.H., Lee, S.M., Cai, Y., Sutton, R.L., and Hovda, D.A. (2004). Differential gene expression in hippocampus following experimental brain trauma reveals distinct features of moderate and severe injuries. J. Neurotrauma *21*, 1141–1153.

Liu, N.-K., Zhang, Y.-P., O'Connor, J., Gianaris, A., Oakes, E., Lu, Q.-B., Verhovshek, T., Walker, C.L., Shields, C.B., and Xu, X.-M. (2013). A bilateral head injury that shows graded brain damage and behavioral deficits in adultmice. Brain Res. *1499*, 121–128.

Luerssen, T.G., Klauber, M.R., and Marshall, L.F. (1988). Outcome from head injury related to patient's age. A longitudinal prospective study of adult and pediatric head injury. J. Neurosurg. *68*, 409–416.

Ma, Y., and Prince, D.A. (2012). Functional alterations in GABAergic fast-spiking interneurons in chronically injured epileptogenic neocortex. Neurobiol. Dis. *47*, 102–113.

Maas, A.I., Stocchetti, N., and Bullock, R. (2008). Moderate and severe traumatic brain injury in adults. Lancet Neurol. *7*, 728–741.

Magiorkinis, E., Sidiropoulou, K., and Diamantis, A. (2010). Hallmarks in the history of epilepsy: epilepsy in antiquity. Epilepsy Behav. EB *17*, 103–108.

Marklund, N., Bareyre, F.M., Royo, N.C., Thompson, H.J., Mir, A.K., Grady, M.S., Schwab, M.E., and McIntosh, T.K. (2007). Cognitive outcome following brain injury and treatment with an inhibitor of Nogo-A in association with an attenuated downregulation of hippocampal growth-associated protein-43 expression. J. Neurosurg. *107*, 844–853.

Markram, H., Toledo-Rodriguez, M., Wang, Y., Gupta, A., Silberberg, G., and Wu, C. (2004). Interneurons of the neocortical inhibitory system. Nat. Rev. Neurosci. *5*, 793–807.

Matsumoto, H., and Marsan, C.A. (1964). Cortical cellular phenomena in experimental epilepsy: Interictal manifestations. Exp. Neurol. *9*, 286–304.

Mazarati, A. (2006). Is posttraumatic epilepsy the best model of posttraumatic epilepsy? Epilepsy Curr. Am. Epilepsy Soc. *6*, 213–214.

Miller, L.M., Escabí, M.A., and Schreiner, C.E. (2001). Feature selectivity and interneuronal cooperation in the thalamocortical system. J. Neurosci. Off. J. Soc. Neurosci. *21*, 8136–8144.

Miller, M.N., Okaty, B.W., Kato, S., and Nelson, S.B. (2011). Activity-dependent changes in the firing properties of neocortical fast-spiking interneurons in the absence of large changes in gene expression. Dev. Neurobiol. *71*, 62–70.

Mishra, A.M., Bai, X., Sanganahalli, B.G., Waxman, S.G., Shatillo, O., Grohn, O., Hyder, F., Pitkanen, A., and Blumenfeld, H. (2014). Decreased Resting Functional Connectivity after Traumatic Brain Injury in the Rat. PLoS ONE *9*.

Mrzljak, L., Uylings, H.B., Van Eden, C.G., and Judás, M. (1990). Neuronal development in human prefrontal cortex in prenatal and postnatal stages. Prog. Brain Res. *85*, 185–222.

Nakamura, T., Matsumoto, J., Takamura, Y., Ishii, Y., Sasahara, M., Ono, T., and Nishijo, H. (2015). Relationships among parvalbumin-immunoreactive neuron density, phase-locked gamma oscillations, and autistic/schizophrenic symptoms in PDGFR-β knock-out and control mice. PloS One *10*, e0119258.

Nathanson, J.L., Yanagawa, Y., Obata, K., and Callaway, E.M. (2009). Preferential labeling of inhibitory and excitatory cortical neurons by endogenous tropism of AAV and lentiviral vectors. Neuroscience *161*, 441–450.

Nelson, S.B., and Turrigiano, G.G. (1998). Synaptic depression: a key player in the cortical balancing act. Nat. Neurosci. *1*, 539–541.

Noctor, S.C., Flint, A.C., Weissman, T.A., Dammerman, R.S., and Kriegstein, A.R. (2001). Neurons derived from radial glial cells establish radial units in neocortex. Nature *409*, 714–720.

Nudo, R.J. (2006). Mechanisms for recovery of motor function following cortical damage. Curr. Opin. Neurobiol. *16*, 638–644.

Pagni, C.A., and Zenga, F. (2005). Posttraumatic epilepsy with special emphasis on prophylaxis and prevention. Acta Neurochir. Suppl. *93*, 27–34.

Pandolfo, M. (2011). Genetics of epilepsy. Semin. Neurol. *31*, 506–518.

Park, E., Bell, J.D., and Baker, A.J. (2008). Traumatic brain injury: Can the consequences be stopped? CMAJ Can. Med. Assoc. J. *178*, 1163–1170.

Perucca, P., and Gilliam, F.G. (2012). Adverse effects of antiepileptic drugs. Lancet Neurol. *11*, 792–802.

Petilla Interneuron Nomenclature Group, Ascoli, G.A., Alonso-Nanclares, L., Anderson, S.A., Barrionuevo, G., Benavides-Piccione, R., Burkhalter, A., Buzsáki, G., Cauli, B., Defelipe, J., et al. (2008). Petilla terminology: nomenclature of features of GABAergic interneurons of the cerebral cortex. Nat. Rev. Neurosci. *9*, 557–568.

Pinto, D.J., Brumberg, J.C., and Simons, D.J. (2000). Circuit dynamics and coding strategies in rodent somatosensory cortex. J. Neurophysiol. *83*, 1158–1166.

Pinto, D.J., Hartings, J.A., Brumberg, J.C., and Simons, D.J. (2003). Cortical damping: analysis of thalamocortical response transformations in rodent barrel cortex. Cereb. Cortex N. Y. N 1991 *13*, 33–44.

Pitkänen, A., and McIntosh, T.K. (2006). Animal models of post-traumatic epilepsy. J. Neurotrauma *23*, 241–261.

Pitkänen, A., Kharatishvili, I., Karhunen, H., Lukasiuk, K., Immonen, R., Nairismägi, J., Gröhn, O., and Nissinen, J. (2007). Epileptogenesis in experimental models. Epilepsia *48 Suppl 2*, 13–20.

Polack, P.-O., Guillemain, I., Hu, E., Deransart, C., Depaulis, A., and Charpier, S. (2007). Deep Layer Somatosensory Cortical Neurons Initiate Spike-and-Wave Discharges in a Genetic Model of Absence Seizures. J. Neurosci. *27*, 6590–6599.

Pouille, F., and Scanziani, M. (2001). Enforcement of temporal fidelity in pyramidal cells by somatic feed-forward inhibition. Science *293*, 1159–1163.

Prince, D.A. (1978). Neurophysiology of Epilepsy. Annu. Rev. Neurosci. *1*, 395–415.

Prinz, A., Selesnew, L.-M., Liss, B., Roeper, J., and Carlsson, T. (2013). Increased excitability in serotonin neurons in the dorsal raphe nucleus in the 6-OHDA mouse model of Parkinson's disease. Exp. Neurol. *248*, 236–245.

Rakic, P. (1988). Specification of cerebral cortical areas. Science *241*, 170–176.

Rheims, S., Holmgren, C.D., Chazal, G., Mulder, J., Harkany, T., Zilberter, T., and Zilberter, Y. (2009). GABA action in immature neocortical neurons directly depends on the availability of ketone bodies. J. Neurochem. *110*, 1330–1338.

Rubio-Garrido, P., Pérez-de-Manzo, F., Porrero, C., Galazo, M.J., and Clascá, F. (2009). Thalamic input to distal apical dendrites in neocortical layer 1 is massive and highly convergent. Cereb. Cortex N. Y. N 1991 *19*, 2380–2395.

Rudy, B., Fishell, G., Lee, S., and Hjerling-Leffler, J. (2011). Three Groups of Interneurons Account for Nearly 100% of Neocortical GABAergic Neurons. Dev. Neurobiol. *71*, 45–61.

Saatman, K.E., Duhaime, A.-C., Bullock, R., Maas, A.I.R., Valadka, A., Manley, G.T., and Workshop Scientific Team and Advisory Panel Members (2008). Classification of traumatic brain injury for targeted therapies. J. Neurotrauma *25*, 719–738.

Salin, P., Tseng, G.F., Hoffman, S., Parada, I., and Prince, D.A. (1995). Axonal sprouting in layer V pyramidal neurons of chronically injured cerebral cortex. J. Neurosci. *15*, 8234–8245.

Scheff, S.W., Price, D.A., Hicks, R.R., Baldwin, S.A., Robinson, S., and Brackney, C. (2005). Synaptogenesis in the Hippocampal CA1 Field following Traumatic Brain Injury. J. Neurotrauma *22*, 719–732.

Schwaller, B., Tetko, I.V., Tandon, P., Silveira, D.C., Vreugdenhil, M., Henzi, T., Potier, M.-C., Celio, M.R., and Villa, A.E.P. (2004). Parvalbumin deficiency affects network properties resulting in increased susceptibility to epileptic seizures. Mol. Cell. Neurosci. *25*, 650–663.

Shatz, C.J. (1990). Impulse activity and the patterning of connections during cns development. Neuron *5*, 745–756.

Shipp, S. (2007). Structure and function of the cerebral cortex. Curr. Biol. *17*, R443–R449.

Smith, C., Gentleman, S.M., Leclercq, P.D., Murray, L.S., Griffin, W.S.T., Graham, D.I., and Nicoll, J.A.R. (2013). The neuroinflammatory response in humans after traumatic brain injury. Neuropathol. Appl. Neurobiol. *39*, 654–666.

Sohal, V.S., Zhang, F., Yizhar, O., and Deisseroth, K. (2009). Parvalbumin neurons and gamma rhythms enhance cortical circuit performance. Nature *459*, 698–702.

Somjen, G.G. (2004). Ions in the Brain : Normal Function, Seizures, and Stroke: Normal Function, Seizures, and Stroke (Oxford University Press).

Steriade, M., Amzica, F., Neckelmann, D., and Timofeev, I. (1998). Spike-wave complexes and fast components of cortically generated seizures. II. Extra- and

intracellular patterns. J. Neurophysiol. *80*, 1456–1479.

Tasker, J.G., and Dudek, F.E. (1991). Electrophysiology of GABA-mediated synaptic transmission and possible roles in epilepsy. Neurochem. Res. *16*, 251–262.

Temkin, O. (1994). The Falling Sickness: A History of Epilepsy from the Greeks to the Beginnings of Modern Neurology (JHU Press).

Thompson, H.J., Lifshitz, J., Marklund, N., Grady, M.S., Graham, D.I., Hovda, D.A., and McIntosh, T.K. (2005). Lateral fluid percussion brain injury: a 15-year review and evaluation. J. Neurotrauma *22*, 42–75.

Thurman, D.J., Beghi, E., Begley, C.E., Berg, A.T., Buchhalter, J.R., Ding, D., Hesdorffer, D.C., Hauser, W.A., Kazis, L., Kobau, R., et al. (2011). Standards for epidemiologic studies and surveillance of epilepsy. Epilepsia *52 Suppl 7*, 2–26.

Timofeev, I., and Steriade, M. (2004). Neocortical seizures: initiation, development and cessation. Neuroscience *123*, 299–336.

Traub, R.D., and Wong, R.K. (1982). Cellular mechanism of neuronal synchronization in epilepsy. Science *216*, 745–747.

Traub, R.D., Bibbig, A., LeBeau, F.E.N., Buhl, E.H., and Whittington, M.A. (2004). Cellular mechanisms of neuronal population oscillations in the hippocampus in vitro. Annu. Rev. Neurosci. *27*, 247–278.

Ueno, M., Hayano, Y., Nakagawa, H., and Yamashita, T. (2012). Intraspinal rewiring of the corticospinal tract requires target-derived brain-derived neurotrophic factor and compensates lost function after brain injury. Brain J. Neurol. *135*, 1253–1267.

Werner, C., and Engelhard, K. (2007). Pathophysiology of traumatic brain injury. Br. J. Anaesth. *99*, 4–9.

Wilson, N.R., Runyan, C.A., Wang, F.L., and Sur, M. (2012). Division and subtraction by distinct cortical inhibitory networks in vivo. Nature *488*, 343–348.

Wöhr, M., Orduz, D., Gregory, P., Moreno, H., Khan, U., Vörckel, K.J., Wolfer, D.P., Welzl, H., Gall, D., Schiffmann, S.N., et al. (2015). Lack of parvalbumin in mice leads to behavioral deficits relevant to all human autism core symptoms and related neural morphofunctional abnormalities. Transl. Psychiatry *5*, e525.

Xu, X., Roby, K.D., and Callaway, E.M. (2010). Immunochemical characterization of inhibitory mouse cortical neurons: Three chemically distinct classes of inhibitory cells. J. Comp. Neurol. *518*, 389–404.

Yang, L., Afroz, S., Michelson, H.B., Goodman, J.H., Valsamis, H.A., and Ling, D.S.F. (2010). Spontaneous epileptiform activity in rat neocortex after controlled cortical impact

injury. J. Neurotrauma *27*, 1541–1548.

Zhang, Z. (2004). Maturation of Layer V Pyramidal Neurons in the Rat Prefrontal Cortex: Intrinsic Properties and Synaptic Function. J. Neurophysiol. *91*, 1171–1182.

van Zundert, B., Izaurieta, P., Fritz, E., and Alvarez, F.J. (2012). Early pathogenesis in the adult-onset neurodegenerative disease amyotrophic lateral sclerosis. J. Cell. Biochem. *113*, 3301–3312.

(2005). Atlas epilepsy care in the world. (Geneva: Programme for Neurological Diseases and Neuroscience, Dept. of Mental Health and Substance Abuse, World Health Organization).

APPENDIX A

CURRICULUM VITAE

Education

Aug. 2012 – Nov. 2015	Ph.D in Biology – Physiology, Arizona State University
Aug. 2010 – May 2010	Bachelor of Arts with Honors, Arizona State University

Honors and Awards

2015	Society for Neuroscience-Press Conference Selection and Presentation
2015	Society for Neuroscience-Press Conference Selection and Presentation
2015	ASU Graduate and Professional Student Associate Travel Grant
2015	Arizona State University-School of Life Sciences Travel Award
2013	Arizona State University-School of Life Sciences Travel Award
2007-2010	Barrett Honors Scholar
2006-2010	Dean's List, Arizona State University, Tempe, AZ

Research Experience and Training

Aug 2012 – Current **Arizona State University – School of Life Sciences & University of Arizona-College of Medicine Phoenix**
Phoenix, AZ
Research Intern/Ph.D Student
Investigating cortical network changes in pediatrics after traumatic brain injury.

Responsibilities:

- Develop and establish a new model in the laboratory studying pediatric traumatic brain injury and post-traumatic epilepsy.
- Perform whole-cell patch clamp from in vitro brain slices and human brain tissue to investigate the efficacy of pharmacological agents in alleviating epileptiform activity.
- Develop transgenic optogentic mice, using cre-lox technology, to understand cortical circuit activity after brain injury.
- Perform immunohistochemistry and utilize laser-scanning confocal microscopy to elucidate cell specific changes after controlled cortical impact.
- Characterize optogenetic properties using whole-cell patch clamp of newly generated transgenic mice with channelrhodopsin.
- Handle rodent models (mice & rats) for experimentation, I.P. injections, and survival surgeries including but not limited to craniotomies, EEG implantation, and xenografts.
- Generate protocols for voltage and current clamp recordings in pClamp software.
- Analyze patch clamp signal data using Clampfit, Excel, and Prism software.

- Perform signal analysis of EEG data recorded from rats and humans suffering from traumatic brain injury using Matlab, Excel, and C.
- Develop computational tools in Matlab, Python, and Exceal to analyze neurophysiological datasets.

Principle Investigators – Trent Anderson, Ph.D. & Jason Newbern, Ph.D.

June 2011-Aug 2012 **University of Arizona-College of Medicine Phoenix**
Phoenix, AZ
Research Technician
Investigated the role of neurosteroids in regulating cortical excitablity.
Responsibilities:

- Performed voltage and current clamp techniques on neurons *in vitro* while pharmacologically inducing epileptiform activity.
- Tested different anti-convulsant drugs concentrations *in vitro* to evaluate intrinsic drug effect.
- Performed data analysis using MiniAnalysis software and Excel.

Principle Investigator – Trent Anderson, Ph.D.

June 2011-Aug 2012 **Arizona State University – School of Life Sciences**
Tempe, AZ
Research Technician
Understanding the development and function of motorneuron dendritic architecture.
Responsibilities:

- Developed protocols for, and conducted dual whole-cell patch clamp recordings of third-star larvae Drosophila.
- Performed Drosophilia husbandry (prepared food and vials, and maintained back-up fly lines).

Principal Investigator: Carsten Duch, Ph.D. (Currently at Johannes Gutenberg University – Mainz)

2008-2011 **Arizona State University – School of Life Sciences**
Tempe, AZ
Honors Research Scholar
Investigate ultrasonic neuromodulation, and homeostatic plasticity using the rodent olfactory system as prime model.

Responsibilities:

- Conducted behavioral assays (Morris water maze, rotarod, wire hang test, reward and aversive conditioning, etc) to understand olfactory synaptic plasticity.
- Assist graduate students with in-vivo two-photon imaging of blood flow rate changes in the cortex while applying pulsed ultrasound to the skull.
- Fluorescently labeled receptors by immunohistochemistry, and imaged tissue slices with laser scanning confocal microscopy.
- Performed continuum modeling of the brain during pulsed ultrasound using Matlab.

Principal Investigator: William Jamie Tyler, Ph.D.

Professional Memberships

2013-Present Society for Neuroscience

Publications & Presentations

Publications:

J.F. Georges*, X. Liu*, J. Eschbacher, **J. Nichols**, R. Spetzler, B.G. Feuerstein, M.C. Preul, K. Van Keuren-Jensen, T. Anderson, H. Yan*, P.Nakaji* (2015) Rapid *ex vivo* identification of central nervous system lymphoma with conformational switching aptamer. *PlosOne* (In Press).

Corey Goddeyne, **Joshua Nichols**, Chen Wu, and Trent Anderson (2015) Repetitive mild brain injury selectively decreases cortical inhibition in juvenile rats. *Journal of Neurophysiology* 113 (5)

Joshua Nichols, Chen Wu, Roxy Perez, Lucy Treiman, and Trent Anderson (2014) Traumatic brain injury induces rapid enhancement of cortical excitability in juvenile rats. *CNS & Therapeutics* 21(2)

Joseph F. Georges, Nikolay L. Martirosyan, Jennifer Eschbacher, **Joshua Nichols**, Maya Tissot, Mark C. Preul, Burt Feuerstein, Trent Anderson, Robert F. Spetzler, Peter Nakaji (2014) Sulforhodamine 101 selectively labels human astrocytoma cells in an animal model of glioblastoma. *Journal of Clinical Neuroscience* 21 (5):

Joseph Georges, BS, Aqib Zehri, BS, Elizabeth Carlson, BS, **Joshua Nichols, BA**, Michael A. Mooney, MD, Nikolay L. Martirosyan, MD, Layla Ighaffari, M. Yashar S. Kalani, MD, PhD, Jennifer Eschbacher, MD, Burt Feuerstein, MD, PhD, Trent Anderson, PhD, Mark C. Preul, MD, Kendall Jensen, PhD, and Peter Nakaji, MD (2014) Contrast-free microscopic assessment of glioblastoma biospecimens prior to biobanking. *Neurosurgical Focus* 36(2):

E8.

In Preparation:

Joshua Nichols, Jason Newbern, Trent Anderson (In Preparation) Severe Traumatic Brain Injury Compromises Inhibitory Network Morphology and Decreases Inhibitory Synaptic Connectivity.

Joshua Nichols, Jason Newbern, Trent Anderson (In Preparation) Preferential loss of parvalubumin immunoreactivity in contralateral motor cortex after severe traumatic brain injury.

J.S. Martinez*, **J.D. Nichols***, T.R. Anderson, J. Newbern (In Preparation) Region-specific requirement ERK/MAPK signaling in regulating GABAergic interneuron number and excitatory synaptic drive during development. *These authors contributed equally to this work.

M. A. Moreno, L. T. Hewitt, **J.D. Nichols**, G. R. Bjorkland, C. W. Daniels, M. F. Olive, F. Sanabria, S. Marsh, D. M. Treiman, W. D. Snider, J. M. Newbern (In Preparation) Hyperactivation of ERK1/2 signaling in developing GABAergic circuits reduces parvalbumin interneuron number and increases cortical excitability.

A. Parga, **J. Nichols**, Z. Killeen, C. Wu, T. Anderson (In Preparation) Cortical spreading depression induced by targeted optogenetic activation of cortical pyramidal neurons.

Li MM, Tufail, Y., **Nichols, J.**, Cruz, Karina, and Tyler, WJ (In Preparation). Serotonin modulates sensory input gains in a context-dependent manner at olfactory glomeruli.

Abstracts:

Society for Neuroscience – **Joshua Nichols**, Jason Newbern, Trent Anderson (2015) Pediatric traumatic brain injury induces selective loss of cortical inhibitory function

Society for Neuroscience – C. Goddeyne, **J. Nichols**, C. Wu, K. Magnuson, Z. Killeen, T.R. Anderson (2015) Repetitive mild traumatic brain injury induces ventriculomegaly and cortical thinning in juvenile rats

Society for Neuroscience – Z. Killeen, A. Parga, **J. Nichols**, C. Wu, T. Anderson (2015) Cortical Spreading depression induced by targeted optogentic activation of cortical pyramidal neurons

Society for Neuroscience – J.S. Martinez, **J.D. Nichols**, T.R. Anderson, J. Newbern (2015) Region-specific requirement ERK/MAPK signaling in regulating GABAergic interneuron number and excitatory synaptic drive during development

Society for Neuroscience– **Joshua Nichols**, Chen Wu, Roxy Perez, Lucy Treiman, and Trent Anderson (2013) Traumatic Brain Injury Induces Rapid Enhancement of Cortical Excitability in Juvenile Rats

American Association of Neurological Surgeons - Joseph F. Georges, Nikolay L. Martirosyan, Jennifer Eschbacher, **Joshua Nichols**, Maya Tissot, Aqib H Zehri, George AC Mendes, Anna Joy, Ali Elhadi, Mark C Preul, Burt G Feuerstein, Robert F Spetzler, Trent Anderson, Peter Nakaji (2013) Ex Vivo Fluorescence Neuropathology: Immediate and Specific Diagnosis of Human Astrocytic Brain Tumors

Neurotrauma Symposium - Trent Anderson, Corey Goddeyne, **Joshua Nichols**, Anna Yoshihiro, Roxy Perez, Lucy Treiman, and P. David Adelson (2012) Enhanced Cortical Excitability in the Peri-Injury Zone of Immature Rats after Experimental TBI

American Association of Neurological Surgeons - Joseph F. Georges, Nikolay L. Martirosyan, Jennifer Eschbacher, **Joshua Nichols**, Maya Tissot, Ali M. Elhadi, George Mendes, Michelle McQuilkin, Burt G. Feuerstein, Robert F. Spetzler, Trent Anderson, Mark C. Preul, Peter Nakaji (2012) Rapid and Specific Diagnosis of Human Astrocytic Brain Tumors by Immediate Imaging with Sulforhodamine 101

Society for Neuroscience - Monica Li Tauchmann, Yusuf Z. Tufail, **Joshua Nichols** and William J. Tyler (2010) Amplitude modulation by 5HT2A receptors at primary olfactory synapses underlies a learning-dependent peripheral sensory gate.

Presentations:

University of Arizona – College of Medicine Phoenix Basic Medical Seminar Series (June 2013) **Enhanced Cortical Excitability in the Peri-Injury Zone of Immature Rats After Experimental TBI**

APPENDIX B

USE OF A CONFORMATIONAL SWITCHING APTAMER FOR RAPID AND SPECIFIC EX VIVO IDENTIFICATION OF CENTRAL NERVOUS SYSTEM LYMPHOMA IN A XENOGRAFT MODEL

PLOS | ONE

RESEARCH ARTICLE

Use of a Conformational Switching Aptamer for Rapid and Specific Ex Vivo Identification of Central Nervous System Lymphoma in a Xenograft Model

Joseph F. Georges[1,2☯¤], Xiaowei Liu[4☯], Jennifer Eschbacher[3], Joshua Nichols[5], Michael A. Mooney[2], Anna Joy[1], Robert F. Spetzler[2], Burt G. Feuerstein[5], Mark C. Preul[2], Trent Anderson[5], Hao Yan[4], Peter Nakaji[2]*

1 Division of Neuroscience, Barrow Neurological Institute, St. Joseph's Hospital and Medical Center, Phoenix, Arizona, **2** Division of Neurological Surgery, Barrow Neurological Institute, St. Joseph's Hospital and Medical Center, Phoenix, Arizona, **3** Division of Neuropathology, Barrow Neurological Institute, St. Joseph's Hospital and Medical Center, Phoenix, Arizona, **4** The Biodesign Institute, Arizona State University, Tempe, Arizona, **5** College of Medicine, University of Arizona, Phoenix, Arizona

☯ These authors contributed equally to this work.
¤ Current Address: Division of Neurosurgery, Ohio University and Grant Medical Center, Columbus, Ohio
* Neuropub@dignityhealth.org

OPEN ACCESS

Citation: Georges JF, Liu X, Eschbacher J, Nichols J, Mooney MA, Joy A, et al. (2015) Use of a Conformational Switching Aptamer for Rapid and Specific Ex Vivo Identification of Central Nervous System Lymphoma in a Xenograft Model. PLoS ONE 10(4): e0123607. doi:10.1371/journal.pone.0123607

Academic Editor: James D. Clelland, The Nathan Kline Institute, UNITED STATES

Received: July 1, 2014

Accepted: March 4, 2015

Published: April 15, 2015

Data Availability Statement: All relevant data are within the paper and its Supporting Information files.

Funding: These authors have no support or funding to report.

Competing Interests: The authors have declared that no competing interests exist.

Abstract

Improved tools for providing specific intraoperative diagnoses could improve patient care. In neurosurgery, intraoperatively differentiating non-operative lesions such as CNS B-cell lymphoma from operative lesions can be challenging, often necessitating immunohistochemical (IHC) procedures which require up to 24-48 hours. Here, we evaluate the feasibility of generating rapid *ex vivo* specific labeling using a novel lymphoma-specific fluorescent switchable aptamer. Our B-cell lymphoma-specific switchable aptamer produced only low-level fluorescence in its unbound conformation and generated an 8-fold increase in fluorescence once bound to its target on CD20-positive lymphoma cells. The aptamer demonstrated strong binding to B-cell lymphoma cells within 15 minutes of incubation as observed by flow cytometry. We applied the switchable aptamer to *ex vivo* xenograft tissue harboring B-cell lymphoma and astrocytoma, and within one hour specific visual identification of lymphoma was routinely possible. In this proof-of-concept study in human cell culture and orthotopic xenografts, we conclude that a fluorescent switchable aptamer can provide rapid and specific labeling of B-cell lymphoma, and that developing aptamer-based labeling approaches could simplify tissue staining and drastically reduce time to histopathological diagnoses compared with IHC-based methods. We propose that switchable aptamers could enhance expeditious, accurate intraoperative decision-making.

Introduction

Surgical resection of brain tumors is guided by intraoperative frozen section analyses. This technique is useful for diagnosing neoplastic tissue and identifying tumor margins [1]; however, some pathologies that require opposing treatment strategies can be a challenge to diagnose by frozen section alone, and instead require more specific staining. For example, differentiating some gliomas, such as oligodendroglioma or subtypes of high-grade astrocytoma from lymphoma can be challenging with frozen section analysis [2]. Specific diagnostic staining is typically achieved with immunohistochemistry (IHC), a staining process which is too slow to be used intraoperatively [3]. When a diagnosis requires IHC, a biopsy will typically be performed, and definitive treatment for the patient can be delayed by several days while awaiting fixation of tissue, performance of IHC studies, and evaluation by a pathologist for a final pathological diagnosis. Definitive treatment in this situation can vary from a return to the operating room for surgical resection of the lesion in the case of glioma, versus chemoradiation therapy in the case of lymphoma.

IHC was developed during the 1940s by Albert Coons [4]. This histopathological technique generates contrast in cells and tissue by specifically targeting proteins with antibodies. IHC undoubtedly revolutionized the study of tissues in laboratory and clinical settings. With a series of tissue preparation and staining procedures, IHC can provide specific tissue information within 24–48 hours [5, 6]. However, with the advent of new imaging technologies and fluorescent molecular probes, it may be possible to develop protocols for generating IHC-like information in a fraction of the time required by antibodies [7]. If these diagnoses could be made within intraoperative timeframes, they could offer immediate information to the surgeon, who can then make surgical decisions intraoperatively. We sought to design a probe with sufficient speed and accuracy to provide IHC-quality diagnoses in a surgically relevant time frame and to test that probe in brain tumor model systems.

Aptamers are a newer class of target-recognizing molecular probes. They are deoxyribonucleic acid (DNA), ribonucleic acid (RNA), or peptide strands with unique secondary or tertiary structures that can bind to target molecules with high affinity and specificity [8–10]. Aptamers can be generated from a synthetic DNA or RNA pool through an *in vitro* selection method known as systemic evolution of ligands by exponential enrichment [9, 10]. The selected aptamer probes can bind molecular targets with IHC-like specificity in a fraction of the time required by antibodies. Reports have been published which describe aptamers used as recognition molecules for tumor cell identification with various molecular targets [11–13]. In this study, we build from these initial findings to investigate the utility of aptamers for intraoperative histopathological assessments.

Histopathological applications, whether antibody- or aptamer-based, require optimized staining protocols to minimize nonspecific staining. Molecules such as blocking serum, bovine serum albumin, and/or transfer RNA (tRNA) are routinely added during the staining process to reduce nonspecific interactions [14, 15]. Then repetitive washing steps are used to minimize nonspecific staining with aptamers and antibodies. To circumvent this, we developed fluorescently coupled aptamers that are activated upon specific binding-induced conformational change and visualized through the principle of Förster Resonance Energy Transfer (FRET), which has been previously described [16–18]. This can effectively produce an agent that is optically silent until bound and "switches on" after binding to a specific target [16]. This decreases the noise due to nonspecific binding and eliminates the need for multiple time-consuming tissue preparation, staining, and rinsing procedures.

To test whether aptamers specifically label neoplastic brain tissue in a manner that would be practical and timely for clinical intraoperative neuropathological use, we constructed a

switchable aptamer complex against a human central nervous system (CNS) lymphoma cell line. We extended a previously reported aptamer [14, 19] to include a fluorophore and a fluorescence quencher to minimize signal in its unbound confirmation. Tested on human tumor cells and fresh tissue from animal models of CNS lymphoma and glioma, we determined whether this probe could rapidly distinguish human lymphoma cells similar to the clinical standard of CD20 immunohistochemistry.

Materials and Methods

Preparation of Q-TD05

All DNA oligonucleotides were purchased from Integrated DNA Technologies, CA with high performance liquid chromatography (HPLC) purification. A truncated version of TD05 aptamer, TD05 [17, 19] was used in our study.

The name and sequence of fluorophore-labeled aptamers are as follows:

TD05: 5' /5Alex488N/AGG AGG ATA GTT AGG TGG CTG TTG AGG GTC TCC TCC TA 3'

Q-TD05: 5' /5Alex488N/AGG AGG AGA TTT TTT TTT TAG GAG GAT AGT TAG GTG GCT GTT GAG GGT CTC CTC CTA /3BHQ_1/ 3'

Random aptamer (LD20t): 5' FITC-TAG CCA AGG TAA CCA GTA CAA GGT GCT AAA CGT AAT GGC TTC GGC TTA C 3'

Cell culture

Human glioma cells (U251) and human CNS lymphoma (Ramos) cell lines were acquired from American Type Culture Collection. U251 cells were cultured with Dulbecco's Modified Eagle Medium media supplemented with 10% fetal bovine serum (FBS), and Ramos cells were cultured in Roswell Park Memorial Institute Medium (RPMI) 1640 supplemented with 10% FBS and 50μM 2-mercaptoethanol (all from Invitrogen, Grand Island, NY). Cells were grown at 37°C in a humidified incubator under 5% CO_2. In some experiments, tumor cells were infected with a lentivirus to introduce expression of red fluorescent protein (RFP) following the manufacturers' protocol.

In vitro labeling

The aptamer probes were diluted to 1μM in aptamer binding buffer (6.05 mM Mg^{2+}, 1.2 mM Ca 2+, 4.5g/L glucose and 0.2% NaN_3 in PBS buffer) and heated to 94°C for 5 minutes, followed by immediate chilling on ice for 10 minutes. The annealed aptamers were mixed with yeast tRNA (0.1 mg/mL) to block nonspecific binding and the prepared acute tissue slices were soaked in the above aptamer solution and incubated on ice for 1 hour before confocal imaging.

Flow cytometry

Cultured U251 cells and Ramos cells were collected and washed twice by the aptamer binding buffer. The annealed aptamers were diluted to 200nM in the binding buffer and added to 5 x 10^5 cells. The aptamer-cell mixture was incubated on ice for 15 minutes, and analyzed by FACSCalibur from BD Biosciences with or without washing.

Animals

Crl:NIH-Foxn1^{rnu} rats (5 weeks age) were obtained from The Charles River Laboratories International, Inc. (Wilmington, MA). All experiments were performed in accordance with the guidelines and regulations set forth by the National Institutes of Health Guide for the Care and

Use of Laboratory Animals. Experiments were approved by the Institutional Animal Care and Use Committee of the Barrow Neurological Institute at St. Joseph's Hospital and Medical Center, Phoenix, Arizona.

Intracranial implantation

Rats were anesthetized by intramuscular injection of 10 mg/kg xylazine and 80 mg/kg ketamine and placed in a small animal stereotactic headframe (Model 900, David Kopf Instruments, Tujunga, CA). A 7-mm incision was made starting between the animal's eyes to expose bregma. A bur hole was made 3.5 mm lateral to bregma. U251 or Ramos cells were infused at a depth of 4.5 mm below the surface of the brain after the syringe (Hamilton) was advanced 5.0 mm to create a 0.5-mm pocket. The cell suspension was infused using a UMP3-1 UltraMicroPump microinjector (WPI, Sarasota, FL) set to a volume of 10 μL with an infusion rate of 3.00 μL/minute. The needle was withdrawn 2 minutes after the injection to minimize backflow of the cell suspension. The bur hole was covered with bone wax, the skin incision was sutured, and the rats were allowed to recover.

Acute slices

Twenty-eight days after implantation, rats were deeply anesthetized using the xylazine/ketamine mixture described previously. They were immediately decapitated, and their brains were removed. Coronal slices (350 μm thick) were immediately cut from the cerebral cortex on a Leica VT1200 vibratome in artificial cerebrospinal fluid containing the following (in mM): 126 NaCl, 26 $NaHCO_3$, 2.5 KCl, 1.25 NaH_2PO_4, 2 $MgSO_4$, 2 $CaCl_2$ and 10 glucose, pH 7.4. Acute slices were incubated in aptamer solution for 60 minutes.

Aptamer and CD20 antibody colabeling

Fixed xenograft slices (3 slices from 2 animals) were washed and incubated in anti-CD20 primary antibody (Millipore; 1:250). Sections were then rinsed, incubated with AlexaFluor594 secondary antibody (Invitrogen), rinsed again, and counterstained with Q-TD05 aptamer. Labeled sections were mounted on slides with vectashield (Vector labs) and No 1.5 coverslips (VWR). Total antibody staining time was 24 hours and aptamer staining time was 1 hour.

Imaging

Aptamer labeled samples were placed in uncoated No.1.5 glass-bottom dishes and positioned on the stage of a Zeiss 710 laser scanning confocal microscope equipped with a 40x/1.2NA water emersion objective. We imaged Q-TD05 by exciting the fluorophore with a 489-nm diode laser and collecting 505nm-535nm emission. We imaged red fluorescent protein by exciting with a 561nm laser and collecting 595nm-625nm emission. Spectral imaging was performed utilizing a 34 channel spectral detector, and separating emission every 10nm between 405nm-745nm. The confocal aperture was set to one Airy unit for imaging. The laser and gain values were set to fill the dynamic range of the photomultiplier tube, and the frame size was set to sample at Nyquist. All post-image processing was conducted with NIH imageJ utilizing linear functions.

Results

Development of a FRET-based aptamer for detecting CD20 positive B cells

Aptamer TD05, which binds to the heavy mu chain of membrane bound immunoglobulin in CD20-positive Burkitt's lymphoma cells, has been reported previously [14, 19]. In this study, a

Use of Laboratory Animals. Experiments were approved by the Institutional Animal Care and Use Committee of the Barrow Neurological Institute at St. Joseph's Hospital and Medical Center, Phoenix, Arizona.

Intracranial implantation

Rats were anesthetized by intramuscular injection of 10 mg/kg xylazine and 80 mg/kg ketamine and placed in a small animal stereotactic headframe (Model 900, David Kopf Instruments, Tujunga, CA). A 7-mm incision was made starting between the animal's eyes to expose bregma. A bur hole was made 3.5 mm lateral to bregma. U251 or Ramos cells were infused at a depth of 4.5 mm below the surface of the brain after the syringe (Hamilton) was advanced 5.0 mm to create a 0.5-mm pocket. The cell suspension was infused using a UMP3-1 UltraMicroPump microinjector (WPI, Sarasota, FL) set to a volume of 10 μL with an infusion rate of 3.00 μL/minute. The needle was withdrawn 2 minutes after the injection to minimize backflow of the cell suspension. The bur hole was covered with bone wax, the skin incision was sutured, and the rats were allowed to recover.

Acute slices

Twenty-eight days after implantation, rats were deeply anesthetized using the xylazine/ketamine mixture described previously. They were immediately decapitated, and their brains were removed. Coronal slices (350 μm thick) were immediately cut from the cerebral cortex on a Leica VT1200 vibratome in artificial cerebrospinal fluid containing the following (in mM): 126 NaCl, 26 $NaHCO_3$, 2.5 KCl, 1.25 NaH_2PO_4, 2 $MgSO_4$, 2 $CaCl_2$ and 10 glucose, pH 7.4. Acute slices were incubated in aptamer solution for 60 minutes.

Aptamer and CD20 antibody colabeling

Fixed xenograft slices (3 slices from 2 animals) were washed and incubated in anti-CD20 primary antibody (Millipore; 1:250). Sections were then rinsed, incubated with AlexaFluor594 secondary antibody (Invitrogen), rinsed again, and counterstained with Q-TD05 aptamer. Labeled sections were mounted on slides with vectashield (Vector labs) and No 1.5 coverslips (VWR). Total antibody staining time was 24 hours and aptamer staining time was 1 hour.

Imaging

Aptamer labeled samples were placed in uncoated No.1.5 glass-bottom dishes and positioned on the stage of a Zeiss 710 laser scanning confocal microscope equipped with a 40x/1.2NA water emersion objective. We imaged Q-TD05 by exciting the fluorophore with a 489-nm diode laser and collecting 505nm-535nm emission. We imaged red fluorescent protein by exciting with a 561nm laser and collecting 595nm-625nm emission. Spectral imaging was performed utilizing a 34 channel spectral detector, and separating emission every 10nm between 405nm-745nm. The confocal aperture was set to one Airy unit for imaging. The laser and gain values were set to fill the dynamic range of the photomultiplier tube, and the frame size was set to sample at Nyquist. All post-image processing was conducted with NIH imageJ utilizing linear functions.

Results

Development of a FRET-based aptamer for detecting CD20 positive B cells

Aptamer TD05, which binds to the heavy mu chain of membrane bound immunoglobulin in CD20-positive Burkitt's lymphoma cells, has been reported previously [14, 19]. In this study, a

single stranded DNA linker is added to the existing TD05 aptamer sequence to create the switchable probe "Q-TD05." The fluorophore, AlexaFluor488, is chemically modified at the 5' end of this probe, while a Black Hole Quencher (Integrated DNA Technology. Coralville, Iowa) is modified at the 3' end during chemical synthesis. Conceptually, the aptamer would be minimally fluorescent in its unbound confirmation (designated as "resting" status) and increase in fluorescence after binding to its target (designated as "bound" status; Fig 1A). Under macrofluorescence, we observed the quenched and unquenched aptamer exhibited markedly altered fluorescence (Fig 1B).

The constructed probe was first analyzed by fluorometry to confirm the quenching of the fluorophore (Fig 1C). Here, we included a positive control where the fluorophore was directly labeled at the 5' end of TD05 aptamer (designated as the "on" TD05 probe). As shown in Fig 1C, the switchable probe in the absence of its target molecule shows a nearly 8 fold decrease in

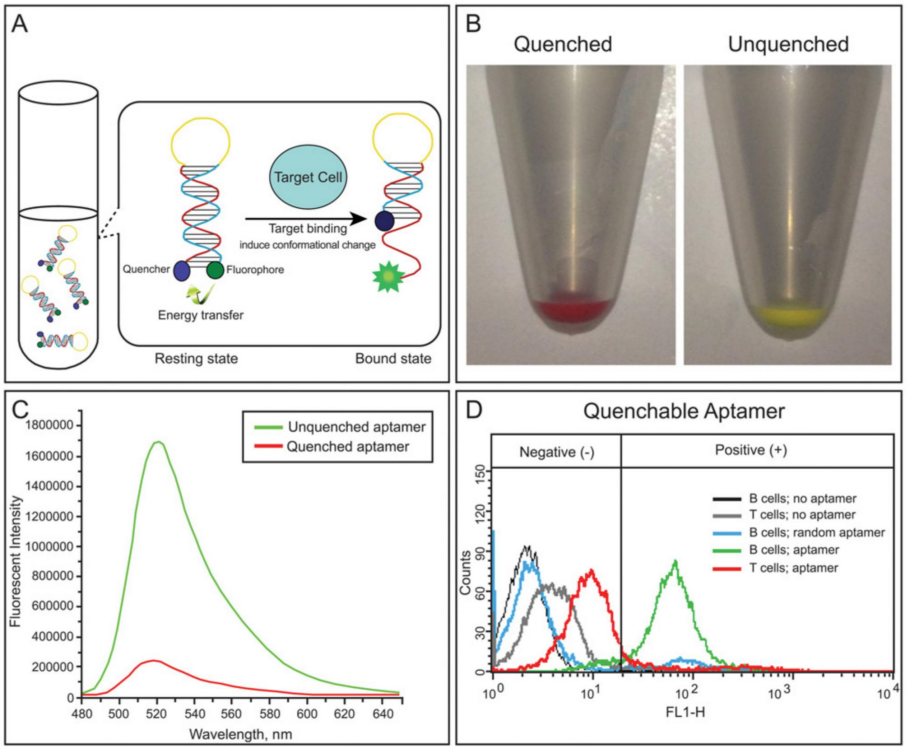

Fig 1. Aptamer fluorescence unquenching. (A, B). A) Illustration of aptamer fluorescence unquenching with binding to molecular target. B) Macrofluorescence change in fluorescence emission between quenched and unquenched aptamers. Target-binding induced change in fluorescence (C, D). C) Fluorescence emission intensity of the unquenched probe versus the quenched. Note a near 8-fold change in fluorescence intensity. D) Fluorescence intensity of the quenchable aptamer tested on negative control T cells and positive control B cells. Note increased fluorescence and number of labeled B cells versus T cells.

doi:10.1371/journal.pone.0123607.g001

fluorescence intensity compared to the "on" probe in the unquenched confirmation. This indicated the switchable probe is truly in resting status, and is expected to exhibit very low background signal when is used for cell or tissue staining.

To confirm this expectation, we then incubated the aptamer probes on cultured human lymphoma cell lines for 15 minutes and analyzed by flow cytometry (S1 Table). Fluorescence signal caused by nonspecific binding is commonly seen in regular aptamer staining without a washing step. This results in artificial positive cell labeling, especially when applied to tissues. Here, the background staining is compared in the cell lines without washing. The percentage of cells that were artificially labeled in the negative control cell line was used as a parameter to compare the background level (also known as noise) between the "on" probe and the switchable probe. In the group stained with the switchable aptamer probe, the background nonspecific labeling of negative control cells was reduced to about 1/7 (11.77% vs. 81.90% in (Fig 1D) of that in the group stained with the "on" aptamer probe. As an additional control, we incubated B cells with a random fluorescent aptamer and found their fluorescence signal to resemble baseline noise (Fig 1D). This demonstrates that the switchable aptamer could reduce the background staining of non-target cells and could potentially provide specific contrast during tissue staining.

Quenched TD05 specifically differentiates B cell lymphoma from astrocytoma cells

To test whether our aptamer could differentiate clinically meaningful tumor cell types, we tested Q-TD05 on human B cell lymphoma and human astrocytoma cells. Human lymphoma and astrocytoma were first virally transduced with lentivirus to constitutively express red fluorescent protein for specific visualization of tumor cells (Fig 2B and 2E). Fluorescence imaging of lymphoma cells incubated with Q-TD05 revealed a ring-like staining pattern that is typically seen when using CD20 antibody, a common lymphoma marker on lymphoma cells (Fig 2A) [20]. Fluorescence imaging of astrocytoma cells revealed no cell-specific staining (Fig 2D). We noted that Q-TD05 produced some fluorescent artifacts in lymphoma and astrocytoma tissues which differed in morphology from the positive ring-like staining characteristic of CD20 immunostaining (Fig 2 arrowheads). This shows Q-TD05 can differentiate human B cell lymphoma and astrocytoma in cell culture based on fluorescence and staining pattern.

Comparison of Q-TD05 staining in xenograft acute slices and fixed slices (Quenched TD05 differentiates human B cell lymphoma from astrocytoma in xenograft acute slices)

In order to test Q-TD05 on tissues that more resemble a clinical biopsy, we generated brain slices from rodents intracranially implanted with human B cell lymphoma and astrocytoma cells (n = 12 lymphoma slices from 5 animals and n = 5 astrocytoma slices from 3 animals), and compared the staining patterns. Fresh acute tissue slices containing tumor were incubated with Q-TD05 for one hour and imaged on a confocal microscope. In acute slices containing B cell lymphoma, we found cells with a fluorescent ring-like staining pattern that resembled classic CD20 antibody staining (Fig 3A). On fresh tissue containing human astrocytoma cells we found minimal nonspecific fluorescence and an absence of a ring-like staining pattern (Fig 3B). Much like astrocytoma samples, fresh tissue from normal rodent brain incubated with Q-TD05 only produced weak fluorescence and fluorescence hypointensity of cell bodies (Fig 3C). Next, we examined if active processes were important to the aptamer signaling by examining for similar staining in fixed tissue. We tested Q-TD05 on fixed xenograft brain slices from animals implanted separately with either a B cell lymphoma or astrocytoma. We found a strong fluorescence ring-like staining pattern of cells within lymphoma tumor regions. This was

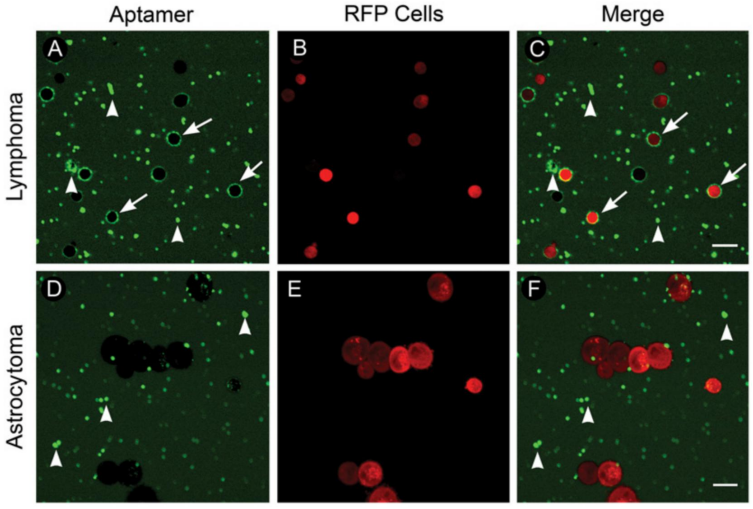

Fig 2. Quenchable aptamer staining of cultured human fluorescent lymphoma and astrocytoma cells. (A-C) Lymphoma. A) B cell lymphoma cells incubated with the quenchable aptamer; note ring-like staining pattern (arrows) and fluorescent artifacts (arrowheads). B) Lymphoma cells expressing RFP. C) Merged image of RFP-lymphoma cells and aptamer staining. (D-F) Astrocytoma. D) Astrocytoma cells incubated with the quenchable aptamer; note fluorescent artifacts (arrowheads) and lack of ring-like staining. E) Astrocytoma cells expressing RFP. F) Merged image of RFP-astrocytoma cells and aptamer staining. Scale bars equal 20*um*.

doi:10.1371/journal.pone.0123607.g002

contrasted to weak fluorescence of tissue outside the lymphoma tumor margin (Fig 3D). Fixed astrocytoma slices incubated with Q-TD05 produced only weak fluorescence and were absent of the observed CD20-like staining pattern from fixed lymphoma tissue (Fig 3E). Spectral imaging verified fluorescence signals we detected were fluorophore-specific (S1 Fig). Unique to fixed tissue, we found increased fluorescent artifacts compared to fresh tissue. However, these artifacts did not recapitulate a CD20 circumferential staining pattern (Fig 3F). These results indicate that specific tissue preparation such as fixation is not needed, and may actually reduce the quality, for Q-TD05 staining. Removing time-consuming washing or fixation procedures significantly reduces the complexity of staining and highlights the benefit of the Q-TD05 staining method.

Quenched TD05 localizes to fluorescent B cell lymphoma cells in xenograft slices

To visualize the localization of Q-TD05 and examine the labeling accuracy, we produced rodent xenografts with human B cell lymphoma and astrocytoma cells expressing red fluorescent protein (RFP) (n = 4 lymphoma and 3 astrocytoma slices). Fresh acute slices generated from these animals were incubated with Q-TD05 for one hour and imaged without rinsing. We found strong circumferential staining of RFP-labeled lymphoma cells with Q-TD05 (Fig 4A–4C). Acute slices from astrocytoma xenografts showed strong RFP expression but lacked circumferential staining (Fig 4D–4F). As an additional negative control, we did not find fluorescently labeled cells in acute slice normal brain regions (Fig 4G–4I). We quantified labeling of

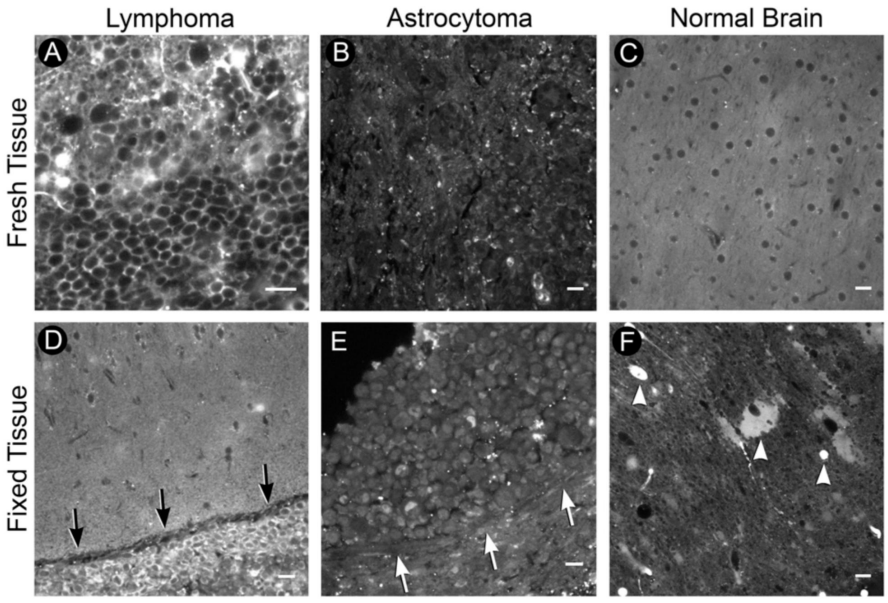

Fig 3. Xenograft acute slices. (A-C) Fresh tissue. A) Tumor region of B cell lymphoma acute slice incubated with the quenchable aptamer. Note the ring-like staining pattern. B) Tumor region of astrocytoma acute slice; note lack of ring-like staining pattern. C) Contralateral normal brain from lymphoma acute slice. Note hypo-fluorescent regions indicating location of cell-bodies. (D-F) Fixed tissue. D) Fixed acute slice containing B cell lymphoma; note positive cells in hypercellular tumor region (arrows). E) Fixed astrocytoma tissue lacking positive staining; note absence of positive cells within hypercellular tumor (arrows). F) Contralateral normal brain from lymphoma fixed slice; note additional fluorescent artifacts (arrowheads). Scale bars equal 20*um*.

doi:10.1371/journal.pone.0123607.g003

Q-TD05 to RFP-labeled lymphoma cells (n = 13 fields of view from 3 acute slices). We found Q-TD05 labeled a significantly greater percentage of RFP-labeled lymphoma cells than non-RFP labeled cells (80.75 ± 2.52% vs. 8.25 ± 1.51%, $p<0.001$), and a strong correlation between aptamer staining and RFP-expressing lymphoma cells ($R^2 = 0.92$, $p<0.001$) (Fig 4J and 4K).

Discussion

We have demonstrated the potential of a FRET-based aptamer for providing antibody-specific diagnostic information in a small fraction of the time required for traditional IHC in cell culture and in an animal model. Specifically, we tested the specificity of Q-TD05 in human cell culture and tissues from orthotopic rodent xenografts. Compared with the current standard of CD20 IHC, Q-TD05 provided significantly faster identification of lymphoma cells with a less complex staining procedure (Supplemental Fig 1). Coupled with fluorescence imaging, Q-TD05 allowed rapid differentiation of human lymphoma cells from a clinically meaningful negative control of human astrocytoma based on staining intensity and morphology.

Antibody staining can be a rate-limiting step for definitive surgical treatment of cancers. When intraoperative histopathological diagnostics cannot differentiate cancers with opposing treatment paradigms such as CNS lymphoma versus astrocytoma, antibody staining is utilized

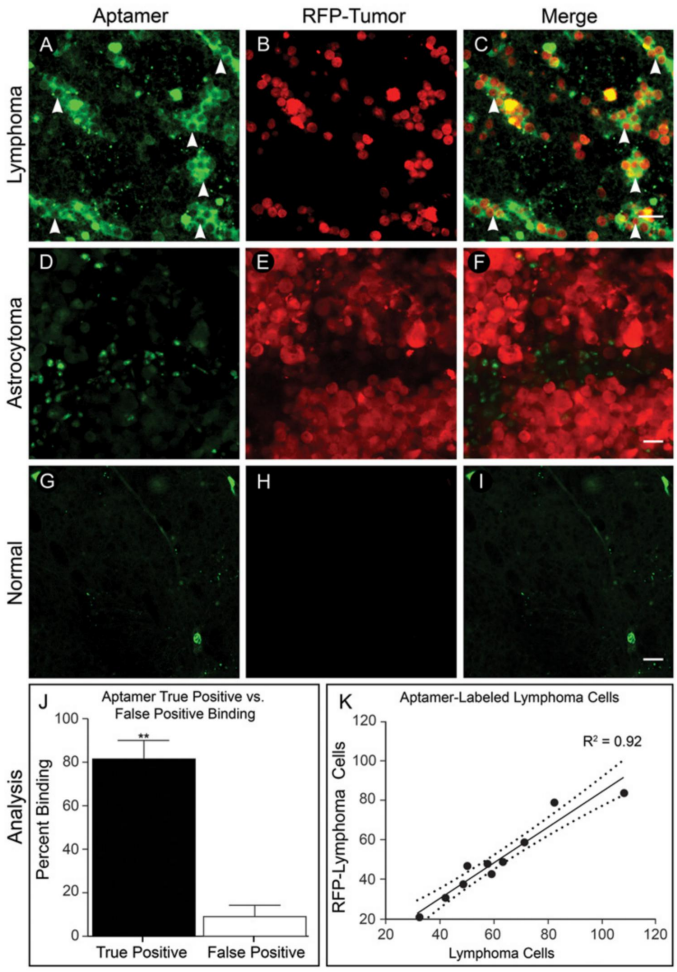

Fig 4. Fluorescent xenograft acute slices. (A-C) Lymphoma. A) Aptamer staining of lymphoma acute slice with positive staining regions (arrowheads). B) RFP-expressing lymphoma cells within tissue slice. C) Merge (D-F) Astrocytoma. D) Aptamer staining of astrocytoma acute slice; note lack of positively stained cells. E) RFP-expressing astrocytoma cells within tissue slice. F) Merge. (G-I) Normal brain. G) Aptamer staining of normal brain lacking aptamer-positive cells. H) Absence of ring-like staining and RFP-expressing cells in normal brain. I) Merge. J) Q-TD05 labels 80.75 ± 2.52% of RFP-expressing lymphoma cells and 8.25 ± 1.51% of non-RFP cells, $p<0.001$. K) Coefficient of correlation between RFP-lymphoma cells and aptamer staining (R^2) = 0.92 with 95% confidence intervals (dotted lines) of 0.87–0.99, $p<0.001$. Scale bars equal 20*um*.

doi:10.1371/journal.pone.0123607.g004

to differentiate tissue based on tumor-specific protein expression [3]. This method requires numerous steps for tissue preparation and staining, and therefore typically requires at least 24–48 hours for processing [2, 6]. In contrast, our Q-TD05 aptamer identified CD20-positive tumor cells in fresh and fixed tissue with a one-step staining protocol with no special tissue preparation. This was evident in tumor core regions and tumor margins which contain more heterogenous cell populations (S1 Fig) [21]. Q-TD05 allowed antibody-like specific detection of CNS lymphoma cells within 15–60 minutes. Though labeling with this proof-of-concept quenchable aptamer exceeds the frozen section time range, it specifically labels lymphoma cells nearly two orders of magnitude faster than IHC. Additionally, development of aptamers with enhanced binding affinities is currently underway and could further decrease this staining time.

Advancements in optical imaging and development of fluorescent probes have provided researchers powerful tools for characterizing tissue, and we believe great advances will be made by applying these tools to intraoperative tissue diagnostics. The ability to make rapid and specific intraoperative diagnoses could decrease surgical times, provide additional guidance to surgeons in the operating suite, decrease the time patients are required to wait for a definitive diagnosis, and potentially decrease healthcare costs by facilitating and expediting diagnosis-based treatment decisions. Though the initial cost of fluorescence imaging equipment may be an obstacle to widespread use of switchable-aptamers, the one-step staining protocol and rapid diagnostic output could justify the expense, making them cost-effective with even moderate use. The attractiveness of much more rapid definitive pathological results will likely drive adoption. In addition, current efforts to miniaturize and economize fluorescence imaging instruments will soon make this imaging modality a realistic option for many pathology departments [22, 23].

Conclusion

We have demonstrated that a conformational FRET-based switchable aptamer targeting human B cell lymphoma can rapidly and specifically identify tumor cells in biopsies from rodent xenograft models of human brain tumors. Translated into clinical pathology, quenchable aptamers have potential for providing intraoperative diagnoses not currently possible with frozen sections. Development of these aptamers against additional clinical targets could provide specific diagnoses in timeframes that support intraoperative decision-making and facilitate clinical management of patients whose treatment depends on their pathological diagnosis.

Supporting Information

S1 Fig. Colabeling: TD05 and CD20 antibody. (A and D) Aptamer. B cell lymphoma xenograft slices incubated with the quenchable aptamer; 1 hour staining. (B and E) CD20 antibody. B cell lymphoma slices incubated with CD20 antibody; 24 hour staining time. (C and F) Merge. Merged image of aptamer and CD20 antibody staining. (G) Spectral analysis. Ring-like staining patterns contain strong 488nm and 594nm fluorescence emissions; wavelengths unique to Q-TD05 and CD20 antibody. Scale bars equal 20μm.
(TIF)

S1 Table. Quantification of probe staining profile in cultured human B lymphoma cells (Ramos, the CD20 positive cell line) and T lymphoma cells (Jurkat, the CD20 negative control cell line). The percentage of the positively stained population in each cell line is listed in the table, and the signal/noise ratios are shown as the ratio between the percentage of positively stained population in Ramos and Jurkat cells.
(DOCX)

Author Contributions

Conceived and designed the experiments: JFG PN HY XL BGF TA JE AJ. Performed the experiments: JFG XL JE JN. Analyzed the data: JFG XL JE BGF TA MCP HY PN. Contributed reagents/materials/analysis tools: JE AJ RFS BGF TA MCP HY PN. Wrote the paper: JFG XL JE JN MAM BGF TA MCP HY PN.

References

1. Haybaeck J, von Campe G, Hainfellner JA. [Rapid frozen sections in neuropathology]. Pathologe. 2012; 33(5): 379–88. Der Schnellschnitt in der Neuropathologie. doi: 10.1007/s00292-012-1604-x PMID: 22868403
2. Schiffer D, Giordana MT, Mauro A, Migheli A. Immunohistochemistry in neuro-oncology. Basic Appl Histochem. 1986; 30(2): 253–65. PMID: 2427063
3. Plesec TP, Prayson RA. Frozen section discrepancy in the evaluation of central nervous system tumors. Arch Pathol Lab Med. 2007; 131(10): 1532–40. PMID: 17922589
4. Hokfelt T. Neurobiology thanks to microbiology: the legacy of Albert H. Coons (1912–1978). Brain Res Bull. 1999; 50(5–6): 371–2. PMID: 10582521
5. Safi MA. An overview of various labeled assays used in medical laboratory diagnosis. Immune and non-immune assays. Saudi Med J. 2010; 31(4): 359–68. PMID: 20383411
6. Hofman FM, Taylor CR. Immunohistochemistry. Curr Protoc Immunol. 2013; 103: Unit 21 4.
7. Nimmerjahn A, Kirchhoff F, Kerr JN, Helmchen F. Sulforhodamine 101 as a specific marker of astroglia in the neocortex in vivo. Nat Methods. 2004; 1(1): 31–7. PMID: 15782150
8. Keefe AD, Pai S, Ellington A. Aptamers as therapeutics. Nat Rev Drug Discov. 2010; 9(7): 537–50. doi: 10.1038/nrd3141 PMID: 20592747
9. Ellington AD, Szostak JW. In vitro selection of RNA molecules that bind specific ligands. Nature. 1990; 346(6287): 818–22. PMID: 1697402
10. Tuerk C, Gold L. Systematic evolution of ligands by exponential enrichment: RNA ligands to bacteriophage T4 DNA polymerase. Science. 1990; 249(4968): 505–10. PMID: 2200121
11. Blank M, Weinschenk T, Priemer M, Schluesener H. Systematic evolution of a DNA aptamer binding to rat brain tumor microvessels. selective targeting of endothelial regulatory protein pigpen. J Biol Chem. 2001; 276(19): 16464–8. PMID: 11279054
12. Sefah K, Meng L, Lopez-Colon D, Jimenez E, Liu C, Tan W. DNA aptamers as molecular probes for colorectal cancer study. PLoS One. 2010; 5(12): e14269. doi: 10.1371/journal.pone.0014269 PMID: 21170319
13. Hicke BJ, Stephens AW, Gould T, Chang YF, Lynott CK, Heil J, et al. Tumor targeting by an aptamer. J Nucl Med. 2006; 47(4): 668–78. PMID: 16595502
14. Tang Z, Shangguan D, Wang K, Shi H, Sefah K, Mallikratchy P, et al. Selection of aptamers for molecular recognition and characterization of cancer cells. Anal Chem. 2007; 79(13): 4900–7. PMID: 17530817
15. Liu X, Yan H, Liu Y, Chang Y. Targeted cell-cell interactions by DNA nanoscaffold-templated multivalent bispecific aptamers. Small. 2011; 7(12): 1673–82. doi: 10.1002/smll.201002292 PMID: 21538862
16. Shi H, He X, Wang K, Wu X, Ye X, Guo Q, et al. Activatable aptamer probe for contrast-enhanced in vivo cancer imaging based on cell membrane protein-triggered conformation alteration. Proc Natl Acad Sci U S A. 2011; 108(10): 3900–5. doi: 10.1073/pnas.1016197108 PMID: 21368158
17. Tang Z, Mallikaratchy P, Yang R, Kim Y, Zhu Z, Wang H, et al. Aptamer switch probe based on intramolecular displacement. J Am Chem Soc. 2008; 130(34): 11268–9. doi: 10.1021/ja804119s PMID: 18680291
18. Wu C, Chen T, Han D, You M, Peng L, Cansiz S, et al. Engineering of switchable aptamer micelle flares for molecular imaging in living cells. ACS Nano. 2013; 7(7): 5724–31. doi: 10.1021/nn402517v PMID: 23746078
19. Mallikaratchy PR, Ruggiero A, Gardner JR, Kuryavyi V, Maguire WF, Heaney ML, et al. A multivalent DNA aptamer specific for the B-cell receptor on human lymphoma and leukemia. Nucleic Acids Res. 2011; 39(6): 2458–69. doi: 10.1093/nar/gkq996 PMID: 21030439
20. Chu PG, Loera S, Huang Q, Weiss LM. Lineage determination of CD20- B-Cell neoplasms: an immunohistochemical study. Am J Clin Pathol. 2006; 126(4): 534–44. PMID: 16938666

21. Georges JF, Martirosyan NL, Eschbacher J, Nichols J, Tissot M, Preul MC, et al. Sulforhodamine 101 selectively labels human astrocytoma cells in an animal model of glioblastoma. J Clin Neurosci. 2014; 21(5): 846–51. doi: 10.1016/j.jocn.2014.02.007 PMID: 24666692

22. Sankar T, Delaney PM, Ryan RW, Eschbacher J, Abdelwahab M, Nakaji P, et al. Miniaturized handheld confocal microscopy for neurosurgery: results in an experimental glioblastoma model. Neurosurgery. 2010; 66(2): 410–7; discussion 7–8. doi: 10.1227/01.NEU.0000365772.66324.6F PMID: 20087141

23. Foersch S, Heimann A, Ayyad A, Spoden GA, Florin L, Mpoukouvalas K, et al. Confocal laser endomicroscopy for diagnosis and histomorphologic imaging of brain tumors in vivo. PLoS One. 2012; 7(7): e41760. doi: 10.1371/journal.pone.0041760 PMID: 22911853

APPENDIX C

SULFORHODAMINE 101 SELECTIVELY LABELS HUMAN ASTROCYTOMA CELLS IN AN ANIMAL MODEL OF GLIOBLASTOMA

Journal of Clinical Neuroscience 21 (2014) 846–851

Contents lists available at ScienceDirect

Journal of Clinical Neuroscience

journal homepage: www.elsevier.com/locate/jocn

Laboratory studies

Sulforhodamine 101 selectively labels human astrocytoma cells in an animal model of glioblastoma

Joseph F. Georges [a,b,e,1], Nikolay L. Martirosyan [b,1], Jennifer Eschbacher [c], Joshua Nichols [d], Maya Tissot [a], Mark C. Preul [b], Burt Feuerstein [d], Trent Anderson [d], Robert F. Spetzler [b], Peter Nakaji [b,*]

[a] Division of Neuroscience, Barrow Neurological Institute, St. Joseph's Hospital and Medical Center, Phoenix, AZ, USA
[b] Division of Neurological Surgery, Barrow Neurological Institute, St. Joseph's Hospital and Medical Center, 350 W. Thomas Road, Phoenix, AZ 85013, USA
[c] Division of Neuropathology, Barrow Neurological Institute, St. Joseph's Hospital and Medical Center, Phoenix, AZ, USA
[d] College of Medicine, University of Arizona, Phoenix, AZ, USA
[e] Arizona College of Osteopathic Medicine, Midwestern University, Glendale, AZ, USA

ARTICLE INFO

Article history:
Received 16 July 2013
Accepted 2 February 2014

Keywords:
Astrocyte
Astrocytoma
In vivo model confocal microscopy
SR101
Sulforhodamine

ABSTRACT

Sulforhodamine 101 (SR101) is a useful tool for immediate staining of astrocytes. We hypothesized that if the selectivity of SR101was maintained in astrocytoma cells, it could prove useful for glioma research. Cultured astrocytoma cells and acute slices from orthotopic human glioma (n = 9) and lymphoma (n = 6) xenografts were incubated with SR101 and imaged with confocal microscopy. A subset of slices (n = 18) were counter-immunostained with glial fibrillary acidic protein and CD20 for stereological assessment of SR101 co-localization. SR101 differentiated astrocytic tumor cells from lymphoma cells. In acute slices, SR101 labeled 86.50% (±1.86; $p < 0.0001$) of astrocytoma cells and 2.19% (±0.47; $p < 0.0001$) of lymphoma cells. SR101-labeled astrocytoma cells had a distinct morphology when compared with *in vivo* astrocytes. Immediate imaging of human astrocytoma cells *in vitro* and in *ex vivo* rodent xenograft tissue labeled with SR101 can identify astrocytic tumor cells and help visualize the tumor margin. These features are useful in studying astrocytoma in the laboratory and may have clinical applications.

1. Introduction

Sulforhodamine 101 (SR101) is a red fluorescent dye that has been used in neuroscience research for the rapid and specific labeling of astrocytes [1,2]. Its underlying mechanism is not completely understood, but much like glial fibrillary acidic protein (GFAP), SR101 labels astrocytic cells and has been used to rapidly label rodent astrocytoma cells in culture [3]. If SR101 also labels glioblastoma (GBM) and other tumor cells of astrocytoma lineage, it could provide a more timely alternative to GFAP for identifying astrocytoma cells in glioma models. Furthermore, it may allow the rapid and definitive differentiation of glioma from other tumors, such as lymphoma, during intraoperative diagnosis. We aimed to establish whether the selective staining of astrocytic tumors by SR101 is a reliable and reproducible method for rapidly identifying human astrocytoma cells in cell culture and animal models, and to test this against a negative control central nervous system (CNS) lymphoma animal model. We hypothesized that the combined use of live-cell imaging with targeted fluorophores could provide a rapid method for confirming the astrocytic lineage of tumors. If so, SR101 may prove to be a rapid alternative to GFAP immunohistochemistry in such models.

2. Materials and methods

2.1. Cell culture

We acquired human glioma cell line U251 and human CNS lymphoma cell line MC116 from American Type Culture Collection. The cell lines were maintained in culture with Dulbecco's Modified Eagle Medium (DMEM) media supplemented with 10% fetal bovine serum (FBS), and Roswell Park Memorial Institute (RPMI) 1640 media supplemented with 20% FBS (all from Invitrogen, Grand Island, NY, USA). Cells were grown at 37°C in a humidified incubator under 5% CO_2.

* Corresponding author. Tel.: +1 602 406 3593; fax: +1 602 406 4104.
E-mail address: Neuropub@dignityhealth.org (P. Nakaji).
[1] These authors have contributed equally to the manuscript.

http://dx.doi.org/10.1016/j.jocn.2014.02.007
0967-5868

2.2. In vitro SR101 labeling

U251 glioma cells were labeled by incubating 100,000 cells on a collagen-coated glass-bottom dish (MatTek, Ashland, MA, USA). After 24 hours, the medium was replaced with artificial cerebrospinal fluid (aCSF) containing 2 μM SR101 (Sigma-Aldrich, St Louis, MO, USA) for 20 minutes, followed by two 5 minute washes with standard aCSF.

2.3. Animals

Fifteen male Crl:NIH-Foxn1rnu rats (5 weeks of age) were obtained from The Charles River Laboratories International (Wilmington, MA, USA). Experiments were performed in accordance with the guidelines and regulations set forth by the USA National Institutes of Health Guide for the Care and Use of Laboratory Animals and were approved by the Institutional Animal Care and Use Committee of the Barrow Neurological Institute of St. Joseph's Hospital and Medical Center, Phoenix, AZ, USA.

2.4. Intracranial implantation

Rats were anesthetized by intramuscular injection of a mixture of 10 mg/kg xylazine and 80 mg/kg ketamine (Wyeth, Madison, NJ, USA) and placed in a small animal stereotactic headframe (Model 900, David Kopf Instruments, Tujunga, CA, USA). A 10 mm incision was made starting between the animal's eyes to expose bregma. A burr hole was made 3.5 mm lateral to bregma. U251 (nine rats) or MC116 cells (six rats) were infused at a depth of 4.5 mm below the surface of the brain after the syringe (Hamilton, Reno, NV, USA) was advanced 5.0 mm to create a 0.5 mm pocket. The cell suspension was infused using a UMP3-1 UltraMicroPump microinjector (WPI, Sarasota, FL, USA) set to a volume of 10 μL with an infusion rate of 3 μL/minute. The needle was withdrawn 2 minutes after the injection to minimize backflow of the cell suspension. The burr hole was covered with bone wax, the skin incision was sutured, and the rats were allowed to recover.

2.5. Acute slices

Twenty-eight days after implantation, rats were deeply anesthetized using the xylazine/ketamine mixture as described previously. They were immediately decapitated, and their brains were removed. Immediately, coronal slices (350 μm thick) were cut from the cerebral cortex on a Leica VT1200 vibratome (Leica Biosystems, Nussloch, Germany), in aCSF containing the following (in mM): 126 NaCl, 26 $NaHCO_3$, 2.5 KCl, 1.25 NaH_2PO_4, 2 $MgSO_4$, 2 $CaCl_2$ and 10 glucose, pH 7.4. Slices were then incubated at room temperature in aCSF containing 2 μM SR101 for 20 minutes followed by a 10 minute wash in aCSF. A two-tailed paired *t*-test with alpha set to 0.05 was used to compare mean fluorescence intensity between tumor cells and reactive astrocytes.

2.6. Co-labeling

SR101 is not amenable to fixation; we therefore used a fixable version of SR101 (Texas Red Hydrazide; Sigma-Aldrich) for these experiments. The staining pattern of fixable SR101 fluorophore mimics the staining pattern of the standard nonfixable SR101 [1,2]. For clarity, the use of the fixable version of SR101 is clearly indicated by the term "fixable-SR101" throughout the text. Fixable-SR101 and the nonfixable version had similar staining patterns, but the intensity and cellular staining of the fixable version was weaker than that of the standard SR101.

Acute xenograft slices were incubated with fixable-SR101, washed at room temperature, and fixed with 4% paraformaldehyde for 12 hours at 4°C. The sections were rinsed in phosphate-buffered saline, permeabilized with 0.3% Iriton, and blocked with CAS block (Invitrogen) [4]. The GBM xenograft slices (nine slices from three animals) were incubated in anti-GFAP primary antibody (EMD Millipore, Billerica, MA, USA; 1:500) for 12 hours, and the lymphoma sections (nine slices from three animals) were incubated in anti-CD20 primary antibody (EMD Millipore; 1:250) for 12 hours. Sections were then rinsed and incubated with Alexa-Fluor488 secondary antibody (Invitrogen), followed by 4′,6-diamidino-phenylindole (DAPI; Invitrogen) nuclear counterstain and mounted on slides with vectashield (Vector Laboratories, Burlingame, CA, USA) and number 1.5 coverslips (VWR, Radnor, PA, USA).

2.7. Stereology

We adapted standard stereology approaches to quantify tumor cells labeled with fixable-SR101 and GFAP or CD20 antibodies [5,6]. We selected one rostral, midline, and caudal acute slice from each brain containing tumor incubated with fixable-SR101. Glioma slices were immunofluorescently stained for GFAP, and slices containing lymphoma were stained for CD20. In each slice, 10 randomly selected tumor regions (150 μm^2) were optically sectioned to 50 μm with a Zeiss 710LSM (Carl Zeiss Surgical, Oberkochen, Germany). The first 5 μm of each image stack was discarded to minimize counts from cells damaged during sectioning. A maximum intensity projection image was generated from the remaining 45 μm, and a stereology dissector was overlaid onto the image. Cells within the dissector and those in contact with its left and bottom edges were counted for either GFAP or CD20 positivity and for SR101 positivity.

The percent overlap between immunostaining and SR101 positivity was calculated. Two-tailed *t*-tests with alpha levels of 0.05 were used to determine statistical differences. A paired *t*-test was used to determine if staining localization between antibody and SR101-labeling differed between cell types. An unpaired *t*-test was used to compare fixable-SR101 staining between glioma and lymphoma models.

2.8. Imaging

SR101-labeled samples were placed in uncoated number 1.5 glass-bottom dishes and positioned on the stage of a Zeiss 710 laser scanning confocal microscope equipped with a 40 ×/1.2 NA water immersion objective (Carl Zeiss Surgical). We imaged SR101 by exciting the fluorophore with a 561 nm diode laser and collecting 595 nm to 625 nm emissions. The confocal aperture was set to one Airy unit for imaging. The laser and gain values were set to fill the dynamic range of the photomultiplier tube, and the frame size was set to sample at Nyquist. Images were collected in 8 and 12-bit format absent of nonlinear processing.

2.9. Rapid uptake

To establish the time course of SR101 uptake, U251 astrocytoma cells were visualized using the confocal microscope as previously described. Astrocytoma cells were cultured on number 1.5 glass-bottom dishes and placed on the stage of an inverted confocal microscope. Time lapse images were collected 30 seconds prior to addition of SR101 to 7 minutes post-incubation. Change in fluorescence intensity of astrocytoma cells and background was calculated with ImageJ software (National Institutes of Health, Bethesda, MD, USA).

3. Results

3.1. SR101 labels human astrocytoma cells and reactive astrocytes

To investigate the potential of SR101 for identifying human astrocytoma cells, we used differential interference contrast with fluorescence overlay to image human astrocytoma cell line U251 after incubation in SR101 (six cultures). The fluorophore filled the cytoplasm of the cultured cells and clearly delineated cell nuclei (Fig. 1A, B).

Next, human astrocytoma cells (U251 cell line) were implanted into the caudate-putamen of six nude rats and allowed to grow for 4 weeks before the rats were sacrificed. This orthotopic xenograft model consistently produced astrocytic tumors as previously characterized [7,8]. Live cell confocal images of acute slices from the cerebral cortex of the implanted animals (Fig. 1C) treated with SR101 showed cells in the tumor core markedly labeled with the fluorophore. The cells were easily distinguished from low level background staining (Fig. 1D–F).

Confocal microscopy imaging of the acute slices treated with SR101 also showed distinct tumor margins that contained SR101-positive astrocytoma cells and reactive astrocytes (Fig. 1G, H). The fluorescence intensity from the astrocytoma cells and reactive astrocytes was quantified. The mean fluorescence intensity did not differ between the two cell types (Fig. 1I). However, reactive astrocytes were easily distinguished based on their distinct morphology (Fig. 1H). Therefore, SR101 can rapidly identify astrocytes and astrocytoma cells in cell culture and animal models, and it can effectively define tumor margins in an animal model.

3.2. Fixable-SR101 labels GFAP-positive human astrocytoma cells and reactive astrocytes

We used confocal microscopy to compare the efficacy and localization of SR101 and GFAP staining. Confocal images from the tumor core regions showed numerous cells simultaneously filled with fixable-SR101 and labeled by GFAP (Fig. 2A–D). In general, GFAP and SR101 labeled the same cells, although

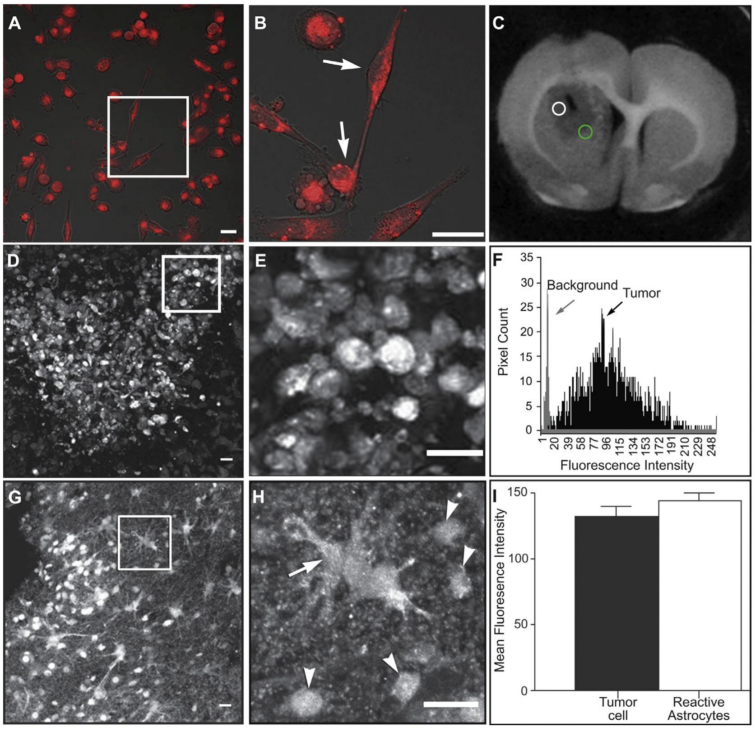

Fig. 1. Non-fixable sulforhodamine 101 (SR101) labels human astrocytoma cells in culture and identifies tumor core and margin in rodent xenografts. (A–B) U251 astrocytoma cell culture. (A) Differential interference contrast image with fluorescent overlay of human U251 astrocytoma cells incubated with SR101. (B) High magnification of inset in (A) demonstrates cytoplasmic filling of cells and delineation of cell nuclei (arrows). (C–H) Acute slices from rodents intracranially implanted with U251 cells. (C) Acute slice containing U251 derived tumor. Representative core and margin regions identified by white circle and green circle, respectively. (D) Confocal fluorescence image of SR101-labeled tumor core. (E) High magnification of inset in (D) shows typical morphology of U251cells. (F) Histogram of SR101 fluorescence distribution in (E) between tumor core and background. Note the clear distinction in mean fluorescence intensity (MFI) between tumor (102.84) and background (8.74). (G) Image of acute slice tumor margin with SR101-labeled cells. (H) Inset of morphologically identified reactive astrocyte (arrow) surrounded by glioma cells (arrowheads) near tumor margin from (G). (I) MFI of U251 cells and reactive astrocytes normalized to background (three acute slices from three rats) showing no significant difference in MFI between the two cell types. Scale bars = 20 μm. *Used with permission from Barrow Neurological Institute.*

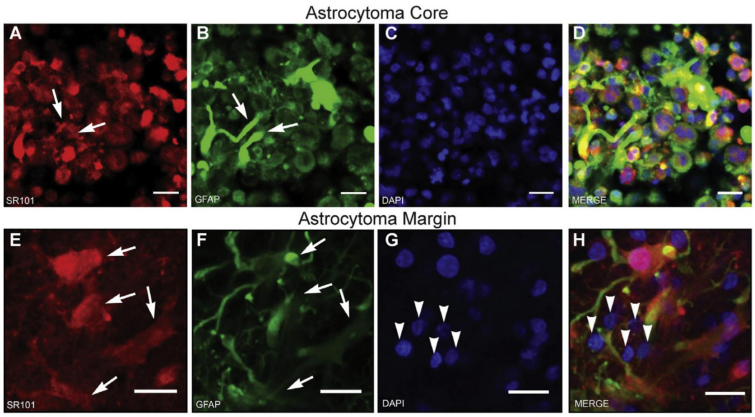

Fig. 2. Fixable-sulforhodamine 101 (SR101) co-localizes with the astrocytic marker glial fibrillary acidic protein (GFAP). (A) Confocal imaging of rodent xenograft acute slices incubated in fixable-SR101. Following incubation, slices were fixed and stained with (B) GFAP and (C) 4′,6-diamidino-phenylindole (DAPI). Images are from the core of the astrocytoma. Fixable-SR101 fills the cell bodies of GFAP-positive cells in the tumor core and weakly fills astrocytic processes (arrows). (D) GFAP, DAPI and SR101 overlap considerably in the merged image. (E–H) Images from the margin of the astrocytoma. Fixable-SR101 fills cell bodies of GFAP-positive cells at the tumor margin. Solid arrows identify (E) SR101-positive and (F) GFAP-positive cells. Note the appearance of (G) DAPI positive cells (arrowheads) unlabeled by SR101 or GFAP that are selectively observed at the astrocytoma margin. (H) Merged image from tumor margin. Scale bars = 20 μm. *Used with permission from Barrow Neurological Institute.*

fixable-SR101 stained some cellular processes less intensely than GFAP (Fig. 2A, B, D). Merged images from the tumor core showed that most cells were positive for both fixable-SR101 and GFAP, indicating that SR101 effectively labels astrocytic tumor cells.

We compared the staining pattern of fixable-SR101 and GFAP to determine if reactive astrocytes could be differentiated from neoplastic astrocytes to help identify tumor borders. Imaging of rat brain regions adjacent to human astrocytoma cells showed that the staining patterns of fixable-SR101 and GFAP were similar (Fig. 2E, F). However, GFAP labeled membrane processes more thoroughly than the fixable-SR101. Cells in the peripheral regions contained extensive membrane projections that could be readily differentiated from cells within the tumor core that lacked this feature. When additional cells in these regions were stained with DAPI (Fig. 2G), groups of cells were negative for both fixable-SR101 and GFAP (Fig. 2G, H). These findings suggest a mixed cell population of tumor cells and nontumor brain cells typical of regions outside the tumor core. Together, the data indicate that SR101-positive cells are the GFAP-positive astrocytoma cell population. Furthermore, fixable-SR101 provides morphological information that appears to differentiate astrocytoma cells from reactive astrocytes.

3.3. SR101 differentiates astrocytoma from lymphoma

In contrast to the findings from astrocytoma cells, confocal imaging indicated minimal SR101 signal from the human CNS lymphoma cell line MC116 (Supp. Fig. 1). In acute slices from astrocytoma and CNS lymphoma animal models incubated with fixable-SR101, we quantified co-localized GFAP for astrocytoma slices and CD20 for lymphoma slices. In astrocytoma tumor regions, fixable-SR101 labeled the majority of cells (Fig. 3A–D, I). The frequency of co-localization of SR101 and GFAP was 86.50% (Fig. 3K, Table 1), with a mean of 22.30 SR101-positive cells and 20.58 GFAP-positive cells per stereology dissector region of interest (ROI) ($p = 0.0004$, Fig. 3I, Table 1). In contrast, fixable-SR101 labeled only a very small number of cells from ROI in CNS lymphoma acute slices (Fig. 3E). SR101 and CD20 co-localized poorly (2.19%), and there were significantly more CD20-positive cells than fixable-SR101-positive cells ($p < 0.0001$) (Fig. 3J, Table 1). However, SR101 labeled a small number of cells in CNS lymphoma tissue that were not CD20-positive and that morphologically resembled reactive astrocytes (Fig. 3E, F). SR101 distinguished astrocytoma from lymphoma tissue and co-localized with GFAP more frequently than CD20 (Fig. 3K). This finding demonstrates the strong relationship of SR101 to GFAP-positive cells in astrocytoma, and the ability of SR101 to differentiate an astrocytic from a non-astrocytic tumor such as CNS lymphoma.

3.4. SR101 uptake is rapid

Astrocytoma cells exposed to SR101 in cell culture took up the fluorophore within 1 minute of incubation. One minute after incubation, astrocytoma cells concentrated SR101 to approximately twice the fluorescence intensity of background, and within 3 minutes contained approximately six times the fluorescence intensity compared to background. These data show the utility of SR101 for rapidly labeling astrocytoma cells in culture (Supp. Fig. 2, 3).

4. Discussion

We have demonstrated a technique for identifying the most common primary brain tumor, astrocytoma, in animal models by *ex vivo* exposure to the fluorescent agent SR101. We tested the specificity of SR101 in human cell culture and orthotopic rodent xenografts. We found SR101-labeling to be preserved in cell culture and animal models of astrocytoma. Compared to GFAP immunocytochemistry, SR101 provided more rapid and equally accurate identification of astrocytic tumors. Our results clearly indicate the potential utility of SR101 for rapidly identifying an astrocytic neoplasm. Compared to *ex vivo* tissue from a negative control animal model, we found SR101 staining could differentiate astrocytoma and CNS lymphoma within 30 minutes of biopsy. Our rapid incubation experiments in cell culture suggest that this time frame could be compressed substantially further.

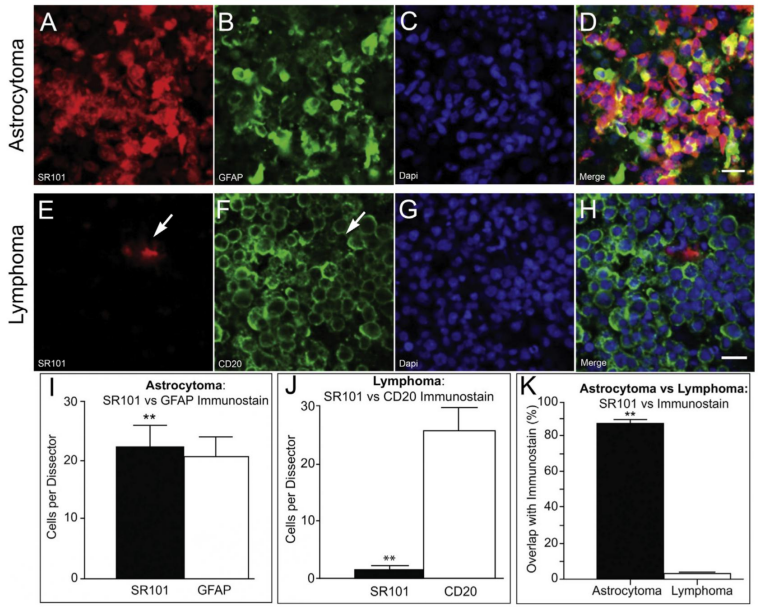

Fig. 3. Sulforhodamine 101 (SR101) rapidly differentiates human astrocytoma from central nervous system (CNS) lymphoma in rodent xenografts. Confocal imaging of acute slices from xenograft animals implanted with astrocytoma cells (U251, top row) or lymphoma cells (MC116, middle row). Slices were stained with fixable-SR101 and specific markers for astrocytoma, glial fibrillary acidic protein (GFAP), or lymphoma (CD20). Nuclei were counterstained with 4′,6-diamidino-phenylindole (DAPI). (A–D) Region from U251 astrocytoma acute slice incubated with fixable-SR101 and counterstained with GFAP and DAPI. (E) SR101 labels a single cell (arrow) in a MC116 xenograft lymphoma region. (F) CD20 immunostaining labels lymphoma cells but does not label region containing SR101-positive cell (arrow). (G) DAPI counterstain of cell nuclei in field of view. (H) Merged lymphoma image indicating poor colocalization of SR101 and CD20. Scale bars = 20 μm. (I–K) Confocal stereology of acute slices. (I) Number of SR101-positive cells slightly outnumber GFAP-positive cells in U251 xenograft astrocytoma regions ($p = 0.0004$). (J) Difference in number of SR101-positive and CD20-positive cells present in MC116 xenograft lymphoma regions is highly significant ($p < 0.0001$). (K) SR101 significantly overlaps with GFAP-positive astrocytoma cells (86.50%) compared with CD20 lymphoma cells (2.19%, $p < 0.0001$). *Used with permission from Barrow Neurological Institute.* vs = *versus.*

Table 1
Co-localization of immunostain-positive and sulforhodamine 101-positive cells from stereology

Tumor	Immunostain	Immunostain positive	SR101 positive	Percent overlap	Total cells counted
Astrocytoma	GFAP	20.58 ± 3.26	22.30 ± 3.55	86.50 ± 1.86	1316
Lymphoma	CD20	25.61 ± 4.05	1.58 ± 0.32	2.20 ± 0.47	1657

GFAP = glial fibrillary acidic protein, SR101 = sulforhodamine 101.
Data are presented as mean ± standard deviation.

We chose a U251 immortalized GBM cell line for this model because, compared to more invasive models, it is easier to distinguish the border zone of the tumor and therefore distinguish tumor cells from native astrocytes. In future studies, additional astrocytoma models will need to be validated for their SR101 avidity.

U251 cells are largely GFAP-positive. GBM contains a heterozygous population of cells that vary in terms of GFAP expression [9]. SR101 labeled slightly more tumor cells in our GBM xenografts than GFAP. This finding resembles data from normal brain showing that SR101 identifies subtypes of astrocytes and precursor cells that are GFAP-negative [2,10]. Future studies on SR101 are needed to identify and characterize GBM precursor cells that uptake SR101. A direct comparison of the sensitivity of SR101 and GFAP in human brain tumors obtained at surgery is being pursued by our group.

These findings have important implications for astrocytoma research, since SR101 can be used to identify astrocytic tumor cells in both *in vitro* and *ex vivo* settings in a more rapid time frame than has previously been possible. In addition, the fact that SR101-labeling appears to occur within minutes could represent an opportunity for clinical neuropathology, in that it could be used intraoperatively to provide a definitive diagnosis that a given tumor is of glioma lineage. While SR101 does not distinguish astrocytoma from astrocytes (also a limitation of GFAP), it is interesting that the selective uptake of SR101 is preserved in malignant astrocytic cells. Further work is required to determine the exact mechanism of uptake. Any variation in the uptake mechanism between astrocytoma and astroctyes could represent an opportunity for a selective therapy.

5. Conclusion

SR101 rapidly and selectively labels human and rodent astrocytic tumor cells. In an orthotopic xenograft model, SR101

staining retained its specificity. This method could provide utility in neuro-oncology research. This technique also provides proof of concept for a method to provide a clinically meaningful immediate *ex vivo* neuropathological diagnosis.

Conflicts of interest/disclosures

The authors declare that they have no financial or other conflicts of interest in relation to this research and its publication.

Acknowledgements

This work was supported by a Barrow Neurological Foundation grant to Peter Nakaji and Jennifer Eschbacher.

Appendix A. Supplementary data

Supplementary data associated with this article can be found, in the online version, at http://dx.doi.org/10.1016/j.jocn.2014.02.007.

References

[1] Nimmerjahn A, Kirchhoff F, Kerr JN, et al. Sulforhodamine 101 as a specific marker of astroglia in the neocortex in vivo. Nat Methods 2004;1:31–7.
[2] Kafitz KW, Meier SD, Stephan J, et al. Developmental profile and properties of sulforhodamine 101–labeled glial cells in acute brain slices of rat hippocampus. J Neurosci Methods 2008;169:84–92.
[3] Lai CP, Bechberger JF, Thompson RJ, et al. Tumor-suppressive effects of pannexin 1 in C6 glioma cells. Cancer Res 2007;67:1545–54.
[4] Beeman SC, Georges JF, Bennett KM. Toxicity, biodistribution, and ex vivo MRI detection of intravenously injected cationized ferritin. Magn Reson Med 2012;69:853–61.
[5] Kim JH, Lee JE, Kim SU, et al. Stereological analysis on migration of human neural stem cells in the brain of rats bearing glioma. Neurosurgery 2010;66:333–42.
[6] Mouton PR. Principles and practices of unbiased stereology: an introduction for bioscientists. United States: John Hopkins University Press; 2002.
[7] Buckingham SC, Campbell SL, Haas BR, et al. Glutamate release by primary brain tumors induces epileptic activity. Nat Med 2011;17:1269–74.
[8] Michaud K, Solomon DA, Oermann E, et al. Pharmacologic inhibition of cyclin-dependent kinases 4 and 6 arrests the growth of glioblastoma multiforme intracranial xenografts. Cancer Res 2010;70:3228–38.
[9] Bonavia R, Inda MM, Cavenee WK, et al. Heterogeneity maintenance in glioblastoma: a social network. Cancer Res 2011;71:4055–60.
[10] Kimelberg HK. The problem of astrocyte identity. Neurochem Int 2004;45:191–202.

APPENDIX D

LABEL-FREE MICROSCOPIC ASSESSMENT OF GLIOBLASTOMA BIOPSY SPECIMENS PRIOR TO BIOBANKING

This article has been updated from its originally published version to correct the title.

Neurosurg Focus 36 (2):E8, 2014

Label-free microscopic assessment of glioblastoma biopsy specimens prior to biobanking

***Joseph Georges, B.S.,[1,6] Aqib Zehri, B.S.,[1,7] Elizabeth Carlson, B.S.,[5] Joshua Nichols, B.A.,[4] Michael A. Mooney, M.D.,[2] Nikolay L. Martirosyan, M.D.,[1,8] Layla Ghaffari,[5] M. Yashar S. Kalani, M.D., Ph.D.,[2] Jennifer Eschbacher, M.D.,[3] Burt Feuerstein, M.D., Ph.D.,[7] Trent Anderson, Ph.D.,[4] Mark C. Preul, M.D.,[1] Kendall Van Keuren-Jensen, Ph.D.,[5] and Peter Nakaji, M.D.[2]**

[1]Neurosurgery Research Laboratory, [2]Division of Neurological Surgery, and [3]Division of Neuropathology, Barrow Neurological Institute, St. Joseph's Hospital and Medical Center, Phoenix; [4]Department of Basic Medical Sciences, The University of Arizona College of Medicine, Phoenix; [5]Neurogenomics Division, Translational Genomics Research Institute, Phoenix; [6]School of Life Sciences, Arizona State University, Tempe; [7]College of Medicine, The University of Arizona, Phoenix; and [8]Division of Neurosurgery, Department of Surgery, The University of Arizona, Tucson, Arizona

Glioblastoma is the most common primary brain tumor with a median 12- to 15-month patient survival. Improving patient survival involves better understanding the biological mechanisms of glioblastoma tumorigenesis and seeking targeted molecular therapies. Central to furthering these advances is the collection and storage of surgical biopsies (biobanking) for research. This paper addresses an imaging modality, confocal reflectance microscopy (CRM), for safely screening glioblastoma biopsy samples prior to biobanking to increase the quality of tissue provided for research and clinical trials. These data indicate that CRM can immediately identify cellularity of tissue biopsies from animal models of glioblastoma. When screening fresh human biopsy samples, CRM can differentiate a cellular glioblastoma biopsy from a necrotic biopsy without altering DNA, RNA, or protein expression of sampled tissue. These data illustrate CRM's potential for rapidly and safely screening clinical biopsy samples prior to biobanking, which demonstrates its potential as an effective screening technique that can improve the quality of tissue biobanked for patients with glioblastoma.
(*http://thejns.org/doi/abs/10.3171/2013.11.FOCUS13478*)

Key Words • **glioblastoma** • **confocal reflectance microscopy** • **biobank** • **biopsy**

Each year, more than 22,000 Americans are diagnosed with high-grade gliomas. More than half of these brain tumors are glioblastomas, the most aggressive and essentially noncurable form of this disease.[3] Standard treatment for newly diagnosed glioblastoma is resection followed by ionizing radiation and chemotherapy.[11] However, current therapeutic approaches provide minimal survival benefit, with median survival remaining formidably at 12 months and 2-year survival remaining less than 30%.[8,16]

A key component to improving patient survival involves a better understanding of the biological mechanisms in tumor formation and seeking targeted molecular therapies.[13] With recent advances in medical genetics, computational biology, and biotechnology, novel molecular approaches such as immunotherapy, vaccine therapy, and gene therapy are being extensively explored in treating brain tumors. Furthering these advances requires collecting surgical biopsy specimens (biobanking) to study gliomagenesis and to assess a patient's eligibility for potentially life-prolonging clinical trials. Unfortunately, due to the necrotic features of malignant gliomas and our inability to assess tissue prior to biobanking, a large portion of biobanked glioblastoma samples lack appropriate cellularity to be used in these two research arenas. A method for safely screening tissue biopsies prior to biobanking is needed to increase the quality of tissue provided for research and clinical trials.

Confocal reflectance microscopy (CRM) is an optical imaging modality that can rapidly assess tissue without physical manipulation or application of exogenous contrast agents.[1,17] In CRM, a laser is raster-scanned across a specimen without generating a detectable Stokes shift. Photons from the laser are scattered back toward

Abbreviations used in this paper: Akt = protein kinase B; CRM = confocal reflectance microscopy; DAPI = 4,6-diamidino-2-phenylindole dihydrochloride; GAPDH = glyceraldehyde-3-phosphate-dehydrogenase; RIN = RNA integrity number.

* Mr. Georges and Mr. Zehri contributed equally to this work.

the objective and passed through a confocal aperture. This allows multiple optical sections to be collected from a sample without physical sectioning. When applied to thick tissue samples, CRM can identify individual cells and structural components within the tissue.[1] Compared with other optical sectioning techniques such as fluorescence confocal microscopy, structured illumination, or nonlinear microscopy, CRM introduces a fraction of the energy into tissue samples that is encountered with these other techniques. Thus, CRM is theoretically less likely to alter tissue characteristics by generation of free radicals or thermal energy.

We hypothesize that CRM will provide a safe and rapid means for screening glioblastoma tissue prior to biobanking. In this study we used CRM to assess tissue cellularity from rodent glioma models, and subsequently evaluated the molecular integrity of tissue imaged with CRM. Lastly, we assessed CRM on clinical samples with a pathology-based CRM system. Our data illustrate CRM's potential for screening clinical biopsy samples prior to biobanking, which can augment information gained from resected tissue for molecular and translational research and for determining the eligibility of patients with glioblastoma for enrollment into clinical trials. Although numerous applications for intraoperative CRM exist, the goal of this study is to determine its efficacy as a rapid screening technique that will improve the quality of tissues collected and biobanked for glioblastoma research.

Methods

Intracranial Implantation

Nude rats were acquired from Charles River Laboratories. Five rats were anesthetized by intramuscular injection of a mixture of 10 mg/kg xylazine and 80 mg/kg ketamine (Wyeth) and placed in a small animal stereotactic headframe (Model 900, David Kopf Instruments). A 10-mm incision was made starting between the animal's eyes to expose bregma. A bur hole was made 3.5 mm lateral to bregma. Human glioma cells (U251; ATCC) were infused at a depth of 4.5 mm below the surface of the brain after the syringe (Hamilton) was advanced 5.0 mm to create a 0.5-mm pocket. The cell suspension was infused using a UMP3–1 UltraMicroPump microinjector (WPI) set to a volume of 10 µl with an infusion rate of 3.00 µl/min. The needle was withdrawn 2 minutes after the injection to minimize backflow of the cell suspension. The bur hole was covered with bone wax and the skin incision was sutured prior to the rats emerging from anesthesia. All animal procedures were performed according to principles outlined in the NIH *Guide for the Care and Use of Laboratory Animals.*

Rodent Tissue

Twenty-eight days after implantation, rodents with xenografts were deeply anesthetized using xylazine and ketamine (as described above), and whole brain specimens were collected. Coronal slices (350 µm thick) were cut from the cerebrum on a Leica VT1200 vibratome and placed in artificial CSF containing the following (in mM): 126 NaCl, 26 $NaHCO_3$, 2.5 KCl, 1.25 NaH_2PO_4, 2 $MgSO_4$, 2 $CaCl_2$ and 10 glucose, pH 7.4). Slices were then fixed in 4% paraformaldehyde at 4°C overnight and washed 3 times with phosphate-buffered saline. Three tumor-containing slices per animal were incubated with DAPI for 45 minutes at room temperature, rinsed 3 times with phosphate-buffered saline, and placed into no. 1.5 glass-bottom dishes (MatTek) for imaging. A coefficient of determination analysis was used to compare cells identified with CRM to cells labeled with DAPI.

The 2 rodents used for molecular experiments were deeply anesthetized using xylazine and ketamine and rapidly decapitated. Whole brains were placed in ice-cold artificial CSF and sectioned into 1-mm coronal sections using a rodent brain block. The cerebrum from each section was blocked into 4 equivalent sections. Two sections were immediately frozen in liquid nitrogen for reference. At 15, 30, 45, 60, 90, and 120 minutes, 2 sections were placed into glass-bottom dishes. At each time point, the cortex, corpus callosum, and caudate/putamen from 1 section was imaged with CRM. As a control, 1 section was simultaneously placed on the stage of the microscope but not imaged. Next, each section was frozen in liquid nitrogen for assessment of DNA, RNA, and protein.

Imaging

All samples were imaged in uncoated no. 1.5 glass-bottom dishes. Confocal reflectance microscopy was conducted with a Zeiss inverted 710 laser-scanning confocal microscope equipped with a ×40/1.2 numerical aperture water emersion objective. For reflectance imaging, a 633-nm diode laser was raster scanned across the sample, and reflected photons were collected by tuning the emission filters to allow photons with the same wavelength of the incident laser passage to the photomultiplier tube. For DAPI imaging, samples were excited with a 405-nm diode laser and 430–490 nm emission was collected. The confocal aperture was set to 1 Airy unit for all imaging. The laser and gain values were set to fill the dynamic range of the photomultiplier tube, and the frame size was set to sample at Nyquist. Images were collected in 12-bit format absent of nonlinear processing.

DNA Isolation and Analysis

DNA was isolated from brain tissue using the QIAamp DNA Mini (Qiagen), per the manufacturer's instructions. DNA was quantified using the Nanodrop Spectrophotometer (Thermo Scientific). Samples were loaded in equal concentrations (100 ng) in a 1% agarose gel with ethidium bromide and imaged on an Alpha Imager.

RNA Isolation and Analysis

Tissue was homogenized in 500 µl of Ambion's Cell Disruption Buffer (Life Technologies) and subsequently isolated using Ambion's mirVana Paris kit (Life Technologies), per the manufacturer's instructions. RNA concentrations were determined using the Nanodrop Spectrophotometer (Thermo Scientific), which gave dilutions necessary to remain within the dynamic range of the Bioanalyzer. The integrity of the RNA was assessed using Agilent 2100 Bioanalyzer Nanochips (Agilent Technologies).

Western Blot Analysis

Frozen tissue was sectioned on dry ice and designated for protein, RNA, or DNA analysis. Protein lysate was made by placing brain sections into 750 μl of Ambion's Cell Disruption Buffer (Life Technologies), triturated using RNase-free pipettes, and sonicated using Covaris Sonolab at 2%–5% for 5 seconds, 2%–20% for 15 seconds, 2%–20% for 15 seconds, and 2%–5% for 5 seconds (Covaris Inc).

Protein concentrations were quantified by bicinchoninic acid assay, and 18 μg/lane was loaded in 4%–12% Bis-Tris gels and run using NuPage electrophoresis reagents (Invitrogen). Protein was transferred onto Novex nitrocellulose membrane (Invitrogen) and thereafter incubated for 1 hour in a blocking solution consisting of 5% bovine serum albumin (Sigma Aldrich) in tris-buffered saline with 0.1% Tween (Thermo Fisher Scientific). Primary antibodies were incubated for 12 hours at 4° C while secondary horseradish peroxidase–conjugated antibodies were incubated for 1 hour at room temperature. Blots were probed for protein kinase B (Akt; 1:1000, Cell Signaling) and GAPDH (1:60,000, Millipore). Horseradish peroxidase–conjugated secondary antibodies were anti-rabbit (1:2000, Cell Signaling) and anti-chicken (Millipore).

Blots were developed by using Pierce SuperSignal Chemiluminescent Substrate (Thermo Fisher Scientific) per the manufacturer's instructions. Protein signal was detected on radiographic film (General Electric).

Statistical Analysis

A coefficient of correlation (R^2 value) was determined between DAPI-stained nuclei and nuclei detected by CRM using Graphpad Prism. Differences were considered statistically significant for probability < 0.05. The Agilent 2100 Bioanalyzer provided an RNA integrity number (RIN), calculated algorithmically by including the 28s/18s (ribosomal subunit) ribosomal RNA bands, the region before the peaks, signal areas, and intensities. An elevated threshold baseline and a decreased 28s/18s ratio are both indicative of RNA degradation, while high 28s and 18s ribosomal RNA peaks as well as a small amount of 5s RNA or an RNA number greater than 7.5 are indicative of intact RNA.[7] Image J was used to determine density (intensity) of bands on a Western blot. Data analysis consisted of determining relative density. Results were expressed as means and mean square error (SEM) data with normal distribution that were compared by 1-way ANOVA and a Student t-test.

Clinical Samples

The clinical research was approved by the Institutional Review Board of St. Joseph's Hospital and Medical Center and Barrow Neurological Institute, where all surgery was performed. Preoperatively, patients signed an informed consent form for participation. Samples (mean size 4 mm × 2 mm × 2 mm) were obtained at the time of craniotomy from within the tumor mass at a location determined to be safe by the surgeon. Tissue samples were placed in ice-cold artificial CSF and transported from the operating room to the pathology-based CRM system. There, the samples were immediately placed in no. 1.5 glass-bottom dishes and imaged. Investigators conducting imaging experiments were unaware of the pathological diagnosis at the time of imaging. Final diagnosis was determined by traditional immunohistochemical analysis and paraffin-embedded H & E staining of the sampled tissue. For the purpose of comparisons, the histopathological diagnosis made by a board-certified neuropathologist (J.E.) was accepted as the final diagnosis.

Results

Differentiating Neoplastic Cellular Tumor From Acellular Tissue

To investigate the potential of reflectance imaging to identify tissue cellularity, we first imaged normal rat brain. We found that CRM adequately contrasted normal brain cytoarchitecture, such as cell bodies and axons, as well as blood vessels (Fig. 1). This prompted us to test the utility of CRM to differentiate cellular and acellular tumor biopsy regions by imaging acute slices generated from rodent glioblastoma xenografts. We incubated slices with DAPI to label all cell nuclei and we subsequently imaged the slices with CRM and laser-scanning confocal microscopy (n = 15 slices from 5 animals). We collected 5 images per acute slice and compared cells identified with CRM to cells identified with DAPI. We found CRM provided definitive contrast between cell nuclei, cytoplasm, and extracellular tissue. Within tumor regions, CRM provided contrast to visualize hypercellular tumor regions (Fig. 2A–C) and relatively acellular peritumoral regions with isolated cell populations (Fig. 2E–G). In hypercellular ($r^2 = 0.97$) and acellular regions ($r^2 = 0.098$) we found CRM contrast strongly correlated with cells labeled with DAPI (Fig. 2D and H).

Effect of CRM on the Molecular Characteristics of Examined Tissue

To determine if CRM alters the molecular characteristics of tissue, we compared DNA, RNA, and protein from tissue imaged with CRM to tissue immediately frozen for analysis and tissue that had reflectance imaging and was left out for varying amounts of time. Although the typical time from resection to reception in pathology and assessment using CRM typically takes 15 minutes, we tested for as long as 180 minutes postresection. Neoplastic tissues are heterogeneous in terms of cellularity and gene and protein expression and may yield interspecimen molecular variability. Therefore, we conducted these experiments on control tissue harvested from rodent normal brain.

DNA quality was assessed in CRM-imaged samples, which showed no differences compared with immediately frozen controls. Discrete DNA bands were detectable up to 180 minutes after extraction (Fig. 3B), suggesting no degradation of DNA elements. An RIN was generated to determine the integrity of isolated RNA. An RIN of 1 suggests strong degradation while an RIN greater than 8 suggest minimal degradation.[3] The RIN was comparably the same between control and CRM-imaged groups (Fig.

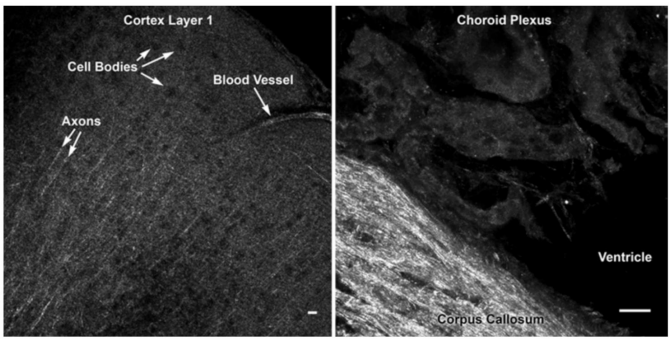

Fig. 1. Acute slices of normal rat brain from the cortex (left) and ventricle and corpus callosum (right) shown using contrast-free reflectance imaging. Left: Confocal reflectance microscopy contrasts cell bodies, axons, and blood vessels in normal rat brain. Cell bodies appear as multiple hypointense circular regions within the tissue. Note the typical lack of cell bodies contrasted in Layer 1 of the cortex. Myelinated axons are visualized as hyperintense fibers extending from cell bodies. Right: White matter tracts in the corpus callosum generate a hyperintense reflectance signal. Individual cell bodies are contrasted in the choroid plexus. A lack of signal is appreciated from the fluid-filled ventricle. Bar = 20 μm.

3C), indicating no effect of CRM on RNA integrity of imaged samples. RNA integrity remained relatively the same up to 120 minutes after biopsy. There was a slight decrease after 120 minutes after biopsy in RIN value that was similar for both the control and CRM tissue, likely due to RNases within the tissue over time. Protein kinase B, a protein involved in glioblastoma pathogenesis, was examined for potential damage after imaging with CRM.

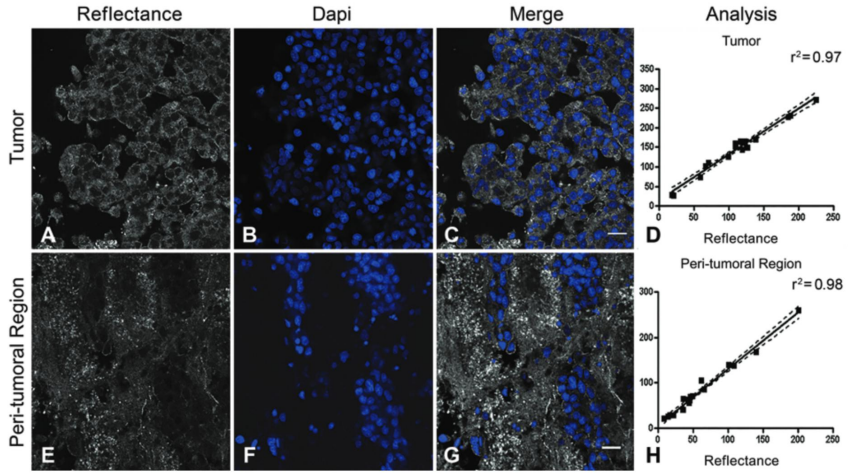

Fig. 2. Confocal reflectance imaging identifies cellular tumor in rodent acute slices. A: Reflectance image of rodent xenograft tumor region; note hypointense cell nuclei. B: DAPI stain of identical tumor region identifies all cells in the field of view. C: Merged image shows location of cells contrasted by reflectance in comparison with cells labeled with DAPI. Bar = 20 μm. D: Plot of coefficient of determination and 95% CIs for tumor cells identified by reflectance imaging ($r^2 = 0.97$). The solid line is the best fit slope. The dotted lines mark the 95% CIs. The dots are the counts from each region of interest. The y axis is actual number of cells (per DAPI staining), and the x axis shows cells counted by reflectance imaging. E: Reflectance image of cellular tumor and adjacent acellular region from rodent xenograft; note isolated cell populations. F: Fluorescence confocal image of identical region labeled with DAPI. G: Merged image of reflectance and fluorescence images from tumor and peritumoral tissue interface. H: Plot of coefficient of determination and 95% CIs for cells identified by reflectance imaging at tumor and acellular tissue interface ($r^2 = 0.98$). Bar = 20 μm.

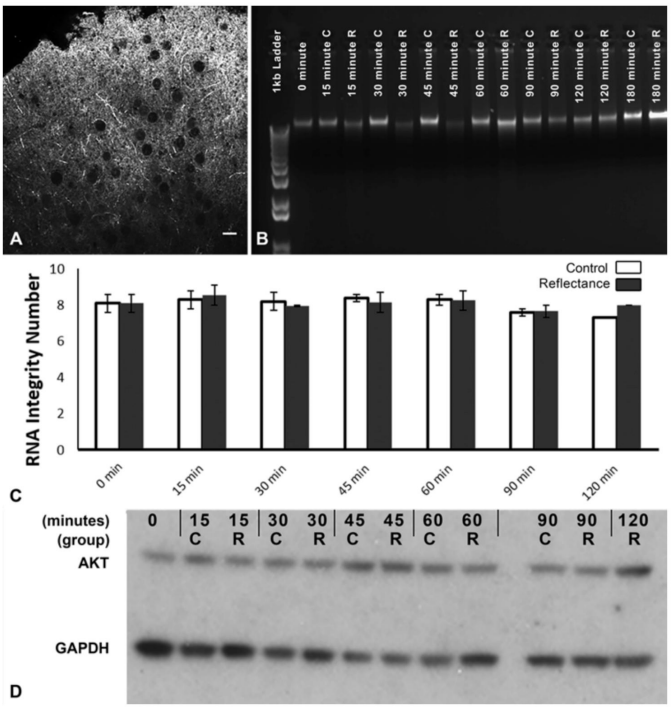

Fig. 3. Images showing CRM does not alter DNA, RNA, or protein of examined tissue in rodent brain. A: Confocal reflectance microscopy image of fresh brain tissue at the cerebral cortex obtained 90 minutes after excision. Bar = 20 μm. B: Gel electrophoresis of genomic DNA extracted from control (C) and CRM-imaged biopsies (R); note similar bands across the time course between imaged and control biopsies. C: Time course comparison of RNA integrity for all imaged and control samples. Note similar RNA integrity for all samples. D: Western blot analysis showing expression of Akt over a 120-minute time course. The protein signal did not degrade over the time course or when exposed to CRM. The GAPDH loading control shows a similar amount of protein lysate was loaded into each well of the Western blot.

Western blot analysis of extracted tissue showed that up to 120 minutes after extraction, discrete Akt bands were detectable and contained similar density to control samples (Fig. 3D).

Differentiating Human Cellular From Acellular Brain Tumor Biopsies

To test the ability of CRM to differentiate cellular tumor from acellular tissue samples in a clinical setting, we imaged 2 fresh human brain tumor biopsy specimens: 1 yielding radiation necrosis tissue and 1 with known glioblastoma cellular tissue. Tissue samples were placed in ice-cold artificial CSF and imaged with CRM. Imaging time per sample was less than 2 minutes. Samples were then compared with final histopathological diagnosis.

Similar to our findings in rodent xenografts, we found that CRM contrasted cellular regions from acellular regions in human biopsy samples. Tissue samples identified as cellular with CRM were found to be cellular with subsequent histopathological assessment (Fig. 4A and C). Confocal reflectance microscopy correctly identified acellular regions in necrotic tissue samples (Fig. 4B and D).

Discussion

Our data illustrate the utility of CRM as a safe and rapid technique for identifying the cellularity of glioma tissue prior to biobanking. This imaging modality can be immediately used on fresh tissue samples without application of exogenous contrast agents and without altering the molecular characteristics of examined tissue. Confocal reflectance microscopy can provide a much-needed tool for neurosurgery and neuropathology teams by maximizing the quality of tissue samples collected during resection. Although other imaging modalities may provide excellent images, their greater energy and the possible

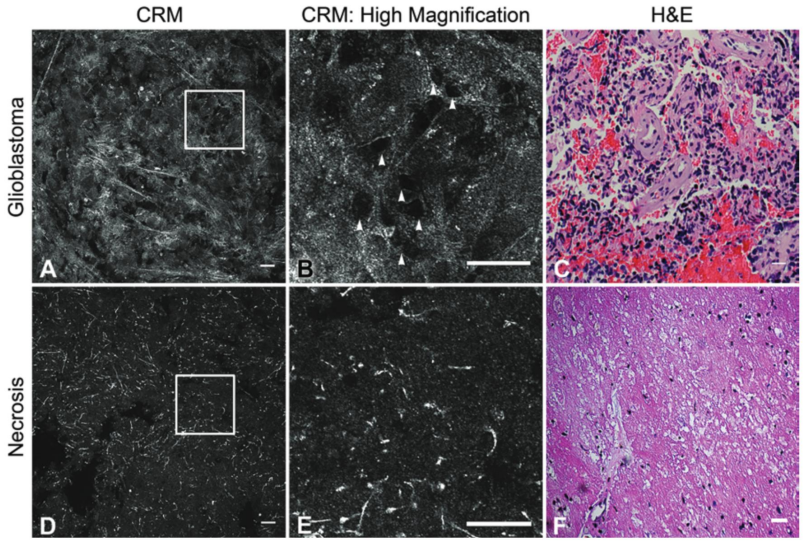

Fig. 4. Reflectance imaging immediately identifies cellular and necrotic fresh human brain tumor biopsies. A: Low-magnification CRM image of ex vivo human glioblastoma biopsy specimen imaged with CRM. B: High magnification of cellular region shown in panel A. Note arrowheads identifying cells within the region. C: Corresponding H & E image from panel B. D: Low magnification image of ex vivo necrotic biopsy specimen imaged with CRM. E: High magnification of inset in panel D. Note the lack of distinct cells. F: Corresponding H & E image from panel E. All bars = 20 μm.

need to use exogenous fluorophores could affect future molecular analysis of the tissues.[12]

We found CRM did not alter the DNA, RNA, or protein that could be extracted and quantified from tissue biopsy specimens screened up to 2 hours after resection. Confocal reflectance microscopy images collected from these samples could be digitally stored and potentially recalled with biobanked specimens. This metadata could prove advantageous to researchers who want more information about tumor morphology or cellularity before they choose it for laborious or costly analyses.

Confocal reflectance microscopy provides cellular and subcellular information. We ascertain CRM to have diagnostic utility, as many images in this study revealed distinct morphological details of glioblastoma such as cellularity, vasculature, and necrosis (Figs. 1, 2, 3A, and 4) typically identified with traditional histopathological H & E staining.

Many translational neurooncology studies rely on human glioblastoma tissue samples that appropriately represent an original tumor. Unintentional utilization of necrotic or nonrepresentative tissue samples can lead to erroneous and biased results that confound molecular and genetic experiments. In studies that advance to clinical trials, patient biopsies are often screened to determine eligibility for a targeted clinical trial. Utilization of CRM can ensure that patients are not mistakenly excluded from these trials after standard therapy has failed. Therefore, screening for high-quality tissue specimens with CRM can facilitate the advancement of our knowledge of glioma biology and can ensure qualified patients receive potential life-prolonging therapies and can enroll in appropriate clinical trials.[14]

Current limitations of CRM include limited imaging depth penetration. With our imaging parameters, CRM could assess tissue from the surface to a depth of 200–300 μm. However, we did not find that this depth limitation altered our assessment of tissues in our study. At present, few pathology departments contain the imaging hardware or personnel required to screen tissue biopsies with CRM. We have a full-scale laboratory Zeiss LSM710 microscope located for research purposes in the hospital's clinical pathology department where operating room specimens are routinely received, but equivalent equipment is rarely found in the pathology departments of most hospitals. However, modernization of pathology departments may include addition of confocal microscopes and other systems capable of CRM that will allow the screening of samples within 2 hours. Lastly, ex vivo CRM is limited by the ability to only assess tissue that is intraoperatively selected to represent tumor. A handheld intraoperative CRM device could potentially overcome sampling error and allow assessment of tissue samples prior to resection.

Past studies have shown the utility of CRM technology in providing cellular and subcellular detail, specifi-

cally in diagnosing dermatological conditions, identifying neoplastic tissue and margins, and assessing diseased and normal liver tissue.[1,2,4–6,9,10,15,18] Our study is the first to assess human brain tumor tissue purely with CRM. By quantifying DNA, RNA, and protein, we also demonstrate for the first time the ability of CRM to preserve the molecular integrity of tissue biopsies.

Conclusions

Confocal reflectance microscopy can screen brain tumor tissue cellularity for inclusion into biobanks while preserving molecular integrity of tissue samples. Confocal reflectance microscopy provides a rapid imaging modality that can accurately provide ex vivo morphological information in animal models and fresh human biopsies. In comparison with traditional histopathological methods, this technique does not rely on exogenous dyes or fixation and sectioning. Furthermore, this technique preserves the DNA, RNA, and protein characteristics of tissues, allowing further analysis of imaged specimens. Future technical developments of CRM include utilization of a handheld confocal endomicroscope for imaging, which would allow rapid and safe histopathological assessments in vivo. Further applications of CRM may include rapid ex vivo and in vivo examination of brain tumors in addition to glioblastoma. This technique ensures that high quality specimens are biobanked for future molecular studies of tumor samples and for assessing patient eligibility for clinical trials based on tumor characteristics.

Disclosure

The authors report no conflict of interest concerning the materials or methods used in this study or the findings specified in this paper.

Author contributions to the study and manuscript preparation include the following. Conception and design: Nakaji, Georges, Zehri, Eschbacher, Feuerstein, Preul, Keuren-Jensen. Acquisition of data: Georges, Zehri, Carlson, Nichols, Martirosyan, Ghaffari, Eschbacher, Anderson, Keuren-Jensen. Analysis and interpretation of data: Georges, Zehri, Carlson, Ghaffari, Eschbacher, Keuren-Jensen. Drafting the article: Georges, Zehri. Critically revising the article: Nakaji, Mooney, Kalani, Eschbacher, Feuerstein, Preul, Keuren-Jensen. Reviewed submitted version of manuscript: Nakaji, Zehri, Preul, Keuren-Jensen. Statistical analysis: Georges, Carlson, Keuren-Jensen. Administrative/technical/material support: Nakaji, Feuerstein, Anderson, Preul, Keuren-Jensen. Study supervision: Nakaji, Eschbacher, Feuerstein, Anderson, Preul, Keuren-Jensen.

References

1. Campo-Ruiz V, Lauwers GY, Anderson RR, Delgado-Baeza E, González S: In vivo and ex vivo virtual biopsy of the liver with near-infrared, reflectance confocal microscopy. **Mod Pathol 18:**290–300, 2005
2. Campo-Ruiz V, Ochoa ER, Lauwers GY, González S: Evaluation of hepatic histology by near-infrared confocal microscopy: a pilot study. **Hum Pathol 33:**975–982, 2002
3. Central Brain Tumor Registry of the United States: **CBTRUS Statistical Report: Primary Brain and Central Nervous System Tumors Diagnosed in the United States 2004-2006.** (http://www.cbtrus.org/2010-NPCR-SEER/CBTRUS-WEB REPORT-Final-3-2-10.pdf) [Accessed December 16, 2013]
4. Clark AL, Gillenwater AM, Collier TG, Alizadeh-Naderi R, El-Naggar AK, Richards-Kortum RR: Confocal microscopy for real-time detection of oral cavity neoplasia. **Clin Cancer Res 9:**4714–4721, 2003
5. Curiel-Lewandrowski C, Williams CM, Swindells KJ, Tahan SR, Astner S, Frankenthaler RA, et al: Use of in vivo confocal microscopy in malignant melanoma: an aid in diagnosis and assessment of surgical and nonsurgical therapeutic approaches. **Arch Dermatol 140:**1127–1132, 2004
6. Drezek RA, Richards-Kortum R, Brewer MA, Feld MS, Pitris C, Ferenczy A, et al: Optical imaging of the cervix. **Cancer 98 (9 Suppl):**2015–2027, 2003
7. Fleige S, Pfaffl MW: RNA integrity and the effect on the real-time qRT-PCR performance. **Mol Aspects Med 27:**126–139, 2006
8. Furnari FB, Fenton T, Bachoo RM, Mukasa A, Stommel JM, Stegh A, et al: Malignant astrocytic glioma: genetics, biology, and paths to treatment. **Genes Dev 21:**2683–2710, 2007
9. González S, Swindells K, Rajadhyaksha M, Torres A: Changing paradigms in dermatology: confocal microscopy in clinical and surgical dermatology. **Clin Dermatol 21:**359–369, 2003
10. Hicks SP, Swindells KJ, Middelkamp-Hup MA, Sifakis MA, González E, González S: Confocal histopathology of irritant contact dermatitis in vivo and the impact of skin color (black vs white). **J Am Acad Dermatol 48:**727–734, 2003
11. Lefranc F, Brotchi J, Kiss R: Possible future issues in the treatment of glioblastomas: special emphasis on cell migration and the resistance of migrating glioblastoma cells to apoptosis. **J Clin Oncol 23:**2411–2422, 2005
12. Liao LD, Tsytsarev V, Delgado-Martínez I, Li ML, Erzurumlu R, Vipin A, et al: Neurovascular coupling: in vivo optical techniques for functional brain imaging. **Biomed Eng Online 12:**38, 2013
13. Mohyeldin A, Chiocca EA: Gene and viral therapy for glioblastoma: a review of clinical trials and future directions. **Cancer J 18:**82–88, 2012
14. Rainov NG, Heidecke V: Clinical development of experimental therapies for malignant glioma. **Sultan Qaboos Univ Med J 11:**5–28, 2011
15. Rajadhyaksha M, González S, Zavislan JM, Anderson RR, Webb RH: In vivo confocal scanning laser microscopy of human skin II: advances in instrumentation and comparison with histology. **J Invest Dermatol 113:**293–303, 1999
16. Stupp R, Mason WP, van den Bent MJ, Weller M, Fisher B, Taphoorn MJ, et al: Radiotherapy plus concomitant and adjuvant temozolomide for glioblastoma. **N Engl J Med 352:**987–996, 2005
17. Tilli MT, Cabrera MC, Parrish AR, Torre KM, Sidawy MK, Gallagher AL, et al: Real-time imaging and characterization of human breast tissue by reflectance confocal microscopy. **J Biomed Opt 12:**051901, 2007
18. White WM, Tearney GJ, Pilch BZ, Fabian RL, Anderson RR, Gaz RD: A novel, noninvasive imaging technique for intraoperative assessment of parathyroid glands: confocal reflectance microscopy. **Surgery 128:**1088–1101, 2000

Manuscript submitted October 14, 2013.
Accepted November 22, 2013.
Please include this information when citing this paper: DOI: 10.3171/2013.11.FOCUS13478.

Address correspondence to: Peter Nakaji, M.D., c/o Neuroscience Publications, Barrow Neurological Institute, St. Joseph's Hospital and Medical Center, 350 W. Thomas Rd., Phoenix, AZ 85013. email: neuropub@dignityhealth.org.